EXPLORING AND EXPLOITING THE REACTIVITY OF GLYCALS IN ORGANIC SYNTHESIS

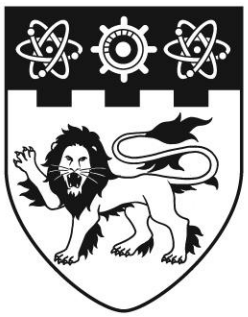

NANYANG TECHNOLOGICAL UNIVERSITY

EXPLORING AND EXPLOITING THE REACTIVITY OF GLYCALS IN ORGANIC SYNTHESIS

YAO HUI

SCHOOL OF PHYSICAL & MATHEMATICAL SCIENCES

2018

YAO HUI

2018

EXPLORING AND EXPLOITING THE REACTIVITY OF GLYCALS IN ORGANIC SYNTHESIS

YAO HUI

School of Physical & Mathematical Sciences

A thesis submitted to the Nanyang Technological University in fulfilment
of the requirement for the degree of
Doctor of Philosophy

2018

ACKNOWLEDGEMENTS

First of all, I would like to express my heartfelt thanks to my supervisor, Assoc. Professor Liu Xuewei, for accepting me and offering this valuable opportunity to continue my studies in his group. I never thought that I could continue to study for a Ph.D. degree at a world-famous university when I did research at the Chinese University of Hong Kong, but it came true here four years ago. Prof. Liu's professional guidance, precious advice, ongoing encouragement and support for the past few years play a crucial role during my Ph.D. study and this thesis writing.

I also thank Nanyang Technological University for funding my study in the form of NTU research scholarship. I would like to thank the faculties of Division of Chemistry and Biological Chemistry in School of Physical and Mathematical Sciences, especially, Dr. Li Yongxin and Dr. Rakesh Ganguly for their help in X-ray crystallography analysis, and Ms. Goh Ee Ling for her assistance in NMR and Ms. Zhu Wenwei for her support of mass spectrometry.

I want to give my deepest gratitude to my seniors: Dr. Xiang Shaohua, Dr. Ronny William, Dr. Leng Wei Ling, Dr. Liao Hongze, Dr. Leow Min Li, Dr. Kim Le Mai Hoang, Dr. Ji Li, Dr. Chai Hua, Dr. Tan Yujia for their advice and help in my Ph.D. study. Thanks to my labmates Zhang Shasha, He Jingxi, Dr. Lin Yichao, Dr. Guo Zhong, Vu Minh Duy, Bati Gabor, Xu Yuan, Kho Shu Hui, Das Mrinmoy, Guo Aoxin, Lin Jun Jie Desmond and Guo Tai for establishing a nice, friendly and positive research atmosphere for this team.

Finally, I am very grateful to my family. This thesis cannot be completed without their encouragements and supports.

TABLE OF CONTENTS

ABSTRACT

Chapter 1 introduces that glycals as one type of unsaturated carbohydrates specialized with a double bond between C1 and C2 on the sugar ring. They demonstrated diverse reactivities and broad applications in organic synthesis, owing to their availability, affordable price and chemical structure with defined chiral centers. Glycals could not only be explored as a glycosyl donor in glycosylation which is the core of carbohydrate chemistry, but also be exploited efficiently as natural chiral pools in total syntheses of natural/unnatural products.

In chapter 2, we have developed the first successful catalyst-controlled *O*-glycosylation *via* palladium catalysis using 3,4-cyclic carbonate glycal as the glycosyl donor. Various 2,3-unsaturated glycosides with C4-OH were synthesized stereoselectively in high yields under mild reaction condition. While hard nucleophiles such as aliphatic alcohols gave β-glycosides, soft nucleophiles such as phenols produced α-glycosides because palladium(II) catalyst coordinated with glycals on the β-face by carbonate group direction. On the other hand, both aliphatic alcohols and phenols generated only β-glycosides directed by hydrogen-bond effect because palladium(0) catalyst coordinated with glycal from α-face due to the steric hindrance. This method serves as a concise approach for constructing glycosides with predictable stereoselectivity and could potentially be applied to the formation of oligosaccharides and natural products.

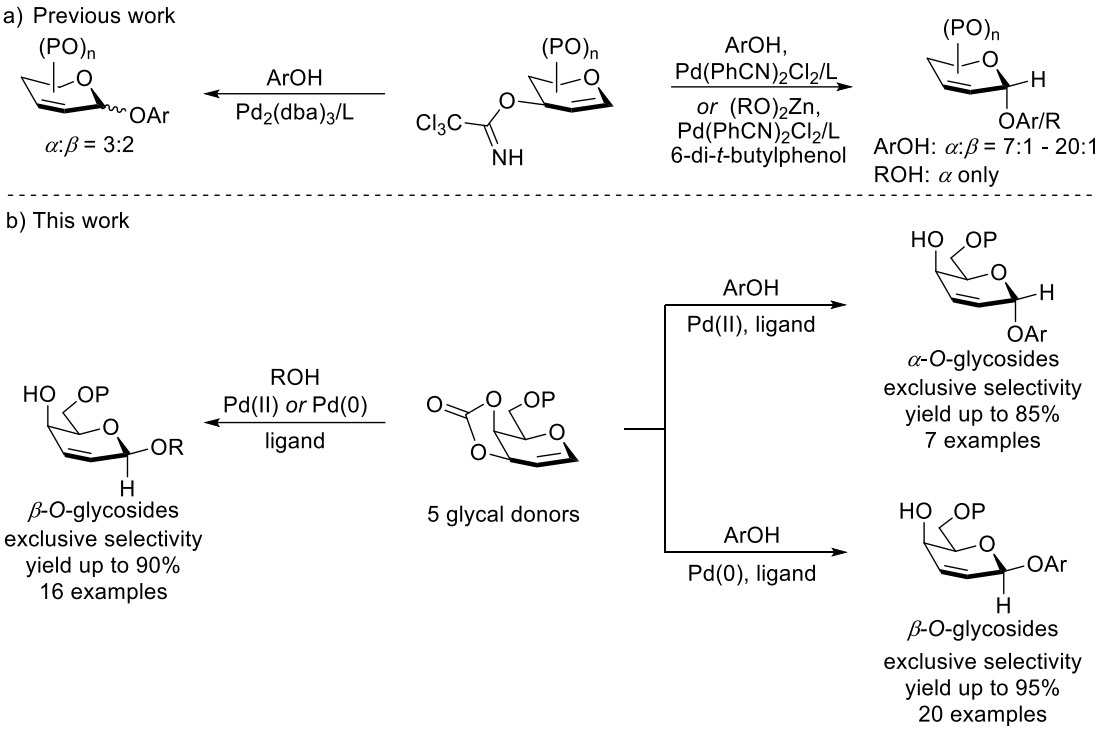

In chapter 3, we exploited glycals as common, inexpensive and affordable synthons to develop a novel synthetic strategy for attaining structurally distinct fused rings in a controlled and stereoselective manner successfully. The overall transformation involves a cascade of Ferrier reaction followed by 4π conrotatory imino-Nazarov cyclization and furnished three different fused-ring structures for divergent further syntheses. The synthesis was performed in one-pot with comparable yields, enabling convenient preparation of complex scaffold motifs from relatively simple starting materials. While reactions employing *ortho*-unsubstituted secondary aniline substrates readily afforded indoline-fused products, those employing *ortho*-hydroxyl-anilines enabled access to 1,4-benzoxazine. In both scenarios, $InBr_3$ acted as a Lewis acid catalyst, and replacement of $InBr_3$ by $Ln(OTf)_3$ converted the indoline-fused products into tetrahydroquinoline-fused cyclopentenones *via* ensuing retro-ene rearrangement.

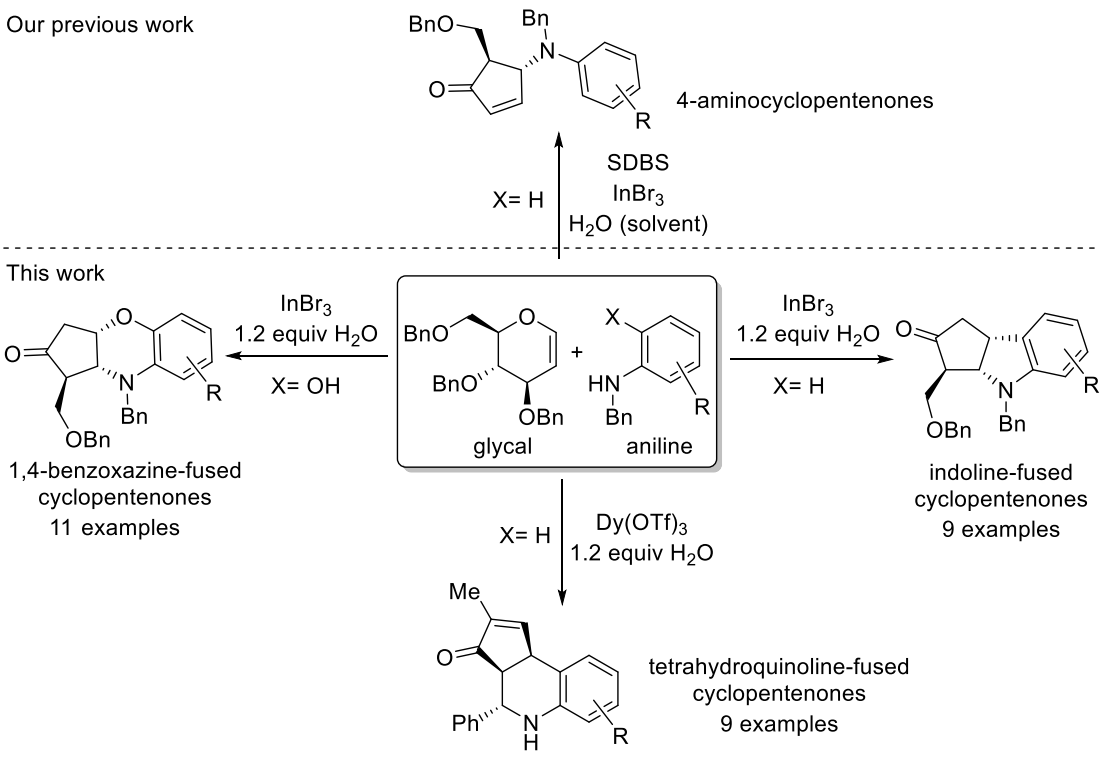
Our previous work
4-aminocyclopentenones
SDBS
InBr3
H2O (solvent)
X= H
This work
InBr3
1.2 equiv H2O
X= OH
1,4-benzoxazine-fused
cyclopentenones
11 examples
glycal
aniline
InBr3
1.2 equiv H2O
X= H
indoline-fused
cyclopentenones
9 examples
X= H
Dy(OTf)3
1.2 equiv H2O
tetrahydroquinoline-fused
cyclopentenones
9 examples

INDEX OF ABBREVIATIONS

δ	chemical shift	DME	dimethoxyethane
^{o}C	degree centigrade	DMF	*N*,*N*-dimethylformamide
Ac	acetyl	DMSO	dimethyl sulfoxide
AcOH	acetic acid	DPPB	1,4-bis(diphenylphosphino) butane
ACN	acetonitrile	equiv	equivalent
aq	aqueous	Et	ethyl
Bn	benzyl	ether	diethyl ether
Boc	*tert*-butoxycarbonyl	Et_3N	triethylamine
brs	broad singlet	EtOAc	ethylacetate
Bz	benzoic	EtOH	ethanol
calcd.	calculated	Fmoc	fluorenylmethoxycarbonyl
cat.	catalytic	g	gram
$CDCl_3$	deuterated chloroform	h	hour (time)
CH_2Cl_2	dichloromethane	Hex	hexane
$CHCl_3$	chloroform	HRMS	high resolution mass spectroscopy
d	doublet	Hz	hertz
dd	doublet of doublets	*i*Pr	isopropyl
dba	dibenzylideneacetone	m	multiplet
DBU	1,8-diazabicycloundec-7-ene	M^+	parent ion peak (mass spectrum)
DMAP	4-(*N*,*N*-dimethylamino) pyridine	Me	methyl
D*i*PPF	1,1'-bis(di-*i*-propylphosphino) ferrocene	MeOH	methanol
D*t*BPF	1,1'-bis(di-*tert*-butyl phosphino)ferrocene	mg	milligram
DCE	dichloroethane	MHz	megahertz
min	minute	Py	pyridine

mL	milliliter	q	quartet
mm	millimeter	RBF	round bottom flask
mmol	millimoles	s	singlet
mol	moles	sat	saturated
MS	mass spectrum	t	triplet
*n*Bu	*n*-butyl	TBAF	tetrabutylammonium fluoride
NMR	nuclear magnetic resonance	TBDPS	*tert*-butyldiphenylsilyl
Nu	nucleophile	TBS	*tert*-butyldimethylsilyl
OTf	trifluromethanesulfonate	TFA	trifluoroacetic acid
p	*para*	THF	tetrahydrofuran
Pd/C	palladium on carbon	TLC	thin layer chromatography
Ph	phenyl	TMS	trimethylsilyl
PMB	*p*-methoxybenzyl	Ts	*p*-toluenesulfonyl
PMP	*p*-methoxyphenyl	*t*Bu	*tert*-butyl
ppm	parts per million	v	volume

Chapter 1

An introduction to glycals

1.1 Background of glycals

Carbohydrates, also known as sugars or saccharides, are one of the four macromolecules required for living organisms besides proteins, nucleic acids and lipids.[1] Carbohydrates and their conjugated complex glycoproteins, glycolipids play essential roles in intercellular recognition, the composition of organisms and life activities.[2] Structurally, carbohydrates are polyhydroxy aldehydes and ketones and their anhydrides as shown in Scheme 1.1.1. If there is no unsaturated bond on the sugar ring, they are named as saturated saccharides. On contrary, they will be classified as an unsaturated saccharide with unsaturated bond on the ring. In particular, one type of the unsaturated saccharides derivatives with a double bond between C1 and C2 are named glycals which have diverse reactivities and broad applications in organic synthesis. Since D-glucal was synthesized from D-glucose by Fischer and Zach in 1913 for the first time,[3] many efforts have been devoted to glycal study by carbohydrate chemists. Almost all the saturated monosaccharides can be converted into the corresponding glycals through monosaccharide halide followed by elimination with zinc powder, for example, D-glucose to D-glucal, D-galactose to D-galactal and D-allose to D-allal (Scheme 1.1.1).

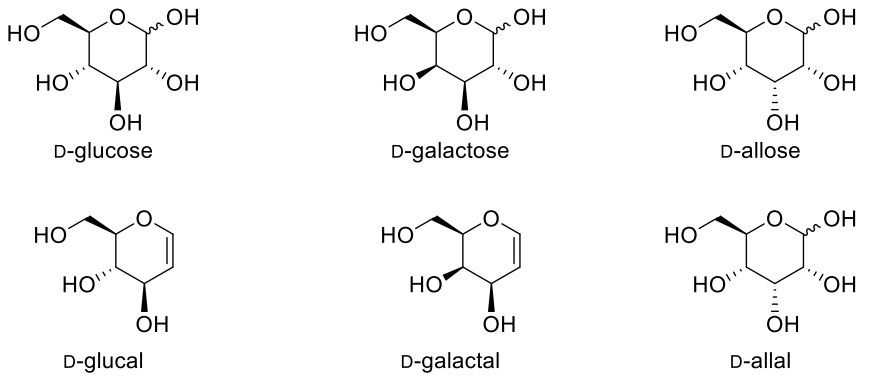

Scheme 1.1.1 Several common saturated sugars and 1,2-unsaturated sugars (glycals)

The structural conformation plays an important role in the reactivity of glycals. The natural form of glycals usually exists as pyranoses or furanoses resembling the six- or five-membered ring structures adopted by saturated monosaccharides. While glucose prefers chair conformation, glucal favors half-chair conformation as shown in Scheme 1.1.2. The conformation will affect the stereoselectivity of reactions by steric effect.

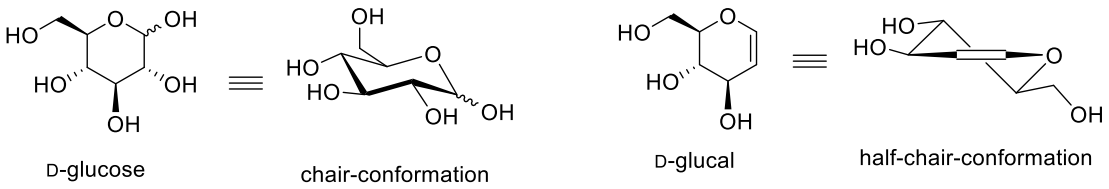

Scheme 1.1.2 The conformation of D-glucose and D-glucal

Glycals can not only be used as glycosyl donors in glycosylation reaction which is the core of carbohydrate chemistry but also be employed as synthetic blocks in the total synthesis of natural products or pharmaceutical agents. The double bond of glycal could play a role as olefin, at the site of which many functional groups can be introduced. When alcohols were attached to the anomeric position, *O*-glycosides will be obtained. Possible rearrangement reactions on the double bond provides potential access to novel scaffolds for natural product syntheses. In this chapter, both aspects of glycosylation with glycals and total syntheses from glycals will be discussed.

1.2 Glycals as glycosyl donors[4]

Efforts in glycochemistry have been centered on glycosylation, the key reaction in glycochemistry. Classic glycosylation strategies typically involve saturated glycosyl donors, proceeding either directly using hydrogen bonds or conformation constraints, or indirectly by installing moieties covalently through neighboring group participation and intramolecular aglycon delivery. Over the past years, new glycosylation strategies, tapping into the rich chemistry provided by transition metal catalyzed reactions, have emerged. To leverage the power of coordination chemistry, unsaturated glycosyl donors (glycals) were introduced. The choice of glycal as glycosyl donor carries advantages over the saturated glycosyl donor as the unsaturated bond readily coordinates with metal, and a multitude of transition metal-catalyzed reactions on olefinic substrates have been well-established with excellent stereoselectivities. Moreover, the resultant unsaturated glycoside provides sites for functionalizations, allowing easy access to a variety of sugars in a facile manner, including rare sugars. Another point highlighted by O'Doherty was the advantage of needing less protecting groups.[5]

First synthesis of glycosides from glycal substrates was reported by Raymond U. Lemieux *et al.* in the early 1960s.[6] They converted glycals into glycosides through two steps: glycals were activated *in situ* into epoxy intermediates, which were in turn subjected to reactions with glycosyl acceptors to afford glycosides (Scheme 1.2.1). This method, seminal as it was, suffers from the steric hindrance between the epoxy ring and C6 position and unsatisfactory stereoselectivity. Glycals could also be reduced first and then employed in glycosylation reactions as saturated glycosyl donors, through which one can gain nil advantage over direct use of corresponding saturated glycosyl donors.

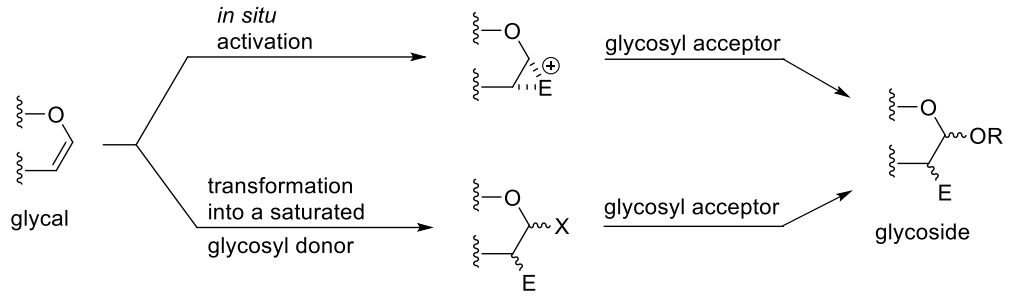

Scheme 1.2.1 Glycal used to glycosylation by Lemieux.

1.2.1 Glycals applied as glycosyl donors in Ferrier rearrangement

While glycals appear to have great potential in selective glycosylation, it remains challenging to employ them in glycosylation reactions due to the absence of a directing functional group on C2, which plays an essential role in imparting stereoselectivity to the reaction through neighbouring-group participation in the glycosylation using saturated glycosyl donors. Among incipient efforts in employing glycals for glycosylation, major products of the reactions generally adopt α-configuration at the anomeric position, presumably resulting from the anomeric effect on the glycoside products, and β-configuration products were not readily accessible.[7]

Notably, later in 1960s, Robert J. Ferrier first developed a method of glycosylation catalyzed by acids, which was later named after him as Ferrier rearrangement, by which glycals were employed as glycosyl donors in a direct fashion (Scheme 1.2.2).[8] In the Ferrier rearrangement reaction, the glycal C3-leaving group is first activated in the presence of the acid catalyst to form an allyloxocarbenium ion, and a following hetero-nucleophilic attack on the oxocarbeneium by the glycoyl acceptor yields a α-glycoside as the major product.[7, 9] Ferrier *et al.* reacted tri-*O*-acetyl-D-glucal with alcohol or phenol, catalyzed by $BF_3 \cdot Et_2O$ acid, and successfully obtained corresponding 2,3-unsaturated glycosides, which could be further functionalized to form other glycosides.

Subsequently, the scope of glycosyl acceptors for Ferrier rearrangement mediated by $BF_3 \cdot Et_2O$ was expanded to many different types of common nucleophiles,[10] and following investigations revealed that some other Lewis acids including $InCl_3$, $AlCl_3$, $ZnCl_2$, etc. are also capable of catalysing the reaction (Scheme 1.2.3).

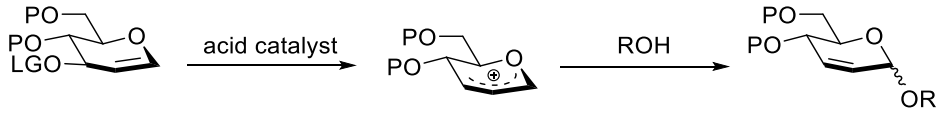

Scheme 1.2.2 Glycals applied in Ferrier rearrangement for *O*-glycosylation.

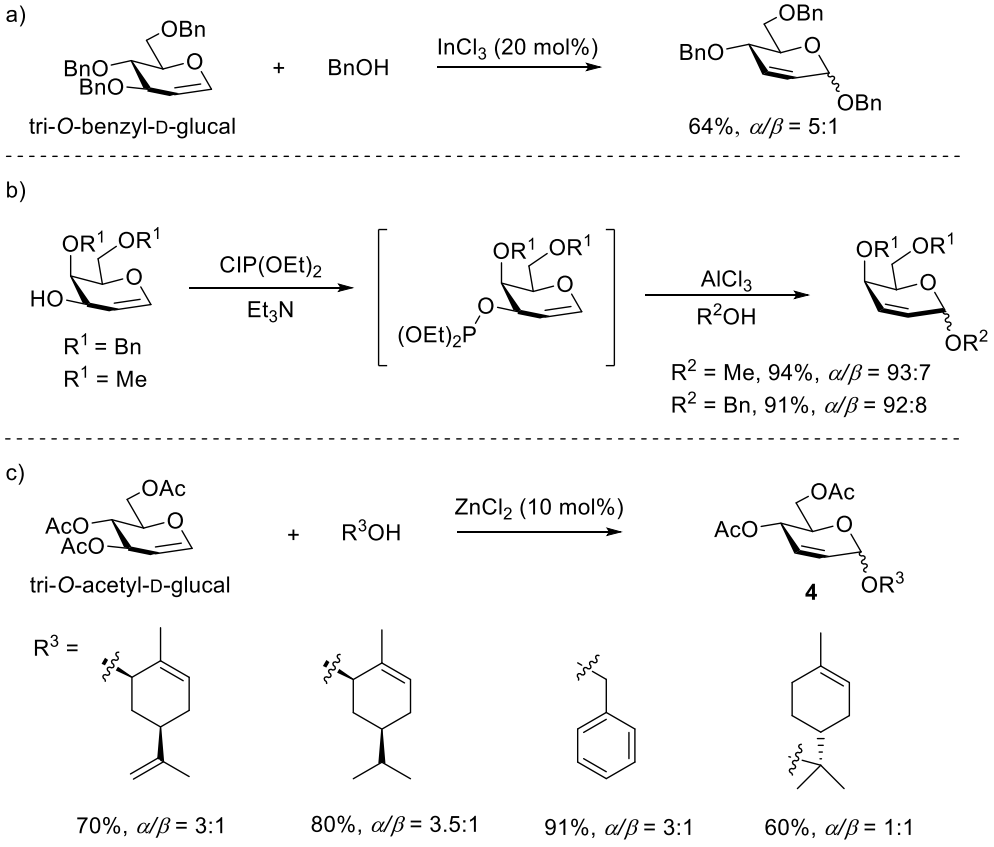

Scheme 1.2.3 Selected examples of Ferrier glycosylation with glycal donors.

In most of the earlier cases of Ferrier rearrangement, Lewis acid catalysts had to be used stoichiometrically.[11] And later developments in the method enabled use of catalytic amount of Pd(II) complexes for the reaction.[12] By far, Ferrier rearrangement

has become the most well-established method for glycosylation using glycal substrates.

Though widely used, conventional Ferrier glycosylations, like other earlier approaches for glycal glycosylation, failed to provide reliable access to *β*-glycosides. Besides the anomeric effect which is believed to contribute to the general α-stereoselectivity in glycosylation reactions using glycals, conformational effect also plays an important role in the α-stereo preference of Ferrier glycosylation, especially among the cases in which the anomeric effect is absent (Scheme 1.2.4).[13] The preferred conformation of activated oxocarbenium intermediate **I** over **II** as well as the favored half-chair conformation $^{O}H_5$ over the high-energy boat conformation $^{1,4}B$, leads to the thermokinetically controlled *α*-selectivity, even for *C*-glycosylation, albeit not exclusively. Initial requirements of stoichiometric Lewis acids, such as $BF_3{\cdot}OEt_2$, $InCl_3$ or $SnCl_4$ later evolved into catalytic amounts of Pd(II) complexes.[12]

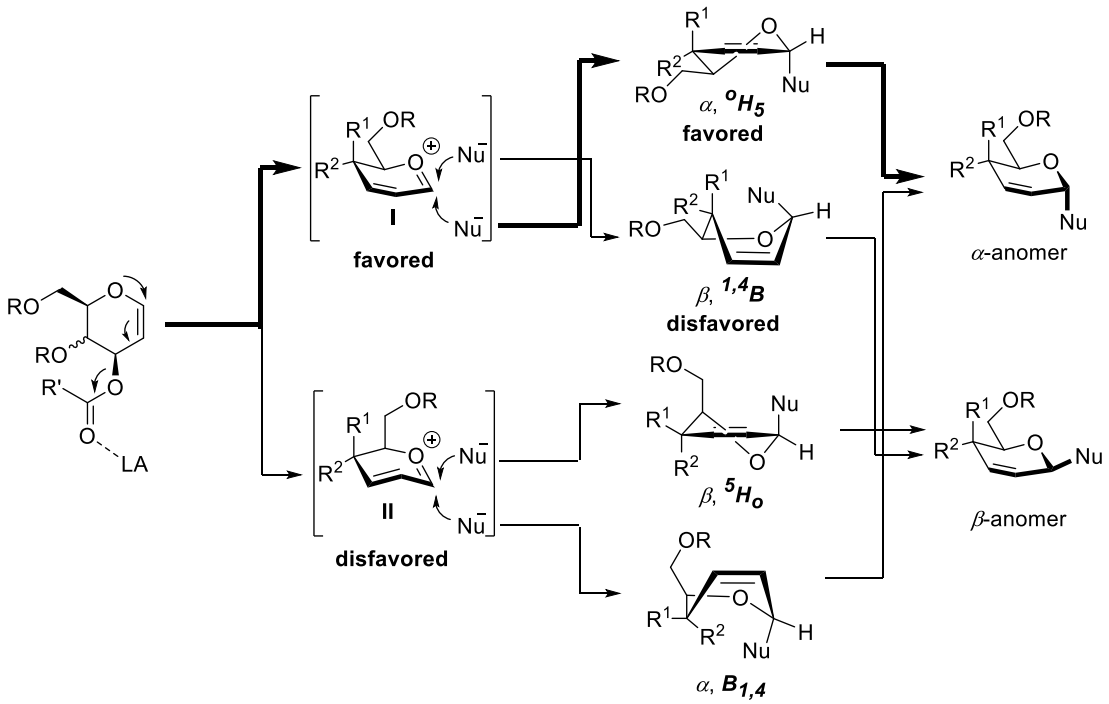

Scheme 1.2.4 The mechanism of Ferrier-type glycosylation using glycals

1.2.2 Glycals applied as glycosyl donors in Heck reaction

Besides Ferrier reaction, Heck reaction with glycals can also be applied in the synthesis of glycosides. Considerable efforts have been devoted to this reaction by many scientists in the past few years. For example, Ye, and our group developed *C*-glycosylation through Heck reaction utilizing phenylboronic acids, phenyl iodides, phenylhydrazines, benzoic acids, aryl diazonium tetrafluoroborates and arylsulfonyl chlorides to successfully synthesize *α*-*C*-glycosides (Scheme 1.2.5).[14] All the desired products 2,3-deoxy-sugars could be furnished in moderate to excellent yields with high regio- and stereo-selectivities, owing to the affinity of metal to the double bond.[14b, 14c, 15]

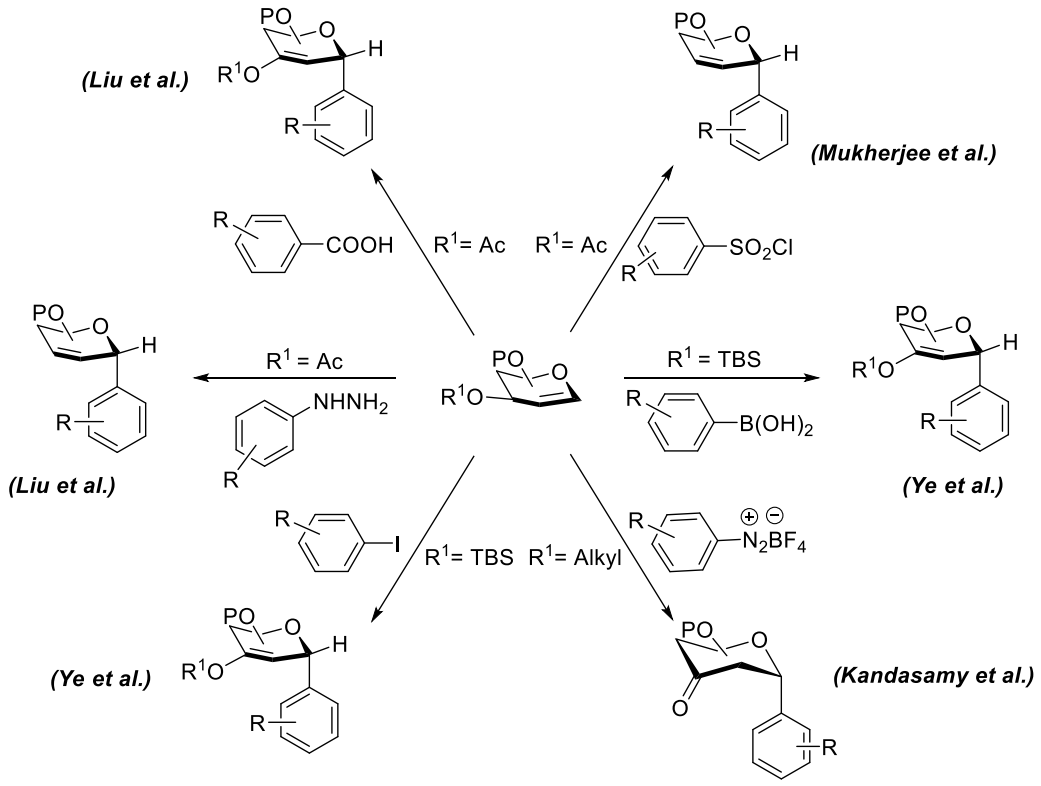

Scheme 1.2.5 Glycals as glycosyl donors *via* Heck reaction

The directing effect of functionalities on other positions can be exploited for achieving stereoselectivity in glycosylation in the absence of a C2 substituent, particularly for metal-catalyzed reactions. Herein the possible mechanism of Heck-type glycosylation was proposed by our group as shown in Scheme 1.2.6.[14d] First, palladium complex **b** is formed through salt exchange, and decarboxylation of **b** gives Pd(II) complex **c**. Then C3 group could direct the *syn* addition of palladium complex from the opposite face due to steric hindrance, accounting for the stereoselectivity of the overall reaction. The silver reagent plays an important role as an additive for *β*-hydride elimination. The silver reagent is an essential additive for *β*-hydride elimination, as the silver cation takes away one of the acetyl group from the palladium complex intermediate **e**, leaving a vacant coordination site and an accessible empty orbital favorable for the rapid *β*-hydride elimination.

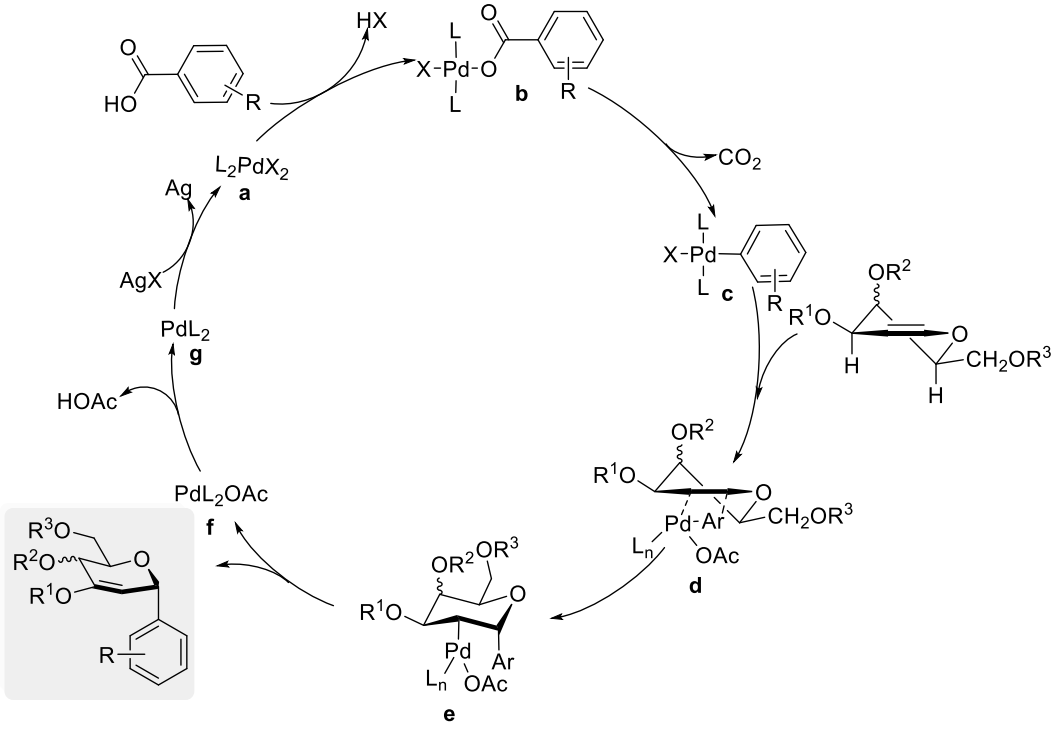

Scheme 1.2.6 Proposed mechanism of a decarboxylative Heck reaction with glycals

1.2.3 Glycals applied as glycosyl donors in Tsuji-Trost reaction

Rapid development in the field of palladium-catalyzed reactions in the past decades has significantly enriched the synthetic approaches available to organic chemists, and our group had recently developed a novel type of glycosylation with glycals based on.[16] Firstly, the problem of poor reactivity was addressed by IAD-like tethering of a glycosyl acceptor to the C3 position of the glycal donor, next to the anomeric position, which could also be released *in situ* upon decarboxylation. Extension of this work to other types of nucleophiles proved the versatility of this reaction, in which *C*-, *N*- and *O*-glycosides could be obtained with similar efficiency (Scheme 1.2.7a-c). In all cases, the reaction proceeded successfully to form β-glycosides stereoselectively.[17]

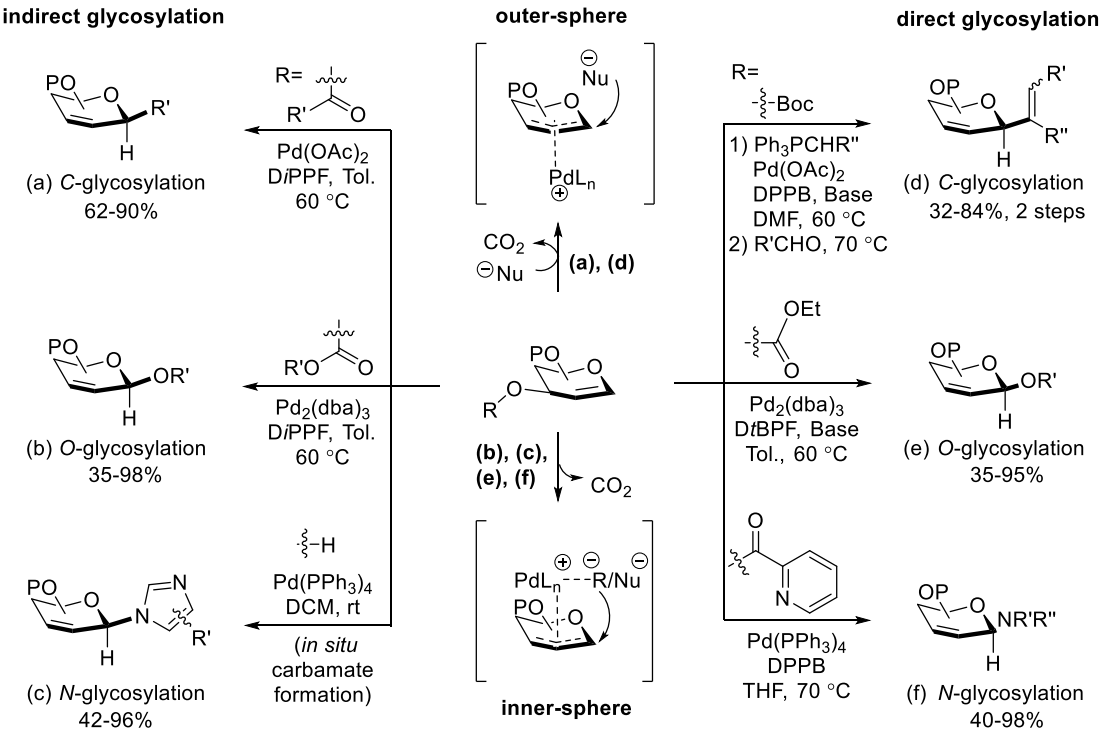

Scheme 1.2.7 Indirect and direct glycosylation by decarboxylative allylation using glycals

On the other hand, reducing the preparative steps for the unsaturated glycal donor in glycosylation was studied. Then the direct glycosylation was developed by our group using an exogenous glycosyl acceptor instead of aglycon installation, through careful consideration of the C3 leaving group and fine-tuning of the acceptors' electronic properties (Scheme 1.2.7d-f).[18] Overall, these approaches demonstrated that *C*-, *O*- and *N*-nucleophiles could be employed and all the reaction results were consistent with either inner-sphere or outer-sphere mechanism raised by Trost,[19] resulting in excellent selectivities. For the inner-sphere mechanism (Scheme 1.2.7b, 1.2.7c, 1.2.7e and 1.2.7f), the facial selectivity arises from the coordination between transition metals and hard

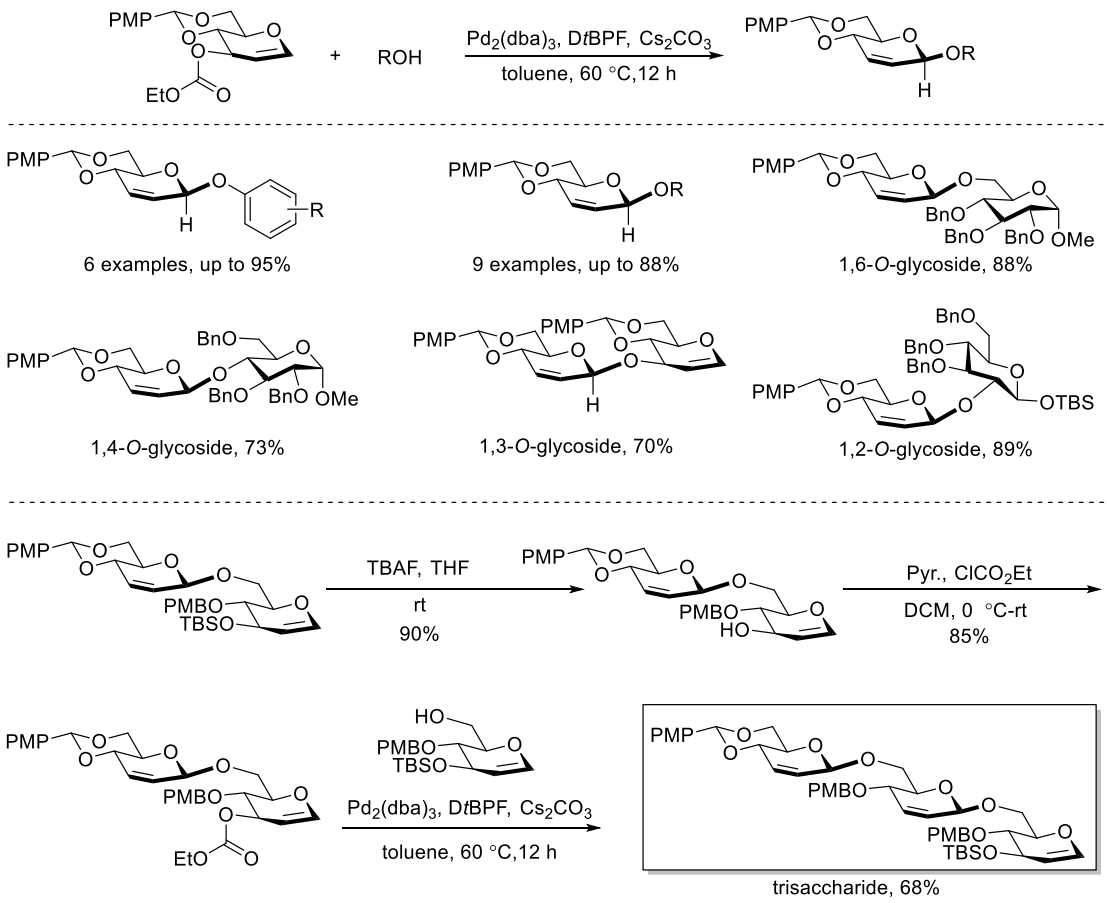

Scheme 1.2.8 Intermolecular *O*-glycosylation by decarboxylative allylation and its application

nucleophiles prior to an intramolecular nucleophilic attack of the anomeric carbon. In contrast, the outer-sphere mechanism (Scheme 1.2.7a and 1.2.7d) arises from the intermolecular attack of soft nucleophiles approaching the π-allylic system from the opposite face of the transition metal, also termed as double inversion.

Furthermore, our group has successfully applied these methodologies to natural product synthesis such as the formal synthesis of the macrolide aspergillide A as well as the syntheses of specific disaccharides and trisaccharides (Scheme 1.2.8).

1.3 Glycals as synthons

Glycals with up to three well-defined chiral centers have long been exploited as versatile starting materials for the synthesis of a wide array of natural products and pharmaceutically relevant compounds.[20] While employing glycals and their readily accessible derivatives as carbon synthon in organic synthesis represents an excellent approach for the preparation of structurally diverse products from relatively inexpensive precursors, the routes arriving at the target compounds often involve a forbidding number of synthetic steps. The new synthetic methodology enabling rapid transformation of a carbohydrate-derived synthon into a number of complex non-carbohydrate compounds with potential in natural product synthesis is highly desirable. Among the repertoire of commercially available carbohydrate derivatives, glycals occupy a prominent position as starting materials for the preparation of a plethora of valuable intermediates for the total synthesis of a wide raft of natural and unnatural products.[21]

1.3.1 Conversion of glycals into Perlin aldehydes

Carbohydrates, intrinsically carrying multiple well-defined chiral centers and attainable from biological resources in large quantities at low costs, have long been deemed as promising precursors for large-scale syntheses of natural products and pharmaceutically active compounds. Glycals can be readily converted into the corresponding *δ*-hydroxyl-*α*,*β*-unsaturated aldehydes, also known as Perlin aldehydes, which have been demonstrated to be remarkably useful building blocks for natural product synthesis owing to the presence of high degree of functionalities amenable to selective functional group manipulations.[22]

Enantiomerically pure *δ*-hydroxy *α*,*β*-unsaturated aldehydes was firstly synthesized by and later named after Arthur S. Perlin in 1975. Treatment of triacetyl-glycals with $HgSO_4$ (0.02 mol equiv) in 5 mM H_2SO_4 at room temperature rapidly converts the glycals into corresponding Perlin aldehydes (Scheme 1.3.1).

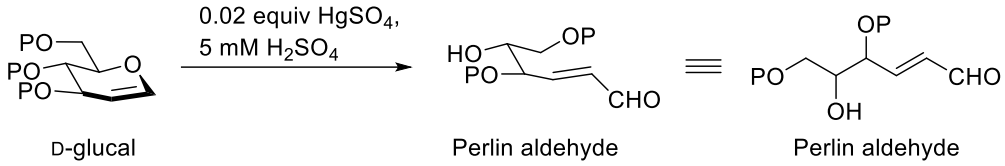

Scheme 1.3.1 Synthesis of Perlin aldehyde from protected D-glucal

The mechanism of forming this type aldehyde was proposed by Perlin *et al.* as shown in Scheme 1.3.2. The 1,2-double bond of triacetate-D-glucal attacks Hg atom of $HgSO_4$ first, and an electron pair on Hg atom attacks the other carbon atom of the double bond to form a three-membered ring mercurinium ion **b**. Then water attacks C1 of sugar ring to hydrolyze the mercurinium **b** and generates two isomeric intermediates **c** and **d** due to the attack from different directions. After elimination of mercurinium and leaving of

C3 substituent, the trans-olefin **g** was generated, which was also the target Perlin aldehyde.

Perlin aldehydes were widely applied in total synthesis as building blocks.[22f] Many carbohydrate chemists devoted a lot of efforts in this field, for example, Herdeis developed the total synthesis of (−)-cassine from L-rhamnose as shown in Scheme 1.3.3.[23] L-Rhamnose was converted into Perlin aldehyde first and the desired chiral center was constructed by methanesulfonyl substitution of the hydroxyl group and a following nucleophilic attack by azide. Then the Perlin aldehyde derivative was subjected to a Horner-Wadsworth-Emmons (HWE) reaction with ketophosphonate to give the key olefinic intermediate. Following deoxygenation and acid hydrolysis converts the intermediate into the target (−)-cassine molecule.

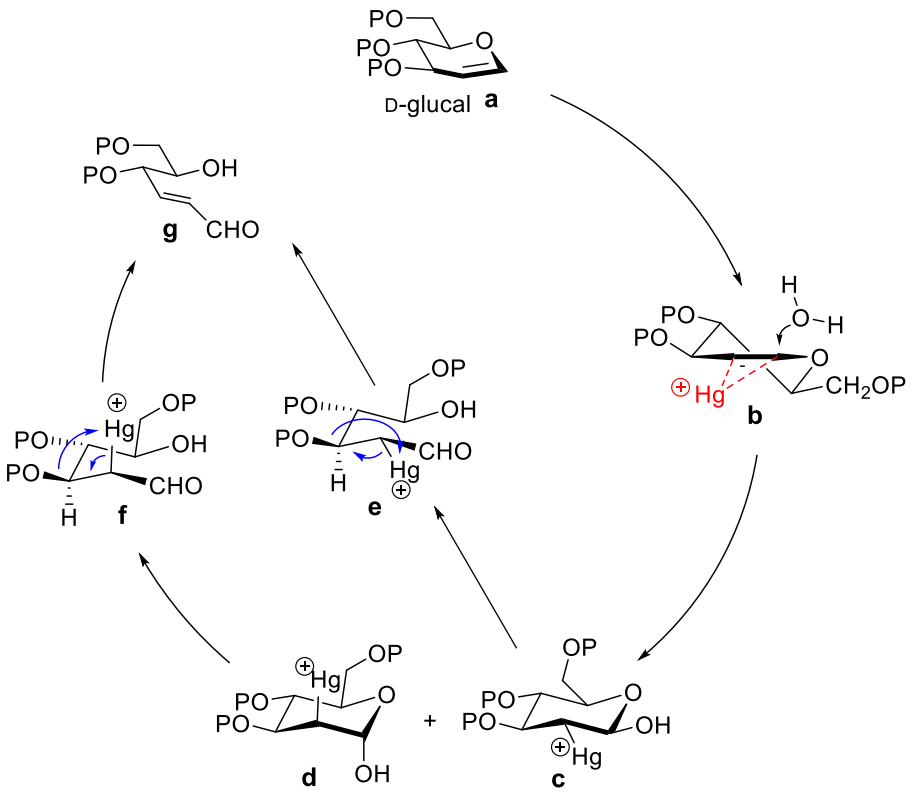

Scheme 1.3.2 Mechanism of Perlin aldehyde synthesis

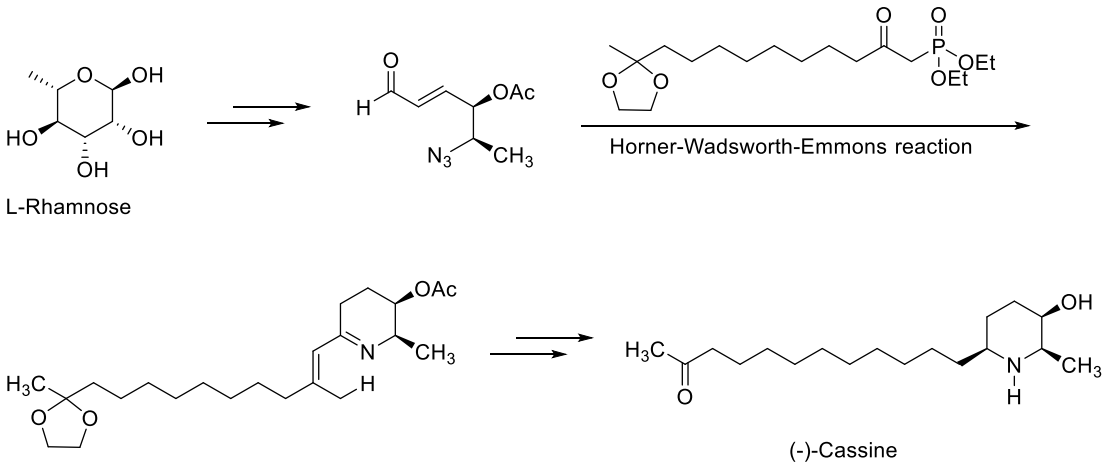

Scheme 1.3.3 Total synthesis of (−)-cassine from L-rhamnose through Perlin aldehydes

Dorrigocin A was reported to exhibit a variety of biological activities.[24] It has been shown to prevent fungal infections by inhibiting carboxymethyltransferase in cell models. The structure of Dorrigocin A as shown in Scheme 1.3.4 is a cycloheximide linked to a long unsaturated carbon chain with two hydroxyl groups and a terminal carboxylic acid, the analogues of which can be synthesized from glycals in a quick access.[25] Murphy's group developed this synthesis methodology using commercially available 3,4,6-tri-*O*-acetyl-D-glucal as the starting material (Scheme 1.3.4). They converted the C6 group of D-glucal into 3-methoxybut-3-en-1-yl group through a reported method firstly. Then the glycal was further modified into a C6-long chain D-glucal by ring-closing metathesis with Grubbs-II catalyst. Followed by Perlin aldehyde forming reaction the key intermediate adehyde was generated. After reduction of the aldehyde group and hydrolysis of the acetyl group, analogue **1** of Dorridocin A was obtained. On the other hand, the key intermediate aldehyde was also able to react with acetic anhydride before the reduction reaction. Another analogue **2** of Dorridocin A would be generated smoothly.

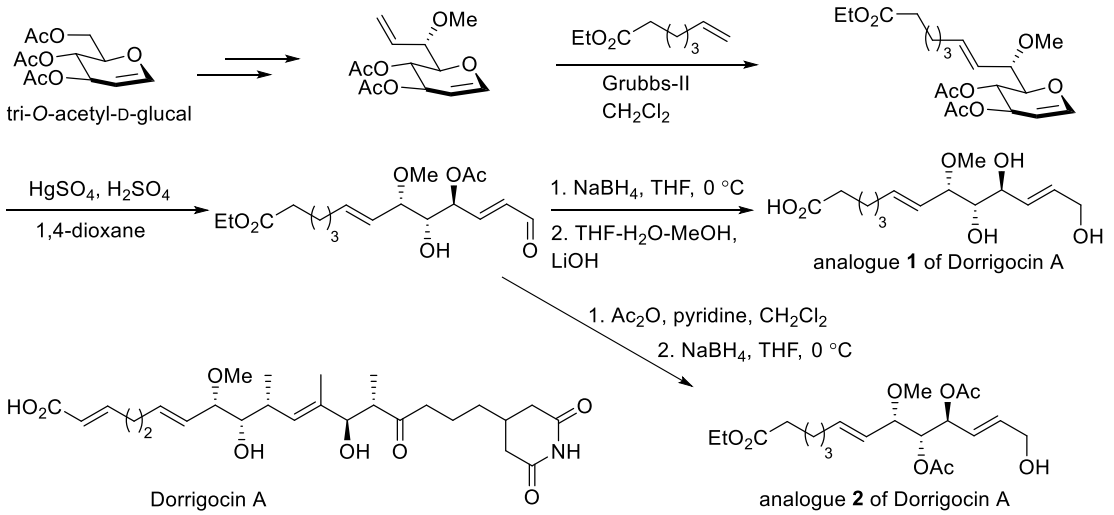

Scheme 1.3.4 Dorrigocin A and total synthesis of its analogues from tri-*O*-acetyl-D-glucal through Perlin aldehydes

1.3.2 Natural product syntheses from glycals

Apart from being used as a Perlin aldehyde source, glycals can also be exploited as affordable biomass materials and natural chiral pools for natural product and drug syntheses.[26] Many efforts have been devoted to this area and we now know that numerous complicated functional molecules could be conveniently synthesized from carbohydrates.[27] Herein, recent representative examples are chosen based on their usage of *O*-, *N*- and *C*-glycosides from glycals as the starting materials to synthesize natural/unnatural products.

Besides being the core units of oligo- and polysaccharides, *O*-glycosides are also widely employed in natural product syntheses. For example, C2-bromoglucal was successfully applied to synthesize the highly substituted chromans and isochromans with *O*-glycosylation being the key step by Werz in 2010 (Scheme 1.3.5).[28] By capitalizing on the rich stereochemistry of carbohydrate starting materials and using Pd-catalyzed domino approach, complex oligocyclic molecules could be generated with minimal effort.

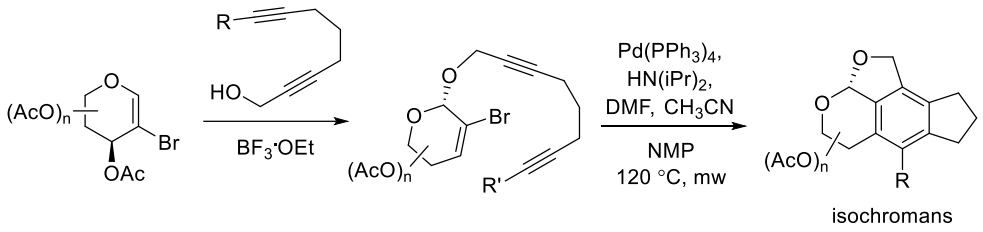

Scheme 1.3.5 Synthesis of isochromans from glycals

N-Glycosides are indispensable components of DNA, RNA, cofactors and various antibacterial, anti-inflammatory, anti-viral and anti-neoplastic agents. Of them, 2-amino-2-deoxyglycopyranosides are commonly found in prokaryotic and eukaryotic glycoconjugates. In order to synthesize this type of glycocojugates, our group developed a sequential reaction: aziridination catalyzed by rhodium and Barbier allylation of D-glycal. Various of 2-amino-2-deoxyglycopyranosides were obtained

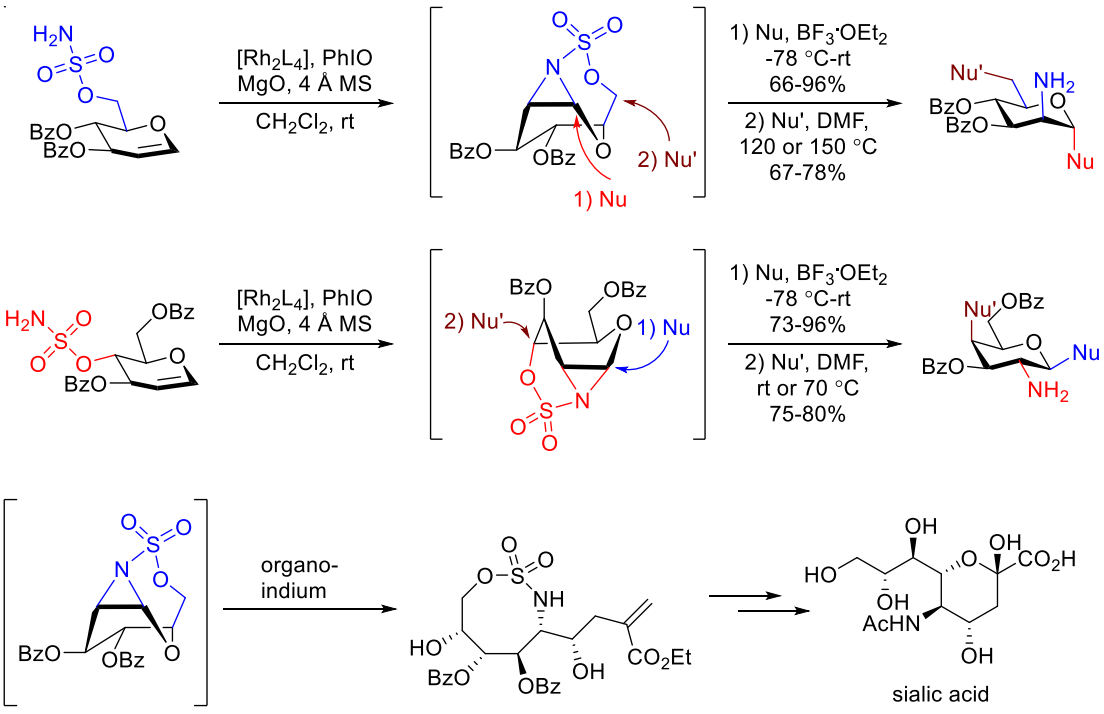

Scheme 1.3.6 Methodology of aziridination and allylation of D-glucal and its application in sialic acid synthesis

seteroselectively in high yields. What's more, the *N*-glycoside intermediates generated by intramolecular *N*-glycosylation could be converted to a highly-substituted [1,2,3]-oxathiazocane-2,2-dioxide, which could be later applied to the total synthesis of sialic acid *N*-acetylneuraminic acid (Neu5Ac) (Scheme 1.3.6).[29]

While *N*-glycosides are mostly found in the biological components, *C*-glycosides occurred more broadly in natural products, particularly for 2,3-unsaturated glycosides. One of their applications is the rational design of intramolecular decarboxylative allylation to form the *β*-*C*-glycoside which was applied as the key step in the formal synthesis of aspergillide A (Scheme 1.3.7).[30]

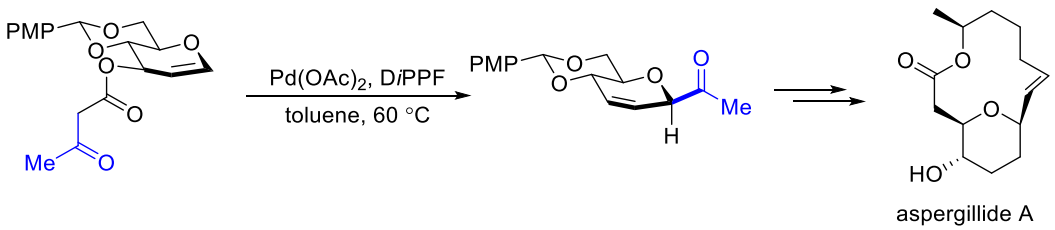

Scheme 1.3.7 Intramolecular decarboxylative allylation for *C*-glycosylation

As described above, *O*-, *N*- and *C*-glycosides play important roles in drug discovery. Vankar further demonstrated this in his report on bicyclic hybrid sugar molecules comprising of oxa-aza, oxa-oxa, and oxa-carbasugar-fused skeletons, synthesized from *O*-, *N*- and *C*-glycosides derived from C2-acetoxyglucal (Scheme 1.3.8).[31] These hybrid sugar molecules were found to exhibit good activity as glycosidase inhibitors.

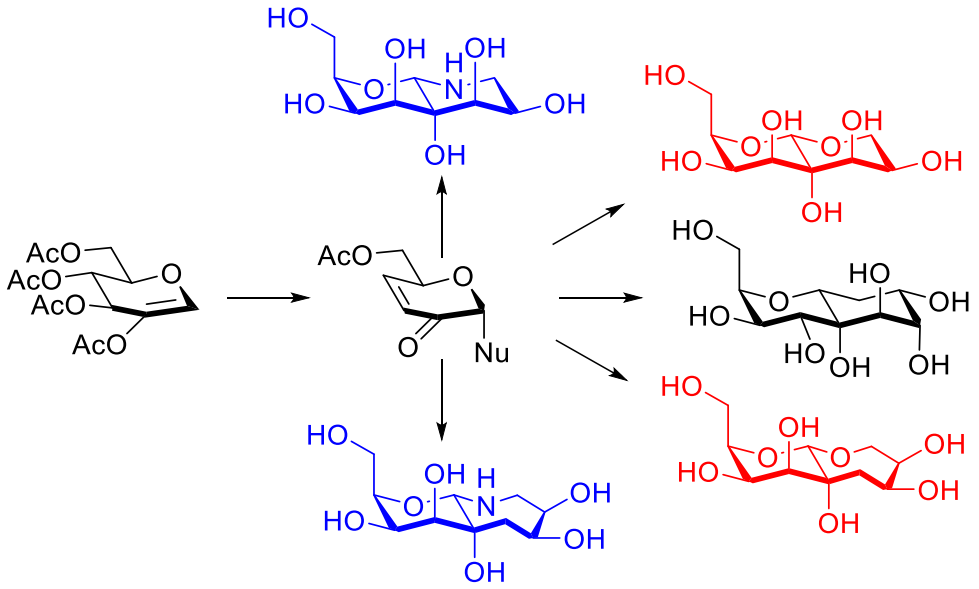

Scheme 1.3.8 Synthesizing glycosidase inhibitors from *C*-, *O*- and *N*-glycosides

Though most reactions on glycosylation discussed above are centred about the anomeric carbon of glycals, it should not be forgotten that functionalization of other positions can also provide access to natural products and carbohydrate derivatives. An example of functionalizing C2 position of glycal with activated alkenes under mild conditions using palladium-catalyzed direct cross-coupling reaction of glycals, it was later applied to the synthesis of bradyrhizose, a unique C10 monosaccharide which is the unit of *O*-antigen polysaccharide related to a nitrogen fixation independent of Nod-factor (Scheme 1.3.9).[15e, 32]

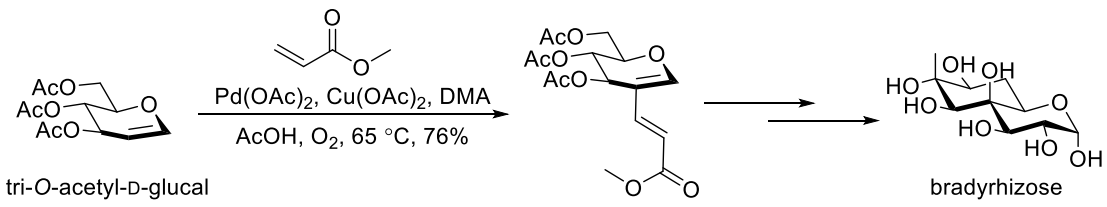

Scheme 1.3.9 Palladium-catalyzed direct cross-coupling reaction and its application

1.4 References

[1] F. V. Toukach, V. P. Ananikov, *Chem. Soc. Rev.* **2013**, *42*, 8376-8415.

[2] a) J. A. Torreno-Pina, B. M. Castro, C. Manzo, S. I. Buschow, A. Cambi, M. F. Garcia-Parajo, *Proc. Natl. Acad. Sci. U. S. A.* **2014**, *111*, 11037-11042; b) S. Yamada, W. J. Nelson, *Annu. Rev. Biochem.* **2007**, *76*, 267-294.

[3] E. Fischer, K. Zach, *Chem. Zentralblatt.* **1913**, *1*, 1968.

[4] Reprinted (adapted) with permission from (W.-L. Leng, J.-X. He, X.-W. Liu, *Acc. Chem. Res.* **2018**, *51*, 628-639.) Copyright (2018) American Chemical Society.

[5] R. S. Babu, Q. Chen, S. W. Kang, M. Q. Zhou, G. A. O'Doherty, *J. Am. Chem. Soc.* **2012**, *134*, 11952-11955.

[6] a) R. U. Lemieux, A. R. Morgan, *Can. J. Chem.* **1965**, *43*, 2190-2197; b) R. U. Lemieux, S. Levine, *Can. J. Chem.* **1964**, *42*, 1473-1480; c) R. U. Lemieux, Fraserre.B, *Can. J. Chem.* **1964**, *42*, 532-538; d) R. U. Lemieux, S. Levine, *Can. J. Chem.* **1962**, *40*, 1926-1932.

[7] A. M. Gomez, F. Lobo, C. Uriel, J. C. Lopez, *Eur. J. Org. Chem.* **2013**, *2013*, 7221-7262.

[8] a) R. J. Ferrier, *J. Chem. Soc.* **1964**, 5443-5449; b) D. M. Ciment, R. J. Ferrier, *J. Chem. Soc. C* **1966**, 441-445.

[9] a) R. Roy, P. Rajasekaran, A. Mallick, Y. D. Vankar, *Eur. J. Org. Chem.* **2014**, 5564-5573; b) B. K. Gorityala, R. Lorpitthaya, Y. G. Bai, X.-W. Liu, *Tetrahedron* **2009**, *65*, 5844-5848.

[10] a) G. R. Morais, R. S. Oliveira, R. A. Falconer, *Tetrahedron Lett.* **2009**, *50*, 1642-1644; b) F. W. Lichtenthaler, S. Ronninger, P. Jarglis, *Liebigs Ann. Chem.* **1989**,

1153-1161; c) R. J. Ferrier, J. O. Hoberg, *Adv. Carbohydr. Chem. Biochem.* **2003**, *58*, 55-119.

[11] a) P. Nagaraj, N. G. Ramesh, *Eur. J. Org. Chem.* **2008**, 4607-4614; b) Y. B. Chen, S. I. Wang, Z. P. Lin, C. H. Lin, M. T. Hsieh, H. C. Lin, *Tetrahedron* **2015**, *71*, 350-358; c) T. Ziegler, U. Seidl, *J. Carbohydr. Chem.* **1991**, *10*, 813-831; d) B. K. Bettadaiah, P. Srinivas, *Tetrahedron Lett.* **2003**, *44*, 7257-7259.

[12] a) F. Ding, R. William, F. Wang, J. Ma, L. Ji, X.-W. Liu, *Org. Lett.* **2011**, *13*, 652-655; b) F. Ding, R. William, S.-T. Cai, J. Ma, X.-W. Liu, *J. Org. Chem.* **2012**, *77*, 5245-5254; c) F. Ding, R. William, X.-W. Liu, *J. Org. Chem.* **2013**, *78*, 1293-1299; d) E. I. Balmond, D. Benito-Alifonso, D. M. Coe, R. W. Alder, E. M. McGarrigle, M. C. Galan, *Angew. Chem. Int. Ed.* **2014**, *53*, 8190-8194.

[13] K. Le Mai Hoang, W.-L. Leng, Y.-J. Tan, X.-W. Liu, in *Selective Glycosylations: Synthetic Methods and Catalysts*, Wiley-VCH Verlag GmbH & Co. KGaA, **2017**, pp. 135-153.

[14] a) H. Li, X. Ye, *Org. Biomol. Chem.* **2009**, *7*, 3855-3861; b) D. Xiong, L. Zhang, X. Ye, *Org. Lett.* **2009**, *11*, 1709-1712; c) Y. Bai, K. L. M. Hoang, H. Liao, X.-W. Liu, *J. Org. Chem.* **2013**, *78*, 8821-8825; d) S. Xiang, S. Cai, J. Zeng, X. Liu, *Org. Lett.* **2011**, *13*, 4608; e) S. K. Yousuf, S. C. Taneja, D. Mukherjee, *J. Org. Chem.* **2010**, *75*, 3097-3100; f) J. Kalikanda, Z. Li, *J. Org. Chem.* **2011**, *76*, 5207-5218.

[15] a) S. Xiang, S.-T. Cai, J. Zeng, X.-W. Liu, *Org. Lett.* **2011**, *13*, 4608-4611; b) Y. Bai, M.-L. Leow, J. Zeng, X.-W. Liu, *Org. Lett.* **2011**, *13*, 5648-5651; c) J. Ma, S. Xiang, H. Jiang, X.-W. Liu, *Eur. J. Org. Chem.* **2015**, 949-952; d) Y. Bai, K.

M. L. Hoang, H. Liao, X.-W. Liu, *J. Org. Chem.* **2013**, *78*, 8821-8825; e) Y. Bai, J. Zeng, S. Cai, X.-W. Liu, *Org. Lett.* **2011**, *13*, 4394-4397.

[16] a) B. M. Trost, D. L. VanVranken, *Chem. Rev.* **1996**, *96*, 395-422; b) B. M. Trost, M. J. Krische, V. Berl, E. M. Grenzer, *Org. Lett.* **2002**, *4*, 2005-2008; c) B. M. Trost, P. E. Strege, *J. Am. Chem. Soc.* **1977**, *99*, 1649-1651.

[17] a) J. Zeng, J. Ma, S. Xiang, S.-T. Cai, X.-W. Liu, *Angew. Chem. Int. Ed.* **2013**, *52*, 5134-5137; b) S. Xiang, Z. Lu, J.-X. He, K. Le Mai Hoang, J. Zeng, X.-W. Liu, *Chem. Eur. J.* **2013**, *19*, 14047-14051; c) S. Xiang, J.-X. He, J. Ma, X.-W. Liu, *Chem. Commun.* **2014**, *50*, 4222-4224.

[18] a) S. Xiang, J.-X. He, Y.-J. Tan, X.-W. Liu, *J. Org. Chem.* **2014**, *79*, 11473-11482; b) L. Ji, S. Xiang, W.-L. Leng, K. Le Mai Hoang, X.-W. Liu, *Org. Lett.* **2015**, *17*, 1357-1360; c) W.-L. Leng, H. Liao, H. Yao, Z.-E. Ang, S. Xiang, X.-W. Liu, *Org. Lett.* **2017**, *19*, 416-419.

[19] B. M. Trost, D. L. Van Vranken, *Chem. Rev.* **1996**, *96*, 395-422.

[20] a) E. J. Corey, D. A. Clark, G. Goto, A. Marfat, C. Mioskowski, B. Samuelsson, S. Hammarstrom, *J. Am. Chem. Soc.* **1980**, *102*, 1436-1439; b) D. A. Griffith, S. J. Danishefsky, *J. Am. Chem. Soc.* **1991**, *113*, 5863-5864; c) R. I. Hollingsworth, G. J. Wang, *Chem. Rev.* **2000**, *100*, 4267-4282; d) Z. J. Witczak, K. Tatsuta, *Carbohydrate Synthons in Natural Products Chemistry, Vol. 841*, American Chemical Society, **2002**; e) A. Zakarian, A. Batch, R. A. Holton, *J. Am. Chem. Soc.* **2003**, *125*, 7822-7824; f) M. Orazov, M. E. Davis, *Proc. Natl. Acad. Sci. U. S. A.* **2015**, *112*, 11777-11782; g) T. Masazumi, Y. Naoto, C. Ji, N. Yoshinao, T. Keiichi, *Angew. Chem. Int. Ed.* **2018**, *57*, doi:10.1002/anie.201803043.

[21] a) M. Yamaguchi, T. Okuma, A. Horiguchi, C. Ikeura, T. Minami, *J. Org. Chem.* **1992**, *57*, 1647-1649; b) D. A. Evans, B. W. Trotter, P. J. Coleman, B. Cote, L. C. Dias, H. A. Rajapakse, A. N. Tyler, *Tetrahedron* **1999**, *55*, 8671-8726; c) F. E. McDonald, K. S. Reddy, *Angew. Chem. Int. Ed.* **2001**, *40*, 3653-3655; d) P. Saidhareddy, A. K. Shaw, *RSC Adv.* **2015**, *5*, 29114-29120; e) C. K. Hill, J. F. Hartwig, *Nat. Chem.* **2017**, *9*, 1213-1221.

[22] a) K. Walczak, E. B. Pedersen, *Synthesis* **1991**, 959-962; b) H. H. A. M. Hassan, M. M. A. Rahman, *Synthetic Commun.* **2000**, *30*, 201-216; c) R. Pathak, S. K. Shaw, A. P. Bhaduri, K. V. G. Chandrasekhar, A. Srivastava, K. K. Srivastava, V. Chaturvedi, R. Srivastava, B. S. Srivastava, S. Arora, S. Sinha, *Biorg. Med. Chem.* **2002**, *10*, 1695-1702; d) M. Saquib, R. Sagar, A. K. Shaw, *Carbohydr. Res.* **2006**, *341*, 1052-1056; e) P. Nagaraj, M. Ganesan, N. G. Ramesh, *Tetrahedron* **2011**, *67*, 769-776; f) L. V. R. Reddy, V. Kumar, R. Sagar, A. K. Shaw, *Chem. Rev.* **2013**, *113*, 3605-3631.

[23] C. Herdeis, P. Kupper, S. Ple, *Org. Biomol. Chem.* **2006**, *4*, 524-529.

[24] a) J. H. Ju, S. K. Lim, H. Jiang, B. Shen, *J. Am. Chem. Soc.* **2005**, *127*, 1622-1623; b) T. Schneider-Poetsch, J. H. Ju, D. E. Eyler, Y. J. Dang, S. Bhat, W. C. Merrick, R. Green, B. Shen, J. O. Liu, *Nat. Chem. Biol.* **2010**, *6*, 209-217.

[25] G. Anquetin, S. L. Rawe, K. McMahon, E. P. Murphy, P. V. Murphy, *Chem. Eur. J.* **2008**, *14*, 1592-1600.

[26] Y. Yang, X. H. Zhang, B. Yu, *Nat. Prod. Rep.* **2015**, *32*, 1331-1355.

[27] P. C. Gao, S. Y. Zhu, H. Cao, J. S. Yang, *J. Am. Chem. Soc.* **2016**, *138*, 1684-1688.

[28] M. Leibeling, D. C. Koester, M. Pawliczek, S. C. Schild, D. B. Werz, *Nat. Chem. Biol.* **2010**, *6*, 199-201.

[29] a) R. Lorpitthaya, Z. Z. Xie, J. L. Kuo, X.-W. Liu, *Chem. Eur. J.* **2008**, *14*, 1561-1570; b) R. Lorpitthaya, S. B. Suryawanshi, S. Wang, K. K. Pasunooti, S.-T. Cai, J. Ma, X.-W. Liu, *Angew. Chem. Int. Ed.* **2011**, *50*, 12054-12057.

[30] J. Zeng, J. Ma, S. Xiang, S.-T. Cai, X.-W. Liu, *Angew. Chem. Int. Ed.* **2013**, *52*, 5134-5137.

[31] A. A. Ansari, P. Rajasekaran, M. M. Khan, Y. D. Vankar, *J. Org. Chem.* **2014**, *79*, 1690-1699.

[32] W. Li, A. Silipo, A. Molinaro, B. Yu, *Chem. Commun.* **2015**, *51*, 6964-6967.

Chapter 2[1]

Catalyst-controlled stereoslective *O*-glycosylation of glycals: Pd(0) *vs* Pd(II)

2.1 Introduction

Glycosylation is the most important reaction in glycochemistry. It is an important biochemical process that gives rise to essential molecules in the cell, including glycans and glycoconjugates such as glycoproteins and glycolipids.[2] Particularly, the rapid development of glycobiology and growing recognition of carbohydrates' significance in recent decades demand access to diverse oligosaccharides and glycoconjugates in a facile and practical manner. As compared to other biologically important macromolecules, such as polypeptides and long-chain fatty acid, polysaccharides are structurally more complex, with not only linear but also branched backbones, significantly more complicated regio chemistry rising from the presence of multiple hydroxy groups on each monomers, as well as unique α- or β-anomeric stereochemistry at each glycosidic linkages connecting the monomer residues. However, many polysaccharides and glycoconjugates of interests are present in the very low concentration in living organisms. The structural complexity coupled with physiochemical similarities make it challenging to purify them in large quantities for biochemical studies, severely hampering progress in glycobiology and glycomedicine. Hence, it is of great research significance to successfully mimic the natural biosynthetic processes of glycosylation artificially, in order to gain facile access to abundant amounts of glycans and glycoconjugates for in-depth studies.

The complications associated with glycosylation, i.e. α- and β-anomeric stereoselectivities, mainly stem from the chiral centers of the sugar ring. This is especially the case for glycosyl donor, as it is the functional groups on glycosyl donors that they closely surround the anomeric carbon and directly interfere with the construction of glycosidic bond. Hence, most efforts have been devoted to tuning the

steric and electronic properties of the functionalities on the glycosyl donor, to achieve stereoselective glycosylation.

2.1.1 Classic glycosylation with saturated glycosyl donors

Classic glycosylation often involves using saturated pyranoses as glycosyl donors, as they can be directly isolated from natural sources in large quantities. Comprising up to five chiral carbon centers, their corresponding hydroxyl groups are available for installation of directing moieties, which can either influence the stereochemistry of glycosidic bonds formed in glycosylation reactions directly or indirectly during the formation of glycosidic bonds.[3] Many efforts have been made in this regard, and selected classic examples are illustrated as follows.

Direct approaches to glycosylation typically involve the formation of weak interactions or intramolecular formation of a covalent bond on the glycosyl donor that block access of the acceptor from certain directions and breaks upon the nucleophilic attack. Demchenko *et al.* demonstrated a strategy for achieving stereoselectivity by making use of a hydrogen bond interaction between a remote pyridine functionality on the glycosyl donor and the hydroxy group of the glycosyl acceptor. The hydrogen bond interaction directs the approach of the nucleophile towards the anomeric carbon exclusively from one side of the sugar ring, resulting in spatially-restricted nucleophilic attack that gives glycoside product stereoselectively (Scheme 2.1.1a).[4]

In a conceptually distinct approach, the selectivity of glycosylation is directly controlled by the conformation of the glycosyl donor. In Crich's example of locking pyranose donors with benzylidene group and fixing C5-O5 and C6-O6 bonds in an antiperiplanar manner, there is a potent electron-withdrawing effect on the oxocarbenium species, leading to increased bond covalency between the anomeric

carbon and the triflate anion. As a result, the favored formation of contact ion pair and shielding effect of the α-leaving group impeded the approach of nucleophile from the same face, resulting in a selective formation of β-mannosides (Scheme 2.1.1b).[5] By substituting O4,O6-benzylidene with benzyl groups, the loss of ring-locked conformation led to reduced selectivity.[6] A similar strategy was employed by Yamada, who used *O*-xylylene to lock a sugar ring into an axial-rich configuration.[7] In this case, steric factors were used instead as 1,2-*cis* repulsion with 2-*O*-benzyl can drive the formation of β-anomers through isomerization after glycosylation.

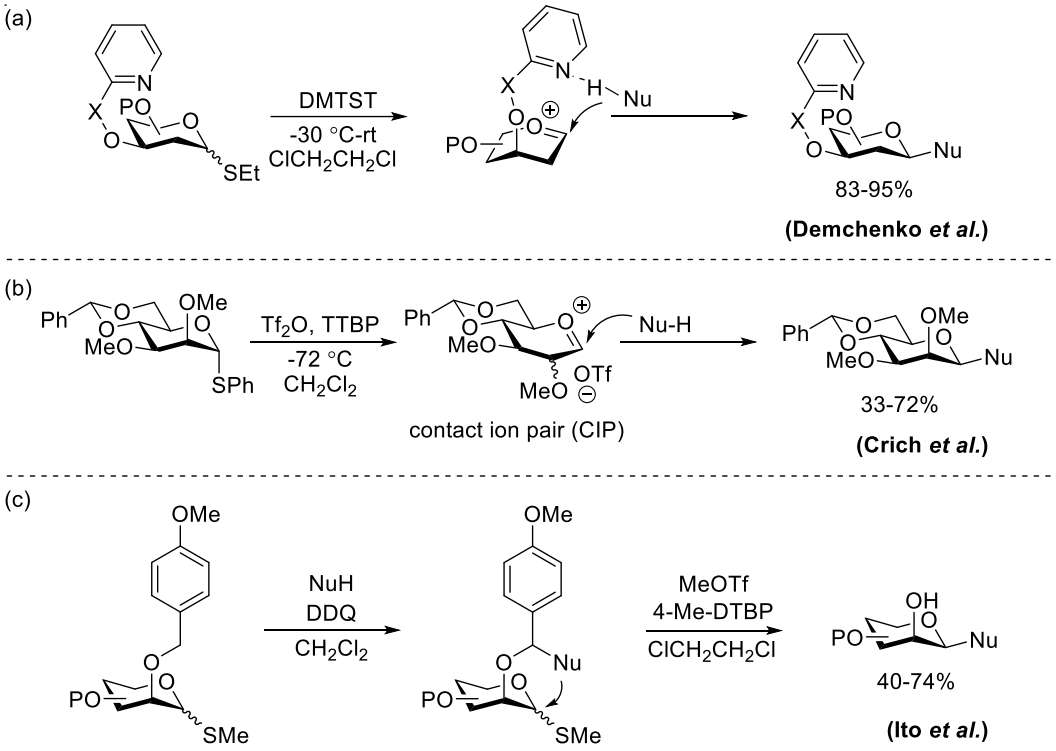

Scheme 2.1.1 Approaches to stereoselective glycosylation using saturated glycosyl donors

Conversely, indirect strategies have been introduced to direct the approaching of nucleophiles more efficiently. The additional steps introduced, results in the formation of an intermediate linked by the covalent bond as opposed to weak interactions. A well-

established example is the utilization of a nearby functionality to deliver a nucleophile instead of docking at the anomeric position by intermolecular nucleophilic attack between the donor and a free acceptor molecule. This intramolecular aglycon delivery approach (IAD) proceeds in a stepwise manner, in which the aglycon is first installed onto other positions of a sugar ring and then transferred to the anomeric carbon subsequently.[8] A well-known example was Ito's use of PMB ethers (Scheme 2.1.1c).[9]

Aligned with our group's long-standing interest in achieving effective glycosylation, we have focused our efforts on developing another type of glycosyl donors, the unsaturated glycosyl donor or glycal. With the presence of a C=C double bond, glycal donors require less protecting groups and it possesses the potential to utilize coordination chemistry, such as transition metal catalysis.

In addition, the unsaturated glycal-generated glycoside can be facilely transformed into diverse carbohydrates.[10] However, the impossibility of exploiting C2 stereo-directing effects in glycal donors raise new challenges in achieving stereoselectivity. Thus, we are forced to rely on other effects. Development of new strategies to address the stereoselectivity challenges is thus a major focus of our work and will be discussed in detail in the following work.

2.1.2 Glycosylation with pyranone glycal donors

Developments in the field of transition metal catalyzed reactions in the past decades have geared up carbohydrate chemists with many novel -and powerful- chemical tools for stereoselective construction of glycosidic bonds and enabled us to expand the substrate scope of glycosylation reactions to not only saturated glycosyl donors but also glycals. Here we will discuss some fascinating applications of transition metal catalyzed reactions in carbohydrate chemistry in detail.

Palladium catalysts were the most studied family of transition-metal catalysts for glycosylation with a variety of glycal donors. Nonetheless, the coordination efficiency of the double bond on glycal pyranose ring to the metal center is impeded by the electronic effect of the oxygen on the ring, which donates electrons to the LUMO of the π system through resonance and cripples the π-backbonding between the metal center and the double bond. In order to increase the reactivity of glycal donors, Feringa oxidized the C3 hydroxyl to form a pyranone starting material which can be applied to a non-Ferrier-type glycosylation (Scheme 2.1.2).[11] Feringa installed formate or benzoate group on the C1 position of pyranones first. The electron-withdrawing inductive effect of C3 ketone moiety could increase the reactivity of glycals to yield the glycosides. The reaction could be catalyzed successfully by palladium acetate with triphenyl phosphite or tris(dibenzylideneacetone)dipalladium(0) with triphenylphosphine. Various anomers gave the corresponding glycosides, in which the chirality was retained.

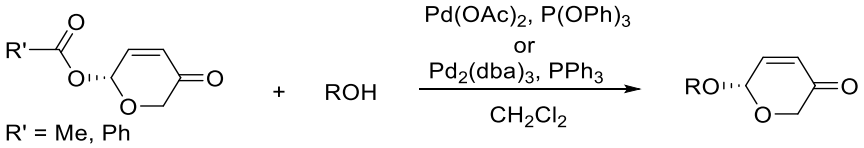

Scheme 2.1.2 Pd-catalyzed *O*-glycosylation with pyranone glycal donors

Almost at the same time, O'Doherty also reported using pyranones to increase the reactivity of glycal donors towards glycosides.[12] As shown in Scheme 2.1.3, the installation of bulky OBoc group on C1 position of pyranone glycal donors could also direct stereoselectivity.[10] Significantly, the ketone glycals showed higher reactivity as a result of the electron-withdrawing effect and stereochemical outcomes resulted from the attack of acceptor from opposite face to the bulky palladium species, which is

opposite to the bulky leaving group (Scheme 2.1.3a), giving rise to double-inversion products. An extension of this strategy to the oligosaccharide synthesis was demonstrated in their 12 steps of repeating glycosylations and reductions to form highly branched all-L-*α*-manno-heptapyranoside (Scheme 2.1.3b).

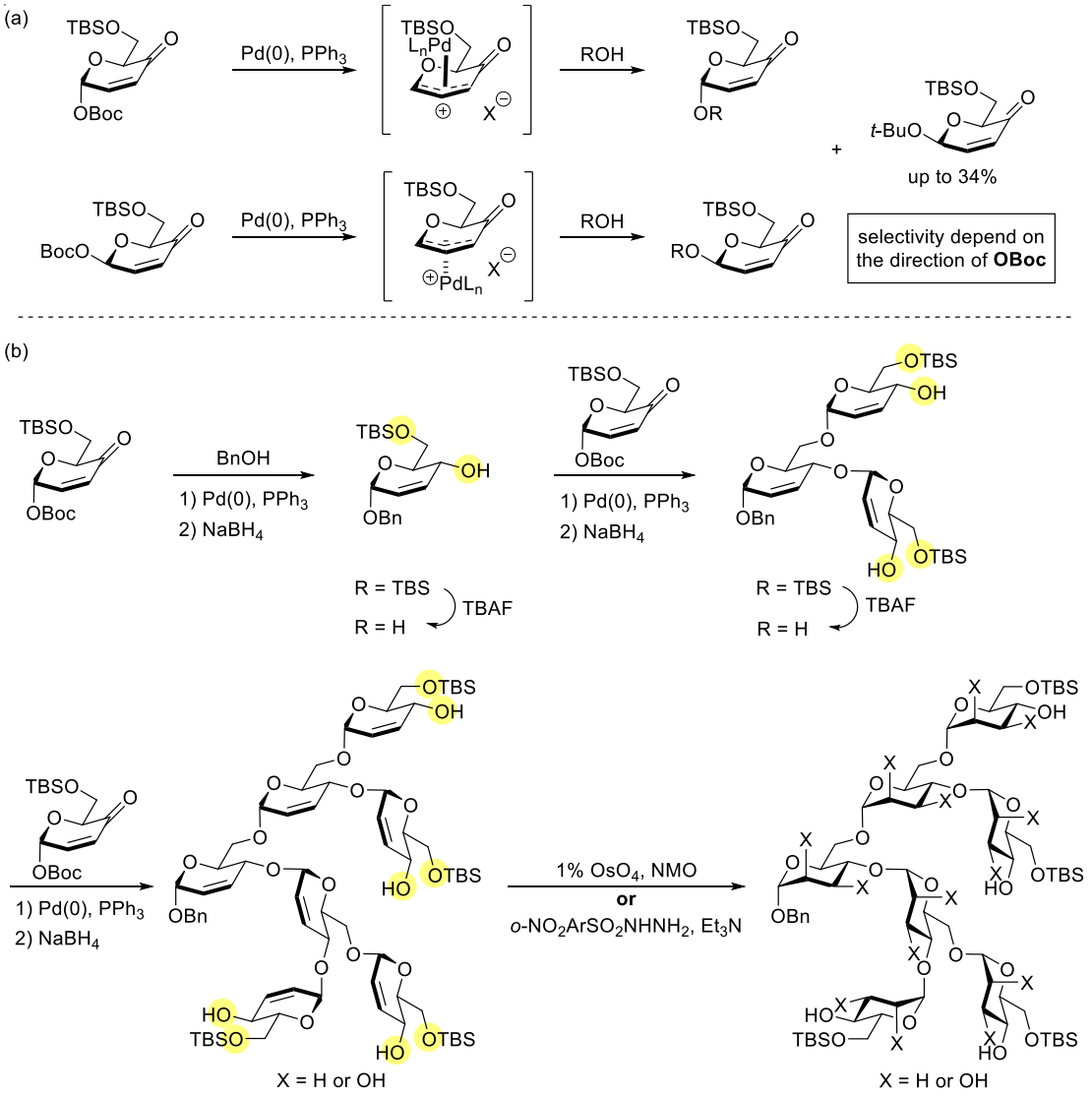

Scheme 2.1.3 Glycosylation with glycal allylic pyranone and its application in syntheses of oligosaccharides

2.1.3 Glycosylation from glycals with Et_2Zn as an additive

Lee's group developed a palladium catalyzed glycosylation using diethyl zinc to

increase the reactivity of glycal donors towards alcohol acceptors.[13] Glycosylation reactions under this conditions could give very good *β*-stereoselectivity in excellent yields. The special ligand di(tert-butyl)-2-biphenylphosphine (DTBBP) significantly contributes to the stereo- preference and addition of the ligand to the reaction system increased the selectivity ratio (*α*/*β*) from 1:5 to more than 1:25. Besides DTBBP ligand, the adduct diethyl zinc played an indispensable role in this reaction. Both acetyl and Boc protected glycals failed to form the glycosidic bond in the absence of diethyl zinc, which possibly takes part in both activating the acceptors and ionizing the leaving group.

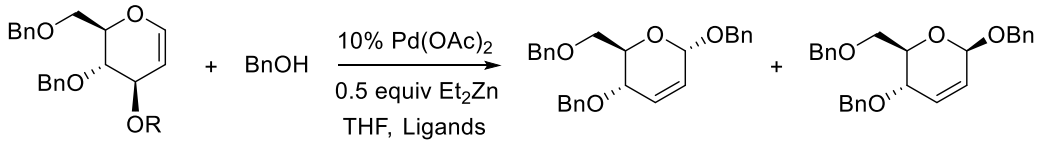

R = Ac, DTBBP, 92%, *α*/*β* < 1:25
P(OMe)$_3$, 90%, *α*/*β* = 7:1

R = Boc, DTBBP, 92%, *α*/*β* < 1:25
P(OMe)$_3$, 90%, *α*/*β* = 5:1

Scheme 2.1.4 Palladium catalyzed glycosylation with DTBBP and Et_2Zn

2.1.4 Glycosylation from glycal donors with directional group

As an extension of Lee's work, Nguyen changed the leaving group from acetyl/Boc to trichloroacetimidate moiety in glycals.[14] In contrast to Lee's results, they obtained *α*-product in quite a high selectivity and good yields from phenol type acceptors. When aliphatic alcohols were used as the acceptors, the yields were still satisfactory. Although the side reaction yield was very low, this reaction system always gave *N*-glycoside as a side-product, which might be from intramolecular rearrangement of trichloroacetimidate moiety and anomeric position. DTBBP also played an important role in the selective control. However, the reversed selectivity was proposed to arise

from the coordination relationship between palladium and the trichloroacetimidate group of glycal donors.

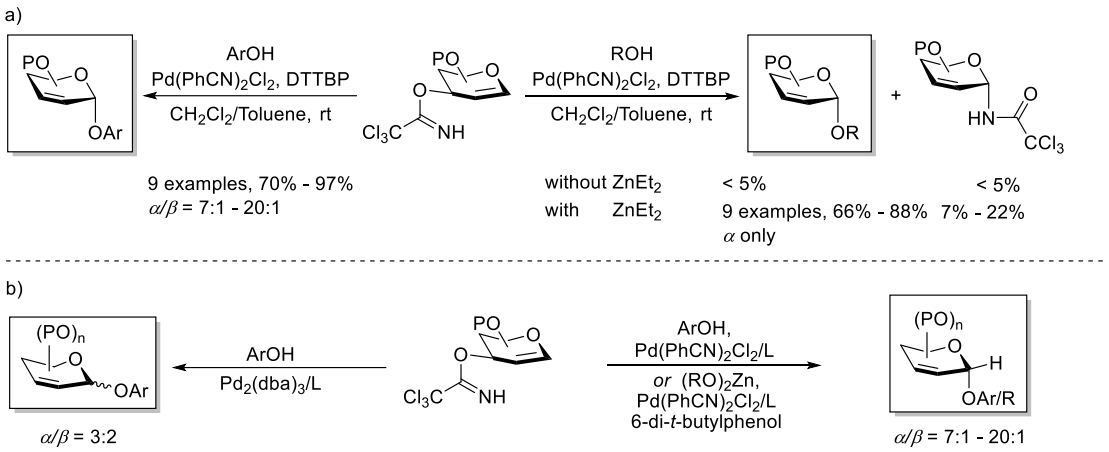

Scheme 2.1.5 Palladium catalyzed glycosylation in trichloroacetimidate glycals

In Nguyen's proposed mechanism (Scheme 2.1.6), trichloroacetimidate is a directing group which can promote palladium complex to approach the allyl system through coordination with imidate from the β face. Acceptors can only attack intermediate **III** from the α-face due to steric hindrance from the upper face. Then trichloroacetamide will be released and the palladium catalyst complex **I** is regenerated simultaneously followed by generation of α-*O*-glycosides.[14]

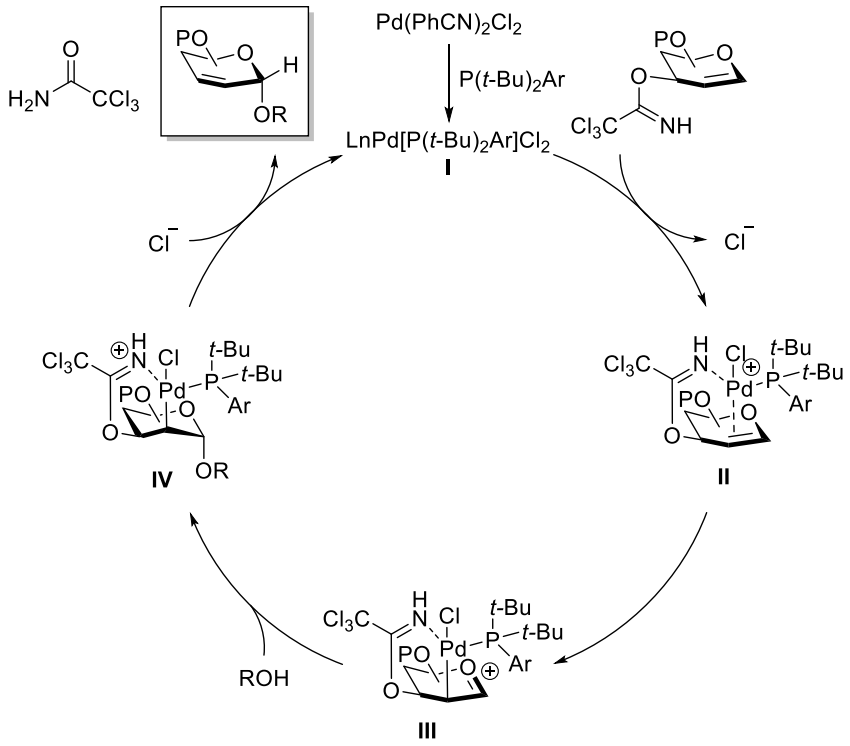

Scheme 2.1.6 Proposed mechanism of palladium-catalyzed glycosylation with C3-trichloroacetimidate glycal

2.1.5 Disaccharide syntheses from unsaturated glycosides

As described before, the double bond of products 2,3-unsaturated glycosides can be functionalized to other groups facilely. When the acceptors of glycosylation were carbohydrates, the glycosides could be converted into disaccharides in both Lee's and Nguyen's products. As shown in Scheme 2.1.7a, while the double bond of 2,3-unsaturated glycosides can be oxidized to *cis*-diol by OsO_4 and NMO, oxone and $BF_3 \cdot Et_2O$ will give *trans*-diol in Scheme 2.1.7b. The olefin moiety can also be oxidized by $Hg(OTf)_2$ and then a following hydroboration to generate 2-deoxyl glycoside in Scheme 2.1.7c, which hold a great potential in bioactive agent synthesis.

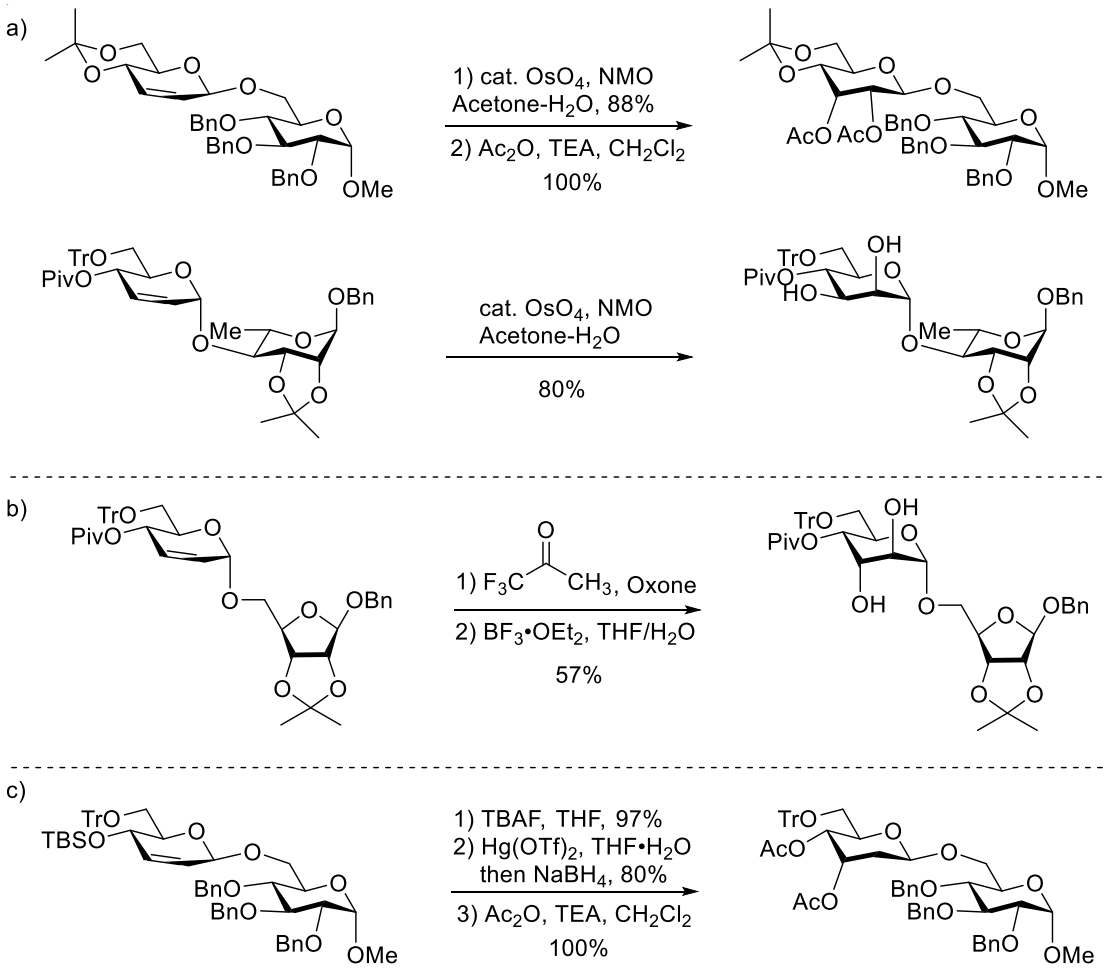

Scheme 2.1.7 Glycosylation products were functionalized to disaccharides

Building on our work on developing unsaturated glycosyl donors, we went on to explore the effect of hardness-softness of acceptors in palladium-catalyzed decarboxylative allylation.[15] Based on our earlier work that the nature of nucleophiles dictates whether the bond breaking and forming processes occur inside or outside the coordination sphere of transition metals, we went on to generalize this trend and looking for a quantitative standard for predicting the stereochemical outcome of the glycosylation reactions based on gauging the hardness of the nucleophile by pK_a values. In order to examine its relevance in predicting anomeric selectivity, the pK_as of various glycosyl acceptors were compared with their α-/β- stereoselectivities. The switchable

anomeric selectivity in the case of trifluoroethanol proved that pK_a 12.5 was an indicative value in distinguishing between hard and soft *O*-nucleophiles for effective acceptor-controlled *O*-glycosylation (Scheme 2.1.8). Hard *O*-nucleophiles (pK_a > 12.5) coordinated with the palladium ion to undergo inner-sphere attack while soft *O*-nucleophiles (pK_a ≤ 12.5) favored the outer-sphere attack on the soft allylic system. Seeberger and Pereira also studied the effect of nucleophilicity on *α*-/*β*-stereoselectivity.[16] Usage of difluorinated weak nucleophile led to *α*-stereoselectivity, while the non-fluorinated strong nucleophile yielded *β*-glycoside (Scheme 2.1.9). Notably, this strategy can be potentially utilized in automated glycan assembly without having adverse effects on binding and immobilization. However, the selectivities of the reaction rely solely different acceptors and the reaction required a high temperature and long hours.

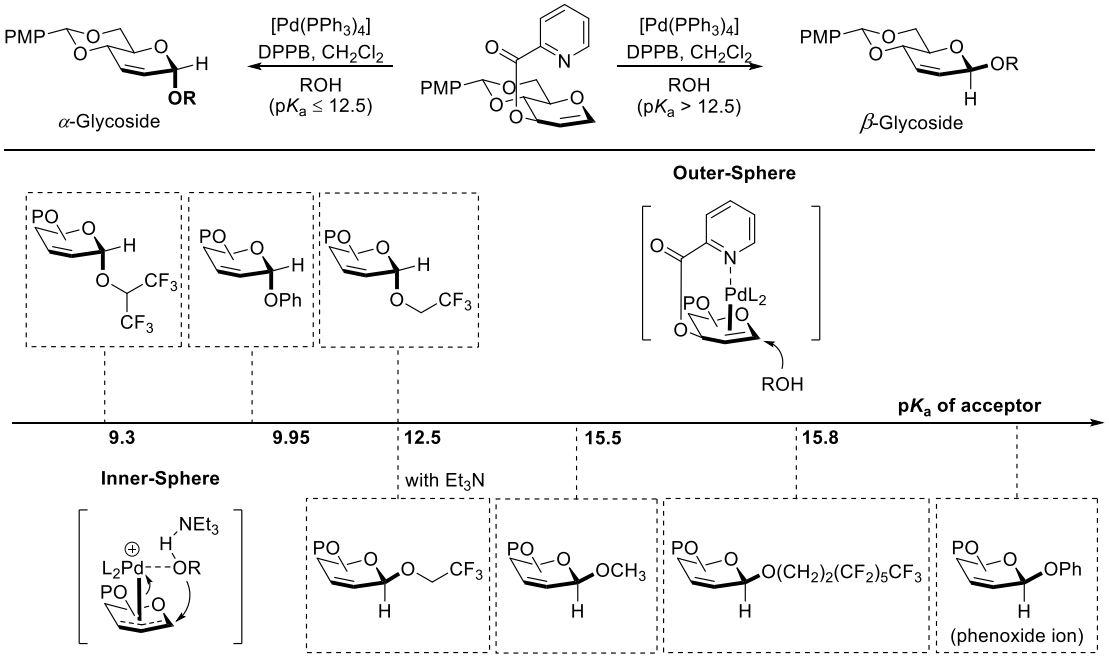

Scheme 2.1.8 Effect of pK_a values on stereoselectivity for acceptor-controlled approach

2.2 Results and Discussion

Exploring highly efficient glycosyl donors for stereo-selective glycosylation has been one of the main focuses in glycoscience which plays a critical role in both chemistry and biology.[4, 17] The rapid development of transition metal chemistry provided more possibilities for catalyst-controlled glycosylation because of its unique coordination effect and the versatility in reactions, this was especially true in the case of palladium.[18] Recently, Zhang's group reported a method of palladium-catalyzed enantioselective decarboxylative cycloaddition under mild condition with vinylethylene carbonates as the starting material.[19] Herein we introduced a cyclic carbonate at the C3,C4 positions of galactal with an aim to form a bicyclic system with greater ring strain to increase the reactivity. Moreover, the alkoxide ion of the intermediate formed could accelerate the substitution reaction of aliphatic alcohols through H-bonding.[20] Meanwhile, a bulky C6-*O*-TBDPS group was chosen to enhance the selectivity by steric hindrance. In addition, density functional theory (DFT) calculations were also carried out to confirm our idea.[21] As shown in Scheme 1a, 3,4-*O*-carbonate D-galactal donor has the weakest and longest C-O bond (1.499 Å) at the C3 position as compared to the rest (1.454-1.461 Å). To the best of our knowledge, reports about catalyst-controlled *O*-glycosylation were extremely rare and Nguyen's group has reported a nearly successful case (Scheme 2.1.5) where α-selectivity from β-Pd(II) complex was directed by trichloroacetimidate and not from Pd(0) as Pd(0) could only generate α/β = 3:2 in a low yield (Scheme 2.1.6).[14] In our strategy, Pd(II) was designed to coordinate at the β-face directed by the carbonate group, while Pd(0) could go to the opposite direction by coordinating at the α-face owing to steric hindrance.

From here, we successfully presented a controllable stereoselective *O*-glycosylation method using Pd(0) and Pd(II) complexes as catalysts (Scheme 2.2.1b).

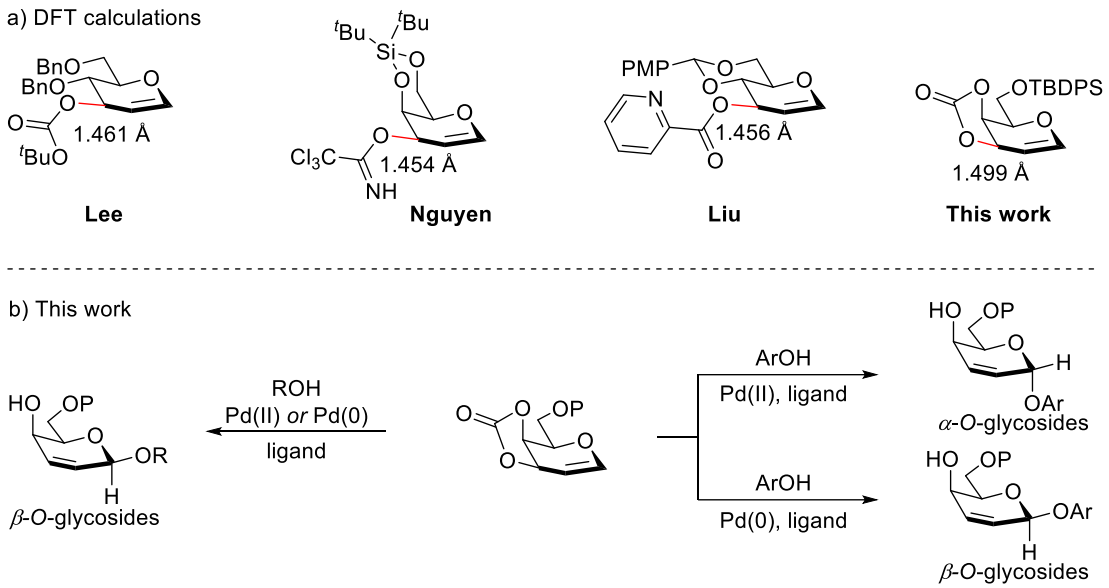

Scheme 2.2.1 Different glycal donors and palladium-catalyzed glycosylation

Firstly, 3,4-*O*-carbonate D-galactal (**1**) was used as the glycosyl donor and the reaction was screened using methanol as the glycosyl acceptor (Table 2.2.1). Both Pd(II) and Pd(0) catalysts were found to afford exclusive *β*-selecvity in different solvents for 12 h (entries 1-7). $Pd(OAc)_2$ in THF was found to provide the best combination (entry 4) while no reaction took place in the absence of ligands (entry 8). During the ligand screening (entries 9-12), Xantphos was found to be the optimal ligand that could reduce the reaction time to 1 h (entry 12), which might be because it is a bidentate ligand with an appropriate bite angle.[22] Therefore, the optimized condition was revealed to be entry 12 and the configuration of *β*-*O*-glycoside **2** was also confirmed by X-ray crystallography.[23]

With the optimal condition in hand, we expanded the substrate scope of glycosyl acceptors to other alcohols (Scheme 2.2.2) such as ethanol, *n*-butanol, benzyl and allyl

Table 2.2.1 Reaction optimization for aliphatic alcohol[a]

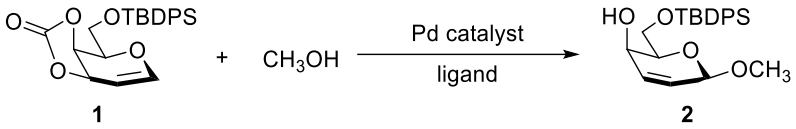

1 **2**

entry	Catalyst	ligand	solvent	Time	yield[b,c]
1[d]	$Pd_2(dba)_3$	PPh_3	THF	12 h	30%
2	$Pd(PPh_3)_4$	PPh_3	THF	12 h	88%
3	$Pd(acac)_2$	PPh_3	THF	12 h	10%
4	$Pd(OAc)_2$	PPh_3	THF	12 h	94%
5	$Pd(OAc)_2$	PPh_3	DMSO	12 h	78%
6	$Pd(OAc)_2$	PPh_3	CH_2Cl_2	12 h	80%
7	$Pd(OAc)_2$	PPh_3	CH_3CN	12 h	85%
8	$Pd(OAc)_2$	-	THF	12 h	N.R.
9[e]	$Pd(OAc)_2$	DPPF	THF	12 h	52%
10[e]	$Pd(OAc)_2$	DPPB	THF	12 h	89%
11	$Pd(OAc)_2$	$P(Cy)_3$	THF	12 h	N.R.
12[e]	$Pd(OAc)_2$	Xantphos	THF	1 h	95%

[a]Unless otherwise specified, all reactions were carried out with 0.1 mmol of **1**, 0.2 mmol of CH_3OH, 10 mol% Pd catalyst, 30 mol% P ligand in 2 mL solvent at room temperature. [b]Isolated yield. [c]Single isomer (β:α > 30:1 by ^{1}H NMR). [d]5 mol% Pd catalyst used and unreacted **1** was recovered. [e]15 mol% P ligand used. N.R. = No reaction. DPPB = DPPButane; DPPF = 1,1'-Bis(diphenylphosphino)ferrocene; Xantphos = 4,5-Bis(diphnyl-phosphino)-9,9-dimethylxanthene.

alcohol to afford the relative product **3**-**6** in high yields and *β*-stereoselectivity. Consequently, heterocyclic alcohols which were important in drug discovery[24] were also introduced as glycosyl acceptors. They were 2-pyridine-methanol, thenyl alcohol, 6-methoxyl-2-pyridine and 6-(3-thienyl)-2-pyridinemethanol which also proceeded to give glycosides **7**-**10** in good yields and *β*-stereoselectivity respectively. The versatility of the methodology was further explored by applying it to the syntheses of disaccharides. Firstly, 3,4-dibenzyl-D-glucal was examined and the corresponding disaccharide **11** was generated in 80% yield with exclusive *β*-selectivity. Subsequently, other screened acceptors with 6-OH monosaccharide also gave disaccharides **12**-**15** in high yields and excellent anomeric selectivity. Since 4-OH glycosyl acceptors are hindered and bulkier than other carbohydrate acceptors,[25] **16** was afforded in a relatively lower yield of 42% as compared to the other substrates. When a less crowded 4-OH acceptor 1,6:2,3-dianhydro-*β*-D-mannopyranose was applied in this condition, the yield of *β*-1,4-*O*-glycoside (**17**) was increased to 71%. Consequently, *β*-1,3-*O*-glycosides (**18**, **19**) could be obtained in 70% yields, while with different types of 2-OH glucose derivatives, *β*-1,2-*O*-glycosides (**20**, **21**) were also formed in very good yields and with exclusive selectivity.

The results showed that aliphatic acceptors including monosaccharide derivatives were able to obtain glycosides in high yields with exclusive *β* stereoselectively. We reasoned that our starting material containing 3,4-*O*-carbonate directed the Pd(II) complex to the *β*-face and through an inner-sphere pathway with hard aliphatic acceptors. Conversely, the soft phenolic nucleophiles would attack Pd-π-allyl intermediate through an outer-sphere pathway to give *α*-products. Therefore, 2-naphthol was used as a phenolic acceptor to optimize the condition (Table 2.2.2). The

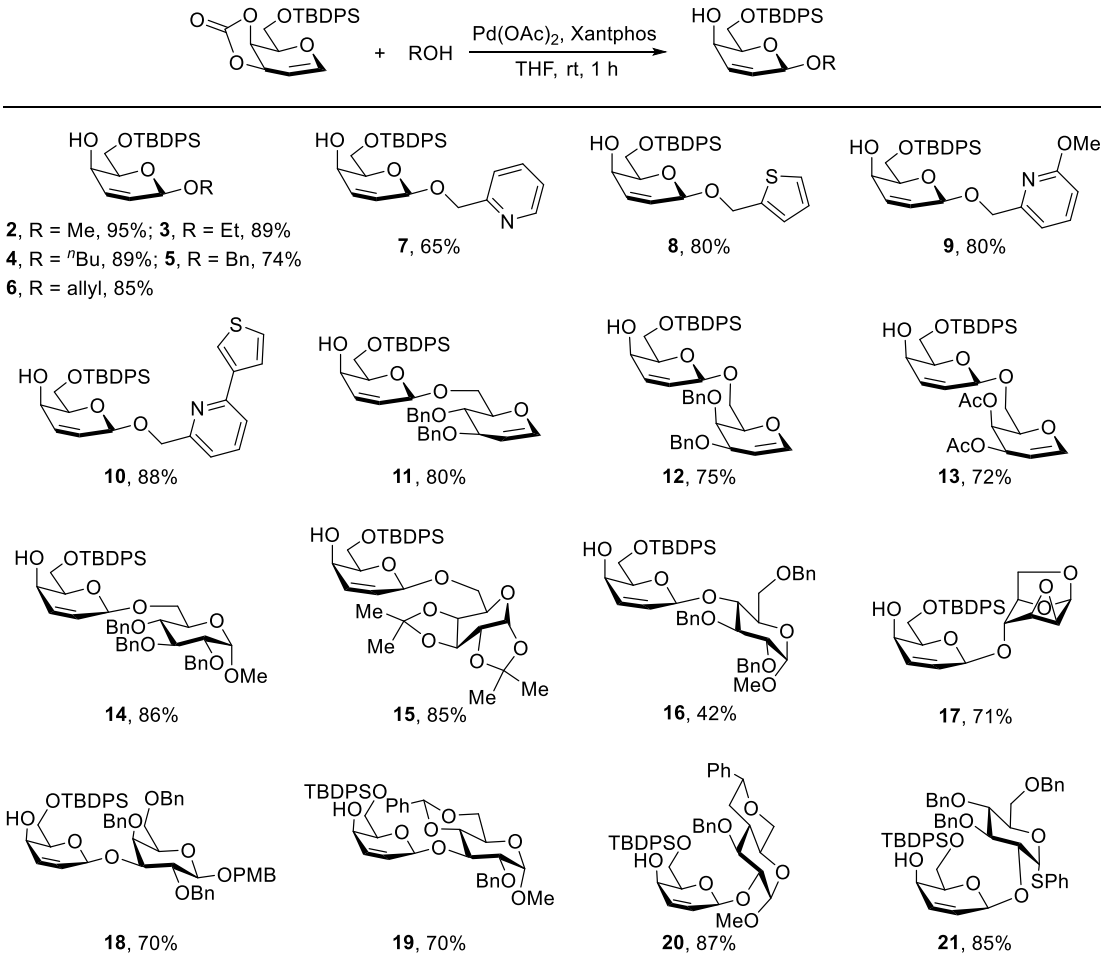

Scheme 2.2.2 Alcohol substrate scope *via* Pd(II) catalyst

previous optimal condition (10% $Pd(OAc)_2$ as a catalyst, 15% Xantphos as a ligand in THF at room temperature for 1 h) was able to generate the expected α-product **22a** in 71% yield (entry 1). This condition was further optimized with different ligands, solvents and Pd(II) catalyst (entries 1-7), but $Pd(OAc)_2$, Xantphos and THF remained the most suitable combination for α-glycosylation. As designed, the stereoselectivity was reversed to β selectivity (**22b**) when $Pd(PPh_3)_4$ was used (entry 8). The same selectivity was also found in the other Pd(0) catalysts: $Pd(dba)_2$ and $Pd_2(dba)_3$ (entries 9, 10). The optimal condition for β-glycosylation was 5% $Pd_2(dba)_3$ as a catalyst, 15% Xantphos as a ligand in THF at room temperature for 12 h using phenols.

Table 2.2.2 Reaction optimization for phenol[a]

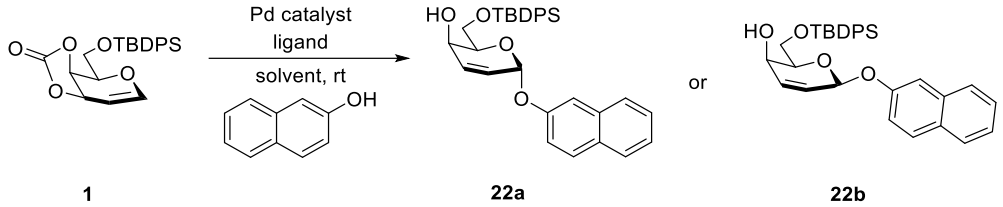

1 **22a** **22b**

entry	catalyst	Ligand	solvent	time	yield[b,c]
1	$Pd(OAc)_2$	Xantphos	THF	1 h	71% **22a**
2[d]	$Pd(OAc)_2$	PPh_3	THF	12 h	47% **22a**
3[d]	$Pd(OAc)_2$	$P(Cy)_3$	THF	12 h	N.R.
4	$Pd(OAc)_2$	DPPF	THF	12 h	14% **22a**
5	$Pd(OAc)_2$	Xantphos	DMSO	12 h	24% **22a**
6	$Pd(OAc)_2$	Xantphos	DMF	12 h	21% **22a**
7	$Pd(acac)_2$	Xantphos	THF	12 h	42% **22a**
8	$Pd(PPh_3)_4$	Xantphos	THF	12 h	66% **22b**
9	$Pd(dba)_2$	Xantphos	THF	12 h	61% **22b**
10[e]	$Pd_2(dba)_3$	Xantphos	THF	12 h	88% **22b**

[a]Unless otherwise specified, all reactions were carried out with 0.1 mmol of **1**, 0.2 mmol of 2-naphthol, 10 mol% Pd catalyst, 15 mol% P ligand in 2 mL solvent at room temperature. [b]Isolated yield. [c]Single isomer (> 30:1 by ^{1}H NMR). [d]30 mol% ligand used. [e]5 mol% Pd catalyst used. N.R. = No reaction.

To our delight, we could produce the desired *α-O*-glycosides or *β-O*-glycosides respectively by using Pd(II) or Pd(0) catalyst. To validate this hypothesis, firstly, the optimal Pd(II) condition was applied to the other phenolic substrates (Scheme 2.2.3). Notably, a variety of phenols were also able to tolerate this Pd(II) condition. For instance, phenol gave a very high yield (**23a**, 85%) with exclusive *α*-selectivity. 4-Phenylphenol (**24a**) and electron donating group substituted phenols (**26a**, **27a**) were able to produce good yields of 1,4-trans-products except for 2,6-dimethyl-phenol (**28a**) which showed a much lower yield due to steric hindrance. Interestingly, with a less nucleophilic, electron withdrawing group being substituted, 4-fluoro-phenol could also generate a good yield of *α-O*-glycoside **25a**. Comparing the reactivity between alcohols

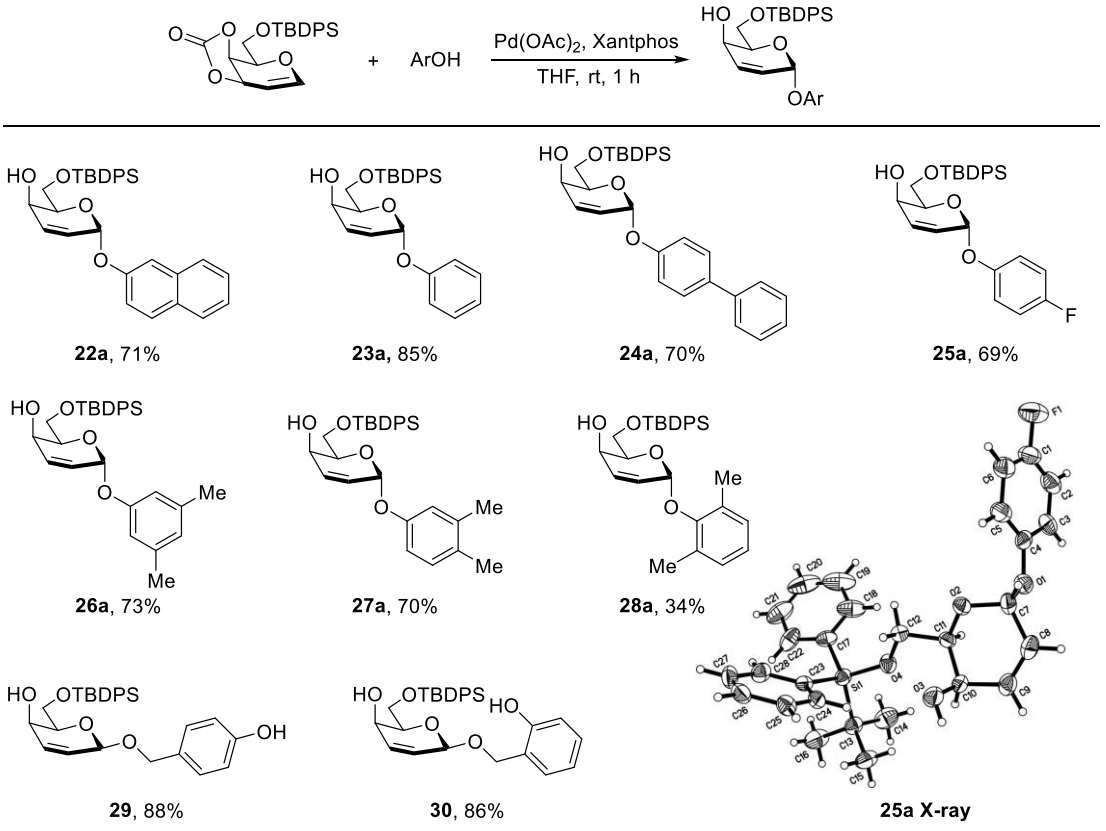

Scheme 2.2.3 Phenol substrate scope *via* Pd(II) catalyst

and phenols, 4-hydroxybenzyl alcohol (**29**) and 2-hydroxy-benzyl alcohol (**30**) were employed to react with our glycal donor. Based on the finding, alcoholic hydroxyl group was shown with significantly higher in reactivity.

Subsequently, Pd(0) condition was also examined by the same types of phenols and some aliphatic acceptors (Scheme 2.2.4). As expected, the selectivity was reversed when compare to the corresponding phenols such as phenol (**23b**), 4-phenylphenol (**24b**) and 4-fluorophenol (**25b**). As we screened before (Table 2.2.1), when the Pd(0) condition was applied to alcohols, only *β*-selectivity were observed. Both simple *β*-*O*-glycosides (**2**, **3**, **5**) and disaccharides (**15**, **21**) were successfully synthesized in high yields.

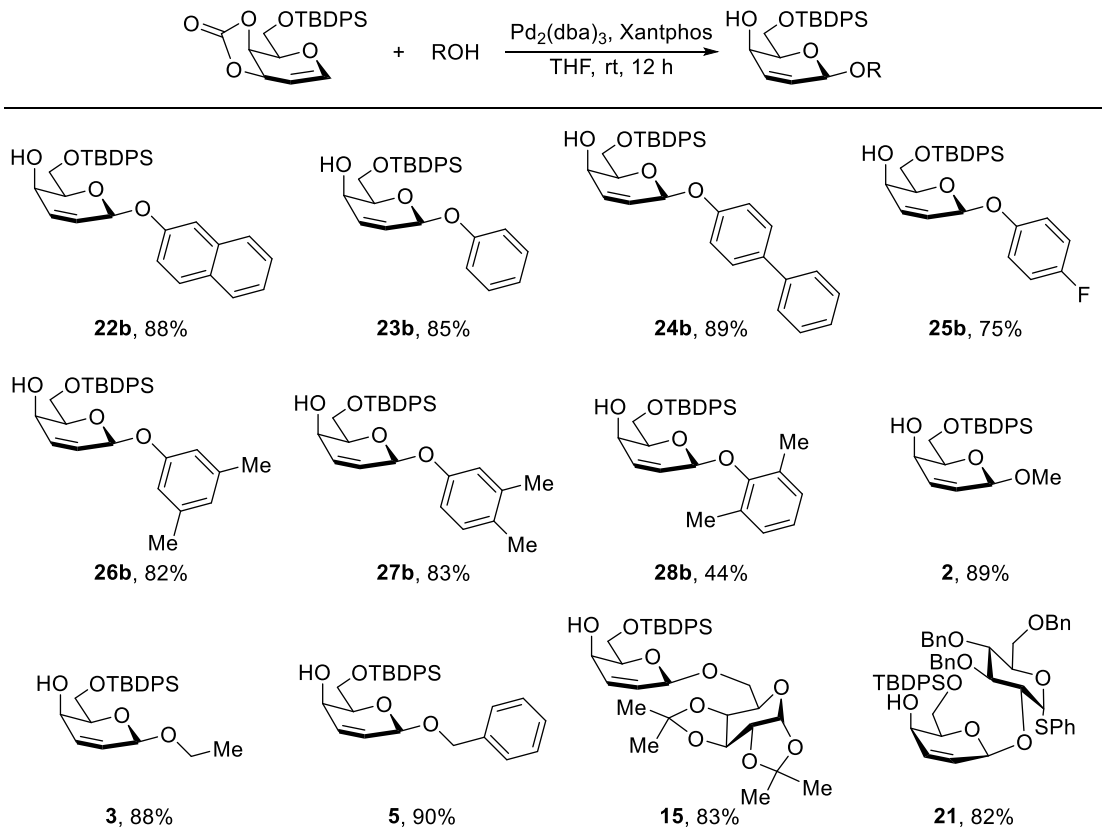

Scheme 2.2.4 Substrate scope *via* Pd(0) catalyst

According to the above results, a plausible mechanism was proposed in Scheme 2.2.5. Pd(0) and Pd(II) opened up two different pathways: firstly, Pd(0) complex was coordinated to the double bond of glycal **1** to form intermediate **A** from the α-face as Pd(0) species with P-ligands was too bulky to coordinate at the β-face. Next, decarboxylation occurred and intermediate **B** was yielded at β-face for both aliphatic or phenolic acceptors due to H-bond.[26] Subsequently, nucleophilic addition formed β-*O*-glycoside **C**. On the other hand, Pd(II) species favored coordination with glycal **1** directly rather than being reduced by P-ligands to give intermediate **D** as it was more oxyphilic and could be directed by the carbonate moiety.[14, 27] After decarboxylation and intermediate **E** was generated, the Pd complex would block H-bond formation and the pathway splits depended on the nature of acceptors. With hard nucleophile alcohols, intermediate **F** was generated by the inner-sphere pathway to give β-glycoside **C**, while for soft nucleophiles phenols, **G** was yielded to form α-glycoside **H** through the outer-sphere pathway.[15, 18a, 18b]

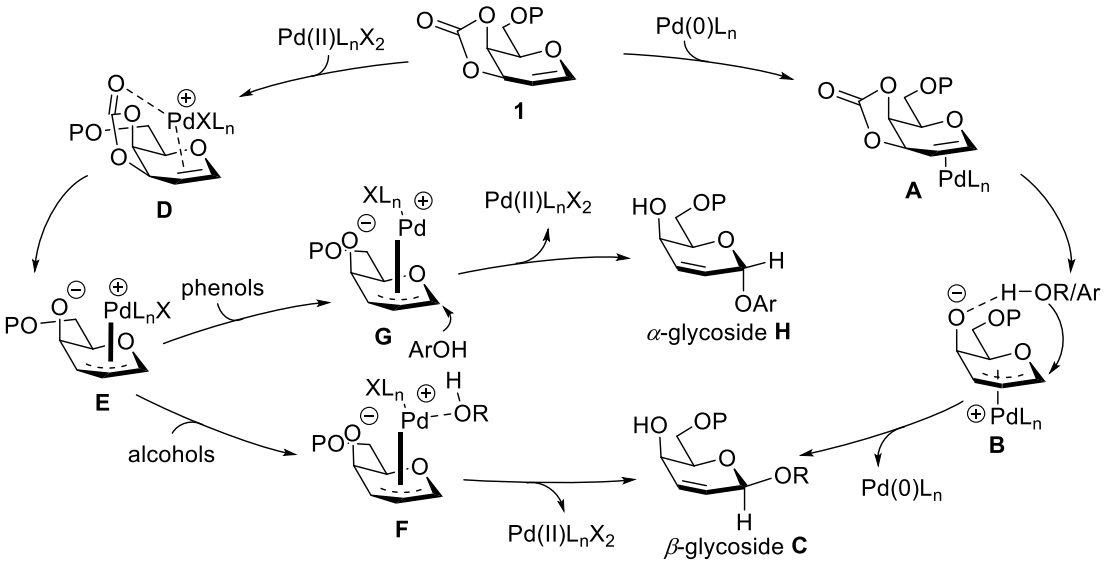

Scheme 2.2.5 Proposed mechanism

To confirm this mechanism, other glycal donors were employed as shown in Table 2.2.3. When the 6-*O*-protecting group was changed from TBDPS to a smaller TBS (entries 1-3), the stereoselectivity was consistent with glycal **1**. When L-fucal **34** was applied, *α*-*O*-glycoside **36a** and *β*-*O*-glycoside **36b** could be obtained stereoselectively in Pd(II) and Pd(0) conditions (entries 5-6) respectively. These results indicated that steric effect from C6 could not affect the selectivity but a less hindered C6-protecting group may decrease the yields due to possible side products (oligosaccharides) from further. glycosylation on 4-OH of the glycosides. In order to investigate coordination relationship between glycal and palladium species, 4,6-*trans*-glycals (D-allal **37** and digitoxal **40**) were also tested (entries 7-12). The aliphatic acceptor gave *α*-selectivity (**38**, **41**), while the phenolic acceptor generated *β*-selectivity (**41b**, **44b**) in the Pd(II) condition and *α*-selectivity (**41a**, **44a**) in the Pd(0) condition. All the results indicated that cyclic carbonate moiety played an important role in the mechanism as we proposed Pd(0) coordinated at its *trans*-face but Pd(II) coordinated at the *cis*-face.

Competitive reactions were carried out to compare the properties of Pd(II) and Pd(0) catalysis as shown in Scheme 2.2.6. Firstly, a reaction was carried out using a mixture of Pd(II):Pd(0) in 1:1 with 2-naphthol. Results showed that majority of the glycosides were able to provide *α*-product **22a** and hence, suggested that Pd(II) could catalyze the reaction at a much faster rate without being reduced. Next, we prestirred Pd(II) catalyst and phosphine ligands before adding glycal donor and naphthol. Then the reduced Pd(II) catalyst could only afford *β*:*α* (phenolic *O*-glycosides) in 5:1. Thus, this result illustrated that Pd(II) was not reduced in a one-pot reaction. On the other side, the aliphatic acceptor methanol demonstrated only *β*-selectivity under the two competitive conditions, which follows our proposed mechanism.

Table 2.2.3 Mechanism study with different glycal donors

entry	glycal	acceptor	condition	glycoside		yield[a,b]
1	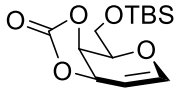 **31**	MeOH	Pd(II)	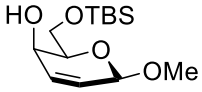	**32**	95%
2	**31**	PhOH	Pd(II)	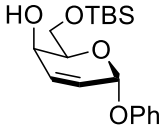	**33a**	61%
3	**31**	PhOH	Pd(0)	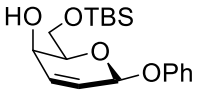	**33b**	72%
4	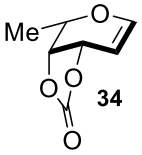 **34**	MeOH	Pd(II)	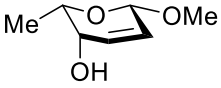	**35**	90%
5	**34**	PhOH	Pd(II)	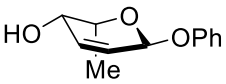	**36a**	60%
6	**34**	PhOH	Pd(0)	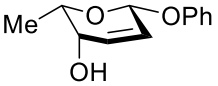	**36b**	58%
7	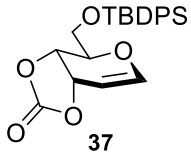 **37**	MeOH	Pd(II)	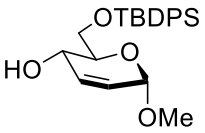	**38**	93%
8	**37**	PhOH	Pd(II)	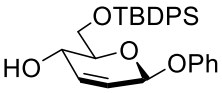	**39b**	71%
9	**37**	PhOH	Pd(0)	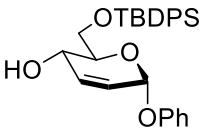	**39a**	76%
10	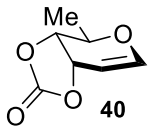 **40**	MeOH	Pd(II)	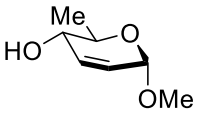	**41**	89%
11	**40**	PhOH	Pd(II)		**42b**	70%
12	**40**	PhOH	Pd(0)	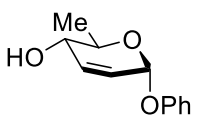	**42a**	75%

[a]Isolated yield. [b]Single isomer (> 30:1 by ^{1}H NMR).

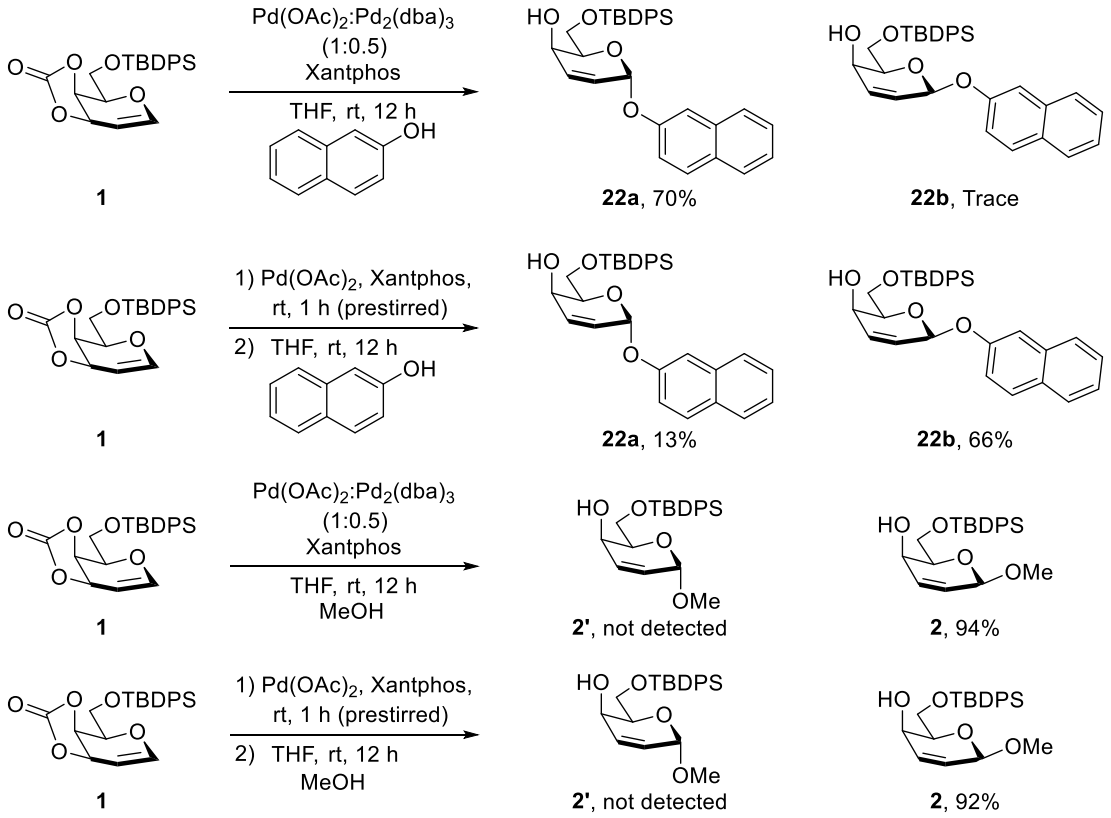

Scheme 2.2.6 Comparison of the reactivity of Pd(0) and Pd(II) catalysts

Four plausible intermediates of galactal-palladium-ligands as proposed in our mechanism were submitted for the DFT calculation.[28] As shown in Scheme 2.2.7, the results demonstrated that Pd(0) complex preferred to stay at α-face with a relative 4.15 kcal/mol lower than β-face. On the other hand, the energy of Pd(II) complex showed 1.77 kcal/mol higher at α-face. Thus, these results also supported our proposed mechanism.

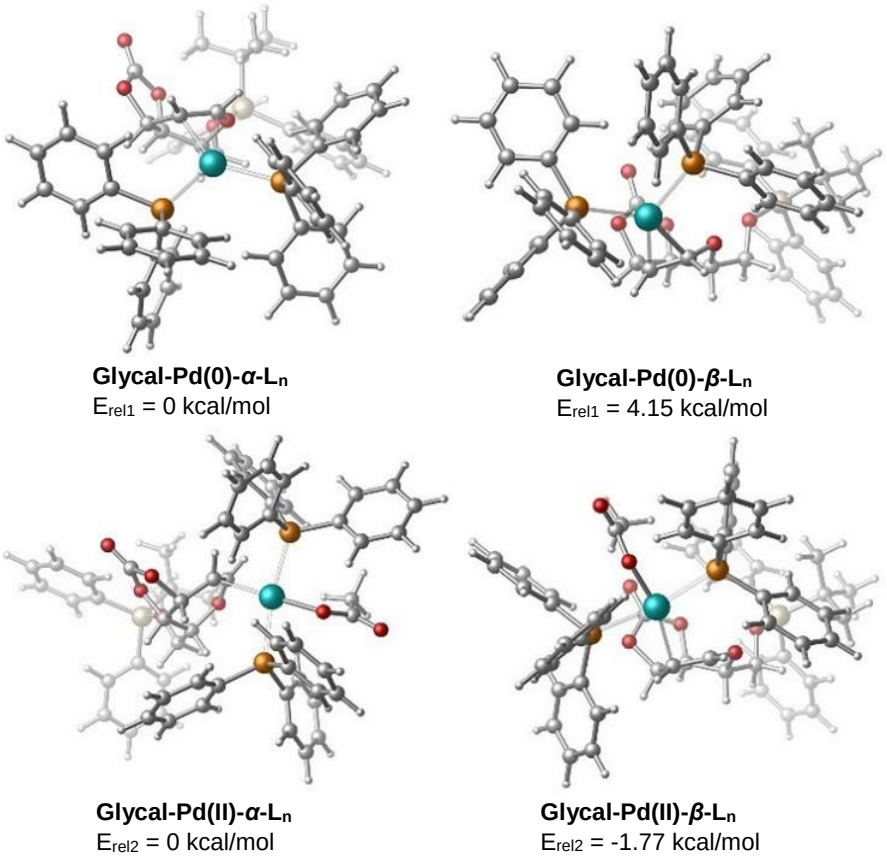

Scheme 2.2.7 Calculated structures and relative energies of plausible glycal-Pd-ligand intermediates

2.3 Conclusion

In conclusion, we have developed a novel strategy to construct *α*- and *β*-*O*-glycosidic bonds with exclusive selectivity under mild conditions through highly efficient 3,4-*O*-carbonate galactal donors. *β*-*O*-Glycosides could be obtained from aliphatic alcohols with both Pd(0) and Pd(II) while *α*- and *β*-*O*-glycosides could be obtained from phenols, using Pd(II) and Pd(0) respectively. Mechanistic studies with varying coordinating pathways for Pd(0) and Pd(II) was proposed and DFT calculations were also performed. A wide range of substrates such as alcohols, saccharides, phenols and glycals were employed and afforded the desired products stereoselectively in high yields. Lastly, these resultant 4-OH glycosides could potentially be acceptors for 4-branched oligosaccharides or natural product synthesis.

The stereoselective *O*-glycosylation controlled by different catalysts has been achieved in this work for the first time, but additional preparation and protection steps cannot be avoided. In order to further enhance the synthetic efficiency, the future efforts could be dedicated to the streamlining of synthetic protocols, through the fine-tuning of reactivity or mimicking enzymatic glycosylation reactions which could proceed without protection. For example, we can apply a reagent to protect the hydroxyl groups of glycosyl donor temporarily and the glycosylation product can be obtained directly after a simple workup without deprotection steps.[29]

2.4 Experimental Section

2.4.1 General experimental procedures and characterization data

General procedure for preparation of cyclic 3,4-*O*-glycal 1, 31, 34, 37, 40

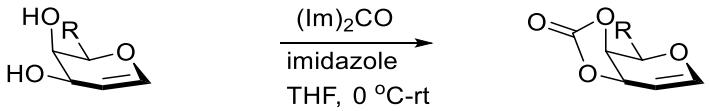

To a solution of D-galatcal or 6-deoxy-D-galactal (1 mmol) in 10 ml THF was added 1,1'-carbonyldiimidazole (1.5 mmol) and one piece of imidazole in the ice bath, and then the mixture was warmed up to room temperature and stirred for overnight. The resulting mixture was diluted with ethyl acetate, then extracted with ethyl acetate (3 × 20 mL). The combined organic phase was washed with water, brine, dried ($MgSO_4$), and concentrated. Purification of the residue by flash column chromatography on silica gel (hexane:EtOAc) gave cyclic 3,4-*O*-glycal.

1,5-Anhydro-6-*O*-(*tert*-butyldiphenylsilyl)-3,4-*O*-carbonate-2-deoxy-D-lyxo-hex-1-enopyranose (1)

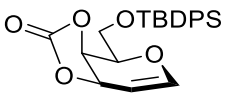

Colorless syrup; yield 76%; ^{1}H NMR (400 MHz, $CDCl_3$): δ 7.74 – 7.65 (m, 4H), 7.50 – 7.38 (m, 6H), 6.63 (d, *J* = 6.3 Hz, 1H), 5.20 (dd, *J* = 7.7, 3.2 Hz, 1H), 5.05 (dd, *J* = 7.7, 0.9 Hz, 1H), 4.94 (ddd, *J* = 6.3, 3.2, 1.3 Hz, 1H), 4.06 – 3.94 (m, 3H), 1.10 (s, 9H); ^{13}C NMR (101 MHz, $CDCl_3$) δ 154.2, 149.2, 135.6, 135.5, 132.8, 132.6, 130.1, 130.1,

128.0, 127.9, 98.1, 73.9, 73.0, 68.9, 61.9, 29.8, 26.9, 19.3; HRMS (ESI) *m/z*: calcd. for $C_{23}H_{26}O_5SiNa^+$ $(M + Na)^+$ 433.1447, found 433.1447; $[\alpha]_D^{24}$ = -29.8 (c = 1.0, $CHCl_3$).

1,5-Anhydro-6-*O*-(*tert*-butyldimethylsilyl)-3,4-*O*-carbonate-2-deoxy-D-lyxo-hex-1-enopyranose (31)

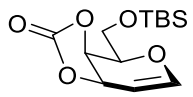

Colorless syrup; yield 80%; ^{1}H NMR (400 MHz, $CDCl_3$) δ 6.63 (d, *J* = 6.2 Hz, 1H), 5.16 (dd, *J* = 7.7, 3.2 Hz, 1H), 4.97 – 4.87 (m, 2H), 3.96 – 3.80 (m, 3H), 0.87 (s, 9H), 0.07 (d, *J* = 2.1 Hz, 6H); ^{13}C NMR (101 MHz, $CDCl_3$) δ 154.3, 149.3, 98.2, 74.1, 72.9, 69.0, 61.2, 25.9, 18.4, -5.3, -5.4; HRMS (ESI) *m/z*: calcd. for $C_{13}H_{22}O_5SiNa^+$ $(M + Na)^+$ 309.1134, found 309.1141; $[\alpha]_D^{24}$ = -37.6 (c = 1.0, $CHCl_3$).

2,6-Anhydro-3,4-*O*-carbonate-1,5-dideoxy-L-arabino-hex-5-enitol (34)

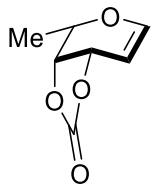

Colorless syrup; yield 58%; ^{1}H NMR (400 MHz, $CDCl_3$) δ 6.61 (d, *J* = 6.3 Hz, 1H), 5.13 (dd, *J* = 7.8, 3.3 Hz, 1H), 4.86 (dd, *J* = 6.4, 3.3 Hz, 1H), 4.68 (d, *J* = 7.8 Hz, 1H), 3.97 (q, *J* = 6.8 Hz, 1H), 1.40 (d, *J* = 6.8 Hz, 3H); ^{13}C NMR (101 MHz, $CDCl_3$) δ 154.3, 149.7, 97.5, 76.3, 70.0, 69.5, 16.6; HRMS (ESI) *m/z*: calcd. for $C_7H_9O_4^+$ $(M + H)^+$ 157.0501, found 157.0504; $[\alpha]_D^{24}$ = +44.7 (c = 1.0, $CHCl_3$).

1,5-Anhydro-6-*O*-(*tert*-butyldiphenylsilyl)-3,4-*O*-carbonate-2-deoxy-D-ribo-hex-1-enitol (37)

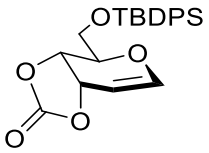

Colorless syrup; yield 73%; ^{1}H NMR (400 MHz, $CDCl_3$) δ 7.71 – 7.62 (m, 4H), 7.50 – 7.35 (m, 6H), 6.76 (d, *J* = 6.0 Hz, 1H), 5.11 (dd, *J* = 6.1, 3.8 Hz, 1H), 5.07 – 4.95 (m, 2H), 3.97 (qd, *J* = 11.8, 3.1 Hz, 2H), 3.80 (dt, *J* = 7.0, 3.3 Hz, 1H), 1.06 (s, 9H); ^{13}C NMR (101 MHz, $CDCl_3$) ^{13}C NMR (101 MHz, $CDCl_3$) δ 154.1, 150.2, 135.6, 135.6, 132.7, 132.7, 130.1, 130.0, 128.0, 127.9, 96.4, 74.2, 71.1, 69.4, 62.0, 26.8, 19.4; HRMS (ESI) *m/z*: calcd. for $C_{23}H_{26}O_5SiNa^+$ $(M + Na)^+$ 433.1447, found 433.1446; $[\alpha]_D^{24}$ = +121.5 (c = 1.0, $CHCl_3$).

1,5-Anhydro-3,4-*O*-carbonate-2,6-dideoxy-D-ribo-hex-1-enitol (40)

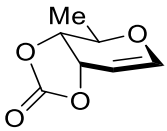

Colorless syrup; yield 74%; ^{1}H NMR (400 MHz, $CDCl_3$) δ 6.71 (d, *J* = 6.0 Hz, 1H), 5.13 (dd, *J* = 6.1, 4.4 Hz, 1H), 5.04 – 4.92 (m, 1H), 4.41 (dd, *J* = 9.1, 6.7 Hz, 1H), 3.87 – 3.73 (m, 1H), 1.46 (d, *J* = 6.4 Hz, 3H); ^{13}C NMR (101 MHz, $CDCl_3$) ^{13}C NMR (101 MHz, $CDCl_3$) δ 154.2, 150.4, 96.9, 76.4, 70.5, 69.7, 17.0; HRMS (ESI) *m/z*: calcd. for $C_7H_9O_4^+$ $(M + H)^+$ 157.0501, found 157.0503; $[\alpha]_D^{21}$ = +99.5 (c = 1.0, $CHCl_3$).

General procedure for syntheses of *O*-glycosides 2-21, 22a-28a, 29, 30, 32, 33a, 35, 36a, 38, 39b, 41, 42b

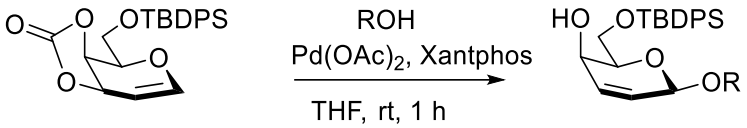

To a mixture of palladium acetate (2.3 mg, 0.01 mmol), Xantphos (8.7 mg, 0.015 mmol) and 3,4-*O*-carbonate glycal donor **1** (0.1 mmol) were added anhydrous THF (2 mL) and a glycosyl acceptor (0.2 mmol) under an atmosphere of Argon. The reaction mixture was stirred at room temperature and monitored by TLC until the glycal donor was consumed completely in 1 h. The solvent was removed under reduced pressure to afford a crude product which was purified by silica gel flash chromatography with a gradient solvent system (EtOAc/hexane as eluent) to yield 4-hydroxyl 2,3-unsaturated *O*-glycoside.

General procedure for syntheses of *O*-glycosides 22b-28b, 2, 3, 5, 15, 21, 33b, 36b, 39a, 42a

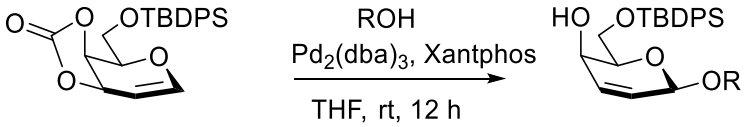

General procedure for synthesis of *O*-glycosides: To a mixture of Tris(dibenzylideneacetone)dipalla-dium(0) (4.6 mg, 0.005 mmol), Xantphos (8.7 mg, 0.015 mmol) and 3,4-*O*-carbonate glycal donor **1** (0.1 mmol) was added anhydrous THF (2 mL) and glycosyl acceptors (0.2 mmol) under an atmosphere of Argon. The reaction mixture was stirred at room temperature and monitored by TLC until the glycal

donor was consumed completely in 12 h. The solvent was removed under reduced pressure to afford a crude product which was purified through silica gel flash chromatography with a gradient solvent system (EtOAc/hexane as eluent) to yield 4-hydroxyl 2,3-unsaturated *O*-glycoside.

Methyl 2,3-dideoxy-6-*O*-[(1,1-dimethylethyl)diphenylsilyl]-*β*-D-*threo*-hex-2-enopyranoside (**2**)

Colorless syrup; 95%; ^{1}H NMR (400 MHz, $CDCl_3$): δ 7.73-7.70 (m, 4H), 7.45-7.37 (m, 6H), 6.16 (dd, J = 10.1 Hz, 4.8 Hz, 1H), 5.82 (d, J = 10.1 Hz, 1H), 4.96 (s, 1H), 4.06 – 3.94 (m, 2H), 3.88 (dd, J = 10.4, 6.2 Hz, 1H), 3.75 (td, J = 6.2, 2.2 Hz, 1H), 3.47 (s, 3H), 1.97 (d, J = 9.7 Hz, 1H), 1.07 (s, 9H); ^{13}C NMR (101 MHz, $CDCl_3$) δ 135.7, 135.7, 133.5, 133.5, 131.1, 130.8, 129.9, 129.9, 127.9, 127.8, 98.9, 75.8, 63.4, 62.7, 55.8, 26.9, 19.4; HRMS (ESI) *m/z*: calcd. for $C_{23}H_{30}O_4SiNa^+$ $(M + Na)^+$ 421.1811, found 421.1813; $[\alpha]_D^{24}$ = -60.2 (c = 1.0, $CHCl_3$).

Ethyl 2,3-dideoxy-6-*O*-[(1,1-dimethylethyl)diphenylsilyl]-*β*-D-*threo*-hex-2-enopyranoside (**3**)

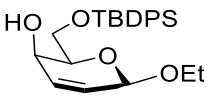

Colorless syrup; 89%; ^{1}H NMR (400 MHz, $CDCl_3$) δ 7.77 – 7.66 (m, 4H), 7.47 – 7.33 (m, 6H), 6.15 (dd, J = 10.1, 5.1, 1H), 5.83 (d, J = 10.1, 1H), 5.04 (s, 1H), 4.06 – 3.95

(m, 2H), 3.95 – 3.82 (m, 2H), 3.75 (td, *J* = 6.3, 2.0, 1H), 3.57 (dq, *J* = 9.3, 7.1, 1H), 1.97 (d, *J* = 9.9, 1H), 1.22 (t, *J* = 7.1 Hz, 3H), 1.07 (s, 9H); ^{13}C NMR (101 MHz, $CDCl_3$) δ 135.8, 135.7, 133.6, 133.5, 131.2, 130.9, 129.9, 129.8, 127.8, 127.8, 97.9, 75.8, 64.3, 63.5, 62.7, 26.9, 19.4, 15.4; HRMS (ESI) *m/z*: calcd. for $C_{24}H_{32}O_4SiNa^+$ $(M + Na)^+$ 435.1968, found 435.1965; $[\alpha]_D^{24}$ = -72.8 (c = 1.0, $CHCl_3$).

_n_-Butyl 2,3-dideoxy-6-*O*-[(1,1-dimethylethyl)diphenylsilyl]-*β*-D-*threo*-hex-2-enopyranoside (**4**)

Colorless syrup; 89%; ^{1}H NMR (400 MHz, $CDCl_3$) δ 7.75 – 7.67 (m, 4H), 7.46 – 7.37 (m, 6H), 6.15 (dd, *J* = 10.1, 5.1, 1H), 5.83 (d, *J* = 10.1 Hz, 1H), 5.02 (s, 1H), 4.05 – 3.95 (m, 2H), 3.91 – 3.81 (m, 2H), 3.75 (td, *J* = 6.3, 2.3 Hz, 1H), 3.54 – 3.43 (m, 1H), 1.98 (d, *J* = 9.9 Hz, 1H), 1.63 – 1.51 (m, 2H), 1.36 (h, *J* = 7.3 Hz, 2H), 1.07 (s, 9H), 0.91 (t, *J* = 7.3 Hz, 3H); ^{13}C NMR (101 MHz, $CDCl_3$) δ 135.8, 135.7, 133.6, 133.5, 131.2, 130.9, 129.9, 129.8, 127.8, 127.8, 98.1, 75.8, 68.7, 63.5, 62.8, 31.9, 26.9, 19.4, 14.0; HRMS (ESI) *m/z*: calcd. for $C_{26}H_{36}O_4SiNa^+$ $(M + Na)^+$ 463.2281, found 463.2288; $[\alpha]_D^{24}$ = -53.8 (c = 1.0, $CHCl_3$).

Benzyl 2,3-dideoxy-6-*O*-[(1,1-dimethylethyl)diphenylsilyl]-*β*-D-*threo*-hex-2-enopyranoside (**5**)

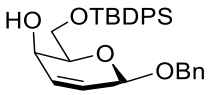

Colorless syrup; 74%; ^{1}H NMR (400 MHz, $CDCl_3$) δ 7.73 (m, 4H), 7.52-7.29 (m, 11H), 6.17 (dd, *J* = 10.0, 5.0 Hz, 1H), 5.87 (d, *J* = 10.1 Hz, 1H), 5.13 (s, 1H), 4.86 (d, *J* = 11.8 Hz, 1H), 4.62 (d, *J* = 11.8 Hz, 1H), 4.02 (m, 2H), 3.93 (m, 1H), 3.79 (td, *J* = 6.1, 2.2 Hz, 1H), 2.04 (d, *J* = 9.7 Hz, 1H), 1.07 (s, 9H); ^{13}C NMR (101 MHz, CDCl3) δ 137.6, 135.77, 135.7, 133.6, 133.4, 131.1, 130.9, 129.9, 129.9, 128.5, 128.2, 127.9, 127.9, 96.9, 75.9, 69.9, 63.6, 62.8, 26.9, 19.4; HRMS (ESI) *m/z*: calcd. for $C_{29}H_{34}O_4SiNa^+$ $(M + Na)^+$ 497.2124, found 497.2126; $[\alpha]_D^{24}$ = -71.0 (c = 1.0, $CHCl_3$).

Allyl 2,3-dideoxy-6-*O*-[(1,1-dimethylethyl)diphenylsilyl]-*β*-D-*threo*-hex-2-enopyranoside (6)

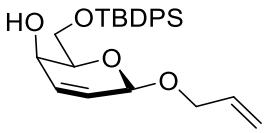

Colorless syrup; 85%; ^{1}H NMR (400 MHz, $CDCl_3$) δ 7.78 – 7.60 (m, 4H), 7.48 – 7.34 (m, 6H), 6.18 (dd, *J* = 10.0, 5.5 Hz, 1H), 6.01 – 5.84 (m, 2H), 5.26 (dd, *J* = 17.2, 1.5 Hz, 1H), 5.17 (d, *J* = 10.4 Hz, 1H), 5.06 (d, *J* = 2.8 Hz, 1H), 4.24 (dd, *J* = 12.7, 5.3 Hz, 1H), 4.14 (td, *J* = 6.2, 2.2 Hz, 1H), 4.04 (dd, *J* = 12.7, 6.3 Hz, 1H), 3.98 – 3.81 (m, 3H), 1.87 (d, *J* = 8.5 Hz, 1H), 1.07 (s, 9H); ^{13}C NMR (101 MHz, $CDCl_3$) δ 135.7, 135.7, 134.2, 133.5, 133.4, 131.1, 130.8, 129.8, 129.8, 127.8, 127.8, 117.6, 97.1, 75.9, 69.2, 63.5, 62.7, 26.9, 19.3; HRMS (ESI) *m/z*: calcd. for $C_{25}H_{32}O_4SiNa^+$ $(M + Na)^+$ 447.1968, found 447.1969; $[\alpha]_D^{24}$ = -63.3 (c = 1.0, $CHCl_3$).

Pyridin-2-ylmethyl 2,3-dideoxy-6-*O*-[(1,1-dimethylethyl)diphenylsilyl]-*β*-D-*threo*-hex-2-enopyranoside (7)

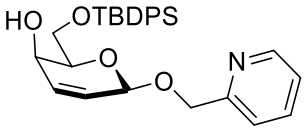

Colorless syrup; 65%; ^{1}H NMR (400 MHz, $CDCl_3$) δ 8.52 (d, *J* = 4.3, 1H), 7.77 – 7.56 (m, 5H), 7.48 – 7.30 (m, 7H), 7.21 – 7.07 (m, 1H), 6.23 (ddd, *J* = 10.1, 5.2, 1.2, 1H), 5.90 (d, *J* = 10.1, 1H), 5.25 (d, *J* = 1.1, 1H), 4.93 (d, *J* = 13.0, 1H), 4.73 (d, *J* = 13.0, 1H), 4.05 (d, *J* = 5.1, 1H), 3.95 (dd, *J* = 10.1, 6.6, 1H), 3.83 (dd, *J* = 10.1, 5.8 Hz, 1H), 3.78 (td, *J* = 6.3, 2.2 Hz, 1H), 2.44 (s, 1H), 1.06 (s, 9H); ^{13}C NMR (101 MHz, $CDCl_3$) δ 154.2, 149.3, 135.6, 135.6, 132.9, 132.7, 130.2, 130.1, 128.0, 128.0, 98.2, 74.0, 73.0, 69.0, 61.9, 26.9, 19.4; HRMS (ESI) *m/z*: calcd. for $C_{28}H_{33}NO_4SiNa^+$ $(M + Na)^+$ 498.2077, found 498.2079; $[\alpha]_D^{24}$ = -49.4 (c = 0.82, $CHCl_3$).

2-Thiophenemethyl 2,3-dideoxy-6-*O*-[(1,1-dimethylethyl)diphenylsilyl]-*β*-D-*threo*-hex-2-enopyrano-side (**8**)

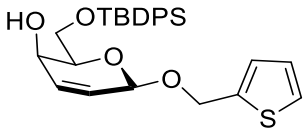

Colorless syrup; 80%; ^{1}H NMR (400 MHz, $CDCl_3$) δ 7.78-7.69 (m, 4H), 7.50-7.36 (m, 6H), 7.29 (dd, *J* = 5.0, 0.8 Hz, 1H), 7.00 (m, 1H), 6.96 (m, 1H), 6.16 (ddd, *J* = 10.0, 5.1, 1.1 Hz, 1H), 5.84 (d, *J* = 10.0 Hz, 1H), 5.14 (d, *J* = 1.1 Hz, 1H), 4.95 (d, *J* = 12.4 Hz, 1H), 4.82 (d, *J* = 12.4 Hz, 1H), 4.02 (m, 2H), 3.93 (dd, *J* = 10.6, 6.1 Hz, 1H), 3.78 (td, *J* = 6.2, 2.2 Hz, 1H), 2.04 (d, *J* = 9.6 Hz, 1H), 1.09 (s, 9H); ^{13}C NMR (126 MHz, $CDCl_3$)

δ 139.9, 135.8, 135.7, 133.6, 133.4, 131.2, 130.7, 129.9, 129.9, 127.9, 127.3, 126.8, 126.3, 96.2, 75.9, 64.1, 63.6, 62.8, 27.0, 19.4; HRMS (ESI) *m/z*: calcd. for $C_{27}H_{32}O_4SiSNa^+$ $(M + Na)^+$ 503.1688, found 503.1690; $[\alpha]_D^{24}$ = -8.7 (c = 1.0, $CHCl_3$).

(6-Methoxypyridin-2-yl)methyl 2,3-dideoxy-6-*O*-[(1,1-dimethylethyl) diphenylsilyl]-*β*-D-*threo*-hex-2-enopyranoside (9)

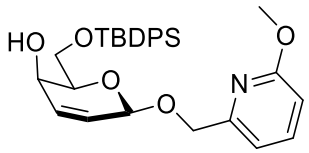

Colorless syrup; 80%; ^{1}H NMR (400 MHz, $CDCl_3$) δ 7.77 – 7.67 (m, 4H), 7.53 (t, *J* = 7.8 Hz, 1H), 7.47 – 7.31 (m, 6H), 6.97 (d, *J* = 7.2 Hz, 1H), 6.62 (d, *J* = 8.2 Hz, 1H), 6.21 (ddd, *J* = 10.0, 5.1, 1.0 Hz, 1H), 5.93 (d, *J* = 10.1 Hz, 1H), 5.24 (d, *J* = 1.0 Hz, 1H), 4.85 (d, *J* = 13.4 Hz, 1H), 4.65 (d, *J* = 13.4 Hz, 1H), 4.06 (s, 1H), 4.01 (dd, *J* = 10.5, 6.6 Hz, 1H), 3.93 – 3.84 (m, 4H), 3.80 (td, *J* = 6.3, 2.1 Hz, 1H), 2.17 (d, *J* = 9.5 Hz, 1H), 1.08 (s, 9H); ^{13}C NMR (101 MHz, $CDCl_3$) δ 163.7, 155.7, 139.0, 135.7, 135.7, 133.5, 133.4, 131.4, 130.7, 129.9, 129.8, 127.8, 114.1, 109.4, 97.6, 75.8, 70.5, 63.5, 62.7, 53.4, 26.9, 19.4; HRMS (ESI) *m/z*: calcd. for $C_{29}H_{35}NO_5SiNa^+$ $(M + Na)^+$ 528.2182, found 521.2183; $[\alpha]_D^{24}$ = -37.9 (c = 1.0, $CHCl_3$).

(6-(Thiophen-3-yl)pyridin-2-yl)methyl 2,3-dideoxy-6-*O*-[(1,1-dimethylethyl) diphenylsilyl]-*β*-D-*threo*-hex-2-enopyranoside (**10**)

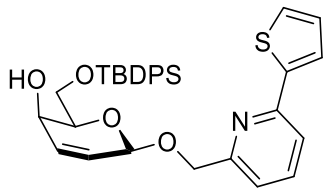

Colorless syrup; 88%; ^{1}H NMR (400 MHz, $CDCl_3$) δ 7.89 (dd, *J* = 3.0, 1.1 Hz, 1H), 7.76 – 7.62 (m, 6H), 7.49 (d, *J* = 7.7 Hz, 1H), 7.46 – 7.35 (m, 7H), 7.32 (d, *J* = 7.6 Hz, 1H), 6.23 (ddd, *J* = 10.1, 5.1, 1.2 Hz, 1H), 5.93 (d, *J* = 10.1 Hz, 1H), 5.29 (d, *J* = 1.2 Hz, 1H), 5.00 (d, *J* = 13.3 Hz, 1H), 4.80 (d, *J* = 13.3 Hz, 1H), 4.06 (br s, 1H), 3.99 (dd, *J* = 10.4, 6.6 Hz, 1H), 3.88 (dd, *J* = 10.4, 5.9 Hz, 1H), 3.81 (td, *J* = 6.3, 2.1 Hz, 1H), 2.29 (br s, 1H), 1.08 (s, 9H); ^{13}C NMR (101 MHz, $CDCl_3$) δ 158.2, 152.9, 142.2, 137.3, 135.7, 135.7, 133.5, 133.4, 131.5, 130.6, 129.9, 127.8, 126.4, 126.3, 123.7, 119.7, 119.0, 97.7, 75.8, 70.8, 63.4, 62.6, 27.0, 19.4; HRMS (ESI) *m/z*: calcd. for $C_{32}H_{35}NO_4SiSNa^+$ $(M + Na)^+$ 580.1954, found 580.1953; $[\alpha]_D^{24}$ = -26.1 (c = 1.0, $CHCl_3$).

1,2-Dideoxy-3,4-*O*-dibenzyl-6-*O*-(2,3-dideoxy-4-hydroxyl-6-*tert*-butyldiphenylsilyl-*β*-D-*threo*-hex-2-enopyranos-1-yl)-D-arabino-hex-1-enopyranose (11)

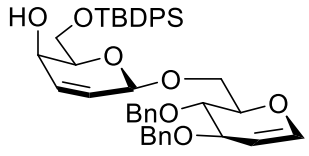

Colorless syrup; 80%; ^{1}H NMR (400 MHz, $CDCl_3$) δ 7.80 – 7.63 (m, 4H), 7.52 – 7.28 (m, 16H), 6.39 (d, *J* = 6.1 Hz, 1H), 6.17 (ddd, *J* = 10.1, 4.2, 0.8 Hz, 1H), 5.83 (d, *J* = 10.1 Hz, 1H), 5.06 (d, *J* = 0.8 Hz, 1H), 4.88 (dd, *J* = 6.1, 2.7 Hz, 1H), 4.83 (d, *J* = 11.5 Hz, 1H), 4.65 (dd, *J* = 15.8, 11.6 Hz, 2H), 4.54 (d, *J* = 11.7 Hz, 1H), 4.23 – 4.14 (m,

1H), 4.13 – 4.05 (m, 2H), 4.05 – 3.91 (m, 2H), 3.91 – 3.72 (m, 4H), 1.88 (s, 1H), 1.07 (s, 9H); ^{13}C NMR (126 MHz, $CDCl_3$) δ 144.7, 138.4, 138.2, 135.7, 135.7, 133.5, 133.4, 131.2, 130.7, 129.9, 129.8, 128.5, 128.0, 128.0, 127.9, 127.9, 127.8, 127.8, 100.0, 98.2, 76.5, 75.7, 75.5, 74.2, 73.6, 70.5, 66.7, 63.2, 62.5, 26.9, 19.3; HRMS (ESI) *m/z*: calcd. for $C_{42}H_{48}O_7SiNa^+$ $(M + Na)^+$ 715.3067, found 715.3063; $[\alpha]_D^{24}$ = -18.8 (c = 1.0, $CHCl_3$).

1,2-Dideoxy-3,4-*O*-dibenzyl-6-*O*-(2,3-dideoxy-4-hydroxyl-6-*tert*-butyldiphenylsilyl-*β*-D-*threo*-hex-2-enopyranos-1-yl)- D-lyxo-hex-1-enopyranose (12)

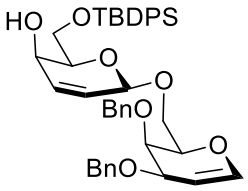

Colorless syrup; 75%; ^{1}H NMR (400 MHz, $CDCl_3$) δ 7.80 – 7.64 (m, 4H), 7.51 – 7.26 (m, 13H), 7.24 – 7.11 (m, 3H), 6.34 (dd, *J* = 6.3, 1.4 Hz, 1H), 6.15 (ddd, *J* = 10.1, 5.2, 1.5 Hz, 1H), 5.83 (d, *J* = 10.1 Hz, 1H), 5.05 (d, *J* = 1.5 Hz, 1H), 4.84 (dd, *J* = 6.2, 2.6 Hz, 1H), 4.80 (d, *J* = 11.9 Hz, 1H), 4.67 – 4.54 (m, 3H), 4.26 – 4.16 (m, 1H), 4.15 – 4.07 (m, 1H), 4.07 – 3.99 (m, 1H), 4.00 – 3.91 (m, 3H), 3.89 – 3.83 (m, 1H), 3.81 (dd, *J* = 10.2, 5.7 Hz, 1H), 3.75 – 3.67 (m, 1H), 1.90 (d, *J* = 9.7 Hz, 1H), 1.05 (s, 9H); ^{13}C NMR (101 MHz, $CDCl_3$) δ 144.2, 138.6, 138.3, 135.7, 135.7, 133.5, 133.4, 131.1, 130.8, 129.9, 128.5, 128.4, 128.1, 127.9, 127.8, 127.7, 127.6, 100.0, 98.5, 76.0, 75.5, 73.2, 72.0, 71.1, 70.4, 67.5, 63.0, 62.4, 26.9, 19.3; HRMS (ESI) *m/z*: calcd. for $C_{42}H_{48}O_7SiNa^+$ $(M + Na)^+$ 715.3067, found 715.3068; $[\alpha]_D^{24}$ = +4.9 (c = 1.0, $CHCl_3$).

1,2-Dideoxy-3,4-diacetyl-6-*O*-(2,3-dideoxy-4-hydroxyl-6-*tert*-butyldiphenylsilyl-*β*-D-*threo*-hex-2-enopyranos-1-yl)-D-lyxo-hex-1-enopyranose (13)

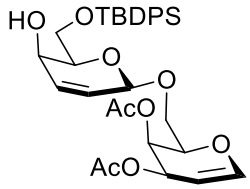

Colorless syrup; 72%; ^{1}H NMR (400 MHz, $CDCl_3$) δ 7.72 – 7.67 (m, 4H), 7.44 – 7.36 (m, 6H), 6.46 (dd, *J* = 6.3, 1.7 Hz, 1H), 6.17 (ddd, *J* = 10.1, 5.3, 1.2 Hz, 1H), 5.79 (d, *J* = 10.1 Hz, 1H), 5.57 – 5.52 (m, 1H), 5.47 – 5.42 (m, 1H), 5.09 (d, *J* = 1.2 Hz, 1H), 4.67 (dt, *J* = 6.3, 2.0 Hz, 1H), 4.26 (t, *J* = 6.4 Hz, 1H), 4.03 – 3.98 (m, 1H), 3.97 – 3.87 (m, 2H), 3.85 – 3.78 (m, 1H), 3.78 – 3.70 (m, 2H), 2.13 (d, *J* = 9.9 Hz, 1H), 2.01 (s, 3H), 1.98 (s, 3H), 1.06 (s, 9H); ^{13}C NMR (101 MHz, $CDCl_3$) δ 170.5, 170.4, 145.7, 135.7, 135.7, 133.5, 133.4, 131.4, 130.2, 129.9, 127.9, 99.0, 97.7, 75.8, 74.4, 65.6, 64.4, 63.8, 63.3, 62.4, 26.9, 20.9, 20.8, 19.4; HRMS (ESI) *m/z*: calcd. for $C_{32}H_{40}O_9SiNa^+$ (M + Na)$^+$ 619.2339, found 619.2338; $[\alpha]_D^{24}$ = -40.1 (c = 1.0, $CHCl_3$).

Methyl 2,3,4-tri-*O*-benzyl-6-*O*-(2,3-dideoxy-4-hydroxyl-6-*tert*-butyldiphenylsilyl-*β*-D-*threo*-hex-2-enopyranos-1-yl)-*α*-D-glucopyranoside (14)

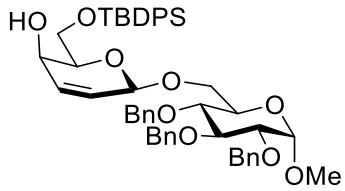

Colorless syrup; 86%; ^{1}H NMR (400 MHz, $CDCl_3$) δ 7.74 – 7.71 (m, 4H), 7.51 – 7.27 (m, 21H), 6.17 (dd, *J* = 10.0, 4.7 Hz, 1H), 5.80 (d, *J* = 10.0 Hz, 1H), 5.02 (d, *J* = 10.9 Hz, 1H), 4.96 (s, 1H), 4.91 – 4.78 (m, 3H), 4.69 (d, *J* = 12.2 Hz, 1H), 4.63 (dd, *J* = 7.3, 3.7 Hz, 2H), 4.09 – 3.94 (m, 4H), 3.85 (dd, *J* = 10.3, 6.1 Hz, 1H), 3.80 – 3.67 (m, 3H),

3.64 – 3.54 (m, 2H),3.38 (s, 3H), 1.88 (d, *J* = 9.9 Hz, 1H), 1.09 (s, 9H); ^{13}C NMR (101 MHz, $CDCl_3$) δ 138.9, 138.4, 138.3, 135.7, 135.7, 133.6, 133.4, 131.1, 130.8, 129.8, 129.8, 128.6, 128.5, 128.2, 128.1, 128.0, 127.9, 127.8, 127.8, 127.7, 98.2, 98.2, 82.3, 79.9, 75.9, 75.0, 73.5, 69.7, 66.5, 63.2, 62.4, 55.3, 26.9, 19.3; HRMS (ESI) *m/z*: calcd. for $C_{50}H_{58}O_9SiNa^+$ $(M + Na)^+$ 853.3748, found 853.3750; $[\alpha]_D^{24}$ = -5.8 (c = 1.0, $CHCl_3$).

1,2:3,4-Di-*O*-isopropylidene-6-*O*-(2,3-dideoxy-4-hydroxyl-6-*tert*-butyldiphenylsilyl-*β*-D-*threo*-hex-2-enopyranos-1-yl)-*α*-D-galactopyranoside (15)

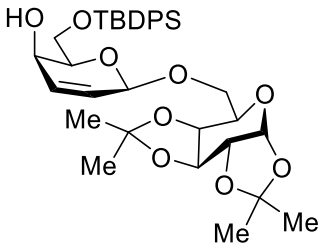

Colorless syrup; 85%; ^{1}H NMR (400 MHz, $CDCl_3$) δ 7.77 – 7.63 (m, 4H), 7.47 – 7.34 (m, 6H), 6.15 (dd, *J* = 10.1, 4.5 Hz, 1H), 5.90 (d, *J* = 10.1 Hz, 1H), 5.53 (d, *J* = 5.0 Hz, 1H), 5.12 (s, 1H), 4.63 – 4.57 (m, 1H), 4.30 (dd, *J* = 4.9, 2.3 Hz, 1H), 4.19 (dd, *J* = 7.9, 1.3 Hz, 1H), 4.08 – 3.93 (m, 4H), 3.91 – 3.79 (m, 1H), 3.79 – 3.65 (m, 2H), 2.04 (d, *J* = 10.2 Hz, 1H), 1.50 (s, 3H), 1.42 (s, 3H), 1.32 (s, 3H), 1.30 (s, 3H), 1.06 (s, 9H); ^{13}C NMR (101 MHz, $CDCl_3$) δ 135.7, 135.7, 133.5, 133.5, 131.1, 130.9, 129.8, 127.9, 109.4, 108.7, 98.7, 96.4, 75.7, 71.5, 70.8, 70.6, 68.2, 67.9, 63.2, 62.5, 27.0, 26.2, 26.1, 25.1, 24.5, 19.4; HRMS (ESI) *m/z*: calcd. for $C_{34}H_{46}O_9SiNa^+$ $(M + Na)^+$ 649.2809, found 649.2808; $[\alpha]_D^{24}$ = -71.7 (c = 1.0, $CHCl_3$).

Methyl 2,3,6-tri-*O*-benzyl-4-*O*-(2,3-dideoxy-4-hydroxyl-6-*tert*-butyldiphenylsilyl-*β*-D-*threo*-hex-2-enopyranos-1-yl)-*α*-D-glucopyranoside (16)

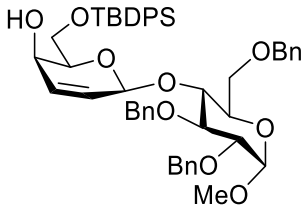

Colorless syrup; 42%; ^{1}H NMR (400 MHz, $CDCl_3$) δ 7.73 – 7.63 (m, 4H), 7.47 – 7.28 (m, 14H), 7.25 (s, 4H), 7.19 – 7.17 (m, 3H), 6.12 (ddd, *J* = 10.1, 5.5, 1.5 Hz, 1H), 5.73 (dd, *J* = 10.1, 1.1 Hz, 1H), 5.20 (q, *J* = 1.5 Hz, 1H), 4.83 (s, 2H), 4.77 (d, *J* = 12.1 Hz, 1H), 4.66 – 4.53 (m, 3H), 4.46 (d, *J* = 12.2 Hz, 1H), 3.99 – 3.80 (m, 5H), 3.70 (dd, *J* = 9.9, 5.6 Hz, 1H), 3.68 – 3.58 (m, 2H), 3.51 (dd, *J* = 11.4, 2.1 Hz, 1H), 3.46 (dd, *J* = 9.5, 3.6 Hz, 1H), 3.36 (s, 3H), 2.42 (d, *J* = 10.5 Hz, 1H), 1.05 (s, 9H); ^{13}C NMR (101 MHz, $CDCl_3$) δ 139.0, 138.4, 137.9, 135.8, 135.7, 133.6, 133.5, 131.7, 130.6, 129.8, 128.5, 128.5, 128.3, 128.2, 128.1, 127.9, 127.9, 127.8, 127.5, 98.4, 98.2, 80.9, 79.6, 76.0, 75.9, 75.2, 73.9, 73.6, 70.7, 68.2, 62.6, 61.6, 55.4, 27.0, 19.4; HRMS (ESI) *m/z*: calcd. for $C_{50}H_{58}O_9SiNa^+$ $(M + Na)^+$ 853.3748, found 853.3747; $[\alpha]_D^{24}$ = +14.3 (c = 1.0, $CHCl_3$).

4-*O*-(2,3-Dideoxy-4-hydroxyl-6-*tert*-butyldiphenylsilyl-*β*-D-*threo*-hex-2-enopyranos-1-yl)-1,6:2,3-dianhydro-*β*-D-mannopyranoside (17)

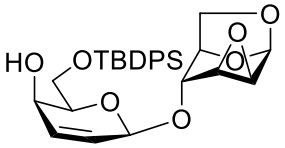

Colorless syrup; 71%; ^{1}H NMR (400 MHz, $CDCl_3$) δ 7.73 – 7.66 (m, 4H), 7.47 – 7.36 (m, 6H), 6.21 (dd, *J* = 10.1, 5.0 Hz, 1H), 5.87 (d, *J* = 10.1, 1H), 5.68 (d, *J* = 3.0 Hz, 1H), 5.27 (s, 1H), 4.47 (t, *J* = 4.2 Hz, 1H), 4.05 (s, 1H), 3.98 (dd, *J* = 8.6, 4.3 Hz, 1H), 3.96 (s, 1H), 3.88 (dd, *J* = 10.6, 5.9 Hz, 1H), 3.78 (td, *J* = 6.1, 2.0 Hz, 1H), 3.67 (d, *J*

= 4.3 Hz, 2H), 3.40 (t, *J* = 3.4 Hz, 1H), 3.30 (d, *J* = 3.6 Hz, 1H), 2.07 (d, *J* = 8.2 Hz, 1H), 1.06 (s, 9H); ^{13}C NMR (101 MHz, $CDCl_3$) δ 135.7, 135.7, 133.3, 133.1, 131.7, 130.2, 130.0, 130.0, 127.9, 127.9, 97.7, 97.7, 75.9, 72.9, 72.3, 65.8, 63.5, 62.5, 54.5, 48.6, 26.9, 19.4; HRMS (ESI) *m/z*: calcd. for $C_{28}H_{34}O_7SiNa^+$ $(M + Na)^+$ 533.1972, found 533.1971; $[\alpha]_D^{22}$ = -63.9 (c = 1.0, $CHCl_3$).

_p_-Methoxyphenyl-2,4,6-_tri_-benzyl-3-_O_-(2,3-dideoxy-4-hydroxyl-6-_tert_-butyldiphenylsilyl-_β_-D-_threo_-hex-2-enopyranos-1-yl)-_β_-D-galactopyranoside (18)

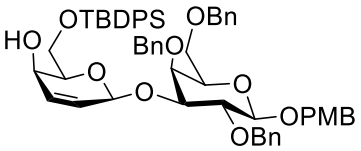

Colorless syrup; 70%; ^{1}H NMR (400 MHz, $CDCl_3$) δ 7.77 – 7.68 (m, 4H), 7.54 – 7.17 (m, 21H), 7.09 – 7.01 (m, 2H), 6.85 – 6.76 (m, 2H), 6.15 (ddd, *J* = 10.1, 5.3, 1.5 Hz, 1H), 5.87 (d, *J* = 10.1 Hz, 1H), 5.31 (d, *J* = 1.5 Hz, 1H), 5.03 (d, *J* = 11.0 Hz, 1H), 4.90 (d, *J* = 11.8 Hz, 1H), 4.86 – 4.74 (m, 2H), 4.63 (d, *J* = 11.9 Hz, 1H), 4.47 – 4.33 (m, 2H), 4.12 – 3.79 (m, 6H), 3.77 (s, 3H), 3.74 (td, *J* = 6.4, 2.1 Hz, 1H), 3.68 – 3.58 (m, 2H), 3.52 – 3.40 (m, 1H), 1.74 (d, *J* = 9.5 Hz, 1H), 1.07 (s, 9H); ^{13}C NMR (101 MHz, $CDCl_3$) δ 155.3, 151.7, 138.8, 138.6, 138.2, 135.7, 135.6, 133.5, 133.3, 131.2, 130.5, 129.9, 128.5, 128.4, 128.2, 128.2, 128.0, 127.9, 127.9, 127.8, 127.7, 127.5, 118.6, 114.6, 103.1, 100.3, 81.7, 79.2, 76.1, 75.6, 75.4, 74.5, 74.2, 73.6, 69.4, 63.2, 62.4, 55.7, 26.9, 19.4; HRMS (ESI) *m/z*: calcd. for $C_{56}H_{62}O_{10}SiNa^+$ $(M + Na)^+$ 945.4050, found 945.4000; $[\alpha]_D^{24}$ = -36.1 (c = 1.0, $CHCl_3$).

Methyl 2-benzyl-4,6-*O*-(*p*-methoxybenzylidene)-3-*O*-(2,3-dideoxy-4-hydroxyl-6-*tert*-butyldiphenylsilyl-*β*-D-*threo*-hex-2-enopyranos-1-yl)-*α*-D-glucopyranoside (19)

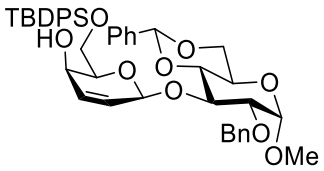

Colorless syrup; 70%; ^{1}H NMR (400 MHz, $CDCl_3$) δ 7.72 – 7.65 (m, 4H), 7.48 – 7.30 (m, 13H), 7.16 (t, *J* = 7.4 Hz, 1H), 7.07 (t, *J* = 7.5 Hz, 2H), 6.22 (ddd, *J* = 10.1, 5.3, 1.1 Hz, 1H), 5.88 (d, *J* = 10.1 Hz, 1H), 5.44 (s, 1H), 5.37 (d, *J* = 1.1 Hz, 1H), 4.77 (d, *J* = 12.1 Hz, 1H), 4.64 (d, *J* = 12.1 Hz, 1H), 4.58 (d, *J* = 3.6 Hz, 1H), 4.26 – 4.15 (m, 2H), 4.09 (s, 1H), 3.97 (t, *J* = 8.2 Hz, 1H), 3.77 (ddd, *J* = 10.8, 7.3, 3.4 Hz, 3H), 3.66 (t, *J* = 10.2 Hz, 1H), 3.56 – 3.43 (m, 2H), 3.37 (s, 3H), 2.13 (d, *J* = 9.6 Hz, 1H), 1.05 (s, 9H); ^{13}C NMR (101 MHz, $CDCl_3$) δ 138.0, 137.3, 135.8, 135.6, 133.5, 133.4, 131.3, 130.7, 129.8, 129.8, 128.8, 128.7, 128.2, 128.1, 127.9, 127.8, 126.0, 100.9, 99.3, 99.0, 79.8, 79.7, 75.4, 73.8, 69.0, 62.8, 62.4, 61.9, 55.4, 27.0, 19.4; HRMS (ESI) *m/z*: calcd. for $C_{43}H_{50}O_9SiNa^+$ $(M + Na)^+$ 761.3122, found 761.3130; $[\alpha]_D^{24}$ = -23.9 (c = 1.0, $CHCl_3$).

Methyl 3-benzyl-4,6-*O*-(*p*-methoxybenzylidene)-2-*O*-(2,3-dideoxy-4-hydroxyl-6-*tert*-butyldiphenylsilyl-*β*-D-*threo*-hex-2-enopyranos-1-yl)-*α*-D-glucopyranoside (20)

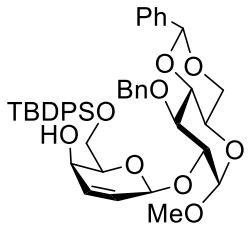

Colorless syrup; 87%; ^{1}H NMR (400 MHz, $CDCl_3$) δ 7.75 – 7.66 (m, 4H), 7.54 – 7.28 (m, 16H), 6.16 (dd, *J* = 10.1, 4.1 Hz, 1H), 5.89 (d, *J* = 10.1 Hz, 1H), 5.57 (s, 1H), 5.26 (d, *J* = 1.0, 1H), 4.90 (d, *J* = 11.4 Hz, 1H), 4.84 (d, *J* = 3.7 Hz, 1H), 4.74 (d, *J* = 11.3 Hz, 1H), 4.29 (dd, *J* = 9.9, 4.6 Hz, 1H), 3.99 (dt, *J* = 10.4, 8.0 Hz, 3H), 3.85 – 3.69 (m, 5H), 3.60 (t, *J* = 9.3 Hz, 1H), 3.35 (s, 3H), 2.00 (d, *J* = 10.2 Hz, 1H), 1.07 (s, 9H); ^{13}C NMR (101 MHz, $CDCl_3$) δ 138.7, 137.5, 135.7, 135.7, 133.5, 133.4, 131.1, 130.4, 129.9, 129.1, 128.5, 128.4, 128.0, 127.9, 127.9, 127.8, 126.2, 101.4, 100.4, 100.1, 82.6, 79.7, 78.2, 75.8, 75.4, 69.3, 63.3, 62.6, 62.3, 55.3, 26.9, 19.4; HRMS (ESI) *m/z*: calcd. for $C_{43}H_{50}O_9SiNa^+$ $(M + Na)^+$ 761.3122, found 761.3128; $[\alpha]_D^{24}$ = -25.5 (c = 1.0, $CHCl_3$).

Phenyl-2-benzyl-4,6-*O*-(*p*-methoxybenzylidene)-3-*O*-(2,3-dideoxy-4-hydroxyl-6-*tert*-butyldiphenylsilyl-*β*-D-*threo*-hex-2-enopyranos-1-yl)-1-thio-*α*-D-glucopyranoside (21)

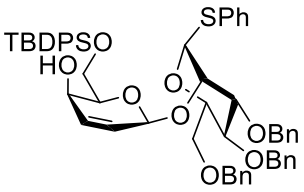

Colorless syrup; 85%; ^{1}H NMR (400 MHz, $CDCl_3$) δ 7.71 – 7.65 (m, 4H), 7.50 – 7.25 (m, 16H), 7.23 – 7.14 (m, 10H), 6.19 (ddd, *J* = 10.1, 5.4, 1.4 Hz, 1H), 5.85 (dd, *J* = 10.1, 1.1 Hz, 1H), 5.65 (d, *J* = 1.7 Hz, 1H), 5.24 (d, *J* = 1.5 Hz, 1H), 4.87 (d, *J* = 10.9 Hz, 1H), 4.72 (d, *J* = 11.3 Hz, 1H), 4.63 (d, *J* = 12.0 Hz, 1H), 4.57 – 4.43 (m, 4H), 4.29 –

4.22 (m, 1H), 4.02 – 3.96 (m, 1H), 3.97 – 3.77 (m, 5H), 3.72 (dt, *J* = 10.9, 3.5, 2H), 1.95 (d, *J* = 10.1, 1H), 1.05 (s, 9H); ^{13}C NMR (101 MHz, $CDCl_3$) δ 138.6, 138.4, 138.0, 135.7, 135.7, 134.5, 133.5, 133.4, 131.8, 131.7, 130.8, 129.9, 129.1, 128.5, 128.4, 128.4, 128.2, 128.0, 127.9, 127.9, 127.9, 127.8, 127.7, 127.6, 127.5, 96.2, 86.5, 78.9, 77.5, 77.4, 77.2, 76.8, 76.1, 75.3, 74.8, 73.4, 73.3, 72.7, 71.7, 69.3, 63.1, 62.2, 27.0, 19.4; HRMS (ESI) *m/z*: calcd. for $C_{55}H_{60}O_8SiSNa^+$ $(M + Na)^+$ 931.3676, found 931.3669; $[\alpha]_D^{24}$ = -36.9 (c = 1.0, $CHCl_3$).

2-Naphthyl 2,3-dideoxy-6-*O*-[(1,1-dimethylethyl)diphenylsilyl]-*α*-D-*threo*-hex-2-enopyranoside (22a)

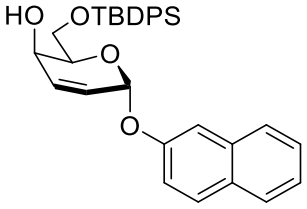

Colorless syrup; 71%; ^{1}H NMR (400 MHz, $CDCl_3$) δ 7.75 (dd, *J* = 12.7, 8.4 Hz, 2H), 7.72 – 7.56 (m, 5H), 7.50 (d, *J* = 2.5 Hz, 1H), 7.47 –7.31(m, 8H), 7.31 – 7.19 (m, 1H), 6.35 (dd, *J* = 9.9, 5.6 Hz, 1H), 6.12 (dd, *J* = 9.9, 3.1 Hz, 1H), 5.88 (d, *J* = 3.1 Hz, 1H), 4.29 (td, *J* = 6.1, 2.2 Hz, 1H), 4.13-4.05 (m, 1H), 4.01 – 3.88 (m, 2H), 2.14 (d, *J* = 7.6 Hz, 1H), 0.96 (s, 9H); ^{13}C NMR (101 MHz, $CDCl_3$) δ 155.2, 135.7, 135.6, 134.5, 133.2, 133.2, 130.6, 129.9, 129.9, 129.8, 129.5, 127.9, 127.7, 127.7, 127.3, 126.4, 124.2, 119.4, 111.3, 93.3, 71.6, 63.5, 61.9, 31.1, 26.8, 19.2; HRMS (ESI) *m/z*: calcd. for $C_{32}H_{34}O_4SiNa^+$ $(M + Na)^+$ 533.2124, found 533.2122; $[\alpha]_D^{24}$ = -53.3 (c = 1.0, $CHCl_3$).

Phenyl 2,3-dideoxy-6-*O*-[(1,1-dimethylethyl)diphenylsilyl]-*α*-D-*threo*-hex-2-enopyranoside (23a)

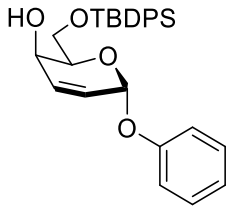

Colorless syrup; 85%; ^{1}H NMR (400 MHz, $CDCl_3$) δ 7.73 – 7.63 (m, 4H), 7.52 – 7.32 (m, 6H), 7.29-2.23 (m, 2H), 7.15 – 7.07 (m, 2H), 7.05 – 6.97 (m, 1H), 6.31 (ddd, *J* = 9.9, 5.6, 1.1 Hz, 1H), 6.06 (dd, *J* = 9.9, 3.2 Hz, 1H), 5.72 (dd, *J* = 3.2, 1.1 Hz, 1H), 4.25 (td, *J* = 6.0, 2.2 Hz, 1H), 4.07 (ddd, *J* = 7.7, 5.6, 2.2 Hz, 1H), 4.01 – 3.87 (m, 2H), 2.21 (d, *J* = 7.5 Hz, 1H), 1.02 (s, 9H); ^{13}C NMR (101 MHz, $CDCl_3$) δ 157.4, 135.7, 135.7, 135.7, 133.2, 133.1, 130.5, 129.9, 129.6, 127.9, 127.7, 122.3, 117.2, 93.3, 71.4, 63.6, 61.9, 26.9, 19.2; HRMS (ESI) *m/z*: calcd. for $C_{28}H_{32}O_4SiNa^+$ $(M + Na)^+$ 483.1968, found 483.1966; $[\alpha]_D^{24}$ = -3.5 (c = 1.0, $CHCl_3$).

4-Phenylphenyl 2,3-dideoxy-6-*O*-[(1,1-dimethylethyl)diphenylsilyl]-*α*-D-*threo*-hex-2-enopyranoside (24a)

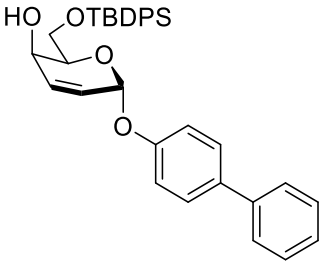

Colorless syrup; 70%; ^{1}H NMR (400 MHz, $CDCl_3$) δ 7.72 – 7.63 (m, 4H), 7.57 – 7.46 (m, 4H), 7.46 – 7.27 (m, 9H), 7.17 (d, *J* = 8.6 Hz, 2H), 6.33 (dd, *J* = 10.0, 5.6 Hz, 1H),

6.09 (dd, *J* = 10.0, 3.2 Hz, 1H), 5.77 (d, *J* = 3.2 Hz, 1H), 4.27 (td, *J* = 6.0, 2.1 Hz, 1H), 4.12 – 4.03 (m, 1H), 4.02 – 3.89 (m, 2H), 2.17 (d, *J* = 7.4 Hz, 1H), 1.02 (s, 9H); ^{13}C NMR (101 MHz, $CDCl_3$) δ 156.8, 140.8, 135.6, 135.6, 135.3, 133.1, 133.1, 130.4, 129.8, 129.8, 128.7, 128.2, 127.7, 127.6, 126.8, 126.8, 117.4, 93.2, 71.4, 63.5, 61.8, 26.8, 19.1; HRMS (ESI) *m/z*: calcd. for $C_{34}H_{36}O_4SiNa^+$ $(M + Na)^+$ 559.2281, found 559.2284; $[\alpha]_D^{24}$ = +40.9 (c = 1.0, $CHCl_3$).

4-Fluorophenyl 2,3-dideoxy-6-*O*-[(1,1-dimethylethyl)diphenylsilyl]-*α*-D-*threo*-hex-2-enopyranoside (25a)

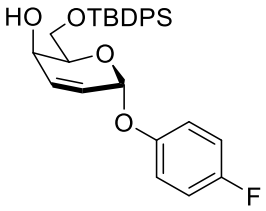

Colorless plate; 69%; ^{1}H NMR (400 MHz, $CDCl_3$) δ 7.72 – 7.61 (m, 4H), 7.48 – 7.34 (m, 6H), 7.03 – 6.96 (m, 2H), 6.95 – 6.88 (m, 2H), 6.10 (dd, *J* = 10.2, 1.5 Hz, 1H), 5.89 (dt, *J* = 10.2, 2.5 Hz, 1H), 5.59 – 5.44 (m, 1H), 4.37 – 4.31 (m, 1H), 3.95 – 3.81 (m, 3H), 2.55 (d, *J* = 4.7 Hz, 1H), 1.05 (s, 9H); ^{13}C NMR (101 MHz, $CDCl_3$) δ 159.5, 157.1, 153.6, 153.6, 135.8, 135.7, 134.1, 132.9, 130.1, 128.0, 127.9, 125.3, 118.7, 118.6, 116.0, 115.8, 93.8, 71.6, 66.1, 65.4, 27.0, 19.3; HRMS (ESI) *m/z*: calcd. for $C_{28}H_{31}O_4SiFNa^+$ $(M + Na)^+$ 501.1873, found 501.1867; $[\alpha]_D^{23}$ = -6.6 (c = 1.0, $CHCl_3$).

3,5-Dimethylphenyl 2,3-dideoxy-6-*O*-[(1,1-dimethylethyl)diphenylsilyl]-*α*-D-*threo*-hex-2-enopyranoside (26a)

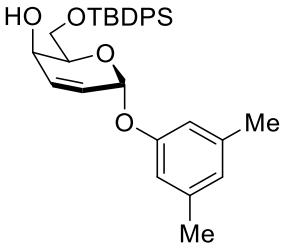

Colorless syrup; 73%; ^{1}H NMR (400 MHz, $CDCl_3$) δ 7.72 – 7.62 (m, 4H), 7.44 – 7.31 (m, 6H), 6.71 (s, 2H), 6.65 (s, 1H), 6.30 (ddd, *J* = 9.9, 5.7, 1.1 Hz, 1H), 6.04 (dd, *J* = 9.9, 3.2 Hz, 1H), 5.70 (d, *J* = 3.3 Hz, 1H), 4.25 (td, *J* = 6.1, 2.2 Hz, 1H), 4.09 – 4.03 (m, 1H), 3.96 – 3.88 (m, 2H), 2.25 (s, 6H), 2.10 (d, *J* = 7.9 Hz, 1H), 1.01 (s, 9H); ^{13}C NMR (101 MHz, $CDCl_3$) δ 157.5, 139.3, 135.7, 135.7, 133.3, 133.2, 130.3, 129.9, 129.9, 127.9, 127.9, 124.1, 114.7, 93.1, 71.4, 63.5, 61.8, 26.9, 21.5, 19.3; HRMS (ESI) *m/z*: calcd. for $C_{30}H_{36}O_4SiNa^+$ $(M + Na)^+$ 511.2281, found 511.2280; $[\alpha]_D^{24}$ = +4.1 (c = 1.0, $CHCl_3$).

3,4-Dimethylphenyl 2,3-dideoxy-6-*O*-[(1,1-dimethylethyl)diphenylsilyl]-*α*-D-*threo*-hex-2-enopyranoside (27a)

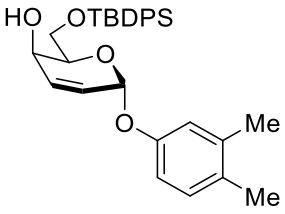

Colorless syrup; 70%; ^{1}H NMR (400 MHz, $CDCl_3$) δ 7.71 – 7.62 (m, 4H), 7.46 – 7.34 (m, 6H), 6.99 (d, *J* = 8.2 Hz, 1H), 6.87 (d, *J* = 2.6 Hz, 1H), 6.83 (dd, *J* = 8.2, 2.7 Hz, 1H), 6.30 (ddd, *J* = 9.9, 5.7, 1.1 Hz, 1H), 6.05 (dd, *J* = 9.9, 3.1 Hz, 1H), 5.67 (dd, *J* = 3.1, 1.1 Hz, 1H), 4.26 (td, *J* = 6.2, 2.2 Hz, 1H), 4.06 (ddd, *J* = 7.7, 5.7, 2.2 Hz, 1H), 4.01 – 3.84 (m, 2H), 2.19 (d, *J* = 2.5 Hz, 6H), 2.13 (d, *J* = 7.7 Hz, 1H), 1.02 (s, 9H);

^{13}C NMR (101 MHz, $CDCl_3$) δ 155.6, 137.8, 135.8, 135.7, 133.3, 133.3, 130.4, 130.4, 130.3, 129.9, 129.9, 128.0, 127.9, 118.6, 114.5, 93.5, 71.3, 63.5, 61.9, 26.9, 20.1, 19.3, 19.0, 0.1; HRMS (ESI) *m/z*: calcd. for $C_{30}H_{36}O_4SiNa^+$ $(M + Na)^+$ 511.2281, found 511.2281; $[\alpha]_D^{23}$= -41.4 (c = 1.0, $CHCl_3$).

2,6-Dimethylphenyl 2,3-dideoxy-6-*O*-[(1,1-dimethylethyl)diphenylsilyl]-*α*-D-*threo*-hex-2-enopyranoside (28a)

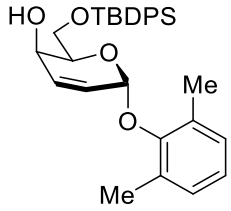

Colorless syrup; 34%; ^{1}H NMR (400 MHz, $CDCl_3$) δ 7.76 – 7.65 (m, 4H), 7.05 – 6.87 (m, 3H), 6.37 (dd, *J* = 10.0, 5.4 Hz, 1H), 6.20 (dd, *J* = 10.0, 3.1 Hz, 1H), 5.28 (dd, *J* = 3.1, 1.2 Hz, 1H), 4.43 (ddd, *J* = 7.8, 5.1, 2.3 Hz, 1H), 4.27 – 4.17 (m, 1H), 4.05 – 3.86 (m, 2H), 2.22 (d, *J* = 4.4 Hz, 1H), 2.18 (s, 6H), 1.07 (s, 9H); ^{13}C NMR (101 MHz, $CDCl_3$) δ 155.1, 135.7, 135.6, 133.2, 133.0, 131.1, 130.1, 130.0, 130.0, 129.0, 128.0, 128.0, 127.9, 127.8, 124.3, 97.3, 71.3, 63.1, 61.5, 27.0, 19.3, 17.1; HRMS (ESI) *m/z*: calcd. for $C_{30}H_{36}O_4SiNa^+$ $(M + Na)^+$ 511.2281, found 511.2282; $[\alpha]_D^{23}$ = -7.2 (c = 1.0, $CHCl_3$).

2-Naphthyl 2,3-dideoxy-6-*O*-[(1,1-dimethylethyl)diphenylsilyl]-*β*-D-*threo*-hex-2-enopyranoside (22b)

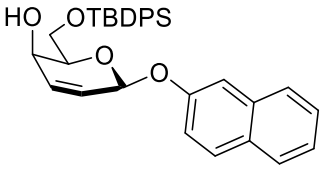

Colorless syrup; 88%; ^{1}H NMR (500 MHz, $CDCl_3$) δ 7.80 – 7.69 (m, 5H), 7.71 – 7.64 (m, 1H), 7.64 (d, *J* = 6.8 Hz, 1H), 7.48 (d, *J* = 2.5 Hz, 1H), 7.45 – 7.34 (m, 4H), 7.37 – 7.22 (m, 5H), 6.29 (ddd, *J* = 10.1, 5.1, 1.8 Hz, 1H), 6.03 (m, *J* = 10.0 Hz, 1H), 5.85 (d, *J* = 1.8 Hz, 1H), 4.15 – 3.92 (m, 4H), 2.13 (d, *J* = 9.9 Hz, 1H), 1.11 (s, 9H); ^{13}C NMR (126 MHz, $CDCl_3$) δ 154.9, 135.8, 135.7, 134.4, 133.4, 133.2, 131.7, 129.9, 129.9, 129.9, 129.8, 129.5, 127.9, 127.9, 127.7, 127.3, 126.4, 124.3, 119.0, 111.0, 96.2, 76.4, 63.8, 62.7, 27.0, 19.4; HRMS (ESI) *m/z*: calcd. for $C_{32}H_{34}O_4SiNa^+$ $(M + Na)^+$ 533.2124, found 533.2120; $[\alpha]_D^{24}$ = -91.0 (c = 1.0, $CHCl_3$).

4-Phenyl 2,3-dideoxy-6-*O*-[(1,1-dimethylethyl)diphenylsilyl]-*β*-D-*threo*-hex-2-enopyranoside (23b)

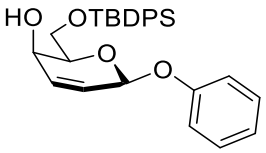

Colorless syrup; 85%; ^{1}H NMR (400 MHz, $CDCl_3$) δ 7.73 – 7.65 (m, 4H), 7.45 – 7.30 (m, 6H), 7.23 (d, *J* = 7.3 Hz, 2H), 7.11 (d, *J* = 7.7 Hz, 2H), 7.00 (t, *J* = 7.3 Hz, 1H), 6.25 (ddd, *J* = 10.0, 5.1, 1.5 Hz, 1H), 6.01 (d, *J* = 10.0 Hz, 1H), 5.70 (q, *J* = 1.5 Hz, 1H), 4.07 – 3.89 (m, 4H), 2.00 (s, 1H), 1.09 (s, 9H); ^{13}C NMR (101 MHz, $CDCl_3$) δ 157.1, 135.8, 133.3, 131.6, 130.1, 129.9, 129.8, 129.6, 127.9, 127.8, 122.5, 116.7, 96.1, 76.5, 63.7, 62.7, 26.9, 19.3; HRMS (ESI) *m/z*: calcd. for $C_{28}H_{32}O_4SiNa^+$ $(M + Na)^+$ 483.1968, found 483.1970; $[\alpha]_D^{23}$ = -105.7 (c = 0.77, $CHCl_3$).

4-Phenylphenyl 2,3-dideoxy-6-*O*-[(1,1-dimethylethyl)diphenylsilyl]-*β*-D-*threo*-hex-2-enopyranoside (24b)

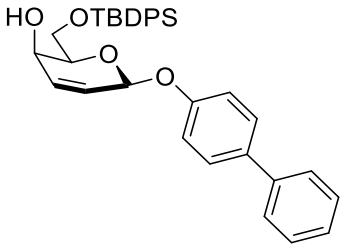

Colorless syrup; 89%; ^{1}H NMR (400 MHz, $CDCl_3$) δ 7.78 – 7.66 (m, 4H), 7.57 – 7.49 (m, 2H), 7.50 – 7.28 (m, 11H), 7.23 – 7.13 (m, 2H), 6.27 (ddd, *J* = 10.1, 5.1, 1.5 Hz, 1H), 6.03 (d, *J* = 10.0 Hz, 1H), 5.74 (d, *J* = 10.0 Hz, 1H), 4.15 – 3.85 (m, 4H), 2.06 (d, *J* = 10.0 Hz, 1H), 1.10 (s, 9H); ^{13}C NMR (101 MHz, $CDCl_3$) δ 156.6, 140.8, 135.8, 135.8, 135.6, 133.3, 133.2, 131.7, 129.9, 129.9, 129.9, 128.8, 128.3, 127.9, 127.8, 127.0, 117.0, 96.1, 76.5, 63.7, 62.7, 27.0, 19.4; HRMS (ESI) *m/z*: calcd. for $C_{34}H_{36}O_4SiNa^+$ $(M + Na)^+$ 559.2281, found 559.2281; $[\alpha]_D^{23}$ = -113.1 (c = 1.0, $CHCl_3$).

4-Fluorophenyl 2,3-dideoxy-6-*O*-[(1,1-dimethylethyl)diphenylsilyl]-*β*-D-*threo*-hex-2-enopyranoside (25b)

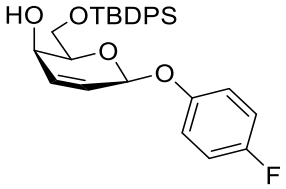

Colorless syrup; 75%; ^{1}H NMR (400 MHz, $CDCl_3$) ^{1}H NMR (400 MHz, $CDCl_3$) δ 7.72 – 7.66 (m, 4H), 7.46 – 7.32 (m, 6H), 7.10 – 7.05 (m, 2H), 6.94 – 6.87 (m, 2H), 6.25 (ddd, *J* = 10.0, 5.1, 1.5 Hz, 1H), 5.99 (d, *J* = 10.0 Hz, 1H), 5.61 (d, *J* = 1.5 Hz, 1H), 4.02 (dd, *J* = 10.1, 5.1 Hz, 1H), 3.99 – 3.89 (m, 3H), 1.97 (d, *J* = 10.1 Hz, 1H), 1.08 (s,

9H); ^{13}C NMR (101 MHz, $CDCl_3$) δ 159.6, 157.2, 153.2, 153.2, 135.8, 135.7, 135.7, 135.7, 133.3, 133.2, 131.7, 130.0, 129.9, 129.9, 127.9, 127.9, 118.2, 118.1, 116.0, 115.8, 96.7, 76.4, 63.6, 62.6, 26.9, 19.3; HRMS (ESI) *m/z*: calcd. for $C_{28}H_{31}O_4SiFNa^+$ $(M + Na)^+$ 501.1873, found 501.1875; $[\alpha]_D^{23}$ = -76.7 (c = 1.0, $CHCl_3$).

3,5-Dimethylphenyl 2,3-dideoxy-6-*O*-[(1,1-dimethylethyl)diphenylsilyl]-*β*-D-*threo*-hex-2-enopyranoside (26b)

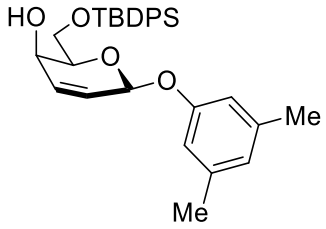

Colorless syrup; 82%; ^{1}H NMR (400 MHz, $CDCl_3$) δ 7.75 – 7.66 (m, 4H), 7.47 – 7.26 (m, 6H), 6.72 (s, 2H), 6.66 (s, 1H), 6.25 (ddd, *J* = 10.0, 5.1, 1.5 Hz, 1H), 5.97 (d, *J* = 10.0 Hz, 1H), 5.69 (d, *J* = 1.5 Hz, 1H), 4.08 – 3.86 (m, 4H), 2.23 (s, 6H), 2.05 (d, *J* = 10.0 Hz, 1H), 1.08 (s, 9H); ^{13}C NMR (101 MHz, $CDCl_3$) δ 157.1, 139.3, 135.8, 135.7, 133.3, 133.3, 131.5, 130.0, 129.9, 129.8, 127.9, 127.8, 124.3, 114.4, 95.9, 76.3, 63.8, 62.7, 27.0, 21.5, 19.3; HRMS (ESI) *m/z*: calcd. for $C_{30}H_{36}O_4SiNa^+$ $(M + Na)^+$ 511.2281, found 511.2278; $[\alpha]_D^{23}$ = -100.6 (c = 1.0, $CHCl_3$).

3,5-Dimethylphenyl 2,3-dideoxy-6-*O*-[(1,1-dimethylethyl)diphenylsilyl]-*β*-D-*threo*-hex-2-enopyranoside (27b)

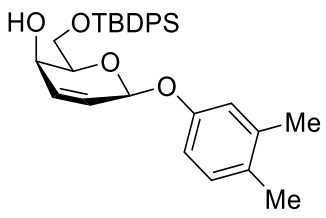

Colorless syrup; 83%; ^{1}H NMR (400 MHz, $CDCl_3$) δ 7.77 – 7.67 (m, 4H), 7.48 – 7.30 (m, 6H), 7.03 – 6.95 (m, 1H), 6.89 (s, 1H), 6.87 (d, *J* = 2.7 Hz, 1H), 6.25 (ddd, *J* = 10.0, 5.0, 1.5 Hz, 1H), 5.99 (d, *J* = 10.0 Hz, 1H), 5.66 (d, *J* = 1.5 Hz, 1H), 4.07 – 3.95 (m, 2H), 3.97 – 3.87 (m, 2H), 2.19 (s, 6H), 2.05 (d, *J* = 13.9 Hz, 1H), 1.10 (s, 9H); ^{13}C NMR (101 MHz, $CDCl_3$) δ 155.2, 137.8, 135.8, 135.7, 133.4, 133.3, 131.5, 130.6, 130.4, 130.1, 129.9, 129.8, 127.9, 127.8, 118.3, 113.9, 96.4, 76.3, 63.6, 62.6, 27.0, 20.1, 19.3, 19.0; HRMS (ESI) *m/z*: calcd. for $C_{30}H_{36}O_4SiNa^+$ $(M + Na)^+$ 511.2281, found 511.2276; $[\alpha]_D^{23}$ = -130.3 (c = 1.0, $CHCl_3$).

2,6-Dimethylphenyl 2,3-dideoxy-6-*O*-[(1,1-dimethylethyl)diphenylsilyl]-*β*-D-*threo*-hex-2-enopyranoside (28b)

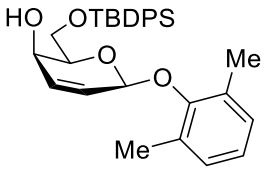

Colorless syrup; 44%; ^{1}H NMR (400 MHz, $CDCl_3$) δ 7.70 – 7.60 (m, 4H), 7.47 – 7.31 (m, 6H), 7.01 (d, *J* = 6.4 Hz, 2H), 6.99 – 6.91 (m, 1H), 6.29 (ddd, *J* = 10.0, 5.2, 1.5 Hz, 1H), 6.15 (d, *J* = 10.0 Hz, 1H), 5.30 (d, *J* = 1.5 Hz, 1H), 4.11 – 4.03 (m, 1H), 3.95 (dd, *J* = 10.3, 7.1 Hz, 1H), 3.81 (dd, *J* = 10.3, 5.7 Hz, 1H), 3.67 (ddd, *J* = 7.5, 5.7, 2.1 Hz, 1H), 2.29 (s, 6H), 2.10 (d, *J* = 9.5 Hz, 1H), 1.02 (s, 9H); ^{13}C NMR (101 MHz, $CDCl_3$) δ 154.7, 135.7, 135.7, 133.4, 133.3, 131.6, 131.6, 130.6, 129.9, 129.8, 128.9, 127.9, 127.8, 124.6, 100.4, 75.8, 63.0, 62.3, 29.8, 26.9, 19.3, 17.5; HRMS (ESI) *m/z*: calcd. for $C_{30}H_{36}O_4SiNa^+$ $(M + Na)^+$ 511.2281, found 511.2278; $[\alpha]_D^{24}$ = -70.8 (c = 1.0, $CHCl_3$).

_p_-Hydroxybenzyl 2,3-dideoxy-6-_O_-[(1,1-dimethylethyl)dimethylsilyl]-_α_-D-_threo_-hex-2-enopyranoside (29)

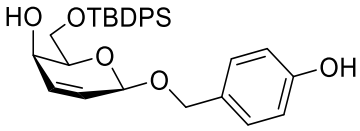

Colorless syrup; 88%; ^{1}H NMR (400 MHz, $CDCl_3$) δ 7.81 – 7.71 (m, 4H), 7.50 – 7.30 (m, 6H), 7.18 (d, *J* = 8.5 Hz, 2H), 6.75 (d, *J* = 8.5 Hz, 2H), 6.15 (ddd, *J* = 10.1, 5.1, 1.5 Hz, 1H), 5.84 (d, *J* = 10.1 Hz, 1H), 5.54 (s, 1H), 5.11 (d, *J* = 1.5 Hz, 1H), 4.77 (d, *J* = 11.3 Hz, 1H), 4.53 (d, *J* = 11.3 Hz, 1H), 4.20 – 3.95 (m, 2H), 3.97 – 3.89 (m, 1H), 3.78 (td, *J* = 6.2, 2.3 Hz, 1H), 2.29 (d, *J* = 9.6 Hz, 1H), 1.09 (s, 9H); ^{13}C NMR (101 MHz, $CDCl_3$) δ 155.7, 135.7, 135.7, 133.5, 133.4, 131.0, 130.1, 129.9, 129.9, 129.3, 127.9, 127.9, 115.4, 96.6, 75.9, 69.8, 63.7, 62.9, 27.0, 19.4; HRMS (ESI) *m/z*: calcd. for $C_{29}H_{34}O_5SiNa^+$ $(M + Na)^+$ 513.2073, found 513.2072; $[\alpha]_D^{24}$ = -49.4 (c = 1.0, $CHCl_3$).

_o_-Hydroxybenzyl 2,3-dideoxy-6-_O_-[(1,1-dimethylethyl)dimethylsilyl]-_α_-D-_threo_-hex-2-enopyranoside (30)

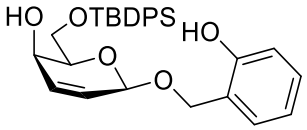

Colorless syrup; 86%; ^{1}H NMR (400 MHz, $CDCl_3$) δ 7.75 – 7.62 (m, 4H), 7.49 – 7.34 (m, 6H), 7.27 – 7.18 (m, 1H), 7.07 (dd, *J* = 7.5, 1.7 Hz, 1H), 6.98 (br s, 1H), 6.93 – 6.79 (m, 2H), 6.21 (ddd, *J* = 10.1, 5.3, 1.5 Hz, 1H), 5.85 (d, *J* = 10.1 Hz, 1H), 5.24 (d, *J* = 1.5 Hz, 1H), 4.92 (d, *J* = 11.8 Hz, 1H), 4.74 (d, *J* = 11.8 Hz, 1H), 4.10 – 3.96 (m, 2H), 3.98 – 3.89 (m, 1H), 3.80 (td, *J* = 6.2, 2.2 Hz, 1H), 1.97 (d, *J* = 9.2 Hz, 1H), 1.08 (s, 9H); ^{13}C NMR (101 MHz, $CDCl_3$) δ 156.0, 135.8, 135.7, 133.4, 133.2, 131.6, 130.2, 130.0, 130.0, 129.6, 127.9, 122.3, 120.1, 116.9, 97.0, 76.1, 68.0, 63.2, 62.5, 27.0, 19.4;

HRMS (ESI) *m/z*: calcd. for $C_{29}H_{34}O_5SiNa^+$ $(M + Na)^+$ 513.2073, found 513.2084; $[\alpha]_D^{24}$ = -43.3 (c = 1.0, $CHCl_3$).

Methyl 2,3-dideoxy-6-*O*-[(1,1-dimethylethyl)dimethylsilyl]-*β*-D-*threo*-hex-2-enopyranoside (32)

Colorless syrup; 95%; ^{1}H NMR (400 MHz, $CDCl_3$) δ 6.14 (ddd, *J* = 10.2, 5.1, 1.4 Hz, 1H), 5.81 (d, *J* = 10.2 Hz, 1H), 4.97 (d, *J* = 1.4 Hz, 1H), 4.00 – 3.88 (m, 2H), 3.81 (dd, *J* = 10.5, 5.8 Hz, 1H), 3.68 (td, *J* = 6.3, 2.3 Hz, 1H), 3.50 (s, 3H), 2.15 (d, *J* = 9.3 Hz, 1H), 0.90 (s, 9H), 0.09 (s, 6H); ^{13}C NMR (101 MHz, $CDCl_3$) δ 131.2, 130.6, 98.8, 75.6, 62.8, 62.7, 55.9, 26.0, 18.4, -5.2, -5.3; HRMS (ESI) *m/z*: calcd. for $C_{13}H_{27}O_4Si^+$ $(M + H)^+$ 275.1679, found 275.1682; $[\alpha]_D^{24}$ = -83.7 (c = 1.0, $CHCl_3$).

2-Phenyl 2,3-dideoxy-6-*O*-[(1,1-dimethylethyl)dimethylsilyl]-*α*-D-*threo*-hex-2-enopyranoside (33a)

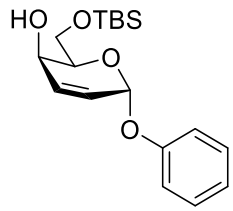

Colorless syrup; 61%; ^{1}H NMR (400 MHz, $CDCl_3$) δ 7.35 – 7.27 (m, 2H), 7.15 – 7.08 (m, 2H), 7.05 – 6.96 (m, 1H), 6.31 (ddd, *J* = 10.0, 5.6, 1.1 Hz, 1H), 6.06 (dd, *J* = 10.0, 3.2 Hz, 1H), 5.77 – 5.67 (m, 1H), 4.17 (td, *J* = 6.1, 2.3 Hz, 1H), 4.07 – 3.99 (m, 1H), 3.95 – 3.76 (m, 2H), 2.35 (d, *J* = 7.0 Hz, 1H), 0.86 (s, 9H), 0.07 (s, 3H), 0.04 (s, 3H); ^{13}C NMR (126 MHz, $CDCl_3$) δ 157.5, 130.5, 129.6, 127.7, 122.3, 117.2, 93.3, 71.2,

62.9, 61.9, 25.9, 18.3, -5.3, -5.4; HRMS (ESI) *m/z*: calcd. for $C_{18}H_{28}O_4SiNa^+$ $(M + Na)^+$ 359.1649, found 359.1647; $[\alpha]_D^{24}$ = +103.3 (c = 1.0, $CHCl_3$).

2-Phenyl 2,3-dideoxy-6-*O*-[(1,1-dimethylethyl)dimethylsilyl]-*β*-D-*threo*-hex-2-enopyranoside (33b)

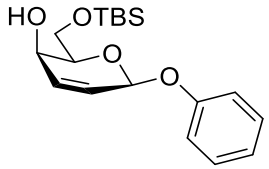

Colorless syrup; 72%; ^{1}H NMR (400 MHz, $CDCl_3$) δ 7.34 – 7.27 (m, 2H), 7.15 – 7.08 (m, 2H), 7.05 – 6.99 (m, 1H), 6.25 (ddd, *J* = 10.1, 4.8, 1.4 Hz, 1H), 5.99 (d, *J* = 10.1 Hz, 1H), 5.68 (d, *J* = 1.7 Hz, 1H), 4.10 – 4.00 (m, 1H), 3.98 – 3.95 (m, 1H), 3.92 – 3.79 (m, 2H), 2.17 (d, *J* = 9.8 Hz, 1H), 0.91 (s, 9H), 0.08 (s, 6H); ^{13}C NMR (101 MHz, $CDCl_3$) δ 157.2, 131.8, 129.6, 129.6, 122.5, 116.8, 96.0, 62.8, 62.8, 26.0, 18.4, -5.2, -5.4; HRMS (ESI) *m/z*: calcd. for $C_{18}H_{28}O_4SiNa^+$ $(M + Na)^+$ 359.1649, found 359.1646; $[\alpha]_D^{24}$ = -137.6 (c = 0.82, $CHCl_3$).

[2*S*-(2*α*,3*α*,6*α*)]-3,6-Dihydro-6-methoxy-2-methyl-2*H*-pyran-3-ol (35)

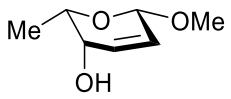

Colorless syrup; 90%; ^{1}H NMR (400 MHz, $CDCl_3$) δ 6.12 (ddd, *J* = 10.0, 5.1, 1.5 Hz, 1H), 5.79 (d, *J* = 10.0 Hz, 1H), 4.94 (d, *J* = 1.5 Hz, 1H), 3.76 – 3.67 (m, 1H), 3.67 – 3.62 (m, 1H), 3.48 (s, 3H), 1.98 (br s, 1H), 1.29 (d, *J* = 6.5 Hz, 3H); ^{13}C NMR (101 MHz, $CDCl_3$) δ 131.5, 130.6, 98.9, 71.5, 64.8, 55.8, 16.7; HRMS (ESI) *m/z*: calcd. for $C_7H_{13}O_3^+$ $(M + H)^+$ 145.0865, found 145.0865; $[\alpha]_D^{24}$ = +118.2 (c = 1.0, $CHCl_3$).

[2*S*-(2*α*,3*α*,6*β*)]-3,6-Dihydro-6-phenoxy-2-methyl-2*H*-pyran-3-ol (36a)

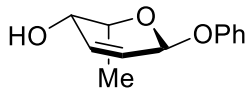

Colorless syrup; 58%; ^{1}H NMR (400 MHz, $CDCl_3$) δ 7.30 (dd, *J* = 8.7, 7.3 Hz, 2H), 7.16 – 7.07 (m, 2H), 7.03 (tt, *J* = 7.3, 1.1 Hz, 1H), 6.33 (ddd, *J* = 9.9, 5.6, 1.0 Hz, 1H), 6.04 (dd, *J* = 9.9, 3.2 Hz, 1H), 5.68 (d, *J* = 3.2 Hz, 1H), 4.28 (qd, *J* = 6.6, 2.2 Hz, 1H), 3.74 – 3.67 (m, 1H), 1.50 (br s, 1H), 1.29 (d, *J* = 6.6 Hz, 3H); ^{13}C NMR (101 MHz, $CDCl_3$) δ 157.6, 131.2, 129.6, 127.6, 122.3, 117.1, 93.4, 67.5, 63.9, 16.2; HRMS (ESI) *m/z*: calcd. for $C_{12}H_{15}O_3^+$ $(M + H)^+$ 207.1021, found 207.1017; $[\alpha]_D^{24}$ = +107.8 (c = 0.74, $CHCl_3$).

[2*S*-(2*α*,3*α*,6*α*)]-3,6-Dihydro-6-phenoxy-2-methyl-2*H*-pyran-3-ol (36b)

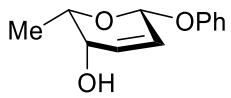

Colorless syrup; 60%; ^{1}H NMR (400 MHz, $CDCl_3$) δ 7.36 – 7.27 (m, 2H), 7.14 – 7.07 (m, 2H), 7.07 – 6.98 (m, 1H), 6.26 (ddd, *J* = 10.0, 5.1, 1.5 Hz, 1H), 5.99 (d, *J* = 10.0 Hz, 1H), 5.69 (q, *J* = 1.5 Hz, 1H), 3.92 (qd, *J* = 6.5, 2.4 Hz, 1H), 3.82 – 3.71 (m, 1H), 1.68 (d, *J* = 11.1 Hz, 1H), 1.38 (d, *J* = 6.5 Hz, 3H); ^{13}C NMR (101 MHz, $CDCl_3$) δ 157.0, 131.8, 129.7, 129.5, 122.4, 116.6, 96.1, 71.8, 64.5, 16.6; HRMS (ESI) *m/z*: calcd. for $C_{12}H_{15}O_3^+$ $(M + H)^+$ 207.1021, found 207.1017; $[\alpha]_D^{24}$ = +65.2 (c = 1.0, $CHCl_3$).

Methyl 2,3-dideoxy-6-*O*-[(1,1-dimethylethyl)dimethylsilyl]-*α*-D-erythro-hex-2-enopyranoside (38)

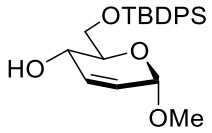

Colorless syrup; 93%; ^{1}H NMR (400 MHz, $CDCl_3$) δ 7.76 – 7.67 (m, 4H), 7.50 – 7.36 (m, 6H), 5.95 (d, *J* = 10.2, 1H), 5.75 (dt, *J* = 10.2, 2.4 Hz, 1H), 4.83 (s, 1H), 4.23 (d, *J* = 8.9 Hz, 1H), 4.00 – 3.83 (m, 2H), 3.78 (dt, *J* = 8.9, 5.6 Hz, 1H), 3.39 (s, 3H), 2.58 (s, 1H), 1.08 (s, 9H); ^{13}C NMR (101 MHz, $CDCl_3$) δ 135.6, 135.6, 133.0, 132.8, 129.9, 127.8, 127.8, 125.9, 95.2, 70.6, 66.5, 65.7, 55.7, 26.8, 19.2; HRMS (ESI) *m/z*: calcd. for $C_{23}H_{30}O_4SiNa^+$ $(M + Na)^+$ 421.1811, found 421.1812; $[\alpha]_D^{24}$ = +37.2 (c = 1.0, $CHCl_3$).

Phenyl 2,3-dideoxy-6-*O*-[(1,1-dimethylethyl)dimethylsilyl]-*β*-D-erythrohex-2-enopyranoside (39b)

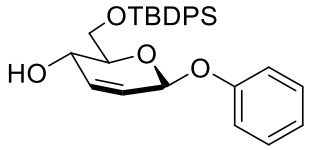

Colorless syrup; 71%; ^{1}H NMR (500 MHz, $CDCl_3$) δ 7.70 – 7.60 (m, 4H), 7.48 – 7.32 (m, 6H), 7.25 – 7.19 (m, 2H), 7.07 – 6.95 (m, 3H), 6.09 (ddd, *J* = 10.2, 2.9, 1.7 Hz, 1H), 5.91 (dt, *J* = 10.2, 1.7 Hz, 1H), 5.76 (d, *J* = 1.7 Hz, 1H), 4.37 (br s, 1H), 3.95 – 3.83 (m, 3H), 2.56 (d, *J* = 5.1 Hz, 1H), 1.06 (s, 9H); ^{13}C NMR (101 MHz, $CDCl_3$) δ 156.9, 135.8, 135.7, 135.7, 132.9, 132.9, 132.3, 130.1, 130.0, 129.5, 128.0, 127.5, 122.4, 116.8, 94.7, 65.3, 65.2, 29.9, 27.0, 19.3; HRMS (ESI) *m/z*: calcd. for $C_{28}H_{32}O_4SiNa^+$ $(M + Na)^+$ 483.1968, found 483.1971; $[\alpha]_D^{24}$ = -13.5 (c = 0.5, $CHCl_3$).

2D-NOESY of **39b**

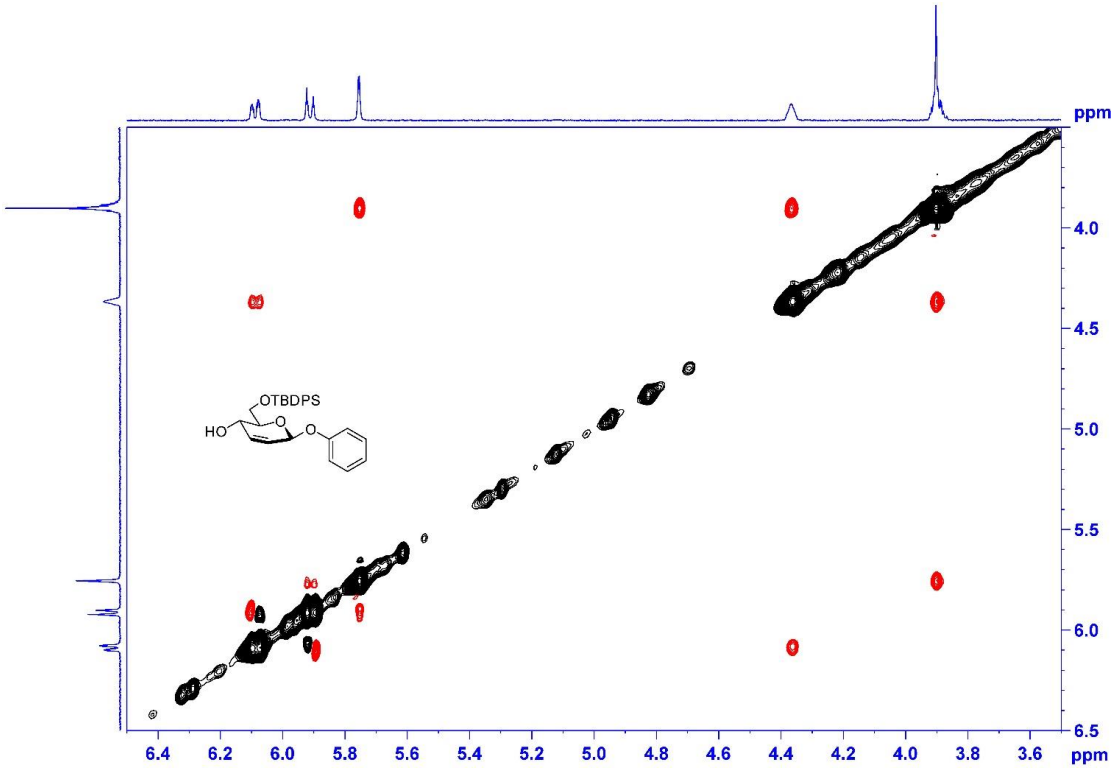

Phenyl 2,3-dideoxy-6-*O*-[(1,1-dimethylethyl)dimethylsilyl]-*α*-D-erythro-hex-2-enopyranoside (39a)

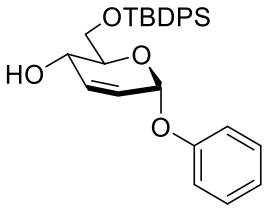

Colorless syrup; 76%; ^{1}H NMR (500 MHz, $CDCl_3$) δ 7.70 – 7.64 (m, 4H), 7.49 – 7.34 (m, 6H), 7.29 – 7.24 (m, 2H), 7.07 – 7.03 (m, 2H), 7.02 – 6.97 (m, 1H), 6.11 (dd, *J* = 10.2, 1.4 Hz, 1H), 5.91 (dt, *J* = 10.1, 2.4 Hz, 1H), 5.62 (d, *J* = 1.4 Hz, 1H), 4.38 (d, *J* = 4.6 Hz, 1H), 3.98 – 3.88 (m, 2H), 3.88 – 3.81 (m, 1H), 2.63 (d, *J* = 4.6 Hz, 1H), 1.05 (s, 9H); ^{13}C NMR (101 MHz, $CDCl_3$) δ 157.5, 135.8, 135.7, 133.9, 132.91, 132.9, 130.0,

130.0, 129.6, 128.0, 127.9, 125.4, 122.3, 117.1, 93.1, 77.5, 77.4, 77.2, 76.9, 76.8, 71.5, 66.2, 65.5, 27.0, 19.3; HRMS (ESI) *m/z*: calcd. for $C_{28}H_{32}O_4SiNa^+$ $(M + Na)^+$ 483.1968, found 483.1968; $[\alpha]_D^{24}$ = +44.6 (c = 1.0, $CHCl_3$)

2D-NOESY of **39a**

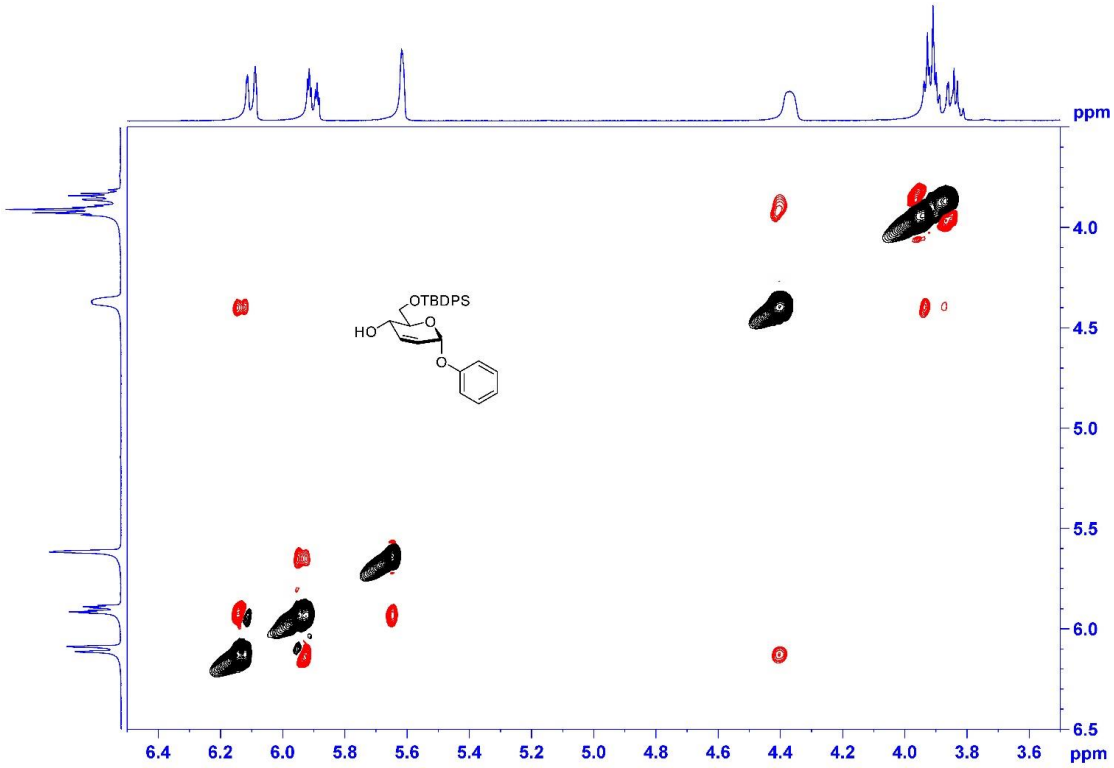

Methyl 2,3,6-trideoxy-*α*-D-erythro-hex-2-enopyranoside (41)

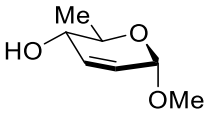

Colorless syrup; 89%; ^{1}H NMR (400 MHz, $CDCl_3$) δ 5.93 (d, *J* = 10.1 Hz, 1H), 5.76 (ddd, *J* = 10.1, 2.7, 2.1 Hz, 1H), 4.84 – 4.82 (m, 1H), 3.85 (dd, *J* = 8.4, 1.9 Hz, 1H), 3.74 – 3.65 (m, 1H), 3.43 (s, 3H), 1.42 (d, *J* = 8.4 Hz, 1H), 1.34 (d, *J* = 6.2 Hz, 3H); ^{13}C NMR (101 MHz, $CDCl_3$) δ 133.6, 126.8, 95.5, 69.9, 68.1, 55.8, 18.1; HRMS (ESI)

m/z: calcd. for $C_7H_{13}O_3^+$ $(M + H)^+$ 145.0865, found 145.0866; $[\alpha]_D^{21}$ = +105.1 (c = 1.0, $CHCl_3$).

Phenyl 2,3,6-trideoxy-*β*-D-erythro-hex-2-enopyranoside (42b)

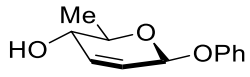

Colorless syrup; 70%; ^{1}H NMR (400 MHz, $CDCl_3$) δ 7.32 – 7.27 (m, 2H), 7.11 – 7.07 (m, 2H), 7.04 – 6.99 (m, 1H), 6.12 (ddd, *J* = 10.2, 3.3, 1.6 Hz, 1H), 5.97 (dt, *J* = 10.2, 1.6 Hz, 1H), 5.77 (d, *J* = 1.7 Hz, 1H), 3.97 (s, 1H), 3.93 – 3.85 (m, 1H), 1.71 (d, *J* = 7.9 Hz, 1H), 1.40 (d, *J* = 6.5 Hz, 3H); ^{13}C NMR (101 MHz, $CDCl_3$) δ 157.2, 131.8, 129.6, 128.0, 122.3, 116.7, 94.1, 74.9, 67.7, 18.8; HRMS (ESI) *m/z*: calcd. for $C_{12}H_{15}O_3^+$ $(M + H)^+$ 207.1021, found 207.1019; $[\alpha]_D^{21}$ = +20.8 (c = 1.0, $CHCl_3$).

Phenyl 2,3,6-trideoxy-*α*-D-erythro-hex-2-enopyranoside (42a)

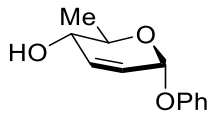

Colorless syrup; 75%; ^{1}H NMR (400 MHz, $CDCl_3$) δ 7.32 – 7.28 (m, 2H), 7.11 – 7.08 (m, 2H), 7.04 – 7.00 (m, 1H), 6.08 (d, *J* = 10.3 Hz, 1H), 5.91 (dt, *J* = 10.1, 2.4 Hz, 1H), 5.62 (d, *J* = 1.2 Hz, 1H), 3.96 – 3.89 (m, 1H), 3.89 – 3.81 (m, 1H), 1.60 (d, *J* = 7.9 Hz, 1H), 1.32 (d, *J* = 6.0 Hz, 3H); ^{13}C NMR (101 MHz, $CDCl_3$) δ 157.6, 134.4, 129.6, 126.1, 122.2, 117.0, 93.2, 69.6, 69.1, 18.1; HRMS (ESI) *m/z*: calcd. for $C_{12}H_{15}O_3^+$ $(M + H)^+$ 207.1021, found 207.1022; $[\alpha]_D^{21}$ = +157.4 (c = 1.0, $CHCl_3$).

2.4.2 Experimental procedure and characterization data of S4

Methyl 2,3-dideoxy-6-*O*-*p*-nitrobenzoyl-*α*-D-*threo*-hex-2-enopyranoside (S4)

To a solution of **2** (39.8 mg, 0.10 mmol) in 2 ml of THF was added TBAF (228.8 mg, 0.11 mmol) and stirred for 2 h at room temperature. The resulting mixture was diluted with ethyl acetate, then extracted with ethyl acetate (3 × 20 mL). The combined organic phase was washed with water, brine, dried ($MgSO_4$), and concentrated. Purification of the residue by flash column chromatography on silica gel (hexane:EtOAc) gave **S3**. A mixture of **S3** (16.0 mg, 0.10 mmol), 4-nitrobenzoyl chloride (18.5 mg, 0.10 mmol) and DMAP (24.4 mg, 0.20 mmol) were stirred in anhydrous CH_2Cl_2 for 1 h, monitored by TLC. When the starting material was consumed completely, the solution was diluted by CH_2Cl_2 and washed with water and brine. The solvent was removed under reduced pressure and the residue was purified by flash column (Hex:EA=3:2). White solid **S4** was obtained in 50% yield, which was used to grow crystal for X-ray analysis.

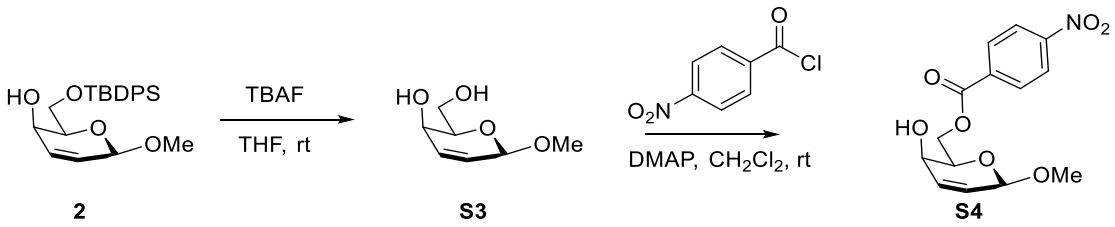

2 **S3** **S4**

^{1}H NMR (400 MHz, $CDCl_3$) δ 8.33 – 8.28 (m, 2H), 8.26 – 8.20 (m, 2H), 6.19 (ddd, *J* = 10.1, 4.9, 1.5 Hz, 1H), 5.90 (d, *J* = 10.1 Hz, 1H), 5.05 (d, *J* = 1.5 Hz, 1H), 4.72 – 4.58 (m, 2H), 4.08 – 3.96 (m, 2H), 3.53 (s, 3H), 1.90 (d, *J* = 10.6 Hz, 1H); ^{13}C NMR (101 MHz, $CDCl_3$) δ 164.7, 150.8, 135.5, 131.2, 130.9, 130.6, 123.7, 98.8, 73.4, 65.0, 62.6,

56.0; HRMS (ESI) *m/z*: calcd. for $C_{14}H_{15}NO_7Na^+$ $(M + Na)^+$ 332.0746, found 332.0751; $[\alpha]_D^{24}$ = -38.9 (c = 1.0, $CHCl_3$).

2.4.3 Azidotrimethylsilane tested as non-hydrogen-bonding acceptor

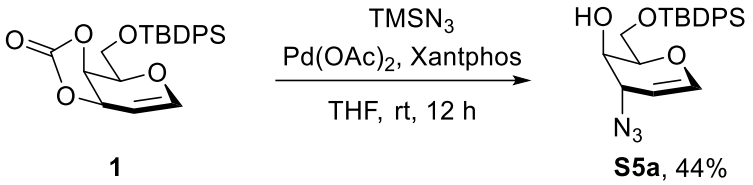

1 **S5a**, 44%

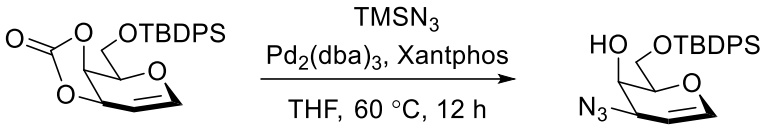

1 **S5b**, 40%

In our proposed mechanism, palladium(II) and palladium(0) condition would go through two opposite intermediates. $TMSN_3$ which cannot form H-bonding was a good glycosyl acceptor to test the direction of the palladium/π-allyl complex after decarboxylation. Although no *N*-glycosides were obtained, the azide group was axial on the C3 position of the product **S5a** from palladium(II) condition but equatorial (**S5b**) in palladium(0) system and the relative configurations were confirmed by NOE experiments. These two opposite selectivities illustrated palladium(II) did coordinate with the *β*-face while palladium(0) went to α-face. These results supported proposed mechanism pathways.

(2*R*,3*R*,4*R*)-4-azido-3,4-dihydro-2-((*tert*-butyldiphenylsilyl)methoxy)-2*H*-pyran-3-ol (S5a)

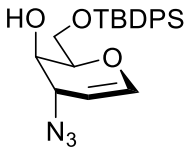

Colorless syrup; 44%; ^{1}H NMR (400 MHz, $CDCl_3$) δ 7.73 – 7.68 (m, 4H), 7.47 – 7.39 (m, 6H), 6.73 (d, *J* = 5.7 Hz, 1H), 4.93 (td, *J* = 5.7, 1.9 Hz, 1H), 4.09 (dd, *J* = 11.3, 4.1 Hz, 1H), 4.04 – 3.94 (m, 2H), 3.79 (d, *J* = 4.6 Hz, 1H), 3.75 (d, *J* = 3.6 Hz, 1H), 3.55 (br s, 1H), 1.07 (s, 9H); ^{13}C NMR (101 MHz, $CDCl_3$) δ 146.5, 135.8, 135.7, 132.9, 132.7, 130.1, 128.0, 97.5, 76.3, 65.8, 63.5, 56.4, 26.9, 19.3; HRMS (ESI) *m/z*: calcd. for $C_{22}H_{27}O_3N_3SiNa^+$ $(M + Na)^+$ 432.1719, found 432.1724; $[\alpha]_D^{24}$ = -27.8 (c = 0.8, $CHCl_3$).

(2*R*,3*R*,4*S*)-4-azido-3,4-dihydro-2-((*tert*-butyldiphenylsilyl)methoxy)-2*H*-pyran-3-ol (S5b)

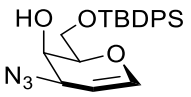

Colorless syrup; 40%; ^{1}H NMR (500 MHz, $CDCl_3$) δ 7.73 – 7.65 (m, 4H), 7.49 – 7.39 (m, 6H), 6.52 (dd, *J* = 6.2, 2.1 Hz, 1H), 4.74 (dt, *J* = 6.2, 2.1 Hz, 1H), 4.24 (s, 1H), 4.10 – 3.96 (m, 2H), 3.94 – 3.84 (m, 2H), 2.78 (d, *J* = 5.1 Hz, 1H), 1.07 (s, 9H); ^{13}C NMR (101 MHz, $CDCl_3$) δ 148.4, 135.8, 135.7, 135.7, 132.5, 132.2, 130.2, 130.2, 128.1, 128.0, 95.2, 72.4, 68.8, 65.2, 55.7, 26.9, 19.3; HRMS (ESI) *m/z*: calcd. for $C_{22}H_{27}O_3N_3SiNa^+$ $(M + Na)^+$ 432.1719, found 432.1720; $[\alpha]_D^{24}$ = +213.0 (c = 1.0, $CHCl_3$).

2D-NOESY of **S5a**

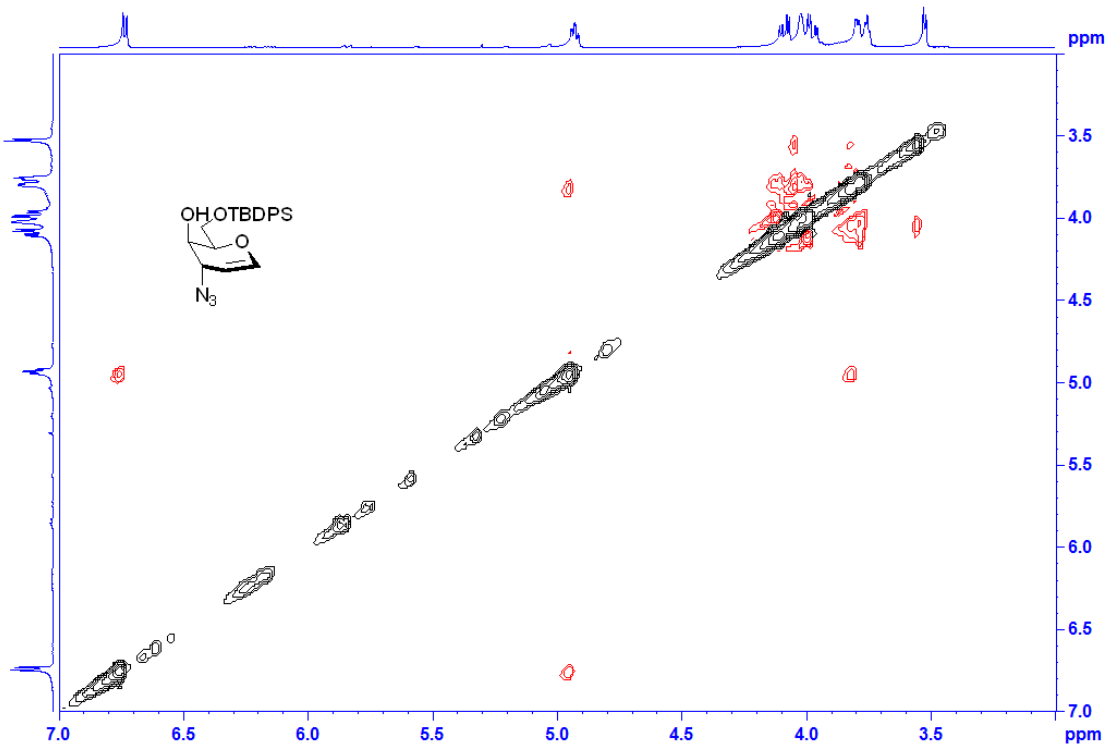

2D-NOESY of **S5b**

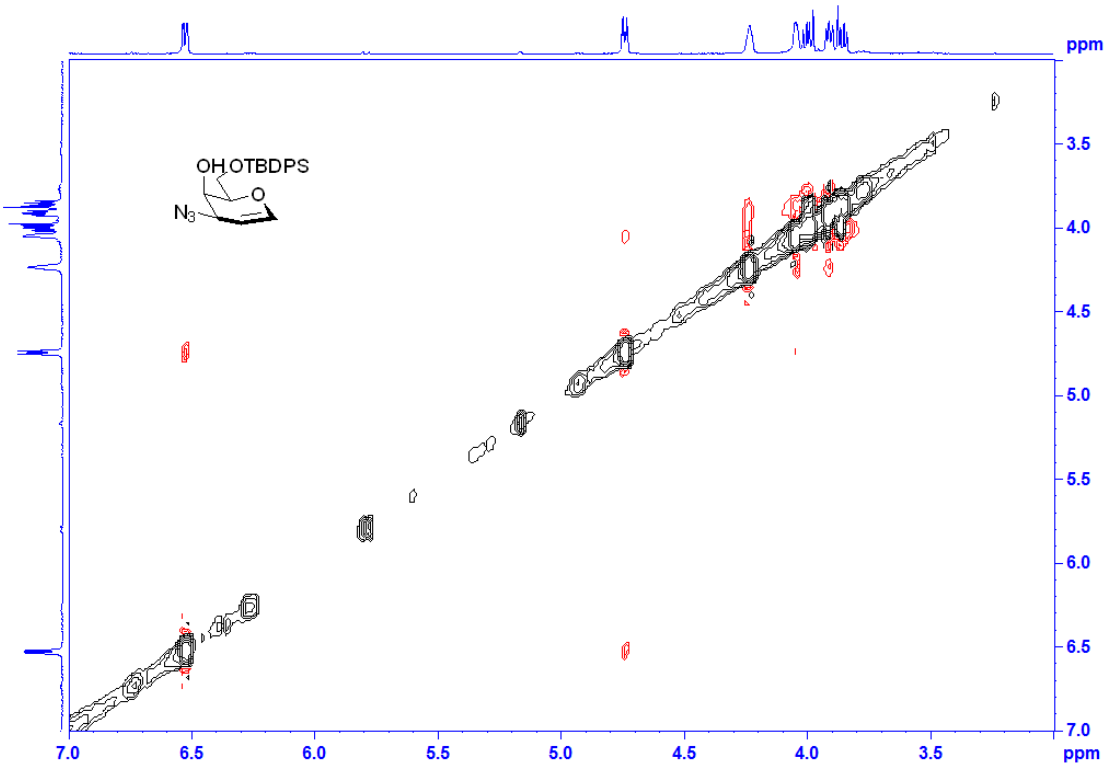

2.4.4 Monitoring the reaction time by ^{1}H NMR kinetic analysis

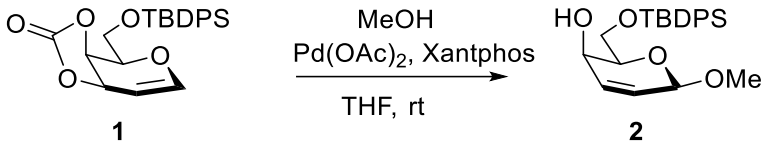

The reaction time was monitored by ^{1}H NMR kinetic analysis and the detected time was 0 min, 5 min, 10 min, 20 min, 30 min, 45 min and 60 min. With the disappearance of peaks from starting material **1**, the peaks of product *β*-*O*-glycoside **2** gradually appeared. This result demonstrated that **1** was consumed completely in one hour and **2** was generated effectively as shown below.

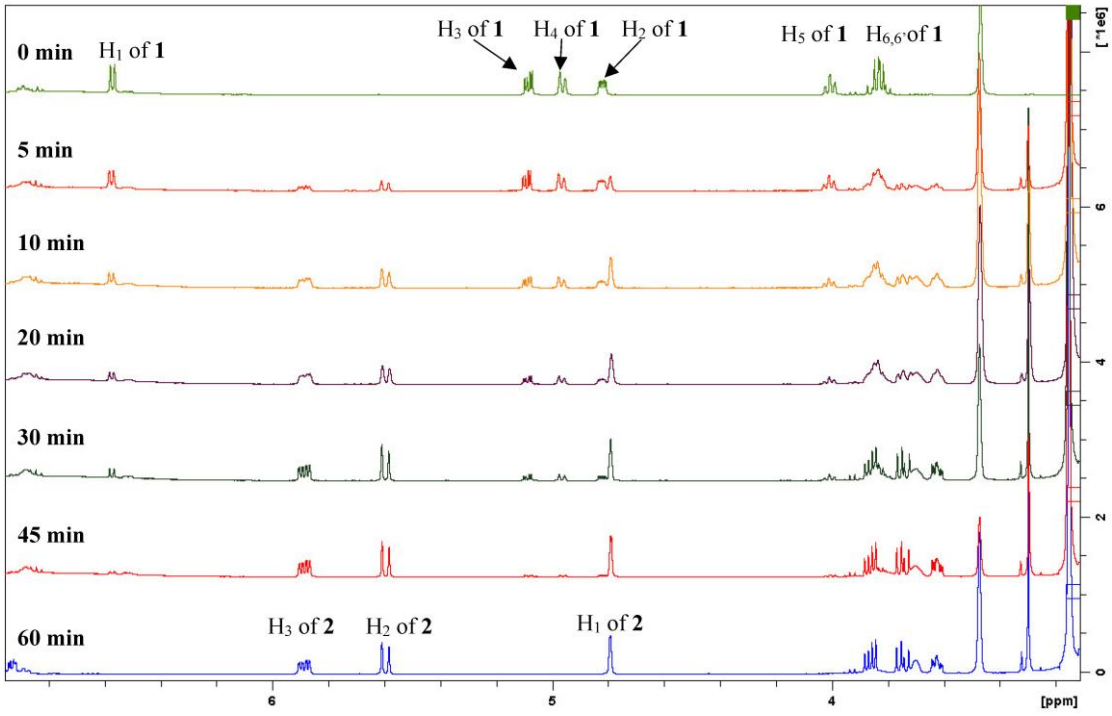

2.4.5 X-ray crystal structure for compound S4 and 25a

X-ray crystal structure for compound **S4** (CCDC number: 1525136)

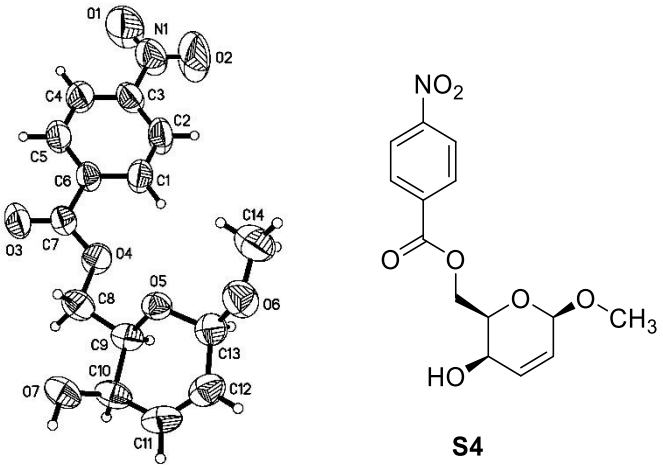

Table 2.4.1. Sample and crystal data for S4.

Chemical formula	$C_{14}H_{15}NO_7$
Formula weight	309.27 g/mol
Temperature	296(2) K
Wavelength	0.71073 Å
Crystal size	0.040 x 0.060 x 0.420 mm
Crystal habit	colorless needle
Crystal system	orthorhombic
Space group	P 21 21 21

Unit cell dimensions	a = 4.2909(2) Å α = 90 °
	b = 10.6038(7) Å β = 90 °
	c = 33.055(2) Å γ = 90 °
Volume	1504.00(16) $Å^3$
Z	4
Density (calculated)	1.366 g/cm^3
Absorption coefficient	0.111 mm^{-1}
F(000)	648

Table 2.4.2 Data collection and structure refinement for S4.

Theta range for data collection	2.02 to 27.00 °
Index ranges	-5<=h<=5, -11<=k<=13, -41<=l<=41
Reflections collected	23616
Independent reflections	3256 [R(int) = 0.0517]
Coverage of independent reflections	98.6%
Absorption correction	Multi-Scan

Max. and min. transmission	0.9960 and 0.9550
Structure solution technique	direct methods
Structure solution program	XT, VERSION 2014/4
Refinement method	Full-matrix least-squares on F^2
Refinement program	SHELXL-2014/7 (Sheldrick, 2014)
Function minimized	$\Sigma\ w(F_o^2 - F_c^2)^2$
Data / restraints / parameters	3256 / 0 / 201
Goodness-of-fit on F^2	1.011
Δ/σ_{max}	0.001
Final R indices	2069 data; R1 = 0.0452, wR2 = 0.0905 $I>2\sigma(I)$ all data R1 = 0.0940, wR2 = 0.1080
Weighting scheme	$w=1/[\sigma^2(F_o^2)+(0.0400P)^2+0.2784P]$ where $P=(F_o^2+2F_c^2)/3$
Absolute structure parameter	1.0(6)
Largest diff. peak and hole	0.134 and -0.134 $eÅ^{-3}$
R.M.S. deviation from mean	0.029 $eÅ^{-3}$

X-ray crystal structure for compound **25a** (CCDC number: 1525137)

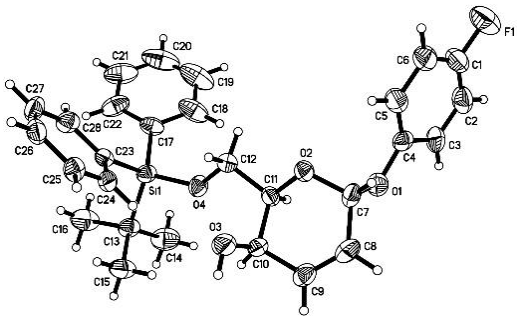

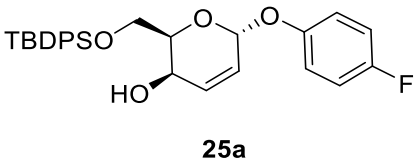

25a

Table 2.4.3 Sample and crystal data for 25a.

Chemical formula	$C_{28}H_{31}FO_4Si$
Formula weight	478.62 g/mol
Temperature	203(2) K
Wavelength	0.71073 Å
Crystal size	0.040 x 0.120 x 0.420 mm
Crystal habit	colorless plate
Crystal system	monoclinic
Space group	P 1 21 1
Unit cell dimensions	a = 12.7802(13) Å α = 90 °
	b = 7.1634(7) Å β = 103.478(3) °

	c = 16.5547(17) Å γ = 90 °
Volume	1473.8(3) $Å^3$
Z	2
Density (calculated)	1.078 g/cm^3
Absorption coefficient	0.113 mm^{-1}
F(000)	508

Table 2.4.5 Data collection and structure refinement for 25a.

Theta range for data collection	1.26 to 25.02 °
Index ranges	-12<=h<=15, -8<=k<=8, -19<=l<=17
Reflections collected	17461
Independent reflections	5193 [R(int) = 0.0971]
Coverage of independent reflections	99.8%
Absorption correction	Multi-Scan

Max. and min. transmission	0.9900 and 0.8400
Structure solution technique	direct methods
Structure solution program	XT, VERSION 2014/5
Refinement method	Full-matrix least-squares on F^2
Refinement program	SHELXL-2014/7 (Sheldrick, 2014)
Function minimized	$\Sigma\, w(F_o^2 - F_c^2)^2$
Data / restraints / parameters	5193 / 1 / 312
Goodness-of-fit on F^2	1.022
Δ/σ_{max}	0.014
Final R indices	2908 data; $I>2\sigma(I)$ R1 = 0.0595, wR2 = 0.1224
	all data R1 = 0.1460, wR2 = 0.1575
Weighting scheme	$w=1/[\sigma^2(F_o^2)+(0.0600P)^2+0.2251P]$ where $P=(F_o^2+2F_c^2)/3$

Absolute structure parameter	-0.17(14)
Extinction coefficient	0.0190(30)
Largest diff. peak and hole	0.270 and -0.298 eÅ^{-3}
R.M.S. deviation from mean	0.059 eÅ^{-3}

2.4.6 Computational section

All the calculations were carried out by using density functional theory B3LYP method with the Gaussian09 program package.[30] Two basis set were used: in basis set I, 6-31G+g(d,p) was employed for all the atoms in reported starting materials and our starting material; in basis set II: a combined basis set Pd and P atoms were described by LANL2DZ basis set and effective core potential implemented and 6-31+G(d) was used for other atoms.[19a, 28b, 28c, 31] Frequency analysis was done at the same level of theory to verify that these optimized structures are real minima or saddle point on the potential energy surface and to get the thermodynamic corrections. Intrinsic reaction coordinate (IRC) calculations were used to confirm that the transition states fond connected the related reactants and products.

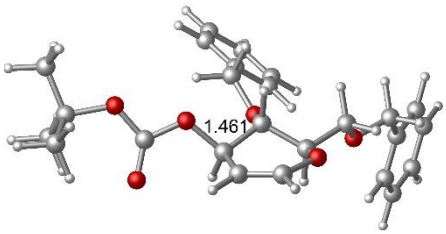

Optimized structure of Lee's starting material

Center Number	Atomic Number	Atomic Type	Coordinates (Angstroms) X	Y	Z

1	6	0	-0.613054	-1.160198	2.218426
2	1	0	-0.409898	-0.081257	2.176211
3	6	0	-2.130443	-1.401527	2.153813
4	1	0	-2.309043	-2.487827	2.135945
5	6	0	-0.548968	-1.564887	-0.120885
6	1	0	0.118495	-1.826873	-0.935227
7	8	0	0.037408	-1.785163	1.090328
8	6	0	0.064990	-1.732543	3.464955
9	1	0	-0.507102	-2.583318	3.867350
10	1	0	1.059213	-2.099091	3.168901
11	6	0	-2.693089	-0.796242	0.861855
12	6	0	-1.783334	-1.079882	-0.299525
13	1	0	-2.146082	-0.891132	-1.302843
14	1	0	-2.864677	0.276007	0.998566
15	8	0	-4.619234	0.277213	-0.717148
16	8	0	-3.997442	-1.422387	0.661612
17	8	0	0.187359	-0.712680	4.441644
18	8	0	-2.699216	-0.821032	3.311108
19	6	0	-3.861831	-1.458766	3.837941

20	1	0	-4.717359	-1.324960	3.164294
21	1	0	-3.675457	-2.543224	3.912437
22	6	0	0.844820	-1.160901	5.618187
23	1	0	1.834705	-1.570236	5.349045
24	1	0	0.272399	-1.978044	6.085752
25	6	0	-4.857712	-0.768279	-0.144085
26	6	0	-4.174565	-0.892868	5.205403
27	6	0	-5.465037	-1.044322	5.731598
28	6	0	-3.195199	-0.251539	5.974496
29	6	0	-5.771442	-0.576297	7.011158
30	1	0	-6.236520	-1.529200	5.136904
31	6	0	-3.504943	0.223520	7.252632
32	1	0	-2.200621	-0.116761	5.562809
33	6	0	-4.789959	0.060897	7.776568
34	1	0	-6.776203	-0.700948	7.405381
35	1	0	-2.737565	0.724090	7.836435
36	1	0	-5.027434	0.432064	8.769553
37	6	0	1.006771	-0.021655	6.598606
38	6	0	1.082537	-0.295809	7.970760

39	6	0	1.124902	1.304607	6.163640
40	6	0	1.285172	0.733185	8.893515
41	1	0	0.977627	-1.319889	8.322200
42	6	0	1.318312	2.335795	7.086787
43	1	0	1.051338	1.523647	5.103845
44	6	0	1.403145	2.054403	8.453219
45	1	0	1.340763	0.503847	9.953949
46	1	0	1.401551	3.360946	6.736820
47	1	0	1.553987	2.857525	9.168852
48	8	0	-5.988044	-1.478759	-0.178511
49	6	0	-7.147642	-1.036222	-0.990985
50	6	0	-8.167123	-2.146880	-0.729266
51	1	0	-8.403701	-2.211101	0.336858
52	1	0	-9.090615	-1.940764	-1.278879
53	1	0	-7.775848	-3.114983	-1.055467
54	6	0	-7.659664	0.311568	-0.474702
55	1	0	-7.879792	0.252465	0.596068
56	1	0	-6.932404	1.106870	-0.644752
57	1	0	-8.586680	0.569114	-0.997573

58	6	0	-6.758620	-0.988894	-2.471584
59	1	0	-6.027811	-0.202981	-2.667884
60	1	0	-6.343189	-1.951100	-2.788119
61	1	0	-7.652191	-0.791317	-3.072926

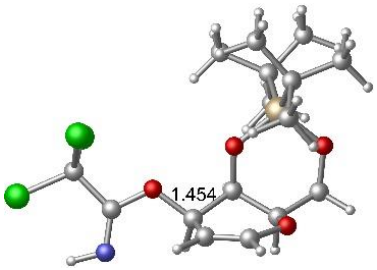

Optimized structure of Nguyen's starting material

Center Number	Atomic Number	Atomic Type	Coordinates (Angstroms) X	Y	Z
1	6	0	-0.780595	-2.821723	-0.995545
2	1	0	-0.550968	-3.420794	-1.870148

3	8	0	0.215600	-2.904873	-0.068718
4	6	0	-2.171882	-1.311888	0.380285
5	6	0	-1.902046	-2.103405	-0.865866
6	1	0	-2.615832	-2.069797	-1.679525
7	1	0	-1.985348	-0.244625	0.217086
8	8	0	-3.556862	-1.433119	0.805131
9	6	0	0.142489	-1.979554	1.031312
10	1	0	0.507577	-1.003463	0.675068
11	6	0	-1.299552	-1.809224	1.543915
12	1	0	-1.293835	-1.037027	2.327273
13	6	0	1.102145	-2.475502	2.112035
14	1	0	2.068369	-2.694244	1.645149
15	1	0	1.250860	-1.659024	2.834120
16	8	0	0.671799	-3.649118	2.784846
17	6	0	-4.455202	-0.641801	0.212083
18	7	0	-4.174423	0.188893	-0.702682
19	1	0	-4.992599	0.704117	-1.018722
20	6	0	-5.851090	-0.922100	0.834192
21	17	0	-6.286401	-2.645887	0.572449

22	17	0	-5.799799	-0.562997	2.598329
23	17	0	-7.110740	0.115115	0.073244
24	8	0	-1.813280	-3.022285	2.060638
25	14	0	-0.938461	-4.021140	3.096293
26	6	0	-1.217224	-5.836304	2.564629
27	6	0	-1.362414	-3.539468	4.909946
28	6	0	-2.893358	-3.432958	5.102050
29	1	0	-3.397646	-4.395956	4.976036
30	1	0	-3.115874	-3.080200	6.119170
31	1	0	-3.343979	-2.727807	4.396329
32	6	0	-0.786263	-4.550247	5.926384
33	1	0	0.298825	-4.665199	5.823283
34	1	0	-0.984123	-4.202405	6.950096
35	1	0	-1.242180	-5.540420	5.828008
36	6	0	-0.737925	-2.154493	5.205865
37	1	0	-0.972847	-1.853688	6.236517
38	1	0	0.352713	-2.167847	5.107429
39	1	0	-1.135527	-1.372548	4.549106
40	6	0	-1.128352	-5.910448	1.021910

41	1	0	-1.908727	-5.313343	0.540944
42	1	0	-0.160230	-5.557430	0.653955
43	1	0	-1.251399	-6.954314	0.700765
44	6	0	-2.602002	-6.362645	3.003401
45	1	0	-2.748447	-7.381457	2.618450
46	1	0	-2.703145	-6.411914	4.092652
47	1	0	-3.418905	-5.745004	2.613571
48	6	0	-0.109776	-6.739555	3.158682
49	1	0	-0.237366	-7.766479	2.788864
50	1	0	0.887937	-6.399775	2.863119
51	1	0	-0.142358	-6.782301	4.251723

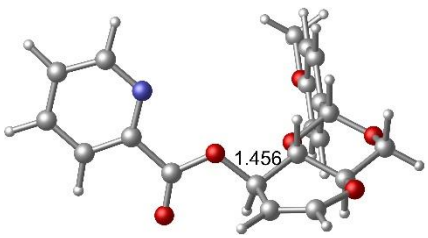

Optimized structure of Liu's starting material

Center Number	Atomic Number	Atomic Type	Coordinates (Angstroms) X	Y	Z
1	6	0	-0.309143	-1.740926	1.888217
2	1	0	0.133135	-0.783732	1.578455
3	6	0	-1.833112	-1.602209	1.925087
4	1	0	-2.278571	-2.578528	2.175533
5	6	0	-0.521525	-2.664212	-0.256294
6	1	0	-0.012506	-3.261627	-1.005033
7	8	0	0.100544	-2.751935	0.958450
8	6	0	0.183379	-2.111124	3.284078
9	1	0	-0.174736	-3.118875	3.547361
10	1	0	1.273684	-2.098708	3.345580
11	8	0	-0.296770	-1.143212	4.216476
12	8	0	-2.180275	-0.641628	2.918236
13	6	0	-1.715844	-1.027959	4.208589
14	1	0	-2.150849	-2.012747	4.454401
15	6	0	-2.352267	-1.174361	0.562312

16	6	0	-1.614152	-1.931556	-0.512154
17	1	0	-2.005272	-1.899929	-1.522325
18	1	0	-2.267820	-0.090826	0.437058
19	6	0	-6.004875	-1.180202	-0.196349
20	6	0	-7.651491	-2.533252	0.637331
21	6	0	-8.645484	-1.858221	-0.079442
22	6	0	-8.268345	-0.789689	-0.892893
23	6	0	-6.920181	-0.441439	-0.956647
24	1	0	-7.909327	-3.372378	1.280051
25	1	0	-9.683012	-2.166939	0.002462
26	1	0	-9.007802	-0.238416	-1.466100
27	1	0	-6.563021	0.377323	-1.570487
28	7	0	-6.356087	-2.208988	0.588588
29	6	0	-4.552535	-0.787947	-0.274065
30	8	0	-4.151348	0.102043	-1.004656
31	8	0	-3.768197	-1.513162	0.535033
32	6	0	-2.129216	0.007977	5.214459
33	6	0	-2.961614	-0.330989	6.279018
34	6	0	-1.681254	1.334304	5.101675

35	6	0	-3.352710	0.621004	7.228733
36	1	0	-3.319044	-1.352607	6.381089
37	6	0	-2.059358	2.290410	6.033310
38	1	0	-1.032642	1.610921	4.277206
39	6	0	-2.898350	1.938558	7.104672
40	1	0	-4.000568	0.323233	8.044244
41	1	0	-1.719301	3.318006	5.956059
42	8	0	-3.211167	2.950919	7.967385
43	6	0	-4.057084	2.665521	9.074315
44	1	0	-4.165488	3.606111	9.615691
45	1	0	-5.044893	2.319800	8.744429
46	1	0	-3.609245	1.914092	9.736782

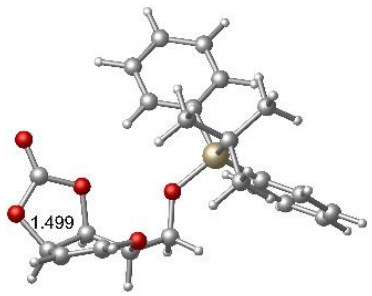

Optimized structure of compound 1

Center Number	Atomic Number	Atomic Type	Coordinates (Angstroms) X	Y	Z
1	6	0	0.218368	-1.415769	-1.944109
2	1	0	-0.738628	-1.895819	-1.782837
3	6	0	0.260770	-0.147029	-2.379915
4	1	0	-0.612365	0.454189	-2.596721
5	8	0	1.425946	0.572865	-2.595381
6	6	0	3.834675	0.834302	-2.447152
7	1	0	3.585483	1.881247	-2.227018
8	1	0	4.685206	0.555021	-1.806636
9	8	0	4.177680	0.623877	-3.810740
10	6	0	1.448897	-2.253744	-1.793016
11	1	0	1.559581	-2.712099	-0.809845
12	6	0	2.723096	-1.514865	-2.278279
13	6	0	2.642695	-0.015176	-2.022839
14	1	0	2.548733	0.084932	-0.926670
15	8	0	1.378630	-3.405666	-2.750381

16	1	0	3.628689	-1.915838	-1.812538
17	8	0	2.765735	-1.872485	-3.710911
18	6	0	2.050942	-3.054164	-3.917606
19	6	0	5.513368	0.547041	-6.306876
20	6	0	6.462710	1.022918	-7.233492
21	6	0	5.173744	-0.821371	-6.331049
22	6	0	7.051725	0.159493	-8.165144
23	1	0	6.756298	2.069617	-7.222798
24	6	0	5.764147	-1.684344	-7.262166
25	1	0	4.454805	-1.207051	-5.615439
26	1	0	7.782628	0.541690	-8.871734
27	1	0	5.490179	-2.734941	-7.269203
28	6	0	5.955859	2.940820	-4.365190
29	6	0	5.740112	4.320222	-4.175131
30	6	0	7.202391	2.408766	-3.965759
31	6	0	6.727212	5.138171	-3.610235
32	1	0	4.800197	4.771505	-4.473066
33	6	0	8.189073	3.221006	-3.397196
34	1	0	7.405841	1.351745	-4.112878

35	1	0	6.538847	6.199458	-3.478507
36	1	0	9.140416	2.789660	-3.100520
37	6	0	7.952683	4.589577	-3.217960
38	1	0	8.718494	5.222600	-2.780157
39	6	0	6.700825	-1.195676	-8.181238
40	1	0	7.156189	-1.866473	-8.903825
41	6	0	3.066900	2.534441	-5.857229
42	6	0	2.187731	1.385004	-6.415608
43	6	0	2.239614	3.310997	-4.803255
44	6	0	3.476532	3.473432	-7.018509
45	1	0	2.707062	0.816404	-7.194655
46	1	0	1.893781	0.687291	-5.624213
47	1	0	1.273389	1.805700	-6.859138
48	1	0	2.796811	4.138883	-4.350074
49	1	0	1.349546	3.743042	-5.284628
50	1	0	1.891905	2.646993	-4.004855
51	1	0	2.575303	3.874184	-7.504658
52	1	0	4.075155	4.325584	-6.675747
53	1	0	4.053456	2.939011	-7.783005

54	14	0	4.659545	1.723067	-5.083010
55	8	0	2.035398	-3.681237	-4.956217

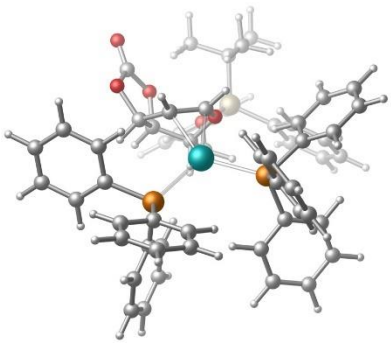

Optimized structure of Glycal-Pd(0)-*α*-L$_n$

Center Number	Atomic Number	Atomic Type	Coordinates (Angstroms) X	Y	Z
1	6	0	-0.229255	-1.616907	-0.487141
2	1	0	-1.168714	-2.111334	-0.257470
3	6	0	-0.192574	-0.742713	-1.584605
4	1	0	-1.016191	-0.591921	-2.269015

5	8	0	1.033077	-0.396370	-2.218805
6	6	0	3.438035	-0.010456	-2.080886
7	1	0	3.199439	0.993116	-2.456943
8	1	0	4.235162	0.097095	-1.328597
9	8	0	3.890116	-0.876773	-3.117595
10	6	0	0.994349	-2.354928	-0.022696
11	1	0	1.116883	-2.361676	1.057924
12	6	0	2.285831	-1.951541	-0.790956
13	6	0	2.203799	-0.538061	-1.358470
14	1	0	2.040654	0.125877	-0.489432
15	46	0	-0.630892	0.431872	0.277866
16	15	0	-1.425432	2.656151	-0.554953
17	1	0	3.178383	-2.051944	-0.165708
18	6	0	-3.084036	3.189468	0.184855
19	6	0	-4.074237	2.203178	0.340426
20	6	0	-3.365673	4.507714	0.575507
21	6	0	-5.328330	2.532010	0.864106
22	1	0	-3.855996	1.176494	0.061185
23	6	0	-4.619748	4.834582	1.110846

24	1	0	-2.612370	5.279856	0.462814
25	1	0	-6.083894	1.761150	0.977770
26	1	0	-4.825836	5.857946	1.409574
27	6	0	-0.332085	4.173043	-0.264844
28	6	0	-0.232189	5.230318	-1.183463
29	6	0	0.413800	4.228647	0.924477
30	6	0	0.597424	6.326136	-0.913086
31	1	0	-0.792915	5.197801	-2.111146
32	6	0	1.237254	5.326614	1.197050
33	1	0	0.361637	3.407269	1.631328
34	1	0	0.670032	7.135311	-1.633280
35	1	0	1.809666	5.351635	2.118952
36	6	0	-1.798838	2.778324	-2.409427
37	6	0	-0.911406	2.162470	-3.309413
38	6	0	-2.928218	3.445358	-2.911935
39	6	0	-1.153964	2.214064	-4.687812
40	1	0	-0.042551	1.628789	-2.937899
41	6	0	-3.168018	3.495078	-4.291310
42	1	0	-3.626285	3.920839	-2.232158

43	1	0	-0.469265	1.722664	-5.371958
44	1	0	-4.047098	4.011104	-4.665087
45	6	0	-5.603997	3.849889	1.251403
46	1	0	-6.576190	4.105005	1.661374
47	6	0	1.331324	6.378068	0.277427
48	1	0	1.975417	7.227166	0.483684
49	6	0	-2.282287	2.879776	-5.182138
50	1	0	-2.472129	2.911859	-6.250385
51	6	0	6.285505	-0.979643	-4.754834
52	6	0	7.099883	-0.809857	-5.894390
53	6	0	6.884894	-1.479963	-3.581467
54	6	0	8.465243	-1.119066	-5.859321
55	1	0	6.672641	-0.434845	-6.820493
56	6	0	8.249052	-1.791741	-3.544044
57	1	0	6.267967	-1.632511	-2.701713
58	1	0	9.074373	-0.979853	-6.747589
59	1	0	8.690708	-2.179120	-2.630558
60	6	0	4.085616	1.230439	-5.209152
61	6	0	2.791937	1.783684	-5.079378

62	6	0	5.122762	2.079307	-5.646533
63	6	0	2.543990	3.126445	-5.388072
64	1	0	1.974433	1.165001	-4.721855
65	6	0	4.875638	3.420229	-5.966064
66	1	0	6.134215	1.695575	-5.730508
67	1	0	1.542774	3.529536	-5.271340
68	1	0	5.690229	4.052950	-6.306059
69	6	0	3.585407	3.946006	-5.839174
70	1	0	3.393652	4.986681	-6.082753
71	6	0	9.042718	-1.609864	-4.682506
72	1	0	10.100873	-1.851977	-4.654884
73	6	0	3.425581	-1.888870	-5.831675
74	6	0	3.865398	-1.787619	-7.311604
75	6	0	3.730491	-3.306053	-5.285820
76	6	0	1.906707	-1.617501	-5.718963
77	1	0	3.686495	-0.786899	-7.725963
78	1	0	4.927302	-2.030688	-7.437360
79	1	0	3.291128	-2.504575	-7.915819
80	1	0	3.410781	-3.409095	-4.244527

81	1	0	3.188389	-4.053963	-5.882496
82	1	0	4.799882	-3.541926	-5.346831
83	1	0	1.353763	-2.403188	-6.254052
84	1	0	1.575636	-1.621407	-4.675186
85	1	0	1.632980	-0.656729	-6.172537
86	14	0	4.411380	-0.605398	-4.757198
87	15	0	-0.522818	0.265223	2.813927
88	6	0	0.982913	1.136882	3.563897
89	6	0	2.090009	1.376099	2.732409
90	6	0	1.036382	1.551038	4.905013
91	6	0	3.234727	2.008569	3.231954
92	1	0	2.041716	1.080102	1.688411
93	6	0	2.179582	2.187176	5.404518
94	1	0	0.186223	1.383976	5.557581
95	1	0	4.081414	2.189120	2.577076
96	1	0	2.207933	2.504460	6.442329
97	6	0	-1.905596	0.834150	3.979059
98	6	0	-2.532682	2.061869	3.711122
99	6	0	-2.311569	0.089805	5.098645

100	6	0	-3.543152	2.541795	4.551487
101	1	0	-2.244069	2.638902	2.839732
102	6	0	-3.327761	0.568039	5.935960
103	1	0	-1.840999	-0.862114	5.317596
104	1	0	-4.021562	3.488943	4.325056
105	1	0	-3.634381	-0.018270	6.796808
106	6	0	-0.274578	-1.527530	3.372775
107	6	0	-1.202486	-2.485182	2.922691
108	6	0	0.800872	-1.945558	4.171876
109	6	0	-1.059524	-3.832273	3.268169
110	1	0	-2.031254	-2.176429	2.292537
111	6	0	0.948396	-3.298528	4.509870
112	1	0	1.524192	-1.222501	4.531648
113	1	0	-1.779055	-4.560414	2.908310
114	1	0	1.788290	-3.609369	5.123568
115	6	0	0.020092	-4.242990	4.061014
116	1	0	0.138745	-5.290450	4.318266
117	6	0	3.281122	2.414996	4.570808
118	1	0	4.166003	2.908638	4.960034

119	6	0	-3.943780	1.794914	5.665691
120	1	0	-4.732207	2.163435	6.314553
121	8	0	2.377238	-2.972461	-1.854712
122	6	0	1.583980	-4.071890	-1.537798
123	8	0	0.853672	-3.810614	-0.390821
124	8	0	1.554149	-5.107476	-2.175252

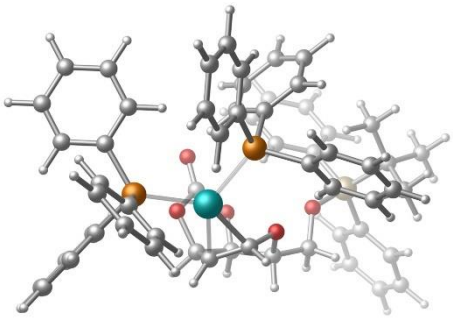

Optimized structure of Glycal-Pd(0)-*β*-L_n

Center Number	Atomic Number	Atomic Type	Coordinates (Angstroms) X	Y	Z

1	6	0	0.930939	-2.352129	-1.346529
2	1	0	0.338040	-2.974228	-0.684610
3	6	0	0.360620	-1.199360	-1.940339
4	1	0	-0.654998	-0.876402	-1.718251
5	8	0	1.226677	-0.088215	-2.232638
6	6	0	2.774600	1.540190	-1.279969
7	1	0	1.930447	2.239993	-1.198093
8	1	0	3.433583	1.712039	-0.414598
9	8	0	3.474326	1.746528	-2.509616
10	6	0	2.417676	-2.427985	-1.172788
11	1	0	2.684215	-3.097449	-0.354569
12	6	0	3.152070	-1.039349	-1.034482
13	6	0	2.187637	0.138192	-1.153532
14	1	0	1.627165	0.141143	-0.200484
15	46	0	0.170056	-2.760681	-3.395015
16	15	0	-0.529296	-1.561234	-5.464486
17	8	0	3.114352	-3.029478	-2.381685
18	1	0	3.695506	-0.972855	-0.087610
19	8	0	4.174920	-1.048536	-2.093306

20	6	0	4.087656	-2.186999	-2.871667
21	6	0	0.996358	-0.928624	-6.374317
22	6	0	0.943167	0.125105	-7.302650
23	6	0	2.232371	-1.525643	-6.081402
24	6	0	2.111248	0.560128	-7.939954
25	1	0	-0.001774	0.615476	-7.515108
26	6	0	3.402306	-1.082429	-6.710017
27	1	0	2.285509	-2.319234	-5.342527
28	1	0	2.062541	1.375868	-8.654951
29	1	0	4.350234	-1.535729	-6.443302
30	6	0	-1.503910	-2.484285	-6.799331
31	6	0	-1.198481	-2.415774	-8.168005
32	6	0	-2.576798	-3.290696	-6.380457
33	6	0	-1.954500	-3.139432	-9.099726
34	1	0	-0.370150	-1.805659	-8.509803
35	6	0	-3.337253	-4.005636	-7.312091
36	1	0	-2.807111	-3.374505	-5.323529
37	1	0	-1.704076	-3.081298	-10.154692
38	1	0	-4.157279	-4.628288	-6.969159

39	6	0	-1.541522	0.025887	-5.247840
40	6	0	-2.759613	0.247486	-5.907283
41	6	0	-1.045304	1.005466	-4.367864
42	6	0	-3.476872	1.432104	-5.689595
43	1	0	-3.153298	-0.497286	-6.589701
44	6	0	-1.761165	2.189391	-4.161259
45	1	0	-0.107342	0.845112	-3.843863
46	1	0	-4.419145	1.590964	-6.205482
47	1	0	-1.365814	2.941521	-3.485110
48	6	0	3.341101	-0.043025	-7.644569
49	1	0	4.247885	0.307788	-8.127100
50	6	0	-3.026311	-3.932259	-8.675278
51	1	0	-3.609910	-4.493011	-9.398831
52	6	0	-2.979250	2.406046	-4.818636
53	1	0	-3.533840	3.324627	-4.652736
54	6	0	5.957266	2.353767	-3.854741
55	6	0	7.044617	3.137156	-4.295362
56	6	0	5.981058	0.968382	-4.106701
57	6	0	8.120905	2.552036	-4.973094

58	1	0	7.064332	4.206812	-4.100039
59	6	0	7.059787	0.381509	-4.779724
60	1	0	5.162407	0.351137	-3.759853
61	1	0	8.951520	3.168547	-5.304715
62	1	0	7.056320	-0.690951	-4.947256
63	6	0	5.056275	4.016311	-1.371016
64	6	0	4.263218	4.953579	-0.675207
65	6	0	6.321931	3.699908	-0.832140
66	6	0	4.716409	5.555424	0.504603
67	1	0	3.282480	5.224903	-1.052719
68	6	0	6.778347	4.298623	0.348328
69	1	0	6.957253	2.984269	-1.344500
70	1	0	4.088974	6.277326	1.019012
71	1	0	7.757257	4.040473	0.741124
72	6	0	5.976647	5.229018	1.018893
73	1	0	6.330248	5.696551	1.932878
74	6	0	8.128874	1.172151	-5.216712
75	1	0	8.966459	0.718328	-5.738669
76	6	0	3.383133	4.217458	-4.161248

77	6	0	3.269943	3.468282	-5.512988
78	6	0	1.956316	4.407341	-3.590511
79	6	0	4.052641	5.593833	-4.384937
80	1	0	4.249395	3.332159	-5.983859
81	1	0	2.814891	2.479640	-5.389236
82	1	0	2.638351	4.046401	-6.203676
83	1	0	1.947908	4.977027	-2.653397
84	1	0	1.341336	4.963390	-4.313272
85	1	0	1.471857	3.440430	-3.414664
86	1	0	3.449933	6.192356	-5.083661
87	1	0	4.148326	6.162989	-3.452748
88	1	0	5.052931	5.490151	-4.823320
89	14	0	4.463454	3.119671	-2.963431
90	8	0	4.784404	-2.409192	-3.849800
91	15	0	0.024179	-5.266375	-3.693729
92	6	0	-1.780411	-5.829144	-3.787317
93	6	0	-2.727609	-5.108585	-3.037451
94	6	0	-2.211440	-6.909741	-4.571094
95	6	0	-4.079840	-5.467466	-3.065280

96	1	0	-2.403167	-4.256880	-2.445934
97	6	0	-3.566866	-7.264327	-4.605279
98	1	0	-1.494829	-7.470880	-5.160532
99	1	0	-4.799999	-4.902780	-2.481181
100	1	0	-3.887740	-8.100447	-5.219155
101	6	0	0.830924	-6.159990	-5.152082
102	6	0	0.981226	-5.457694	-6.358442
103	6	0	1.286620	-7.486402	-5.070624
104	6	0	1.568344	-6.073796	-7.469395
105	1	0	0.645208	-4.429201	-6.427873
106	6	0	1.877545	-8.100501	-6.181474
107	1	0	1.192093	-8.036717	-4.140594
108	1	0	1.679793	-5.517414	-8.394473
109	1	0	2.230197	-9.124567	-6.105503
110	6	0	0.671685	-6.278241	-2.227369
111	6	0	2.001703	-6.065309	-1.820881
112	6	0	-0.115155	-7.208650	-1.531501
113	6	0	2.532934	-6.779692	-0.741724
114	1	0	2.613571	-5.332503	-2.336339

115	6	0	0.416911	-7.914230	-0.442959
116	1	0	-1.141499	-7.386760	-1.832145
117	1	0	3.563610	-6.612310	-0.443397
118	1	0	-0.204617	-8.628637	0.088504
119	6	0	1.741630	-7.704516	-0.047583
120	1	0	2.154282	-8.254640	0.792528
121	6	0	-4.502964	-6.546632	-3.852130
122	1	0	-5.552329	-6.823540	-3.878504
123	6	0	2.018245	-7.396083	-7.382882
124	1	0	2.480751	-7.871825	-8.242075

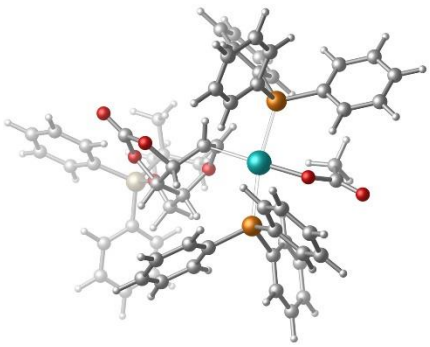

Optimized structure of Glycal-Pd(II)-*α*-L_n

Center Number	Atomic Number	Atomic Type	Coordinates (Angstroms) X	Y	Z
1	6	0	9.464767	5.062927	-0.748166
2	1	0	10.490606	4.833257	-1.016579
3	6	0	8.683116	4.003159	-0.301330
4	1	0	9.101589	3.064494	0.039861
5	8	0	7.342401	3.975642	-0.304493
6	6	0	5.208141	4.560601	-1.280423
7	1	0	4.754753	4.187578	-0.350643
8	1	0	4.596084	5.408610	-1.625814
9	8	0	5.313012	3.539589	-2.259236
10	6	0	8.844340	6.155326	-1.594876
11	1	0	8.957950	7.161476	-1.201912
12	6	0	7.382796	5.820506	-1.995947
13	6	0	6.585711	5.106134	-0.915874
14	1	0	6.448438	5.836549	-0.109459
15	8	0	9.537072	6.141275	-2.908533

16	1	0	6.837773	6.723309	-2.285010
17	8	0	7.584131	5.007609	-3.211607
18	6	0	8.809282	5.332022	-3.792921
19	6	0	4.324386	2.771259	-4.881417
20	6	0	3.349923	2.374456	-5.821511
21	6	0	5.563475	3.245888	-5.356044
22	6	0	3.609547	2.445772	-7.195210
23	1	0	2.378312	2.019391	-5.486983
24	6	0	5.821878	3.319082	-6.730102
25	1	0	6.318268	3.568911	-4.648612
26	1	0	2.848894	2.138217	-7.906154
27	1	0	6.781999	3.691071	-7.074238
28	6	0	2.346887	3.455275	-2.563084
29	6	0	1.611824	3.142309	-1.399785
30	6	0	1.843842	4.470439	-3.406462
31	6	0	0.420727	3.810770	-1.093304
32	1	0	1.958020	2.364684	-0.726964
33	6	0	0.654714	5.142908	-3.101046
34	1	0	2.377694	4.724228	-4.317202

35	1	0	-0.133466	3.545147	-0.198313
36	1	0	0.282995	5.913819	-3.768951
37	6	0	-0.060044	4.813198	-1.943791
38	1	0	-0.986888	5.327510	-1.710062
39	6	0	4.847225	2.917074	-7.650891
40	1	0	5.047766	2.972565	-8.716376
41	6	0	4.250177	0.793258	-2.377042
42	6	0	4.449708	0.763125	-0.842007
43	6	0	3.030067	-0.070328	-2.777677
44	6	0	5.528644	0.223709	-3.044468
45	1	0	5.297662	1.389689	-0.542170
46	1	0	3.561491	1.097074	-0.293529
47	1	0	4.658943	-0.266861	-0.518662
48	1	0	2.885636	-0.085098	-3.864875
49	1	0	3.185435	-1.109217	-2.454338
50	1	0	2.102022	0.287424	-2.316948
51	1	0	5.702412	-0.801929	-2.688349
52	1	0	5.439105	0.190144	-4.135179
53	1	0	6.411775	0.823799	-2.794429

54	14	0	4.008400	2.616422	-3.015467
55	8	0	9.187041	4.970694	-4.884035
56	15	0	8.492938	7.410657	2.067919
57	6	0	7.070649	7.084550	3.239237
58	6	0	6.694457	5.763131	3.522334
59	6	0	6.348470	8.148675	3.811685
60	6	0	5.621000	5.503866	4.383409
61	1	0	7.232571	4.937208	3.070791
62	6	0	5.281029	7.885340	4.675774
63	1	0	6.607816	9.176267	3.579966
64	1	0	5.338803	4.478765	4.598285
65	1	0	4.733646	8.710110	5.119277
66	6	0	9.758390	8.501120	2.928817
67	6	0	9.570656	8.980666	4.231308
68	6	0	10.957193	8.785699	2.251832
69	6	0	10.556133	9.771925	4.833445
70	1	0	8.682886	8.722748	4.794090
71	6	0	11.936825	9.579576	2.855184
72	1	0	11.148555	8.367865	1.267878

73	1	0	10.404278	10.132924	5.844803
74	1	0	12.858093	9.794367	2.323888
75	6	0	7.697453	8.528577	0.760535
76	6	0	8.459806	9.470441	0.046588
77	6	0	6.324569	8.408440	0.475264
78	6	0	7.864036	10.262266	-0.943218
79	1	0	9.509053	9.615063	0.274459
80	6	0	5.731074	9.203943	-0.513301
81	1	0	5.706250	7.724616	1.047049
82	1	0	8.464198	10.990126	-1.478659
83	1	0	4.667461	9.112714	-0.708379
84	6	0	6.500530	10.128631	-1.229615
85	1	0	6.039946	10.747741	-1.991692
86	6	0	4.918631	6.563603	4.965775
87	1	0	4.091347	6.363201	5.637985
88	6	0	11.734610	10.079848	4.146882
89	1	0	12.496256	10.690999	4.618964
90	8	0	10.325864	5.695607	3.471038
91	6	0	9.983879	4.944410	4.551630

92	8	0	10.174130	5.404940	5.686931
93	6	0	9.434667	3.546775	4.340268
94	1	0	8.968490	3.420685	3.358857
95	1	0	10.257832	2.827684	4.427396
96	1	0	8.710488	3.318466	5.125654
97	46	0	9.877562	5.375279	1.503408
98	15	0	11.923429	3.943638	1.326536
99	6	0	11.653202	2.386973	0.315184
100	6	0	12.222542	2.228756	-0.958396
101	6	0	10.812303	1.378416	0.828355
102	6	0	11.956356	1.075020	-1.708050
103	1	0	12.875527	2.992244	-1.365670
104	6	0	10.557357	0.225281	0.078793
105	1	0	10.366295	1.484943	1.813347
106	6	0	11.127757	0.073460	-1.192317
107	1	0	12.399417	0.962806	-2.691617
108	1	0	9.916522	-0.549969	0.484986
109	1	0	10.925372	-0.818469	-1.775009
110	6	0	13.261090	4.909890	0.424301

111	6	0	12.956916	6.080928	-0.286721
112	6	0	14.589393	4.449757	0.466029
113	6	0	13.965901	6.777876	-0.962999
114	1	0	11.940915	6.458881	-0.309830
115	6	0	15.593809	5.148146	-0.211161
116	1	0	14.841879	3.558071	1.029748
117	6	0	15.283722	6.311012	-0.927920
118	1	0	13.720830	7.679300	-1.514384
119	1	0	16.615730	4.786348	-0.175417
120	1	0	16.065404	6.850374	-1.451821
121	6	0	12.769157	3.409944	2.913103
122	6	0	13.157863	2.077745	3.132483
123	6	0	13.069946	4.396984	3.869542
124	6	0	13.834825	1.735276	4.309546
125	1	0	12.948276	1.311297	2.395963
126	6	0	13.743205	4.043434	5.042870
127	1	0	12.755985	5.422488	3.718028
128	6	0	14.124663	2.714786	5.265838
129	1	0	14.136078	0.705989	4.473075

130	1	0	13.956259	4.805439	5.784046
131	1	0	14.643676	2.444907	6.179279

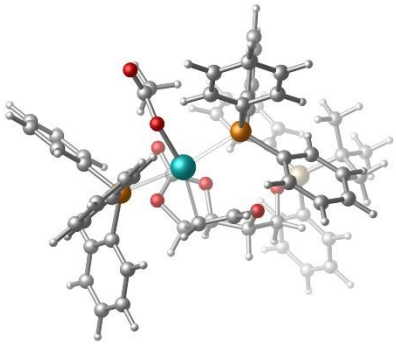

Optimized structure of Glycal-Pd(II)-*β*-L_n

Center Number	Atomic Number	Atomic Type	Coordinates (Angstroms) X	Y	Z
1	6	0	9.279845	4.522097	-2.025190
2	1	0	10.339256	4.744674	-2.015813
3	6	0	8.479369	5.180453	-1.125503
4	1	0	8.857753	5.685038	-0.247126

5	8	0	7.135855	5.339866	-1.271182
6	8	0	4.364387	4.509441	-2.243247
7	6	0	8.704780	3.959932	-3.306880
8	1	0	9.242105	4.335502	-4.176955
9	6	0	7.162256	4.135837	-3.435400
10	8	0	8.840436	2.475401	-3.376498
11	1	0	6.858458	4.204741	-4.484375
12	8	0	6.647129	2.853239	-2.913255
13	6	0	7.621781	1.878044	-3.046800
14	6	0	2.388088	2.483720	-2.860271
15	6	0	3.501525	1.620978	-2.896805
16	6	0	1.108139	1.937078	-3.093556
17	6	0	3.340578	0.252128	-3.150350
18	1	0	4.493400	2.027341	-2.738242
19	6	0	0.947111	0.569646	-3.345556
20	1	0	0.228737	2.575622	-3.093089
21	1	0	4.213818	-0.392602	-3.177792
22	1	0	-0.044793	0.166443	-3.524092
23	6	0	2.157435	5.354739	-4.064901

24	6	0	1.948322	6.750846	-4.039028
25	6	0	2.045769	4.694953	-5.308063
26	6	0	1.635763	7.458615	-5.205338
27	1	0	2.018731	7.297903	-3.103985
28	6	0	1.733894	5.400403	-6.476383
29	1	0	2.190796	3.620442	-5.360381
30	1	0	1.471108	8.530652	-5.159933
31	1	0	1.645530	4.870653	-7.419700
32	6	0	1.527544	6.783564	-6.427061
33	1	0	1.279391	7.330528	-7.331025
34	6	0	2.063543	-0.275803	-3.371588
35	1	0	1.937308	-1.335784	-3.568535
36	6	0	1.730617	4.912934	-0.864703
37	6	0	0.219549	5.132794	-1.123275
38	6	0	1.913377	3.807654	0.205377
39	6	0	2.364601	6.220848	-0.328553
40	1	0	0.036016	5.903000	-1.880390
41	1	0	-0.274991	4.210751	-1.451199
42	1	0	-0.272395	5.451643	-0.193668

43	1	0	2.972647	3.619405	0.416275
44	1	0	1.433716	4.120089	1.143813
45	1	0	1.457241	2.861718	-0.105003
46	1	0	1.882695	6.497769	0.620076
47	1	0	3.436500	6.093469	-0.136036
48	1	0	2.232741	7.066608	-1.013334
49	14	0	2.613972	4.337758	-2.506418
50	8	0	7.454251	0.684956	-2.899530
51	15	0	8.357504	3.296436	1.767377
52	6	0	6.863394	2.166171	1.779197
53	6	0	6.002877	2.157097	0.665327
54	6	0	6.626652	1.294362	2.854095
55	6	0	4.910788	1.282432	0.636972
56	1	0	6.168623	2.822552	-0.176833
57	6	0	5.533951	0.419409	2.815406
58	1	0	7.288949	1.289176	3.711628
59	1	0	4.255265	1.274828	-0.226335
60	1	0	5.359284	-0.254885	3.647030
61	6	0	9.211272	3.038393	3.436558

62	6	0	10.343099	2.221068	3.585668
63	6	0	8.648606	3.659074	4.569861
64	6	0	10.908705	2.038388	4.855303
65	1	0	10.770248	1.716024	2.730137
66	6	0	9.218082	3.467448	5.831890
67	1	0	7.771261	4.288077	4.473842
68	1	0	11.778235	1.398060	4.958848
69	1	0	8.774028	3.947657	6.697596
70	6	0	7.699164	5.049657	1.988514
71	6	0	8.631731	6.076382	2.235595
72	6	0	6.333301	5.356689	1.932814
73	6	0	8.198233	7.392837	2.420817
74	1	0	9.691093	5.845926	2.314190
75	6	0	5.903230	6.677132	2.124548
76	1	0	5.603329	4.577576	1.748731
77	1	0	8.922554	8.175422	2.621560
78	1	0	4.842533	6.902653	2.090398
79	6	0	6.830658	7.695402	2.364740
80	1	0	6.493550	8.715422	2.515794

81	6	0	4.677305	0.411990	1.709737
82	1	0	3.834942	-0.270896	1.679092
83	6	0	10.352423	2.658945	5.977200
84	1	0	10.792517	2.511267	6.957864
85	8	0	10.487682	1.268323	0.723528
86	6	0	10.055454	-0.030643	0.821067
87	8	0	10.688533	-0.766644	1.591029
88	6	0	8.850687	-0.472461	0.038736
89	1	0	7.944220	-0.011304	0.444372
90	1	0	8.923324	-0.190902	-1.013604
91	1	0	8.753966	-1.556523	0.114844
92	46	0	9.777332	2.846514	-0.323833
93	15	0	11.815776	2.229964	-1.689991
94	6	0	12.147899	3.181008	-3.285023
95	6	0	12.550187	4.528188	-3.194650
96	6	0	11.977901	2.600995	-4.551269
97	6	0	12.767303	5.282586	-4.352887
98	1	0	12.729268	4.981012	-2.223327
99	6	0	12.198819	3.358678	-5.709076

100	1	0	11.686673	1.562212	-4.642252
101	6	0	12.588691	4.699355	-5.614041
102	1	0	13.089389	6.315426	-4.269765
103	1	0	12.076708	2.894665	-6.682167
104	1	0	12.765206	5.280940	-6.512624
105	6	0	13.339924	2.634683	-0.663658
106	6	0	13.243885	2.772715	0.729788
107	6	0	14.591267	2.775833	-1.292393
108	6	0	14.386722	3.066067	1.484283
109	1	0	12.293961	2.619286	1.223019
110	6	0	15.729419	3.062026	-0.531585
111	1	0	14.681789	2.664903	-2.367301
112	6	0	15.628196	3.212818	0.857074
113	1	0	14.303398	3.169652	2.560968
114	1	0	16.690923	3.165377	-1.023338
115	1	0	16.512285	3.437061	1.444529
116	6	0	11.936198	0.409168	-2.115043
117	6	0	13.003572	-0.364525	-1.631884
118	6	0	10.939303	-0.192500	-2.904721

119	6	0	13.083055	-1.723844	-1.955445
120	1	0	13.764277	0.079966	-1.002118
121	6	0	11.031244	-1.550151	-3.229894
122	1	0	10.087281	0.380810	-3.248973
123	6	0	12.103056	-2.317149	-2.758057
124	1	0	13.907284	-2.315906	-1.572806
125	1	0	10.257628	-2.006455	-3.838207
126	1	0	12.167349	-3.371567	-3.004566
127	6	0	5.145183	5.622001	-2.673788
128	1	0	4.996028	6.491947	-2.019045
129	1	0	4.873208	5.929033	-3.695404
130	6	0	6.639977	5.338746	-2.679179
131	1	0	7.116784	6.215636	-3.146520

2.5 References

[1] a) Reprinted (adapted) with permission from (W.-L. Leng, J.-X. He, X.-W. Liu, *Acc. Chem. Res*. **2018**, *51*, 628-639.) Copyright (2018) American Chemical Society; b) Reprinted (adapted) with permission from (H. Yao, W.-L. Leng, M.-L. Leow, S. Xiang, J.-X. He, H. Liao, K. Le Mai Hoang, X.-W. Liu, *ACS Catal.* **2017**, *7*, 5456-5460). Copyright (2018) American Chemical Society.

[2] a) X. Zhu, R. R. Schmidt, *Angew. Chem. Int. Ed.* **2009**, *48*, 1900-1934; b) L. L. Kiessling, R. A. Splain, *Annu. Rev. Biochem.* **2010**, *79*, 619-653; c) B. Lepenies, J. Yin, P. H. Seeberger, *Curr. Opin. Chem. Biol.* **2010**, *14*, 404-411.

[3] T. G. Frihed, M. Bols, C. M. Pedersen, *Chem. Rev.* **2015**, *115*, 4963-5013.

[4] J. P. Yasomanee, A. V. Demchenko, *J. Am. Chem. Soc.* **2012**, *134*, 20097-20102.

[5] M. Huang, G. E. Garrett, N. Birlirakis, L. Bohe, D. A. Pratt, D. Crich, *Nat. Chem.* **2012**, *4*, 663-667.

[6] D. Crich, *Acc. Chem. Res.* **2010**, *43*, 1144-1153.

[7] Y. Okada, N. Asakura, M. Bando, Y. Ashikaga, H. Yamada, *J. Am. Chem. Soc.* **2012**, *134*, 6940-6943.

[8] A. Ishiwata, Y. J. Lee, Y. Ito, *Org. Biomol. Chem.* **2010**, *8*, 3596-3608.

[9] Y. Ito, T. Ogawa, *Angew. Chem. Int. Ed.* **1994**, *33*, 1765-1767.

[10] R. S. Babu, Q. Chen, S. W. Kang, M. Q. Zhou, G. A. O'Doherty, *J. Am. Chem. Soc.* **2012**, *134*, 11952-11955.

[11] A. C. Comely, R. Eelkema, A. J. Minnaard, B. L. Feringa, *J. Am. Chem. Soc.* **2003**, *125*, 8714-8715.

[12] R. S. Babu, G. A. O'Doherty, *J. Am. Chem. Soc.* **2003**, *125*, 12406-12407.

[13] H. Kim, H. Men, C. Lee, *J. Am. Chem. Soc.* **2004**, *126*, 1336-1337.

[14] B. P. Schuff, G. J. Mercer, H. M. Nguyen, *Org. Lett.* **2007**, *9*, 3173-3176.

[15] S. Xiang, K. Le Mai Hoang, J.-X. He, Y.-J. Tan, X.-W. Liu, *Angew. Chem. Int. Ed.* **2015**, *54*, 604-607.

[16] B. Schumann, S. G. Parameswarappa, M. P. Lisboa, N. Kottari, F. Guidetti, C. L. Pereira, P. H. Seeberger, *Angew. Chem. Int. Ed.* **2016**, *55*, 14431-14434.

[17] a) K. H. Jung, M. Muller, R. R. Schmidt, *Chem. Rev.* **2000**, *100*, 4423-4442; b) J. H. Kim, H. Yang, J. Park, G. J. Boons, *J. Am. Chem. Soc.* **2005**, *127*, 12090-12097; c) X. M. Zhu, R. R. Schmidt, *Angew. Chem. Int. Ed.* **2009**, *48*, 1900-1934; d) Y. Zhu, B. Yu, *Angew. Chem. Int. Ed.* **2011**, *50*, 8329-8332; e) P. Shu, X. Xiao, Y. Zhao, Y. Xu, W. Yao, J. Tao, H. Wang, G. Yao, Z. Lu, J. Zeng, Q. Wan, *Angew. Chem. Int. Ed.* **2015**, *54*, 14432-14436.

[18] a) B. M. Trost, D. L. VanVranken, *Chem. Rev.* **1996**, *96*, 395-422; b) B. M. Trost, F. D. Toste, *J. Am. Chem. Soc.* **1999**, *121*, 4545-4554; c) G. J. Mercer, J. Yang, M. J. McKay, H. M. Nguyen, *J. Am. Chem. Soc.* **2008**, *130*, 11210-11218; d) B. M. Trost, J. Xu, T. Schmidt, *J. Am. Chem. Soc.* **2009**, *131*, 18343-18357; e) A. Recio, III, J. D. Heinzman, J. A. Tunge, *Chem. Commun.* **2012**, *48*, 142-144; f) G. Wu, W. Su, *Org. Lett.* **2013**, *15*, 5278-5281.

[19] a) A. Khan, R. Zheng, Y. Kan, J. Ye, J. Xing, Y. J. Zhang, *Angew. Chem. Int. Ed.* **2014**, *53*, 6439-6442; b) A. Khan, L. Yang, J. Xu, L. Y. Jin, Y. J. Zhang, *Angew. Chem. Int. Ed.* **2014**, *53*, 11257-11260; c) A. Khan, J. Xing, J. Zhao, Y. Kan, W. Zhang, Y. J. Zhang, *Chem. Eur. J.* **2015**, *21*, 120-124.

[20] Y. S. Reddy, R. Lahiri, Y. D. Vankar, *Eur. J. Org. Chem.* **2012**, 4751-4761.

[21] See the Supporting Information for computation details.

[22] P. W. N. M. van Leeuwen, P. C. J. Kamer, J. N. H. Reek, P. Dierkes, *Chem. Rev.* **2000**, *100*, 2741-2769.

[23] Colorless syrup **2** was modified with p-nitrobenzoyl to grow a crystal. For details on procedures and X-ray data, see the Supporting Information.

[24] S. A. Wang, J. A. Cuesta-Seijo, D. Lafont, M. M. Palcic, S. Vidal, *Chem. Eur. J.* **2013**, *19*, 15346-15357.

[25] a) D. Crich, V. Dudkin, *J. Am. Chem. Soc.* **2001**, *123*, 6819-6825; b) D. Crich, A. U. Vinod, *Org. Lett.* **2003**, *5*, 1297-1300.

[26] Azidotrimethylsilane was examined as a non-hydrogen-bonding acceptor in both Pd(0) and Pd(II) conditions. Two epimers were obtained as products, which also supported the proposed mechanism as shown in the Supporting Information.

[27] M. J. McKay, H. M. Nguyen, *ACS Catal.* **2012**, *2*, 1563-1595.

[28] a) J. D. Weaver, A. Recio, 3rd, A. J. Grenning, J. A. Tunge, *Chem. Rev.* **2011**, *111*, 1846-1913; b) T. Sperger, I. A. Sanhueza, I. Kalvet, F. Schoenebeck, *Chem. Rev.* **2015**, *115*, 9532-9586; c) D. C. Bai, F. L. Yu, W. Y. Wang, D. Chen, H. Li, Q. R. Liu, C. H. Ding, B. Chen, X. L. Hou, *Nat. Commun.* **2016**, *7*, 11806.

[29] K. Le Mai Hoang, J.-X. He, G. Bati, M. B. Chan-Park, X.-W. Liu, *Nat. Commun.* **2017**, *8*, 1146.

[30] M. J. T. Frisch, G. W.; Schlegel, H. B.; Scuseria, G. E.; Robb, M. A.; Cheeseman, J. R.;, G. B. Scalmani, V.; Mennucci, B.; Petersson, G. A.; Nakatsuji, H.; Caricato, M.; Li, X.; Hratchian,, A. F. B. H. P.; Izmaylov, J.; Zheng, G.; Sonnenberg, J. L.; Hada, M.; Ehara, M.; Toyota, K.; Fukuda,, J. I. R.; Hasegawa, M.; Nakajima, T.; Honda, Y.; Kitao, O.; Nakai, H.; Vreven, T.; Montgomery, J., J. P. A., J. E.; Ogliaro, F.; Bearpark, M.; Heyd, J. J.; Brothers, E.; Kudin, K. N.; Staroverov, V.

N.;, R. N. Kobayashi, J.; Raghavachari, K.; Rendell, A.; Burant, J. C.; Iyengar, S. S.; Tomasi, J.;, M. R. Cossi, N.; Millam, J. M.; Klene, M.; Knox, J. E.; Cross, J. B.; Bakken, V.; Adamo, C.;, J. G. Jaramillo, R.; Stratmann, R. E.; Yazyev, O.; Austin, A. J.; Cammi, R.; Pomelli, C.;, J. W. M. Ochterski, R. L.; Morokuma, K.; Zakrzewski, V. G.; Voth, G. A.; Salvador, P.;, J. J. D. Dannenberg, S.; Daniels,A.D.;Farkas,O.; Foresman, J. B.; Ortiz, J. V.; Cioslowski, J.; Fox,, D. J., *Gaussian, Inc.* **2009**, *Wallingford CT*.

[31] a) J. A. Keith, D. C. Behenna, J. T. Mohr, S. Ma, S. C. Marinescu, J. Oxgaard, B. M. Stoltz, W. A. Goddard, 3rd, *J. Am. Chem. Soc.* **2007**, *129*, 11876-11877; b) S. L. Zhang, Y. Fu, R. Shang, Q. X. Guo, L. Liu, *J. Am. Chem. Soc.* **2010**, *132*, 638-646; c) W. S. Guo, L. Martinez-Rodriguez, R. Kuniyil, E. Martin, E. C. Escudero-Adan, F. Maseras, A. W. Kleij, *J. Am. Chem. Soc.* **2016**, *138*, 11970-11978.

Chapter 3

Cascade transformation of glycal into diverse fused cyclic compounds

3.1 Introduction

Carbohydrates as starting material for total synthesis has been devoted many efforts in past decades because they are economical and contain multiple well-defined chiral centers. Unsaturated carbohydrates glycals occupy a significant position in this field because they possess not only chiral centers with hydroxyl groups but also double bonds which can be functionalized facilely by many reactions.[1] As we discussed in the first chapter, huge efforts have been made on the research of converting glycals into synthons, for example, Perlin aldehydes, functionalized furans.[2] They hold a great potential application in many organic reactions because of the double bonds or the functionalized moieties. Herein, we only discuss the Nazarov cyclization reaction using glycal-derived Perlin aldehydes.

3.1.1 Introduction of Nazarov reaction

The typical Nazarov cyclization reaction is a rearrangement of allyl vinyl ketones forming cyclopentenones. A typical Nazarov reaction is initiated by activation of dienone by a strong Lewis/protic acid resulting in pentadienyl cation intermediate. This is followed by electrocyclic ring closure to give cyclopentyl cation intermediate. After a sequence of elimination and protonation, this would give us the cyclopentenone product. Imino-Nazarov reaction is the analogous variant of Nazarov reaction involving amino substituted pentadienyl group instead of the normal oxide group. This special class of Nazarov reaction has received far less attention compared to traditional Nazarov reaction mainly due to unfavorable energetics associated with ring closure of 3-aminopentadienyl cation. It is thought that the lone pair of nitrogen stabilized acyclic 3-aminopentadienyl cation to the extent that ring closure is disfavoured. According to

the computational calculation of energy activation barrier for cyclization of pentadienyl with different X group carried out by Smith group, the energy barrier for cyclization is about 10 kcal/mol higher when X=NH_2 than OH.[3]

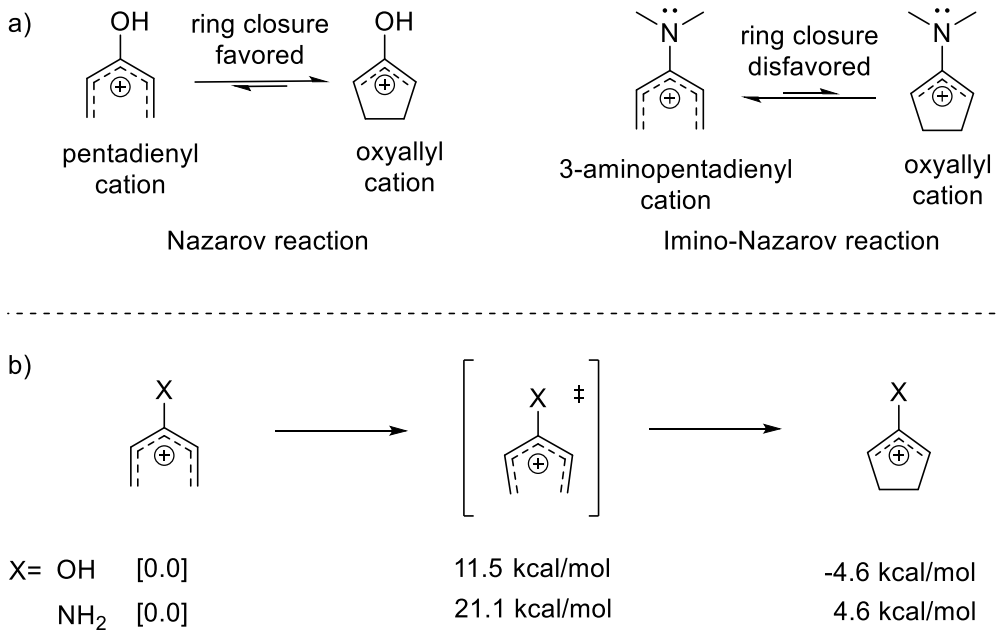

Scheme 3.1.1 Comparison of Nazarov and imino-Nazarov reaction: a) transition states and b) energy barriers.

3.1.2 Imino-Nazarov reaction of glycal-derived dienals and anilines

Inspired by the Perlin aldehydes and imino-Nazarov reaction, our group developed a novel cascade reaction between glycal-derived dienals and secondary anilines mediated by Lewis-acid affording fused indoline and tetrahydroquinoline products.[4] To obtain the required dienal starting material, we subjected permethylated D-glucal to mercury sulfate in H_2SO_4 solution which promoted the ring opening reaction to give Perlin aldehyde. Subsequent mesylation followed by elimination provided dienal as an inseparable mixture of Z/E isomers. With the dienal in hand, we proceeded to react dienal and *N*-benzyl p-methoxyaniline with $AgClO_4$ as a catalyst. It was found that 4-

aminocyclopentenone products can be obtained in high yields as single diastereomer although a *Z*/*E* mixture of dienal was utilized.

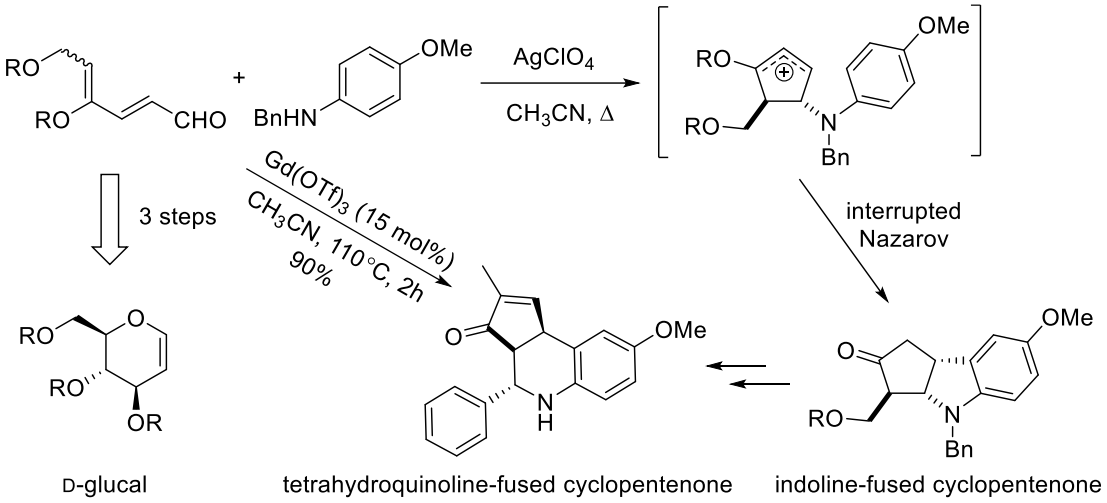

Scheme 3.1.2 Interrupted imino-Nazarov reaction between glycal-derived dienals and secondary anilines.

During the investigation of Lewis acid for interrupted Nazarov reaction, it was found that lanthanide-triflate $Gd(OTf)_3$ was able to catalyze the reaction of dienal and aniline to form tetrahydroquinoline fused products at 110 ℃ after 12 h in a yield of 72%. In summary, this facile cyclization of 1-aminopentadienyl cation generated from the condensation of glycal-derived dienal and aniline has been accomplished successfully. Intramolecular arene trapping enables the reaction to afford tricyclic indoline-fused cyclopentanone diastereoeselectively. Serendipitous Ln-catalyzed cascade transformation resulted in a formation of tetrahydroquinoline-fused cyclopentenone. However, the starting material is not easy to be prepared and the toxic reagent $HgSO_4$ is needed. It took several steps to synthesize the dienals and the total yields would be quite low if we calculate from glycals. Hence it is urgent to develop a more efficient

method from readily available glycals to generate complicate natural or unnatural products directly.

3.1.3 Direction reactions between glycals and anilines

Nevertheless, few investigations on the reactivity of glycal towards aniline derivatives have been reported to date. Yadav reported a mild Lewis acid-mediated reaction between glycals and primary anilines affording tetrahydroquinoline products in 2003.[5] In most cases, both catalytic $InBr_3$ and stoichiometric TMSOTf could produce desired molecules in high yields (75%-89%) with a good stereoselectivity which was confirmed by various 2D-NMR. They reported the substrates sope of this method with 19 examples and only 2,6-dimethylaniline was not able to give the product because of steric hindrance.

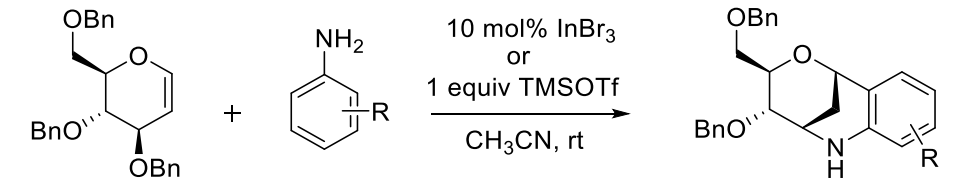

tri-*O*-Benzyl-D-glucal anilines

n.r. - 89%
ratio of regioisomers 7:3 - 1:0

Scheme 3.1.3 Synthesis of tetrahydroquinolines from glycals and primary anilines

In 2011, Yao and Zhang disclosed that appropriately substituted glycal substrates underwent reactions with primary anilines in the presence of $InBr_3$ to yield 4-aminocyclopentenones.[6] In the condition, a novel $InBr_3$ catalyzed glycosidation of C3 alkyl substituted glycals with anilines to form 4-aminocyclopent-2-enones. However, the reaction of aniline with 3,4,6-tri-*O*-acetyl-L-rhamnal under their identical reaction conditions gave the corresponding product in an extremely poor yield (<5%) as shown in Scheme 3.1.4. We noticed that the synthetic utility of the method is limited to C3

alkyl substituted glycals. Furthermore, the condensation of primary arylamines with glycals, which only contain hydrogen on C3, to form tetrahydroquinolines have been extensively studied by Yadav's group and others.[5b, 7]

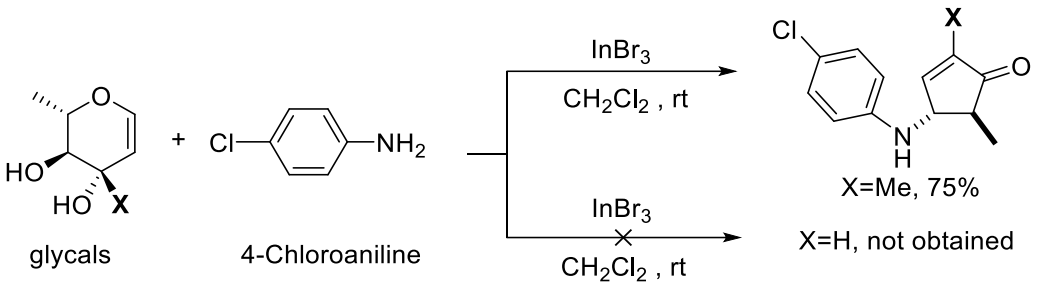

Scheme 3.1.4 4-Aminocyclopentenone synthesis from glycals and primary anilines catalyzed by $InBr_3$

Recently our group has successfully developed an environmentally benign process for construction of 4-aminocyclopentenone utilizing a combination of Lewis acid and surfactant to facilitate the reaction of glycals and secondary anilines in water (Scheme 3.1.5).[8] This is a green method to construct bioactive 4-aminocyclopentenone in a quick access from a readily available glucals and secondary anilines mediated by a Lewis acid-surfactant-combination catalyst system. The mechanism of this reaction was proposed to be carried out through 4π conrotatory electrocyclization between glycal-derived Perlin aldehydes and anilines.

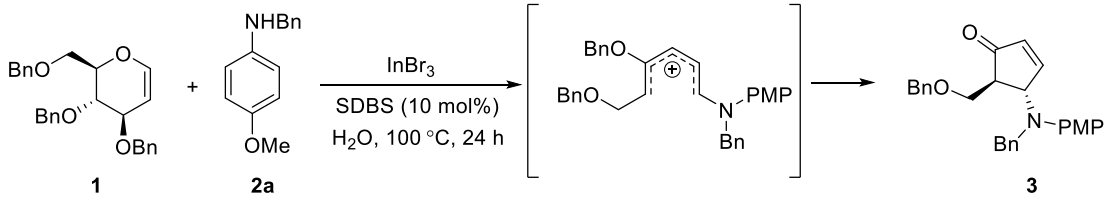

Scheme 3.1.5 Green synthesis of 4-aminocyclopentenone from glycals and primary anilines

Drawing inspirations from the previous works and in continuation of our strong interest in the synthesis of complex natural/unnatural products starting from comparatively simple glycals as starting material. Herein, we envisioned that treatment of protected D-glucal **1** and aniline **2** in the presence of suitable Lewis acid could lead to cascade reaction which entails ring-opening of glycal and subsequent interrupted imino-Nazarov reaction to ultimately furnish indoline-fused cyclopentanone **5** in a straightforward manner. The key feature of the present protocol is the practical use of readily available glycal, rendering the overall process much more step-economical as opposed to employing the corresponding dienal prepared beforehand.

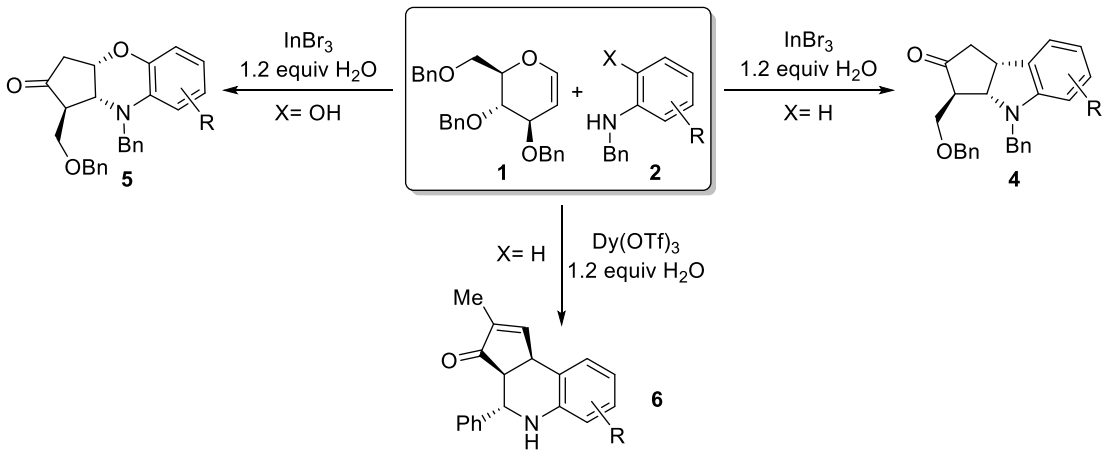

Scheme 3.1.6 Diversity-oriented synthesis of three different fused-ring scaffolds from glycal.

3.2 Results and Discussion

We first performed a systematic investigation to pin down favorable reaction conditions for the reaction between 3,4,6-tri-*O*-benzyl-D-glucal **1** and *N*-benzyl-4-methoxyaniline **2a** by trialing different combinations of various reaction parameters, including temperature setting, Lewis acid catalyst species, and solvents used (Table **3.2.1)**. Testing the reaction at different temperature revealed that the reaction requires a temperature of around 100 ℃ to proceed at an appreciable rate to give a satisfactory yield. Lowering the reaction temperature to 80 ℃ with other conditions held constant severely impedes the reaction and roughly halves the yield (Table **3.2.1**, entry 7 and entry 8), while the reaction performed at room temperature hardly proceeds at all (Table **3.2.1**, entry 9). At favorable temperature, a number of different metal catalysts including AgOTf, $AlCl_3$, $Cu(OTf)_2$, $Sc(OTf)_3$, $ZnCl_2$, $InCl_3$ and $InBr_3$ were proven to be able to catalyze the formation of indoline-fused cyclopentanone product **4a**, with $InBr_3$ identified as the most efficient (Table **3.2.1**, entries 1-7). The results of testing the reaction at favorable temperature catalyzed by $InBr_3$ in a variety of organic solvents including toluene, DCE, DMF, dioxane and nitromethane (Table **3.2.1**, entries 10-14) suggest that the choice of a polar and aprotic solvent is crucial for the success of the reaction, with nitromethane being the most superior choice in terms of the product yield obtained. The reason is possible that the lone pairs of the nitro group can stabilize the key oxyallyl cation intermediate. Hence, the most favorable combination of reaction conditions affording the desired product **4a** in highest yield (62%) is established to be performing the reaction with $InBr_3$ as the Lewis acid catalyst in nitromethane at 100 ℃ for around 4 h (Table **3.2.1**, entry 14), and altering the solvent to acetonitrile affords a comparable yield of 58% (Table **3.2.1**, entry 7).

Table 3.2.1 Optimization study of reaction conditions.[a]

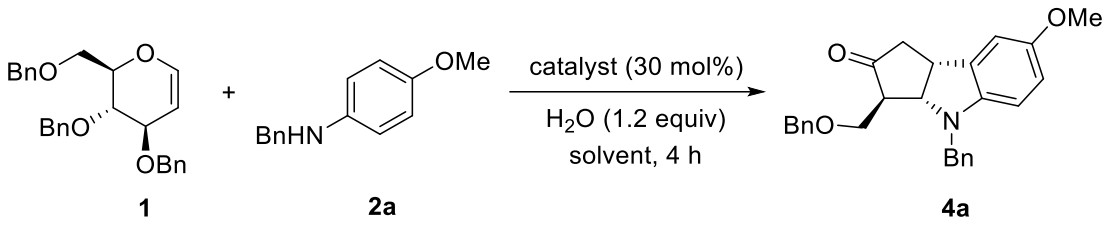

Entry	Catalyst (mol%)	Solvent	T (°C)	Yield[b]
1	AgOTf (30)	CH_3CN	100	49%
2	$AlCl_3$ (30)	CH_3CN	100	-
3	$Cu(OTf)_2$ (30)	CH_3CN	100	8%
4	$Sc(OTf)_3$ (30)	CH_3CN	100	55%
5	$ZnCl_2$ (30)	CH_3CN	100	35%
6	$InCl_3$ (30)	CH_3CN	100	52%
7	$InBr_3$ (30)	CH_3CN	100	58%
8	$InBr_3$ (30)	CH_3CN	80	29%
9	$InBr_3$ (30)	CH_3CN	25	-
10	$InBr_3$ (30)	toluene	100	-
11	$InBr_3$ (30)	DCE	100	12%
12	$InBr_3$ (30)	DMF	100	-
13	$InBr_3$ (30)	1,4-dioxane	100	-
14	$InBr_3$ (30)	CH_3NO_2	100	62%

[a] Unless otherwise noted, all reactions were performed using glycal **1** (0.24 mmol, 1.0 equiv), aniline **2a** (0.24 mmol, 1.0 equiv) and H_2O (0.29 mmol, 1.2 equiv) with 30 mol% of catalyst in 2.4 mL of solvent. [b] Isolated yield. DCE= 1,2-dichloroethane.

With the optimized condition in hand, we went on to explore the scope of secondary aniline substrates for the reaction to demonstrate its general applicability. Reactions of perbenzylated glycal **1** with various secondary anilines **2a-2i** carrying different substituents on the phenyl ring or the nitrogen center proceeded smoothly under the optimized conditions affording the corresponding indoline-fused product **4a-4i** in yields ranging from 40%-62% (Scheme 3.2.1). In general, the present methodology is limited to the use of secondary anilines which possess only electron-donating groups on the aromatic ring, as the presence of an electron-withdrawing group is not well-tolerated. Additionally, anilines with allyl group on the nitrogen center also underwent the cascade transformation with the glycal to furnish the corresponding indoline **4i** in 40% yield.

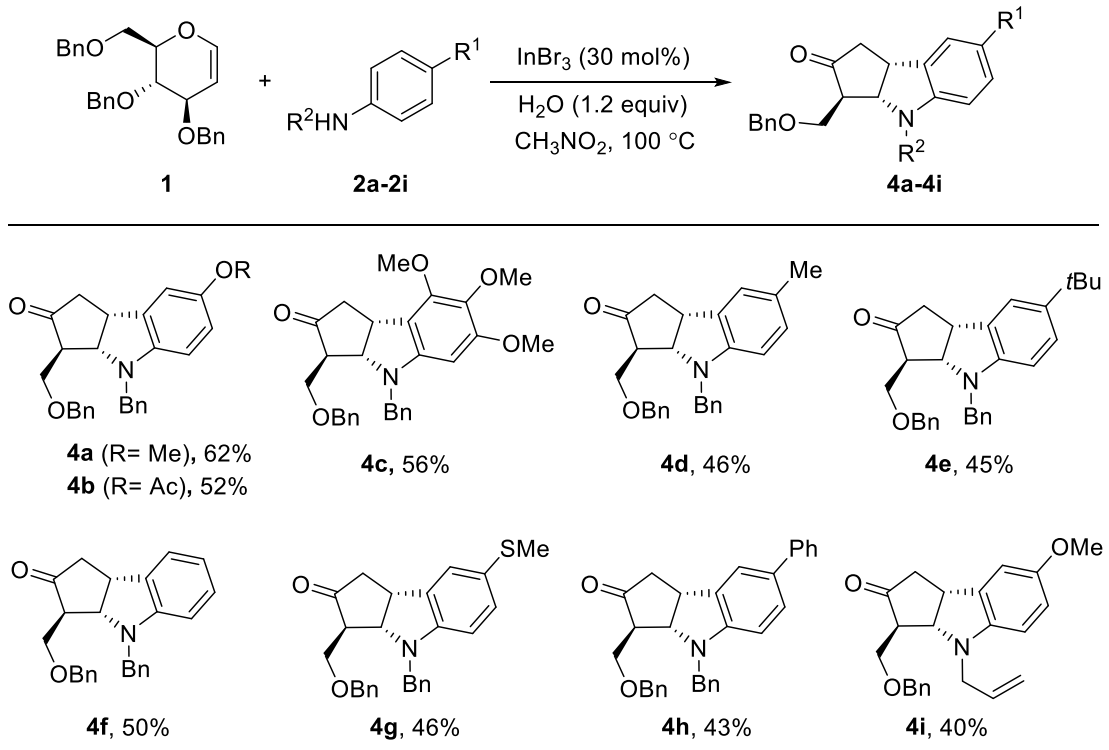

Scheme 3.2.1 Substrate scope of secondary anilines for formation of indoline product.

Serendipitously, during exploring the scope of secondary aniline substrates, a disparate fuse-ring product with 1,4-benzoxazine core structure **5** was obtained in place of the expected indoline product when a secondary aniline bearing an *ortho*-hydroxyl group was subjected to the reaction with glycal **1** (Scheme 3.2.2). This fortuitous observation prompted us to prepare a small library of benzoxazine-fused compounds **5a-5k** by carrying out reactions of glycal **1** with differently substituted *N*-benzyl-*2*-hydroxyaniline derivatives **2h-2r**. The yields for preparation of benzoxazines, ranging from 51% to 65%, are generally slightly higher than those obtained for the indolines. The higher yields might be attributed to the more thermodynamically favorable conformation adopted by the six-membered ring in the benzoxazine fused-ring systems, as contrary to the more strained conformation adopted by the five-membered ring constituting the indolines. Additionally, in reactions involving 2-hyroxyanilines **2h-2r**, we speculate that it is the nucleophilic attack by the hydroxyl group on the phenolic ring to the cyclic carbocation closes the fused-ring to give 1,4-benzoxazines, while in the reactions involving simple anilines **2a-2j** the aromatic conjugated system fulfills the role of the nucleophile, and the superior nucleophilicity of hydroxy group over simple aromatic system may also contribute to the higher yields in the formation of 1,4-benzoxazines. The substrate scope of the direct transformation from glycal **1** to 1,4-benzoxazines includes *N*-benzyl-2-hydroxyanilines with electron donating groups at different positions on phenyl ring (**5b-5j**) as well as those with substitution groups with varied electron-withdrawing capability on the phenyl ring (**5f-5i**), though presence of an electron-withdrawing group marginally diminishes the reaction yields. *N*-methyl-2-hydroxyaniline reagent **2r,** in which the benzyl group on the nitrogen center of the *N*-benzyl-2-hydroxyaniline **2j** is replaced by a methyl group, also reacted smoothly with

glycal **1** to afford the corresponding 1,4-benzoxazine product with a moderate 51% yield. Importantly, based on the crude ^{1}H NMR studies of the reaction mixtures, in each of the reactions for preparation of the benzoxazines, only one diastereomer of the possible 1,4-benzoxazine fused-ring products was formed. Removal of the benzyl protecting group from **5k** allowed unequivocal determination of the diastereo-selectivity of the reaction by a single crystal X-ray diffraction analysis. It is particularly noteworthy that the synthesized 1,4-benzoxazines hold a great potential in natural product synthesis.[9]

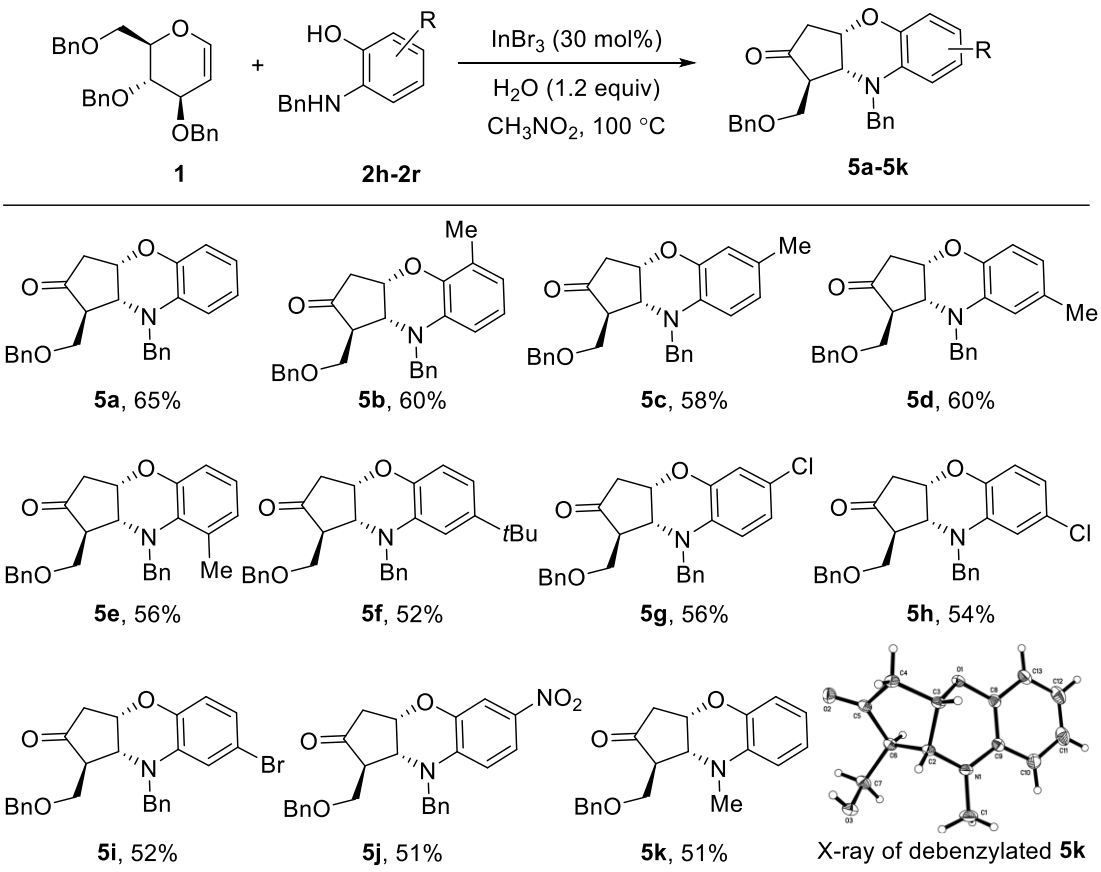

Scheme 3.2.2 Substrate scope of 2-hydroxyaniline for formation of 1,4-benzoxazine product.

In parallel with the preparation of indoline-fused cyclopentenone compounds, further investigation on the reaction between 3,4,6-tri-*O*-benzyl-D-glucal **1** and *N*-benzyl-anilines employing an enriched repository of Lewis acid catalysts revealed that this cascade reaction can, with the use of lanthanide metal catalysts in place of $InBr_3$ and addition of water to the reaction system, provide an alternative access to tetrahydroquinoline-fused cyclopentenone products. This result is within expectation as it is in line with our previous findings on interrupted Nazarov reaction between Perlin aldehydes and anilines. $Dy(OTf)_3$ was identified as the optimal catalyst for facilitating conversion of reacting substrates into tetrahydroquinoline-fused cyclopentenones. And favorable conditions for the transformation include a temperature of 100 ^oC, addition 1.2 equivalent of water in acetonitrile solvent, use of $Dy(OTf)_3$ catalyst and a reaction time of 12 h.

The scope of this reaction under the specified conditions include a variety of secondary anilines bearing electron-donating substitutes on the aromatic ring (**2a-h**), and reaction of glycal **1** with anilines **2a-h** under the favorable conditions afford corresponding desired complex fused-ring products **6a-6i** in a straightforward manner, as shown in Scheme **3.2.3**, with yields ranging from 38%-52%.

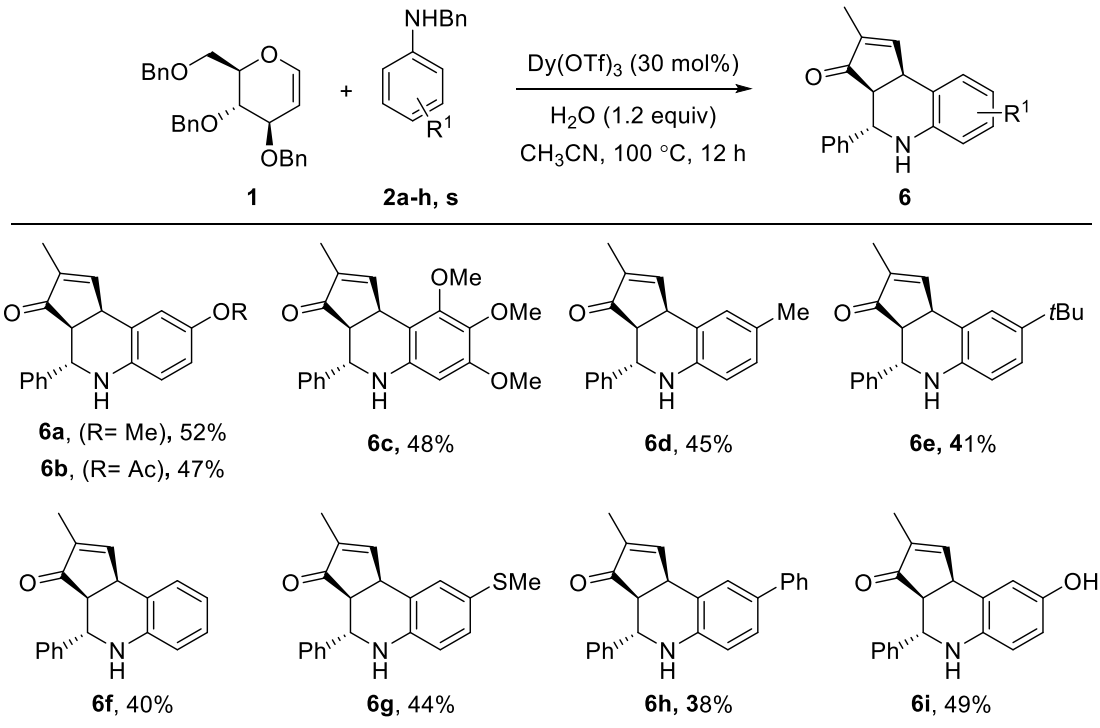

Scheme 3.2.3 $Dy(OTf)_3$-catalyzed cascade interrupted Nazarov/rearrangement.

Apropos of the results and our previous investigation on imino-Nazarov reaction, a plausible reaction mechanism was proposed to illustrate the formation of compound **4**, **5** and **6** as shown in Scheme **3.2.4**. A Lewis acid-catalyzed Ferrier reaction between tri-*O*-benzyl-D-glucal **1** and water initiates the cascade of reactions, furnishing 2,3-dideoxysugar **A** as the first intermediate. The hemiacetal readily undergoes ring opening under the reaction conditions to give *α*,*β*-unsaturated aldehyde **B**. Through a condensation reaction, aldehyde **B** and aniline substrate **2** coalesce into iminium ion **C**, which, upon formation, spontaneously tautomerizes to dienamine **D**. With elimination of a molecule of water from **D** under the acidic condition, facilitated by delocalization of the tertiary amine lone pair to the conjugated system, the sequence of reactions arrives at the key intermediate pentadienyl cation **E**. The dienyl cation **E** is favorably poised for a facile (thermally induced) 4π symmetry-allowed conrotatory ring closure

to transform into the cyclic oxy-allyl cation **F** with *trans* configuration.[10] When X is a hydrogen atom and no lanthanide catalyst is present, intramolecular arene trapping of the oxy-allyl intermediate ensued the formation of oxy-allyl cation **F**, and the following hydrolysis of benzyloxy group completes the reaction sequence to afford indoline-fused ring **4** as the final product. On the other hand, when X is a hydrogen atom and a lanthanide(III) triflate is present in the reaction system, the indoline-fused ring **4** further loses the remaining benzyloxy group by the previously reported mechanism[4] and transforms into intermediate **J**. An intramolecular retro-ene-type reaction proceeds to convert the alkene intermediate **J** into the iminium intermediate **K**, which through enolization readily transforms into enolate **L**. Intramolecular *Re* face attack on the imine by the enolate on **L** *via* Mannich reaction mechanism completes the reaction cascade to finally yield indoline-fused cyclopentenone product **6** diastereo-selectively. The stereoselectivity results from the energetically-favored pseudo-half-chair transition state conformation of *Re* face attack by enolate, as contrary to the unfavored pseudo-boat transition state conformation of the *Si* face attack.[4] When X is a hydroxyl group, as in the case of reactions involving 2-hydroxy aniline substrates, intramolecular trapping with *ortho*-OH leads to the formation of 1,4-benzoxazine (**5**).

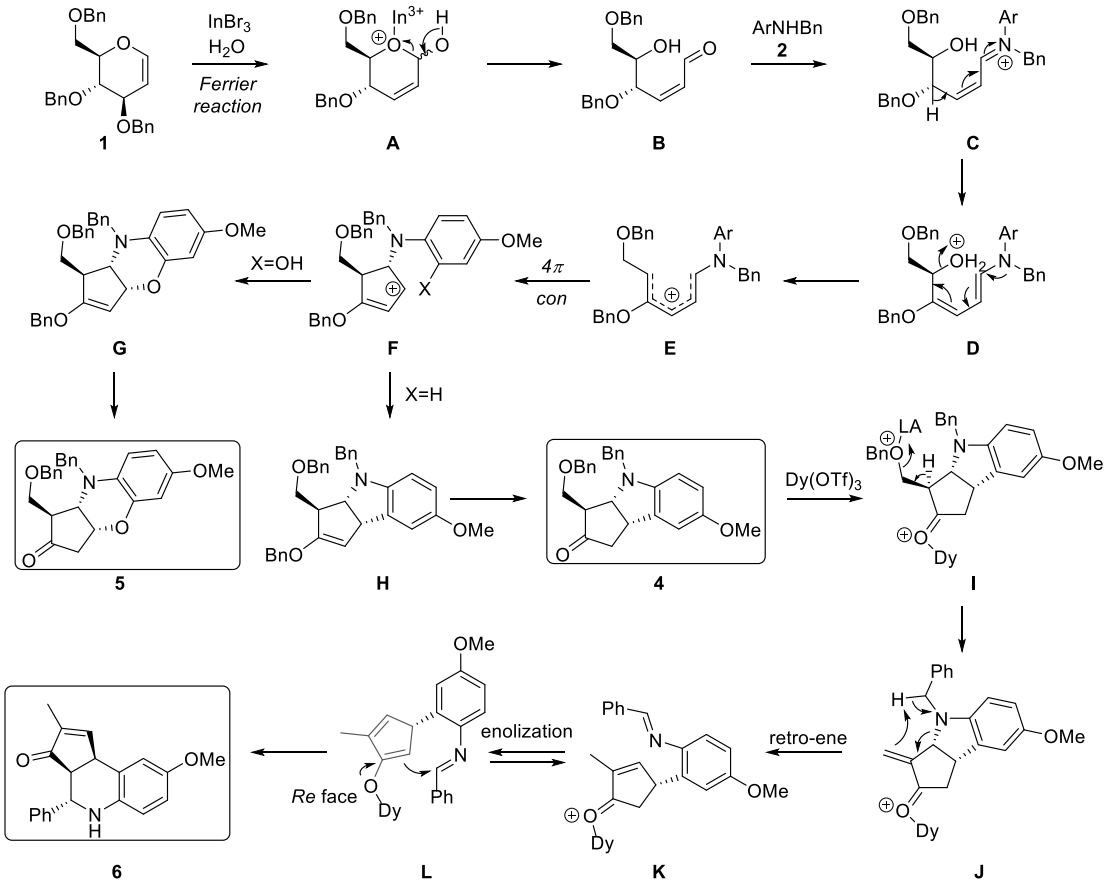

Scheme 3.2.4 Plausible mechanism for formation of the three different scaffolds.

Here we focused on presenting the experimental evidence supporting the first several steps involved in the proposed mechanism, as the rest following steps in the proposed mechanism leading to the formation of **4** and **6** have been discussed in detail and corroborated with deuterium-isotope studies in our previous work.[4] To vindicate the formation of the proposed aldehyde intermediate **B** by first step Ferrier reaction between the glucal substrate and water and ensuing ring opening reaction, high-temperature ^{1}H NMR experiments were carried out to monitor the reaction progress. The reaction was set up in a sealed NMR tube with tri-*O*-benzyl-D-glucal dissolved in CD_3CN solvent containing catalyst and water and without aniline substrate. An initial ^{1}H NMR spectrum of the solution was measured at room temperature over an extended

period of time and from the spectrum no reaction was observed. The solution in the NMR tube was then heated to and maintained at 80 ºC, and a series of spectra were collected in real time. In agreement to the prediction by the proposed mechanism, an aldehyde peak (around δ 9.5) indicating formation of intermediate **B** rose quickly and significantly on the spectra, shown in Scheme **3.2.5**. Upon further addition of aniline **2a** to the solution, the aldehyde peak diminished gradually, indicating consumption of intermediate **B** by the condensation reaction with aniline, and from the NMR spectra we observed slow formation of product **4**.

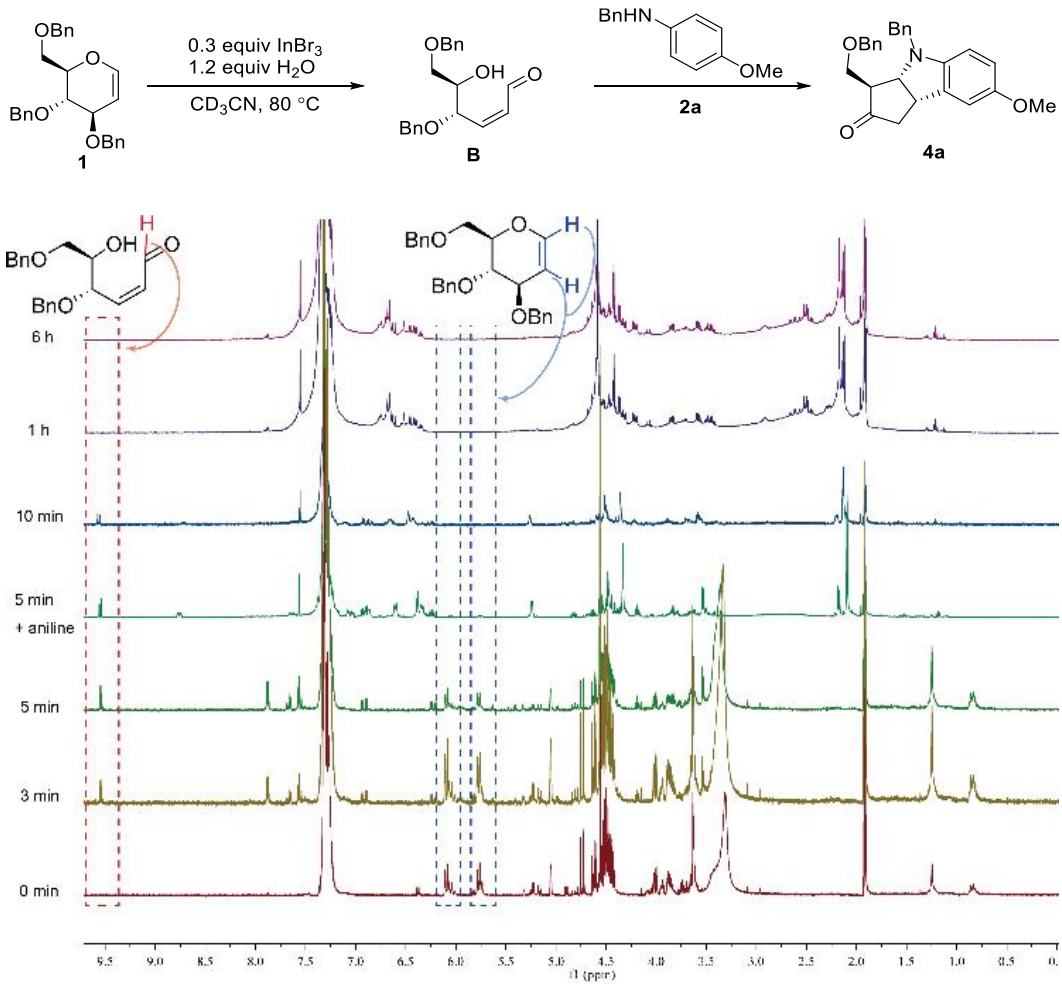

Scheme 3.2.5 High-temperature NMR monitoring reaction.

The trapping experiment of cyclic oxyallyl cation **F** with hydroxymethyl (-CH_2OH) group was conducted to support the mechanism further. Fortunately, the *ortho*-substituent group on the phenyl ring of aniline could also be extended to hydroxymethyl group which enables construction of 1,2,3,5-tetrahydro-1,4-benzoxazepine **7** as a single diastereomer (Scheme 3.2.6). This result not only proved the formation of cyclic oxyallyl cation **F** because the hydroxymethyl moiety could also capture the cation intermediate, but also demonstrated another novel type of fused compound synthesized from D-glucal directly. This experiment indicates that our methodology could be applied to various more nucleophiles and furnish more complicated fused rings. To our best knowledge, there is no precedent in the literature pertaining to the synthesis of 1, 2,3,5-tetrahydro-1,4-benzoxazepine. This fused ring scaffold might hold the keys to some natural product syntheses. For instance, tetrahydro-1,4-benzoxazepine could potentially serve as the core structure in the synthesis of yohimbine analogs with promising efficacy in the treatment or prevention of some diseases, such as proliferative diseases, tumors, inflammatory diseases, autoimmune diseases and infectious diseases.[11]

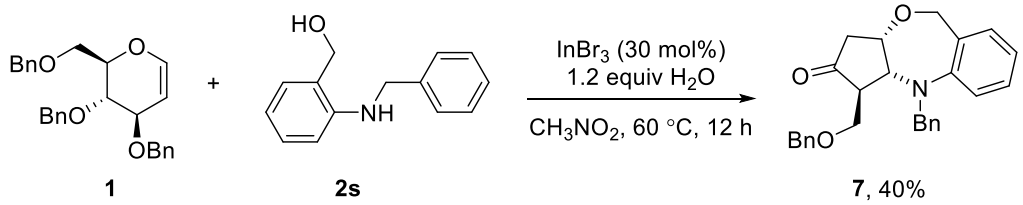

Scheme 3.2.6 2-Methylhydroxyaniline trapping cyclic oxyallyl cation to furnish tetrahydro-1,4-benzoxazepine.

3.3 Conclusion

In conclusion, we have developed a versatile cascade transformation of commercially available D-glycal and anilines directly into three different types of fused cyclic compounds with high molecular complexity, including indoline-fused cyclopentanone, 1,4-benzoxazine-fused cyclopentanone, tetrahydroquinoline-fused cyclopentenone in the exclusive diastereoselectivity. High-temperature NMR study confirmed D-glucal is first converted into *α,β*-unsaturated aldehyde through Ferrier reaction, followed by symmetry-allowed conrotatory ring closure which gives rise to the excellent diastereoselectivity. The formation of cyclic oxyallyl cation was confirmed by a trapping experiment with *N*-benzyl-2-methylhydroxylaniline, generating a fused five-seven-six-membered ring compound 1,2,3,5-tetrahydro-1,4-benzoxazepine-fused cyclopentanone has not been synthesized before. All the fused cyclic products could be found as the core structure of different natural products or potential pharmaceutical molecules.

This work provides a step-economical and more environment-friendly strategy of generating drug-like fused *N*-heterocycles from abundant biomass-derived glucal, anilines and water directly. Therefore, we believe the advances reported herein can intrigue researchers to develop more efficient one-pot reactions based on biomass-derived compounds and substrates, thus boosting the expansion of the library of potential drug candidates, which may greatly accelerate time and economic efficiency of drug discovery in the future.

3.4 Experimental Section

3.4.1 General Procedures

General procedure for preparation of Indoline-fused Cyclopentanones 4

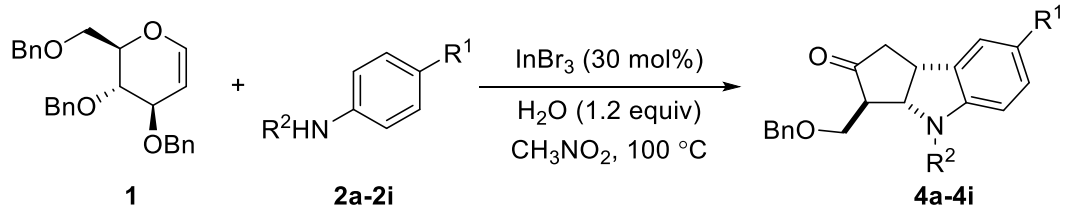

1 **2a-2i** **4a-4i**

To a suspension of 3,4,6-tri-*O*-benzyl-D-glucal **1** (100 mg, 0.24 mmol, 1.0 equiv), aniline **2a-2i** (0.24 mmol, 1.0 equiv) in CH_3NO_2 (2.4 mL) was added $InBr_3$ (25.5 mg, 0.072 mmol, 0.30 equiv) and DI water (5.2 μL, 0.29 mmol, 1.2 equiv). The reaction mixture was stirred at 100 °C for 4 h. Then the reaction mixture was extracted with EtOAc (3 × 50 mL), washed with 10% $NaHCO_3$ (2 × 50 mL) and brine (2 × 50 mL). The organic layers were dried over anhydrous Na_2SO_4, filtered and concentrated under reduced pressure to yield the crude residue as dark yellow oil. The crude residue was purified by flash column chromatography on silica gel (EtOAc/hexane) to afford **4** as an oil.

General procedure for preparation of 1,4-benzoxazine 5

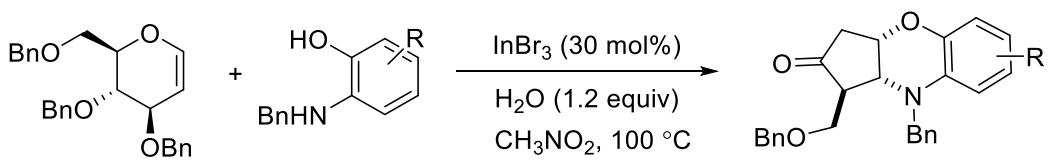

1 **2h-2r** **5a-5k**

To a suspension of 3,4,6-tri-*O*-benzyl-D-glucal **1** (100 mg, 0.24 mmol, 1.0 equiv), aniline **2h-2r** (0.24 mmol, 1.0 equiv) in CH_3NO_2 (2.4 mL) was added $InBr_3$ (25.5 mg, 0.072 mmol, 0.30 equiv) and DI water (5.2 μL, 0.29 mmol, 1.2 equiv). The reaction

mixture was stirred at 100 °C for 4 h. Then the reaction mixture was extracted with EtOAc (3 × 50 mL), washed with 10% $NaHCO_3$ (2 × 50 mL) and brine (2 × 50 mL). The organic layers were dried over anhydrous Na_2SO_4, filtered and concentrated under reduced pressure to yield the crude residue as dark yellow oil. The crude residue was purified by flash column chromatography on silica gel (EtOAc/hexane) to afford **5** as an oil

General procedure for preparation of tetrahydroquinoline-fused cyclopentenone 6

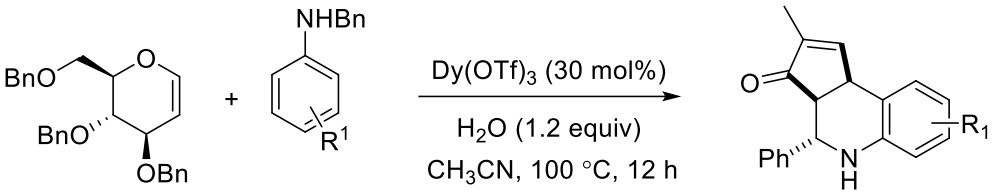

1 **2a-h, j** **6**

To a suspension of 3,4,6-tri-*O*-benzyl-D-glucal **1** (100 mg, 0.24 mmol, 1.0 equiv), aniline **2a-h, j** (24 mmol, 1.0 equiv) in CH_3CN (2.4 mL) was added $Dy(OTf)_3$ (43.9 mg, 0.072 mmol, 0.30 equiv) and DI water (5.2 μL, 0.29 mmol, 1.2 equiv). The reaction mixture was stirred at 100 °C for 12 h. Then the reaction mixture was extracted with EtOAc (3 × 50 mL), washed with 10% $NaHCO_3$ (2 × 50 mL) and brine (2 × 50 mL). The organic layers were dried over anhydrous Na_2SO_4, filtered and concentrated under reduced pressure to yield the crude residue as dark yellow oil. The crude residue was purified by flash column chromatography on silica gel (EtOAc/hexane) to afford **6** as a solid.

3.4.2 Characterization Data

4-Benzyl-3-((benzyloxy)methyl)-7-methoxy-3,3a,4,8b-tetrahydrocyclopenta[*b*]indol-2(*1H*)-one (**4a**)

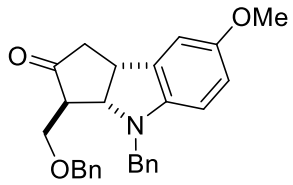

Brown oil; yield 58%; ^{1}H NMR (500 MHz, CD_3CN) δ 7.35 – 7.25 (m, 10H), 6.76 (dd, *J* = 2.7, 0.8 Hz, 1H), 6.58 (dd, *J* = 8.4, 2.6 Hz, 1H), 6.33 (d, *J* = 8.5 Hz, 1H), 4.41 (s, 2H), 4.35 (d, *J* = 15.6 Hz, 1H), 4.25 (dd, *J* = 8.4, 2.5 Hz, 1H), 4.21 (d, *J* = 15.6 Hz, 1H), 3.82 (td, *J* = 8.9, 7.1 Hz, 1H), 3.67 (s, 3H), 3.66 (d, *J* = 5.0 Hz, 1H), 3.53 (dd, *J* = 9.1, 3.8 Hz, 1H), 2.68 (dd, *J* = 18.9, 9.8 Hz, 1H), 2.58 (d, *J* = 5.5 Hz, 1H), 2.28 (ddd, *J* = 18.9, 7.2, 1.3 Hz, 1H); ^{13}C NMR (126 MHz, CD_3CN) δ 218.8, 154.1, 146.5, 139.7, 139.4, 135.5, 129.4, 129.3, 128.9, 128.5, 128.1, 127.9, 113.2, 112.6, 109.1, 73.8, 72.1, 70.4, 56.4, 54.6, 52.5, 44.9, 42.0; HRMS (ESI) *m/z*: calcd. for $C_{27}H_{28}NO_3$ $(M + H)^+$ 414.2070, found 414.2069.

4-Benzyl-3-((benzyloxy)methyl)-2-oxo-1,2,3,3a,4,8b-hexahydrocyclopenta[*b*]indol-7-yl acetate (**4b**)

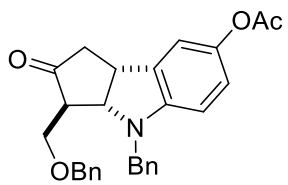

Brown oil; yield 51%; ^{1}H NMR (400 MHz, CD_3CN) δ 7.35 – 7.27 (m, 10H), 6.83 (d, *J* = 2.3 Hz, 1H), 6.69 (dd, *J* = 8.4, 2.3 Hz, 1H), 6.36 (d, *J* = 8.4 Hz, 1H), 4.49 – 4.34 (m,

4H), 4.28 (d, *J* = 16.0 Hz, 1H), 3.88 (q, *J* = 8.6 Hz, 1H), 3.67 (dd, *J* = 9.2, 5.2 Hz, 1H), 3.56 (dd, *J* = 9.2, 3.7 Hz, 1H), 2.71 (dd, *J* = 18.9, 9.9 Hz, 1H), 2.63 (s, 1H), 2.30 (dd, *J* = 18.9, 7.2 Hz, 1H), 2.18 (d, *J* = 1.4 Hz, 3H); ^{13}C NMR (101 MHz, CD_3CN) δ 218.4, 171.2, 150.0, 143.9, 139.3, 135.0, 129.5, 129.3, 128.9, 128.7, 128.5, 128.1, 127.7, 121.7, 119.2, 108.1, 73.8, 72.0, 70.4, 54.5, 51.5, 44.9, 41.6, 21.2; HRMS (ESI) *m/z*: calcd. for $C_{28}H_{28}NO_4$ $(M + H)^+$ 442.2018, found 442.2013.

4-Benzyl-3-((benzyloxy)methyl)-6,7,8-trimethoxy-3,3a,4,8b-tetrahydrocyclopenta[*b*]indol-2(*1H*)-one (**4c**)

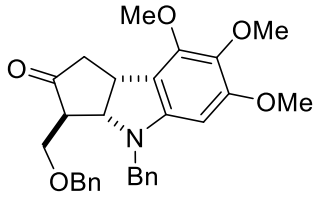

Brown oil; yield 55%; ^{1}H NMR (300 MHz, CD_3CN) δ 7.39 – 7.20 (m, 10H), 5.97 (s, 1H), 4.45 – 4.35 (m, 3H), 4.29 – 4.19 (m, 2H), 3.94 – 3.85 (m, 1H), 3.83 (s, 3H), 3.68 (s, 3H), 3.66 (s, 3H), 3.63 (d, *J* = 5.3 Hz, 1H), 3.58 – 3.49 (m, 1H), 2.70 (ddd, *J* = 18.9, 9.7, 0.7 Hz, 1H), 2.63 – 2.56 (m, 1H), 2.31 – 2.20 (m, 1H); ^{13}C NMR (75 MHz, CD_3CN) δ 219.0, 155.2, 151.3, 149.1, 139.4, 134.7, 129.5, 129.4, 129.1, 128.9, 128.6, 128.2, 128.2, 116.5, 90.5, 73.9, 71.8, 70.4, 61.3, 61.0, 56.8, 54.7, 51.6, 45.1, 39.5; HRMS (ESI) *m/z*: calcd. for $C_{29}H_{32}NO_5$ $(M + H)^+$ 474.2280, found 474.2283.

4-Benzyl-3-((benzyloxy)methyl)-7-methyl-3,3a,4,8b-tetrahydrocyclopenta[*b*]indol-2(*1H*)-one (**4d**)

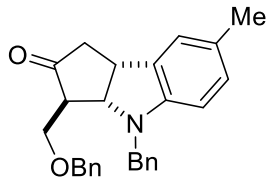

Brown oil; yield 49%; ^{1}H NMR (300 MHz, CD_3CN) δ 7.34 – 7.25 (m, 10H), 6.91 (t, *J* = 1.2 Hz, 1H), 6.85 – 6.74 (m, 1H), 6.32 (d, *J* = 8.0 Hz, 1H), 4.45 – 4.36 (m, 3H), 4.31 – 4.19 (m, 2H), 3.82 (td, *J* = 9.1, 7.0 Hz, 1H), 3.66 (dd, *J* = 9.1, 5.2 Hz, 1H), 3.54 (dd, *J* = 9.2, 3.8 Hz, 1H), 2.70 (ddd, *J* = 18.8, 9.8, 0.7 Hz, 1H), 2.59 (d, *J* = 4.0 Hz, 1H), 2.26 (ddd, *J* = 19.0, 7.1, 1.3 Hz, 1H), 2.19 (s, 3H); ^{13}C NMR (75 MHz, CD_3CN) δ 218.8, 150.1, 139.6, 139.4, 134.2, 129.4, 129.3, 129.1, 128.8, 128.7, 128.6, 128.2, 128.0, 126.1, 108.5, 73.8, 71.6, 70.5, 54.5, 51.7, 45.1, 41.8, 20.8; HRMS (ESI) *m/z*: calcd. for $C_{27}H_{28}NO_2$ $(M + H)^+$ 398.2120, found 398.2118.

4-Benzyl-3-((benzyloxy)methyl)-7-(tert-butyl)-3,3a,4,8b-tetrahydrocyclopenta[*b*]indol-2(*1H*)-one (**4e**)

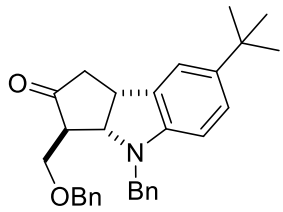

Brown oil; yield 45%; ^{1}H NMR (300 MHz, CD_3CN) δ 7.36 – 7.25 (m, 10H), 7.21 – 7.14 (m, 1H), 7.04 (dd, *J* = 8.2, 2.1 Hz, 1H), 6.32 (d, *J* = 8.2 Hz, 1H), 4.40 (d, *J* = 12.0 Hz, 3H), 4.31 – 4.23 (m, 2H), 3.91 – 3.80 (m, 1H), 3.67 (dd, *J* = 9.2, 5.2 Hz, 1H), 3.55 (dd, *J* = 9.2, 3.8 Hz, 1H), 2.71 (ddd, *J* = 18.8, 9.8, 0.7 Hz, 1H), 2.59 (s, 1H), 2.36 – 2.24 (m, 1H), 1.24 (s, 9H); ^{13}C NMR (75 MHz, CD_3CN) δ 219.5, 150.6, 142.7, 140.4, 140.0,

134.4, 130.1, 130.0, 129.4, 129.2, 128.7, 126.0, 123.2, 118.9, 108.6, 74. 5, 72.3, 71.1, 55.1, 52.2, 45.8, 42.6, 35.4, 32.6; HRMS (ESI) *m/z*: calcd. for $C_{30}H_{34}NO_2$ $(M + H)^+$ 440.2590, found 440.2597.

4-Benzyl-3-((benzyloxy)methyl)-3,3a,4,8b-tetrahydrocyclopenta[*b*]indol-2(*1H*)-one (**4f**)

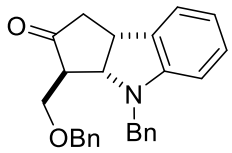

Brown oil; yield 52%; ^{1}H NMR (400 MHz, CD_3CN) δ 7.38 – 7.22 (m, 10H), 7.14 – 7.05 (m, 1H), 7.00 (td, *J* = 7.7, 1.3 Hz, 1H), 6.63 (td, *J* = 7.4, 1.0 Hz, 1H), 6.42 (d, *J* = 7.8 Hz, 1H), 4.50 – 4.41 (m, 3H), 4.35 – 4.25 (m, 2H), 3.88 (q, *J* = 8.8 Hz, 1H), 3.73 – 3.66 (m, 1H), 3.56 (dd, *J* = 9.1, 3.8 Hz, 1H), 2.72 (ddd, *J* = 18.9, 9.9, 0.7 Hz, 1H), 2.61 (s, 1H), 2.29 (ddt, *J* = 19.0, 7.1, 0.7 Hz, 1H); ^{13}C NMR (101 MHz, CD_3CN) δ 218.7, 152.2, 139.6, 139.4, 133.9, 129.5, 129.4, 128.9, 128.8, 128.6, 128.1, 125.3, 118.9, 118.3, 108.4, 73.9, 71.4, 70.5, 54.5, 51.2, 45.2, 41.7; HRMS (ESI) *m/z*: calcd. for $C_{26}H_{26}NO_2$ $(M + H)^+$ 384.1964, found 384.1966.

4-Benzyl-3-((benzyloxy)methyl)-7-(methylthio)-3,3a,4,8b-tetrahydrocyclopenta[*b*]indol-2(*1H*)-one (**4g**)

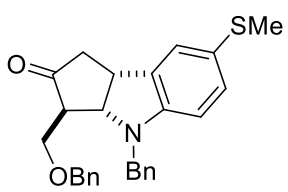

Brown oil; yield 46%; ^{1}H NMR (300 MHz, CD_3CN) δ 7.32 – 7.28 (m, 11H), 7.15 – 7.10 (m, 1H), 7.03 (dd, *J* = 8.1, 2.0 Hz, 1H), 6.36 (d, *J* = 8.2 Hz, 1H), 4.48 – 4.39 (m, 3H), 4.34 (dd, *J* = 8.7, 2.7 Hz, 1H), 4.27 (d, *J* = 15.9 Hz, 1H), 3.87 (q, *J* = 8.8 Hz, 1H), 3.67 (dd, *J* = 9.2, 5.2 Hz, 1H), 3.55 (dd, *J* = 9.1, 3.8 Hz, 1H), 2.72 (dd, *J* = 18.9, 9.9 Hz, 1H), 2.65 – 2.59 (m, 1H), 2.36 (s, 3H), 2.33 – 2.27 (m, 1H); ^{13}C NMR (75 MHz, CD_3CN) δ 219.1, 151.8, 140.0, 139.9, 135.8, 131.2, 130.1, 130.0, 129.4, 129.2, 128.8, 128.5, 127.8, 126.5, 109.4, 74.5, 72.0, 71.0, 55.1, 51.7, 45.6, 42.2, 19.6; HRMS (ESI) *m/z*: calcd. for $C_{27}H_{28}NO_2S$ $(M + H)^+$ 430.1841, found 430.1841.

4-Benzyl-3-((benzyloxy)methyl)-7-phenyl-3,3a,4,8b-tetrahydrocyclopenta[*b*]indol-2(*1H*)-one (**4h**)

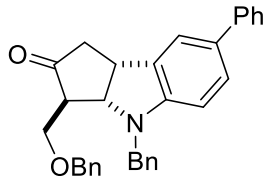

Brown oil; yield 43%; ^{1}H NMR (400 MHz, CD_3CN) δ 7.54 (d, *J* = 7.7 Hz, 2H), 7.40 – 7.27 (m, 15H), 6.48 (d, *J* = 8.2 Hz, 1H), 4.51 (d, *J* = 15.9 Hz, 1H), 4.43 (s, 2H), 4.42 – 4.31 (m, 2H), 3.95 (q, *J* = 8.8 Hz, 1H), 3.69 (dd, *J* = 9.2, 5.3 Hz, 1H), 3.58 (dd, *J* = 9.1, 3.8 Hz, 1H), 2.77 (dd, *J* = 18.9, 9.9 Hz, 1H), 2.65 (t, *J* = 4.1 Hz, 1H), 2.40 (dd, *J* = 18.9, 6.8 Hz, 1H); ^{13}C NMR (101 MHz, CD_3CN) δ 218.6, 151.8, 142.3, 139.4, 134.8, 131.6, 129.7, 129.5, 129.3, 128.9, 128.7, 128.6, 128.1, 127.7, 127.1, 127.1, 127.00, 124.1, 108.4, 73.9, 71.4, 70.4, 54.5, 51.0, 45.1, 41.7; HRMS (ESI) *m/z*: calcd. for $C_{32}H_{30}NO_2$ $(M + H)^+$ 460.2277, found 460.2284.

4-Allyl-3-((benzyloxy)methyl)-7-methoxy-3,3a,4,8b-tetrahydrocyclopenta[*b*]indol-2(*1H*)-one (**4i**)

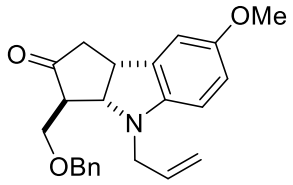

Brown oil; yield 40%; ^{1}H NMR (400 MHz, CD_3CN) δ 7.38 – 7.29 (m, 5H), 6.75 (dd, *J* = 2.6, 0.8 Hz, 1H), 6.63 (dd, *J* = 8.5, 2.7 Hz, 1H), 6.43 (d, *J* = 8.5 Hz, 1H), 5.86 (dddd, *J* = 17.2, 10.2, 6.3, 5.4 Hz, 1H), 5.25 – 5.11 (m, 2H), 4.48 (s, 2H), 4.23 (dd, *J* = 8.4, 2.2 Hz, 1H), 3.83 – 3.71 (m, 3H), 3.68 (s, 3H), 3.67 – 3.60 (m, 2H), 2.71 – 2.63 (m, 1H), 2.63 – 2.56 (m, 1H), 2.28 – 2.16 (m, 1H); ^{13}C NMR (101 MHz, CD_3CN) δ 219.1, 154.0, 146.2, 139.4, 135.7, 135.1, 129.3, 129.0, 128.5, 117.9, 113.3, 112.5, 109.2, 73.9, 71.8, 70.6, 56.4, 54.7, 50.8, 45.0, 42.0; HRMS (ESI) *m/z*: calcd. for $C_{23}H_{26}NO_3$ $(M + H)^+$ 364.1913, found 364.1916.

9-Benzyl-1-((benzyloxy)methyl)-3,3a,9,9a-tetrahydrobenzo[*b*]cyclopenta[*e*][1,4]oxazin-2(*1H*)-one (**5a**)

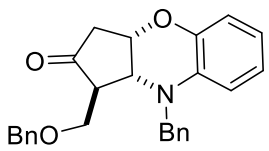

Brown oil; yield 66%; ^{1}H NMR (400 MHz, Acetone-d_6) δ 7.34 – 7.24 (m, 10H), 6.82 – 6.72 (m, 2H), 6.64 (dd, *J* = 8.1, 1.5 Hz, 1H), 6.57 (td, *J* = 7.6, 1.5 Hz, 1H), 4.68 – 4.59 (m, 3H), 4.48 – 4.35 (m, 3H), 3.92 (dd, *J* = 9.5, 3.0 Hz, 1H), 3.63 (dd, *J* = 9.5, 3.4 Hz, 1H), 2.67 – 2.52 (m, 2H), 2.33 (dt, *J* = 10.0, 3.2 Hz, 1H); ^{13}C NMR (101 MHz, Acetone-

d$_6$) δ 212.3, 142.4, 138.7, 138.2, 132.3, 128.4, 128.1, 127.5, 127.4, 126.8, 126.7, 122.0, 117.0, 116.2, 112.8, 72.7, 70.5, 66.0, 55.9, 54.4, 51.3, 45.20; HRMS (ESI) *m/z*: calcd. for $C_{26}H_{26}NO_3$ $(M + H)^+$ 400.1913, found 400.1914.

9-Benzyl-1-((benzyloxy)methyl)-5-methyl-3,3a,9,9a-tetrahydrobenzo[*b*]cyclopenta[*e*][1,4]oxazin-2(*1H*)-one (**5b**)

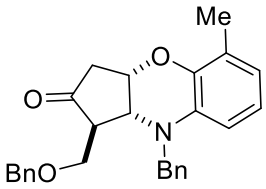

Brown oil; yield 59%; ^{1}H NMR (400 MHz, Acetone-*d*$_6$) δ 7.46 – 7.15 (m, 10H), 6.69 – 6.58 (m, 1H), 6.52 – 6.42 (m, 2H), 4.61 (d, *J* = 12.5 Hz, 3H), 4.47 – 4.37 (m, 2H), 4.35 (d, *J* = 3.3 Hz, 1H), 3.91 (dd, *J* = 9.6, 3.0 Hz, 1H), 3.62 (dd, *J* = 9.5, 3.4 Hz, 1H), 2.63 (d, *J* = 2.4 Hz, 2H), 2.31 (dt, *J* = 10.0, 3.2 Hz, 1H), 2.14 (s, 3H); ^{13}C NMR (101 MHz, Acetone-*d*$_6$) δ 213.5, 141.5, 140.0, 139.3, 133.0, 129.4, 129.1, 128.5, 128.4, 127.8, 127.7, 126.2, 122.2, 119.9, 111.8, 73.8, 71.4, 67.0, 59.9, 55.6, 52.4, 46.3, 16.0; HRMS (ESI) *m/z*: calcd. for $C_{27}H_{28}NO_3$ $(M + H)^+$ 414.2069, found 414.2071.

9-Benzyl-1-((benzyloxy)methyl)-6-methyl-3,3a,9,9a-tetrahydrobenzo[*b*]cyclopenta[*e*][1,4]oxazin-2(*1H*)-one (**5c**)

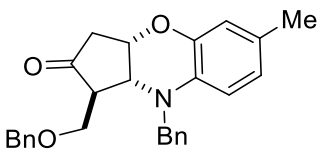

Brown oil; yield 60%; ^{1}H NMR (300 MHz, CD_3CN) δ 7.39 – 7.10 (m, 10H), 6.67 (d, *J* = 8.0 Hz, 1H), 6.53 (d, *J* = 1.9 Hz, 1H), 6.39 (dd, *J* = 8.1, 2.0 Hz, 1H), 4.64 (d, *J* = 5.6 Hz, 2H), 4.55 (td, *J* = 3.1, 1.8 Hz, 1H), 4.48 – 4.29 (m, 3H), 3.91 (dd, *J* = 9.5, 3.0 Hz, 1H), 3.61 (dd, *J* = 9.5, 3.4 Hz, 1H), 2.58 (dd, *J* = 2.8, 1.5 Hz, 2H), 2.30 (dt, *J* = 9.9, 3.2 Hz, 1H), 2.11 (s, 3H); ^{13}C NMR (75 MHz, CD_3CN) δ 213.5, 141.5, 139.9, 139.3, 133.0, 129.4, 129.1, 128.5, 128.4, 127.8, 127.7, 126.2, 122.2, 119.9, 111.8, 73.8, 71.4, 67.0, 59.9, 55.6, 52.4, 46.3, 15.9; HRMS (ESI) *m/z*: calcd. for $C_{27}H_{28}NO_3$ $(M + H)^+$ 414.2069, found 414.2070.

9-Benzyl-1-((benzyloxy)methyl)-7-methyl-3,3a,9,9a-tetrahydrobenzo[*b*]cyclopenta[*e*][1,4]oxazin-2(*1H*)-one (**5d**)

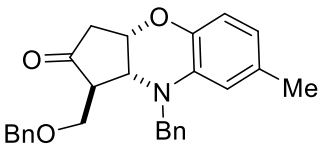

Brown oil; yield 61%; ^{1}H NMR (500 MHz, Acetone-d_6) δ 7.40 – 7.24 (m, 13H), 6.68 (d, *J* = 8.0 Hz, 1H), 6.53 (d, *J* = 1.8 Hz, 1H), 6.39 (dd, *J* = 8.1, 1.8 Hz, 1H), 4.71 – 4.59 (m, 3H), 4.55 (t, *J* = 2.3 Hz, 1H), 4.45 – 4.35 (m, 2H), 4.33 (dd, *J* = 10.0, 3.1 Hz, 1H), 3.91 (dd, *J* = 9.6, 3.0 Hz, 1H), 3.61 (dd, *J* = 9.5, 3.4 Hz, 1H), 2.64 – 2.50 (m, 2H), 2.30 (dt, *J* = 9.9, 3.2 Hz, 1H), 2.11 (s, 3H); ^{13}C NMR (126 MHz, Acetone-d_6) δ 213.4, 141.4, 139.8, 139.2, 133.0, 132.1, 129.4, 129.1, 128.5, 128.3, 127.8, 127.7, 118.6, 117.1, 114.4, 73.7, 71.4, 667.0, 59.8, 55.3, 52.3, 46.2, 21.2; HRMS (ESI) *m/z*: calcd. for $C_{27}H_{28}NO_3$ $(M + H)^+$ 414.2069, found 414.2069.

9-Benzyl-1-((benzyloxy)methyl)-8-methyl-3,3a,9,9a-tetrahydrobenzo[*b*]cyclopenta[*e*][1,4]oxazin-2(*1H*)-one (**5e**)

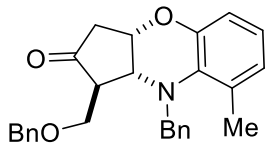

Brown oil; yield 56%; ^{1}H NMR (400 MHz, Acetone-d_6) δ 7.62 (d, *J* = 7.6 Hz, 2H), 7.46 – 7.37 (m, 2H), 7.32 – 7.17 (m, 4H), 7.07 – 6.99 (m, 2H), 6.89 (t, *J* = 7.7 Hz, 1H), 6.81 (ddd, *J* = 7.6, 1.7, 0.8 Hz, 1H), 6.68 (dd, *J* = 8.0, 1.6 Hz, 1H), 4.79 (t, *J* = 3.4 Hz, 1H), 4.32 (d, *J* = 15.2 Hz, 1H), 4.23 (s, 2H), 4.06 (d, *J* = 15.2 Hz, 1H), 3.90 (dd, *J* = 11.3, 3.3 Hz, 1H), 3.78 (dd, *J* = 9.1, 2.8 Hz, 1H), 3.59 (dd, *J* = 9.1, 2.8 Hz, 1H), 2.51 (dd, *J* = 18.2, 1.5 Hz, 1H), 2.42 (s, 3H), 2.40 (d, *J* = 3.5 Hz, 1H), 1.82 (dq, *J* = 11.2, 2.4 Hz, 1H); ^{13}C NMR (101 MHz, Acetone-d_6) δ 212.7, 148.4, 139.4, 139.3, 134.7, 130.9, 129.4, 129.1, 128.9, 128.3, 128.2, 128.0, 124.5, 124.4, 115.4, 73.6, 66.9, 66.2, 60.4, 56.7, 49.9, 46.9, 18.3. HRMS (ESI) *m/z*: calcd. for $C_{27}H_{28}NO_3$ $(M + H)^+$ 414.2069, found 414.2069.

9-Benzyl-1-((benzyloxy)methyl)-7-(tert-butyl)-3,3a,9,9a-tetrahydrobenzo[*b*]cyclopenta[*e*][1,4]oxazin-2(*1H*)-one (**5f**)

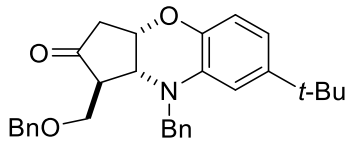

Brown oil; yield 53%; ^{1}H NMR (300 MHz, Acetone-d_6) δ 7.43 – 7.18 (m, 10H), 6.74 – 6.64 (m, 2H), 6.60 (dd, *J* = 8.3, 2.2 Hz, 1H), 4.73 – 4.55 (m, 3H), 4.51 – 4.29 (m, 3H),

3.94 (dd, *J* = 9.6, 3.0 Hz, 1H), 3.65 (dd, *J* = 9.6, 3.4 Hz, 1H), 2.66 – 2.50 (m, 2H), 2.32 (dt, *J* = 9.9, 3.0 Hz, 1H), 1.12 (s, 9H); ^{13}C NMR (75 MHz, Acetone-d_6) δ ^{13}C NMR (75 MHz, Acetone) δ 213.4, 145.5, 141.4, 140.1, 139.3, 132.4, 129.3, 129.1, 128.5, 128.4, 127.8, 127.8, 116.5, 114.9, 111.7, 73.7, 71.5, 67.0, 60.2, 56.0, 52.2, 46.2, 34.8, 31.8; HRMS (ESI) *m/z*: calcd. for $C_{30}H_{34}NO_3$ $(M + H)^+$ 456.2534, found 456.2539.

9-Benzyl-1-((benzyloxy)methyl)-6-chloro-3,3a,9,9a-tetrahydrobenzo[*b*]cyclopenta[*e*][1,4]oxazin-2(*1H*)-one (**5g**)

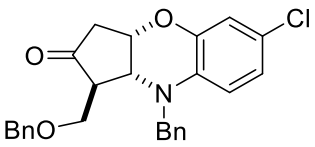

Brown oil; yield 56%; ^{1}H NMR (400 MHz, Acetone-d_6) δ 7.36 – 7.22 (m, 10H), 6.81 (d, *J* = 2.5 Hz, 1H), 6.75 (dd, *J* = 8.7, 2.4 Hz, 1H), 6.61 (d, *J* = 8.7 Hz, 1H), 4.72 – 4.58 (m, 3H), 4.49 – 4.35 (m, 3H), 3.92 (dd, *J* = 9.6, 3.1 Hz, 1H), 3.64 (dd, *J* = 9.6, 3.4 Hz, 1H), 2.65 – 2.61 (m, 2H), 2.36 (dt, *J* = 10.0, 3.4 Hz, 1H); ^{13}C NMR (101 MHz, Acetone-d_6) δ 212.9, 144.0, 139.2, 139.2, 132.4, 129.5, 129.1, 128.6, 128.4, 127.9, 127.6, 122.7, 121.7, 117.2, 114.6 73.7, 72.1, 66.9, 59.8, 55.4, 52.2, 46.0; HRMS (ESI) *m/z*: calcd. for $C_{26}H_{25}ClNO_3$ $(M + H)^+$ 434.1523, found 434.1524.

9-Benzyl-1-((benzyloxy)methyl)-7-chloro-3,3a,9,9a-tetrahydrobenzo[*b*]cyclopenta[*e*][1,4]oxazin-2(*1H*)-one (**5h**)

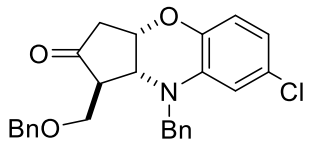

Brown oil; yield 54%; ^{1}H NMR (300 MHz, Acetone-d_6) δ 7.37 – 7.21 (m, 10H), 6.77 (d, *J* = 8.4 Hz, 1H), 6.59 (d, *J* = 2.4 Hz, 1H), 6.54 (dd, *J* = 8.4, 2.4 Hz, 1H), 4.75 – 4.59 (m, 3H), 4.50 – 4.36 (m, 3H), 3.93 (dd, *J* = 9.6, 3.1 Hz, 1H), 3.67 (dd, *J* = 9.6, 3.4 Hz, 1H), 2.72 – 2.53 (m, 2H), 2.42 – 2.31 (m, 1H); ^{13}C NMR (75 MHz, Acetone-d_6) δ^{13}C NMR (75 MHz, Acetone-d_6) δ 212.9, 142.2, 139.2, 138.9, 134.7, 129.6, 129.1, 128.9, 128.6, 128.4, 128.0, 127.6, 118.3, 117.2, 112.9, 73.8, 71.9, 67.0, 59.7, 55.0, 52.5, 46.0; HRMS (ESI) *m/z*: calcd. for $C_{26}H_{25}ClNO_3$ $(M + H)^+$ 434.1523, found 434.1525.

9-Benzyl-1-((benzyloxy)methyl)-7-bromo-3,3a,9,9a-tetrahydrobenzo[*b*]cyclopenta[*e*][1,4]oxazin-2(*1H*)-one (**5i**)

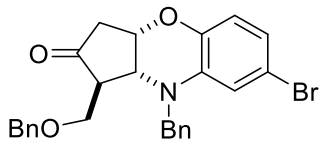

Brown oil; yield 53%; ^{1}H NMR (400 MHz, Acetone-d_6) δ 7.40 – 7.23 (m, 10H), 6.78 – 6.64 (m, 3H), 4.73 – 4.61 (m, 3H), 4.51 – 4.36 (m, 3H), 3.94 (dd, *J* = 9.6, 3.1 Hz, 1H), 3.67 (dd, *J* = 9.6, 3.4 Hz, 1H), 2.71 – 2.55 (m, 2H), 2.38 (dt, *J* = 10.0, 3.3 Hz, 1H); ^{13}C NMR (101 MHz, Acetone-d_6) δ 212.9, 142.6, 139.1, 138.9, 135.0, 129.5, 129.1, 128.6, 128.4, 128.4, 128.0, 127.5, 120.2, 118.8, 115.7, 115.0, 73.8, 71.9, 66.9, 59.6, 55.0, 52.4, 46.0; HRMS (ESI) *m/z*: calcd. for $C_{26}H_{25}BrNO_3$ $(M + H)^+$ 478.1018, found 478.1016.

9-Benzyl-1-((benzyloxy)methyl)-6-nitro-3,3a,9,9a-tetrahydrobenzo[*b*]cyclopenta[*e*][1,4]oxazin-2(*1H*)-one (**5j**)

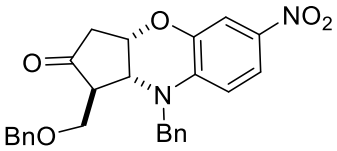

Yellow oil; yield 50%; ^{1}H NMR (400 MHz, Acetone-d_6) δ 7.51 (dd, *J* = 8.7, 2.6 Hz, 1H), 7.46 (d, *J* = 2.6 Hz, 1H), 7.40 – 7.23 (m, 11H), 6.97 (d, *J* = 8.7 Hz, 1H), 4.86 (t, *J* = 3.2 Hz, 1H), 4.84 – 4.70 (m, 2H), 4.57 (dd, *J* = 10.1, 3.2 Hz, 1H), 4.52 – 4.41 (m, 2H), 3.96 (dd, *J* = 9.7, 3.2 Hz, 1H), 3.72 (dd, *J* = 9.7, 3.4 Hz, 1H), 2.80 – 2.76 (m, 1H), 2.73 (d, *J* = 3.7 Hz, 1H), 2.71 (t, *J* = 1.2 Hz, 1H), 2.44 (ddt, *J* = 10.1, 3.8, 1.9 Hz, 1H); ^{13}C NMR (101 MHz, Acetone-d_6) δ 211.5, 148.0, 142.9, 138.2, 137.4, 132.6, 128.7, 128.2, 127.7, 127.5, 127.3, 126.7, 116.3, 112.9, 107.2, 72.9, 72.1, 66.0, 58.6, 54.3, 51.3, 45.0; HRMS (ESI) *m/z*: calcd. for $C_{26}H_{25}N_2O_5$ $(M + H)^+$ 445.1763, found 445.1761.

1-((Benzyloxy)methyl)-9-methyl-3,3a,9,9a-tetrahydrobenzo[*b*]cyclopenta[*e*][1,4]oxazin-2(*1H*)-one (**5k**)

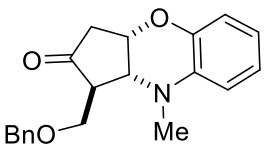

Brown oil; yield 51%; ^{1}H NMR (400 MHz, Acetone-d_6) δ 7.43 – 7.28 (m, 5H), 6.84 (td, *J* = 7.7, 1.6 Hz, 1H), 6.71 (ddd, *J* = 20.6, 8.0, 1.5 Hz, 2H), 6.56 (td, *J* = 7.6, 1.5 Hz, 1H), 4.61 – 4.52 (m, 3H), 4.23 (dd, *J* = 9.9, 3.1 Hz, 1H), 3.98 (dd, *J* = 9.7, 3.1 Hz, 1H), 3.78 (dd, *J* = 9.6, 3.3 Hz, 1H), 3.03 (s, 3H), 2.66 – 2.50 (m, 2H), 2.23 (dt, *J* = 9.9, 3.2 Hz, 1H); ^{13}C NMR (101 MHz, Acetone-d_6) δ 213.5, 143.4, 139.3, 134.1, 129.1, 128.6, 128.4,

123.1, 117.7, 116.7, 112.5, 73.9, 71.7, 67.5, 60.3, 51.8, 46.2, 38.3. HRMS (ESI) *m/z*: calcd. for $C_{20}H_{22}NO_3$ $(M + H)^+$ 324.1600, found 324.1599.

The characterization data of **6a-6f** is consistent with our previous work (*Angew. Chem. Int. Ed.* **2014**, *53*, 10742 –10746).

2-Methyl-8-(methylthio)-4-phenyl-3a,4,5,9b-tetrahydro-*3H*-cyclopenta[*c*]quinolin-3-one (**6g**)

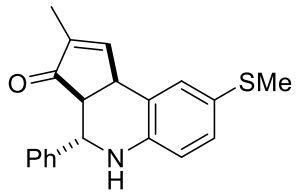

White solid; yield 44%; ^{1}H NMR (400 MHz, CD_3CN) δ 7.44 – 7.39 (m, 1H), 7.39 – 7.18 (m, 7H), 6.96 (dd, *J* = 8.3, 2.0 Hz, 1H), 6.54 (d, *J* = 8.3 Hz, 1H), 4.83 (s, 1H), 4.52 (t, *J* = 2.8 Hz, 1H), 4.13 (d, *J* = 5.9 Hz, 1H), 3.14 (dd, *J* = 7.0, 4.1 Hz, 1H), 2.40 (d, *J* = 1.3 Hz, 3H), 1.73 (d, *J* = 1.7 Hz, 3H); ^{13}C NMR (101 MHz, CD_3CN) δ 209.4, 160.8, 144.0, 143.9, 139.7, 130.3, 129.3, 129.0, 128.3, 128.2, 127.1, 124.1, 117.3, 56.8, 52.8, 40.4, 18.1, 10.2; HRMS (ESI) *m/z*: calcd. for $C_{20}H_{20}NOS$ $(M + H)^+$ 322.1266, found 322.1265.

2-Methyl-3-oxo-4-phenyl-3a,4,5,9b-tetrahydro-*3H*-cyclopenta[*c*]quinolin-8-yl acetate (**6h**)

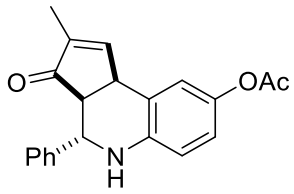

White solid; yield 47%; ^{1}H NMR (400 MHz, Acetone-d_6) δ 7.44 (dq, *J* = 3.0, 1.5 Hz, 1H), 7.41 – 7.34 (m, 2H), 7.34 – 7.25 (m, 2H), 7.23 – 7.18 (m, 1H), 7.05 (d, *J* = 2.3 Hz, 1H), 6.73 – 6.66 (m, 2H), 5.37 (s, 1H), 4.55 – 4.49 (m, 1H), 4.23 – 4.15 (m, 1H), 3.14 (ddd, *J* = 6.9, 4.2, 0.9 Hz, 1H), 2.20 (s, 3H), 1.74 (t, *J* = 1.7 Hz, 3H); ^{13}C NMR (101 MHz, Acetone-d_6) δ 208.3, 170.0, 160.1, 144.3, 143.9, 143.3, 139.5, 129.1, 128.2, 127.8, 123.4, 122.2, 121.2, 116.6, 57.0, 52.9, 40.4, 20.9, 10.1; HRMS (ESI) *m/z*: calcd. for $C_{21}H_{20}NO_3$ $(M + H)^+$ 334.1443, found 334.1439.

8-Hydroxy-2-methyl-4-phenyl-3a,4,5,9b-tetrahydro-*3H*-cyclopenta[*c*]quinolin-3-one (**6i**)

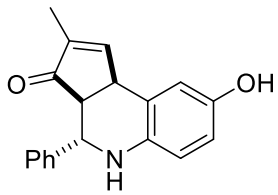

White solid; yield 49%; ^{1}H NMR (400 MHz, CD_3CN) δ 7.44 – 7.34 (m, 1H), 7.33 – 7.18 (m, 6H), 6.73 (d, *J* = 2.5 Hz, 1H), 6.49 – 6.38 (m, 2H), 6.34 (s, 1H), 4.44 (d, *J* = 4.2 Hz, 1H), 4.08 (d, *J* = 6.6 Hz, 1H), 3.10 (dd, *J* = 6.8, 4.1 Hz, 1H), 1.73 (s, 3H); ^{13}C NMR (101 MHz, CD_3CN) δ 209.8, 160.8, 150.7, 144.2, 139.7, 138.5, 129.2, 128.4, 128.0, 124.4, 117.5, 115.9, 115.3, 57.7, 52.7, 41.0, 10.2; HRMS (ESI) *m/z*: calcd. for $C_{19}H_{18}NO_2$ $(M + H)^+$ 292.1338, found 292.1344.

10-Benzyl-1-((benzyloxy)methyl)-1,3,3a,5,10,10a-hexahydro-*2H*-benzo[*e*]cyclopenta[*b*][1,4]oxazepin-2-one (**7**)

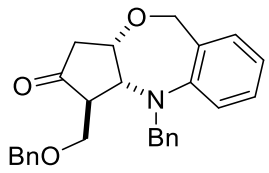

Colorless oil; yield 40%; ^{1}H NMR (400 MHz, Acetone-d_6) δ 7.47 – 7.14 (m, 13H), 6.95 (td, *J* = 7.3, 1.3 Hz, 1H), 4.79 (d, *J* = 12.6 Hz, 1H), 4.73 (d, *J* = 14.2 Hz, 1H), 4.69 – 4.58 (m, 2H), 4.58 – 4.46 (m, 2H), 4.09 (t, *J* = 3.6 Hz, 1H), 4.01 (dd, *J* = 11.7, 3.0 Hz, 1H), 3.84 (dd, *J* = 9.5, 2.7 Hz, 1H), 3.62 (dd, *J* = 9.5, 3.4 Hz, 1H), 2.26 (dd, *J* = 18.2, 4.2 Hz, 1H), 2.23 – 2.13 (m, 1H), 1.99 – 1.88 (m, 1H); ^{13}C NMR (126 MHz, Acetone-d_6) δ 213.0, 148.1, 140.4, 139.4, 133.2, 129.9, 129.7, 129.3, 129.2, 129.1, 128.7, 128.4, 128.0, 122.8, 121.3, 77.4, 73.8, 72.0, 66.8, 62.4, 59.0, 48.4, 47.0; HRMS (ESI) *m/z*: calcd. for $C_{27}H_{28}NO_3$ $(M + H)^+$ 414.2069, found 414.2070.

1-(hydroxymethyl)-9-methyl-3,3a,9,9a-tetrahydrobenzo[b]cyclopenta[e][1,4]oxazin-2(1H)-one (8)

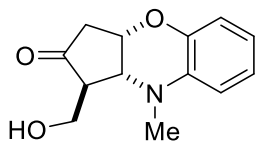

The product was obtained as white solid. Yield: 49%. ^{1}H NMR (400 MHz, $CDCl_3$) δ 6.96 (m, 1H), 6.85 (dd, *J*=8.0, 1.6 Hz, 1H), 6.71 (m, 2H), 4.56 (t, *J*=4.0 Hz, 1H), 4.25 (dd, *J*=11.2, 2.0 Hz, 1H), 4.06 (dd, *J*=10.4, 3.2 Hz, 1H), 3.86 (dd, *J*=11.2, 4.0 Hz, 1H), 3.13 (s, 3H), 2.77 (dd, *J*=19.2, 1.6 Hz, 1H), 2.52 (dd, *J*=19.2, 4.0 Hz, 1H), 2.40 (d, *J*=10.4 Hz, 1H), 1.97 (brs, 1H); ^{13}C NMR (100 MHz, $CDCl_3$) δ 215.2, 142.3, 132.7,

122.5, 117.6, 116.4, 111.8, 70.2, 59.1, 59.1, 52.7, 45.5, 38.5; HRMS (ESI):*m/z* calcd for $C_{13}H_{16}NO_3$ $[M+H]^+$ 234.1130, found, 234.1124.

3.4.3 Mechanism study by the high-temperature NMR

1. Confirmation of the aldehyde intermediate

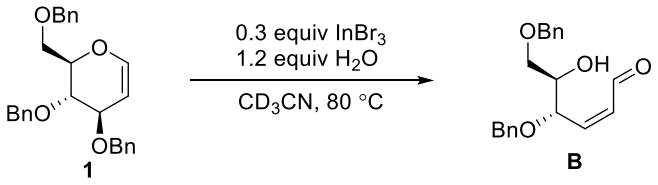

To a suspension of 3,4,6-tri-*O*-benzyl-D-glucal **1** (20 mg, 0.048 mmol, 1.0 equiv) dissolved by CD_3CN (480 μL) in a sealed NMR tube was added $InBr_3$ (5.1 mg, 0.014 mmol, 0.30 equiv) and DI water (1.0 μL, 0.058 mmol, 1.2 equiv). The ^1H NMR was run at room temperature to obtain the original spectra first. No reaction occurred when there was no heating. Then the temperature was increased to 80 ℃ and the ^1H NMR was run every 2 min. A series of spectra were obtained as shown below. The highest peak of aldehyde was observed at 5 min, which was not stable and decreased slowly.

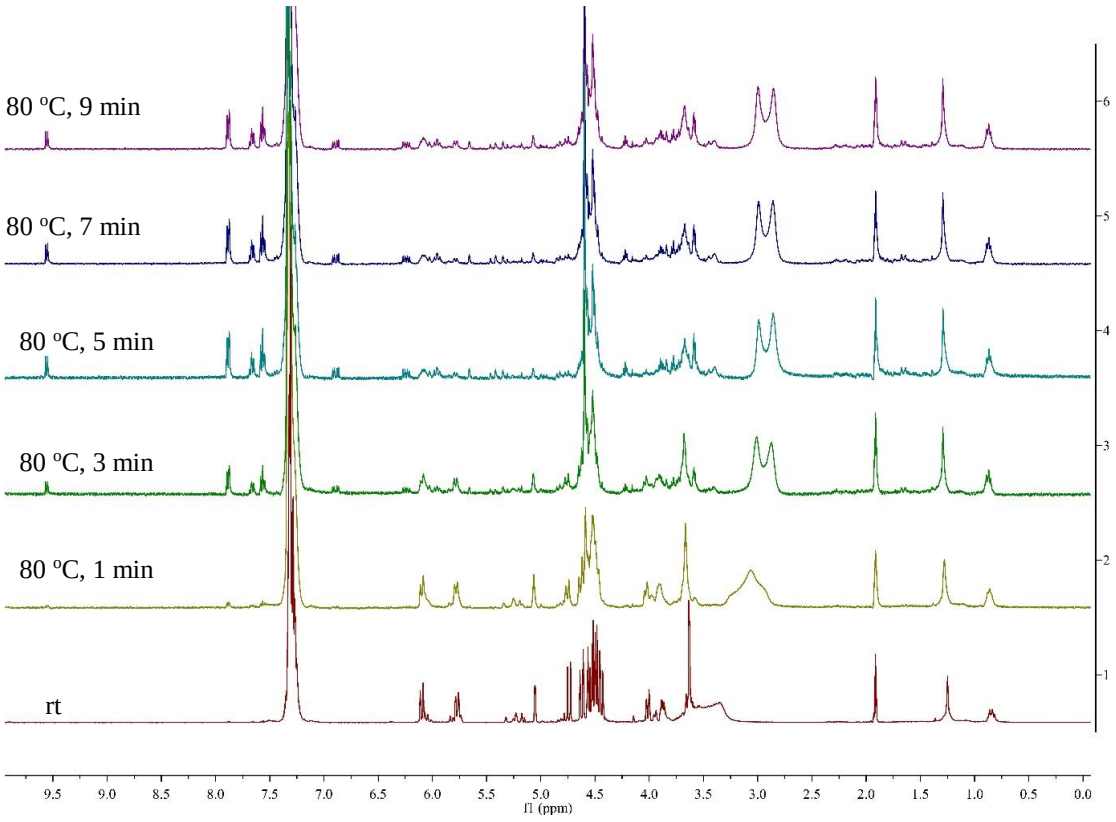

2. Monitoring the reaction process

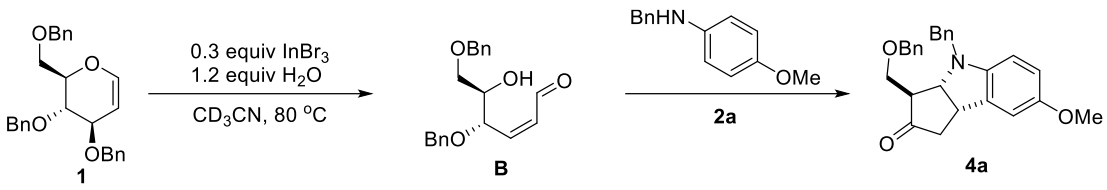

To a suspension of 3,4,6-tri-*O*-benzyl-D-glucal **1** (20 mg, 0.048 mmol, 1.0 equiv) dissolved by CD_3CN (480 μL) in a sealed NMR tube was added $InBr_3$ (5.1 mg, 0.014 mmol, 0.3 equiv) and DI water (1.0 μL, 0.058 mmol, 1.2 equiv). Then the temperature was increased to 80 ℃ and maintained for 5 min. When the aldehyde peak arrived the highest position, *N*-benzyl-4-methoxyaniline **2a** (10.2 mg, 0.048 mmol, 1.0 equiv) was added immediately and ^1H NMR was run every one hour. A series of spectra were obtained, and selected spectra are shown as below. The consumption of aldehyde after adding aniline could be found from the NMR spectra.

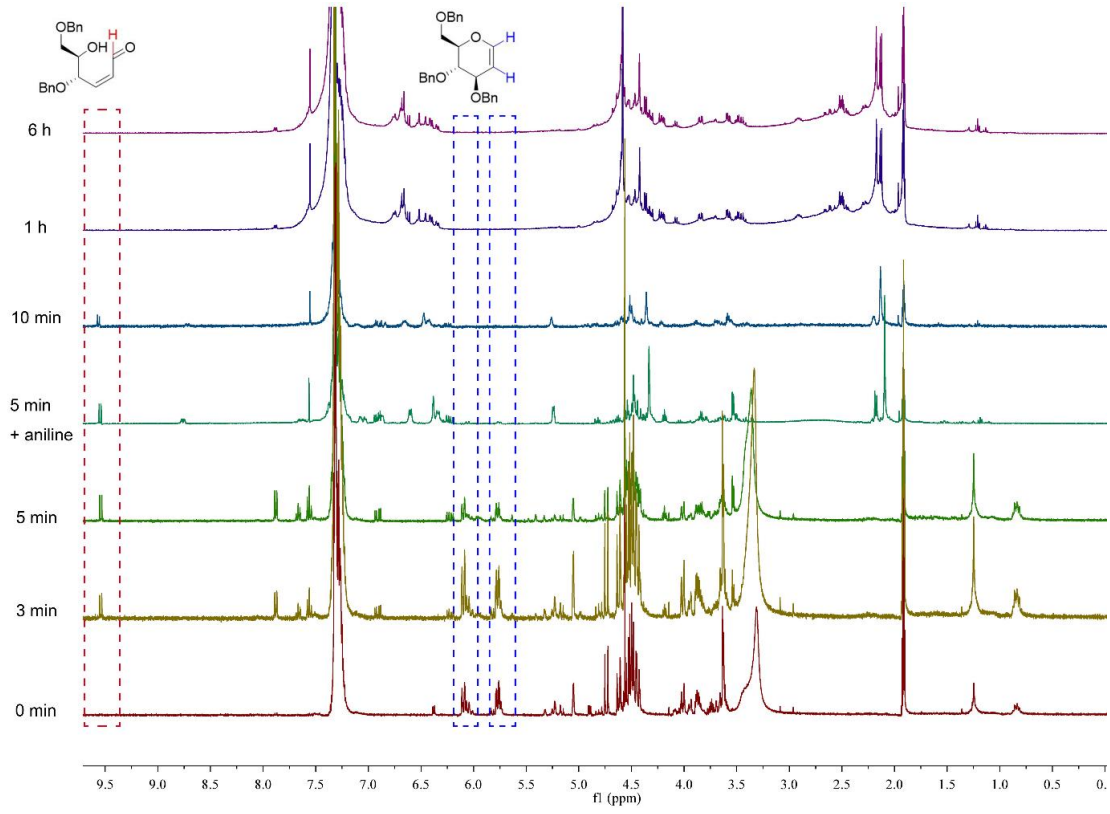

3.4.4 X-ray crystal structure and data

X-ray crystal structure for **8** (CCDC number: 1844841)

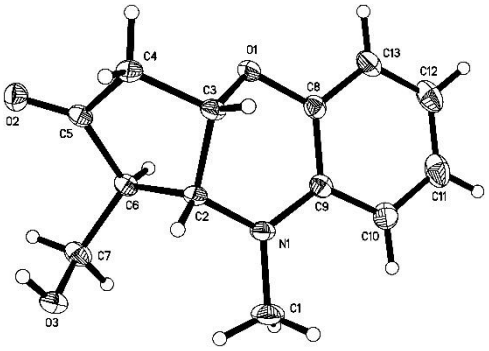

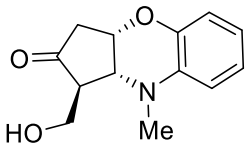

8

Table 3.4.1 Sample and crystal data for 8.

Chemical formula	$C_{13}H_{15}NO_3$	
Formula weight	233.26 g/mol	
Temperature	103(2) K	
Wavelength	0.71073 Å	
Crystal size	0.220 x 0.380 x 0.400 mm	
Crystal system	monoclinic	
Space group	P 1 21/c 1	
Unit cell dimensions	a = 17.2388(8) Å	α = 90 °
	b = 9.0530(5) Å	β = 96.162(3) °
	c = 7.3181(3) Å	γ = 90 °
Volume	1135.49(9) $Å^3$	
Z	4	
Density (calculated)	1.364 g/cm^3	
Absorption coefficient	0.097 mm^{-1}	
F(000)	496	

Table 3.4.2 Data collection and structure refinement for 8.

Theta range for data collection	2.54 to 29.11 °
Index ranges	-23<=h<=23, -12<=k<=11, -8<=l<=9
Reflections collected	10949
Independent reflections	3029 [R(int) = 0.0328]
Max. and min. transmission	0.9790 and 0.9620
Refinement method	Full-matrix least-squares on F^2
Refinement program	SHELXL-2016/6 (Sheldrick, 2016)
Function minimized	$\Sigma\ w(F_o^2 - F_c^2)^2$
Data / restraints / parameters	3029 / 0 / 156
Goodness-of-fit on F^2	1.046
Δ/σ_{max}	0.001
Final R indices	2483 data; $I>2\sigma(I)$ R1 = 0.0427, wR2 = 0.1101

	all data R1 = 0.0535, wR2 = 0.1177
Weighting scheme	$w=1/[\sigma^2(F_o^2)+(0.0613P)^2+0.2849P]$ where $P=(F_o^2+2F_c^2)/3$
Largest diff. peak and hole	0.448 and -0.194 eÅ^{-3}
R.M.S. deviation from mean	0.050 eÅ^{-3}

3.5 References

[1] a) K. Walczak, E. B. Pedersen, *Synthesis* **1991**, 959-962; b) H. H. A. M. Hassan, M. M. A. Rahman, *Synthetic Commun.* **2000**, *30*, 201-216; c) R. Pathak, S. K. Shaw, A. P. Bhaduri, K. V. G. Chandrasekhar, A. Srivastava, K. K. Srivastava, V. Chaturvedi, R. Srivastava, B. S. Srivastava, S. Arora, S. Sinha, *Biorg. Med. Chem.* **2002**, *10*, 1695-1702; d) M. Saquib, R. Sagar, A. K. Shaw, *Carbohydr. Res.* **2006**, *341*, 1052-1056; e) P. Nagaraj, M. Ganesan, N. G. Ramesh, *Tetrahedron* **2011**, *67*, 769-776; f) L. V. R. Reddy, V. Kumar, R. Sagar, A. K. Shaw, *Chem. Rev.* **2013**, *113*, 3605-3631; g) G. Anquetin, S. L. Rawe, K. McMahon, E. P. Murphy, P. V. Murphy, *Chem. Eur. J.* **2008**, *14*, 1592-1600.

[2] S. K. Yousuf, S. C. Taneja, D. Mukherjee, *J. Org. Chem.* **2010**, *75*, 3097-3100.

[3] D. A. Smith, C. W. Ulmer, *J. Org. Chem.* **1997**, *62*, 5110-5115.

[4] R. William, S. Wang, F. Ding, E.-N. Arviana, X.-W. Liu, *Angew. Chem. Int. Ed.* **2014**, *53*, 10742-10746.

[5] a) J. S. Yadav, B. V. S. Reddy, K. V. Rao, K. S. Raj, A. R. Prasad, S. K. Kumar, A. C. Kunwar, P. Jayaprakash, B. Jagannath, *Angew. Chem. Int. Ed.* **2003**, *42*, 5198-5201; b) J. S. Yadav, B. V. S. Reddy, M. Srinivas, B. Padmavani, *Tetrahedron* **2004**, *60*, 3261-3266.

[6] F. Li, C. Ding, M. Wang, Q. Yao, A. Zhang, *J. Org. Chem.* **2011**, *76*, 2820-2827.

[7] a) C. Y. Ding, S. H. Tu, F. Y. Li, Y. X. Wang, Q. Z. Yao, W. X. Hu, H. Xie, L. H. Meng, A. Zhang, *J. Org. Chem.* **2009**, *74*, 6111-6119; b) N. Maugel, B. B. Snider, *Org. Lett.* **2009**, *11*, 4926-4929.

[8] S. Wang, R. William, K. K. G. E. Seah, X.-W. Liu, *Green Chem.* **2013**, *15*, 3180.

[9] a) F. Touzeau, A. Arrault, G. Guillaumet, E. Scalbert, B. Pfeiffer, M.-C. Rettori, P. Renard, J.-Y. Mérour, *J. Med. Chem.* **2003**, *46*, 1962-1979; b) J. W. Blunt, B. R. Copp, R. A. Keyzers, M. H. G. Munro, M. R. Prinsep, *Nat. Prod. Rep.* **2013**, *30*, 237-323.

[10] a) R. J. Fradette, M. Y. Kang, F. G. West, *Angew. Chem. Int. Ed.* **2017**, *56*, 6335-6338; b) Y. Kwon, D. J. Schatz, F. G. West, *Angew. Chem. Int. Ed.* **2015**, *54*, 9940-9943.

[11] R. W. Huigens III, N. G. Paciaroni, PCT Int. Appl., WO 2017190038 A1 20171102, **2017**.

LIST OF PUBLICATIONS

1. Hui Yao, Shasha Zhang, Wei-Lin Leng, Min-Li Leow, Shaohua Xiang, Jingxi He, Hongze Liao, Kim Le Mai Hoang, Xue-Wei Liu, Catalyst-Controlled Stereoselective *O*-Glycosylation: Pd(0) vs Pd(II), *ACS Catal.*, **2017**, *7*, 5456–5460.
2. Wei-Lin Leng‡, Hui Yao‡, Jing-Xi He‡, and Xue-Wei Liu, Venturing beyond Donor-Controlled Glycosylation: New Perspectives toward Anomeric Selectivity, *Acc. Chem. Res.*, **2018**, *51*, 628–639.
3. Hui Yao, Minh Duy Vu, Xue-Wei Liu, Recent advances in reagent-controlled stereoselective/stereospecific glycosylation, *Carbohydr. Res.* **2018**, doi.org/10.1016/j.carres.2018.10.006. (invited paper)
4. Hui Yao,+ Ronny Willam,+ Siming Wang, Tai Guo, Xue-Wei Liu, Cascade Transformation of Glycal into Structurally Diverse Chiral Fused Rings, *Angew. Chem. Int. Ed.* **2018**, submitted.
5. Hongze Liao, Jimei Ma, Hui Yao, Xue-Wei Liu, Recent progress of *C*-glycosylation methods in the total synthesis of natural products and pharmaceuticals, *Org. Biomol. Chem.*, **2018**, *16*, 1791–1806.
6. Nianyu Huang, Hongze Liao, Hui Yao, Tianpeng Xie, Shasha Zhang, Kun Zou, and Xue-Wei Liu, Diastereoselective Synthesis of *C*-Vinyl Glycosides *via* Gold(I)-Catalyzed Tandem 1,3-Acyloxy Migration/Ferrier Rearrangement, *Org. Lett.*, **2018**, *20*, 16–19.
7. Wei-Lin Leng, Hongze Liao, Hui Yao, Zi-En Ang, Shaohua Xiang, Xue-Wei Liu, Palladium-Catalyzed Decarboxylative Allylation/Wittig Reaction: Substrate-Controlled Synthesis of *C*-Vinyl Glycosides, *Org. Lett.*, **2017**, *19*, 416-419.
8. Hongze Liao, Wei-Lin Leng, Kim Le Mai Hoang, Hui Yao, Jingxi He, Amanda Ying

Chapter 3 Cascade transformation of glycal into diverse fused cyclic compounds

Hui Voo, Xue-Wei Liu, Asymmetric syntheses of 8-oxabicyclo[3,2,1]octane and 11-oxatricyclo[5.3.1.0]undecane from glycals, *Chem. Sci.*, **2017**, *8*, 6656-6661.

9. Ho Sup Yoon, Sreekanth Rajan, Hui Ting Toh, Xuewei Liu, Hui Yao, Co-Crystals of Nurr1-LBD In Complex With A Cyclopentenone Prostaglandin And Modulators Of Nurr1, PCT Application No. PCT/SG2017/050476 (as a second filing) based on Singapore Patent Application No. 10201607854Q.
10. Wei-Lin Leng, Jingxi He, Hui Yao and Xue-Wei Liu, "Methodologies in chemical synthesis of carbohydrates", Chapter in book *Synthetic Glycomes*, Chapter 2, Royal Society of Chemistry, **2018**.

Note: ‡Equally Contributing Authors.

Conference

"Catalyst-Controlled Stereoselective *O*-Glycosylation: Pd(0) vs Pd(II)" Hui Yao, Shasha Zhang, Wei-Lin Leng, Min-Li Leow, Shaohua Xiang, Jingxi He, Hongze Liao, Kim Le Mai Hoang, and Xue-Wei Liu. "*255th ACS National Meeting & Expo: Nexus of Food, Energy & Water"*, New Orleans, LA, USA. March 18-22, **2018** (poster presentation).